COMPUTERS IN ELECTROCARDIOGRAM ANALYSIS AND DIAGNOSIS

by

N.A. BOBEY

Submitted in partial fulfillment
of the requirements
for the degree of
Master of Science

Department of Electrical Engineering,
Faculty of Pure and Applied Science,
The University of Ottawa,
Ottawa, Canada

1964

ABSTRACT

This investigation is concerned with the processing of electrocardiographic (ECG) signals using analog and digital computers. A review of the work reported in the literature on displaying and/or analyzing the ECG signal using analog and digital techniques is presented. The limitations and difficulties encountered in a number of analog instruments reported to date are discussed and suggestions for a more general approach given.

The results of digital computer programs written to give the spherical coordinate transformation (magnitude, azimuth and elevation), rate of change of magnitude, linear velocity, rate of change of azimuth, rate of change of elevation, and the magnitude of angular velocity of the "heart vector" is presented along with a discussion on preparing the analog ECG signals (x(t), y(t), z(t), Frank lead system) into a suitable format for presentation to the digital computer input. No one has previously reported all of these curves simultaneously. Angular velocity has been previously discussed only briefly by Brinberg. The coordinate conventions and notations presently in use are discussed.

In addition, the Fourier analysis of the ECG signal is considered along with a recently proposed technique of analyzing the ECG signal using a set of orthogonalized exponential functions which form the basis of a multi-dimensional signal space.

ACKNOWLEDGEMENTS

The author wishes to express his appreciation to Professor G. Glinski, Chairman of the Department of Electrical Engineering at the University of Ottawa, for his patient guidance in directing the author's work and encouraging the author to gain a broad understanding and outlook on clinical research techniques associated with displaying and representing ECG signals. In addition, the author wishes to thank: Dr. F. Berkman, Assistant Professor of Medicine at the University of Ottawa, for constructive discussions, and for supplying electrocardiograms and some pertinent references to the literature; Miss O. Boshko, Research Assistant at the University of Ottawa, for preparing a number of digital computer programs.

A series of seminars dealing with various aspects of heart research and theory proved to be helpful and interesting. The series of seminars were attended by Professor G. Glinski, Dr. F. Berkman, the author, Dr. G.W. Mainwood and Dr. P.A. Robertson of the Department of Medicine at the University of Ottawa, Mr. J.A. Hopps and Mr. O.Z. Roy of the Medical Electronics Group, Radio and Electrical Engineering Division, National Research Council, and other interested persons.

Financial assistance was received from the National Research Council of Canada under Grant No. A-875 and this is gratefully acknowledged.

PREFACE

As a good portion of this investigation is of a survey nature indicating recent advances and the state of the art of electrocardiography and vectorcardiography, the author makes no claim to the originality of the material presented. The source of a particular idea or comment may not at all times be accredited to a particular reference. The reference in question, however, could be traced through the bibliography.

The material is of necessity drawn from a variety of fields and disciplines. Consequently, in the interest of helping to establish a common ground of communication between members of the medical science profession and other consulting professions, some statements may at times appear naive to a person thoroughly familiar with the material. The author would ask the reader for his patient understanding in such instances as these may be quite foreign to the uninitiated person.

TABLE OF CONTENTS

CHAPTER 1

INTRODUCTION - COMPUTERS IN ELECTROCARDIOGRAM ANALYSIS AND DIAGNOSIS [1]

Summary

The purpose of this introduction is to unify and lend an integrated insight into the material in the chapters that follow, which otherwise might give the appearance of being disjointed or haphazard. An attempt is made to achieve this purpose by presenting a summary of the chronological development and overall philosophy of this study together with important topics of interest in related theory and recent advances in the field. It is the author's hope that the introduction will help place the following chapters in proper perspective.

[1] Webster's Collegiate Dictionary, Fifth Edition, 1948.
Diagnosis is "the art or act of recognizing disease from its symptoms - also the decision reached."
Analysis is "the separation of anything into constituent parts or elements; also, an examination of anything to distinguish its component parts, separately, or in their relation to the whole".

The electrocardiogram (ECG) figure 1.1 is a strip chart record of the time variation of the potential field at the body surface arising from the electrochemical activity of the heart. It has for sometime been an invaluable aid to the cardiologist in diagnosing heart disorders. Electrocardiographic (ECG)[2] theory is somewhat emperical and qualitative. Interpretation of the ECG demands an experienced eye.

The ECG signal is normally recorded using German silver electrodes placed on the body surface (1, 2, 3)[3] and connected to a biological amplifier and a direct writing strip chart recorder, or to a string or moving coil galvanometer and a moving photographic film recorder. The frequency response required of such an equipment is to this day an open question (4); DC or close to DC, to several hundred cycles is generally accepted as suitable for research work.

ECG analysis is a "black box technique", that is, the cardiologist attempts either to diagnose (1, pp. 132 - 133; 5, 6) the heart condition by surface measurements on the body without making incisions or inserting probes into the body, or to monitor externally the effects of treatment.

The theory evolved (1, 3, 7, 8) to explain and correlate the waveform of the ECG signal with the electrochemical and muscular or mechanical activity of the heart, models the body as a homogeneous spherical volume conductor containing a dipole current source at its center, figure 1.2. A vector varying in both magnitude and orientation with time in three dimensional geometric space is used to characterize the electrical activity of the dipole. ~~(that is, the SA node in the heart).~~ In

---

[2] It will be obvious from the context as to whether the abbreviation ECG refers to electrocardiogram or electrocardiographic. Similarly, VCG will be used to refer to vectorcardiogram or vectorcardiographic.

[3] Numbers in parenthesis refer to the list of references.

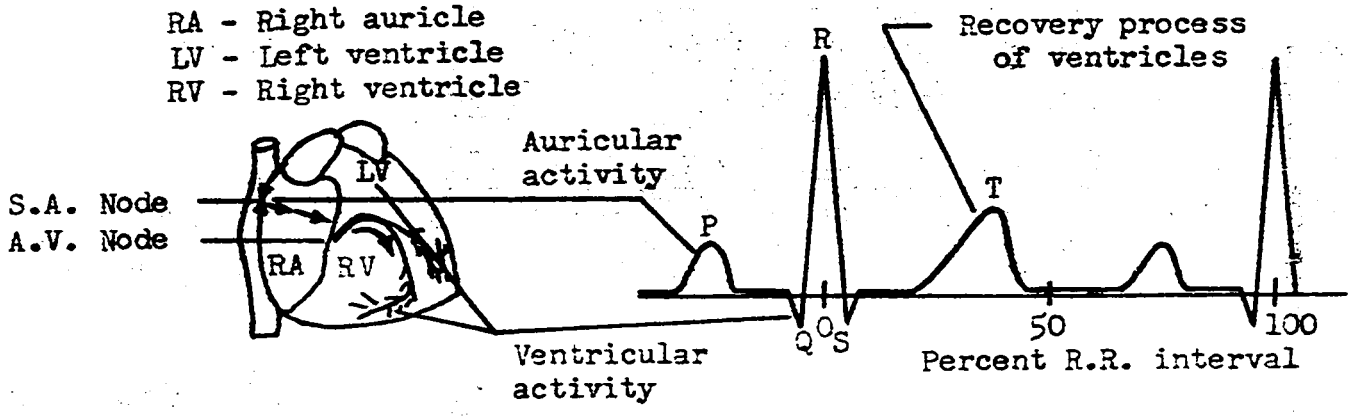

Figure 1.1

Components of ECG signal and sites of origin in the heart

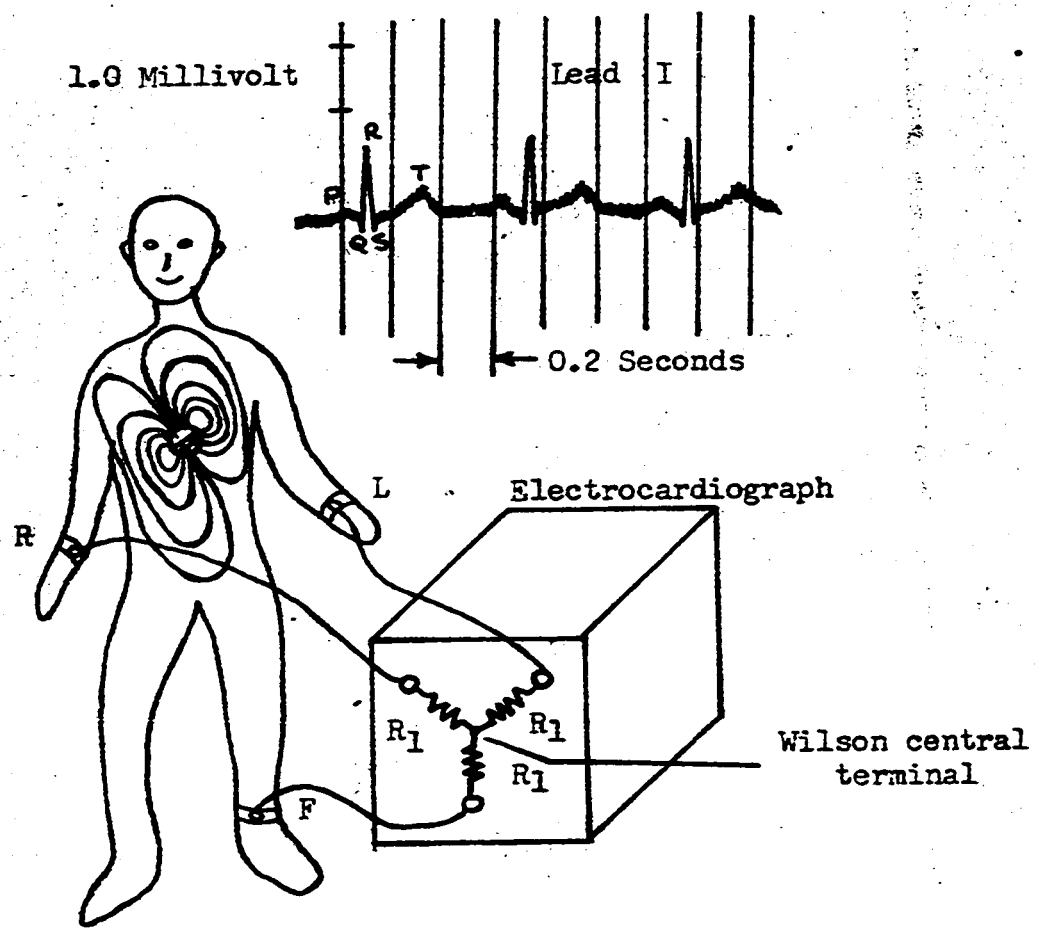

Figure 1.2a

Standard electrodes R, L, and F connected from subject to an electrocardiograph. A typical Lead I recording for three heart beats is also shown.

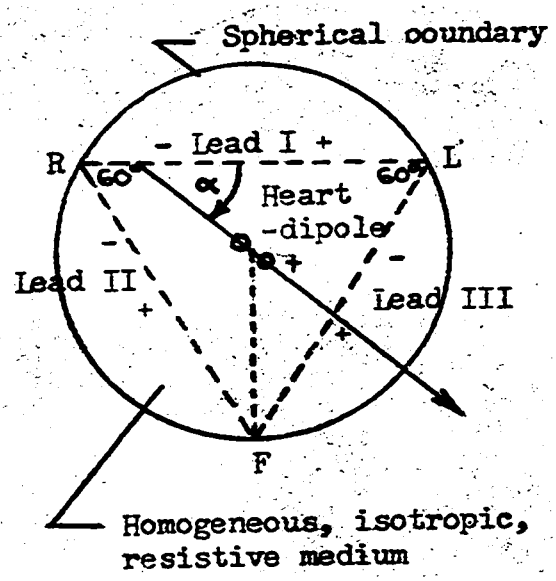

Figure 1.2b

Approximate model of the body and heart which was the basis in developing electrocardiographic theory. Standard bipolar Leads I, II, and III developed by Einthoven and his associates are shown.

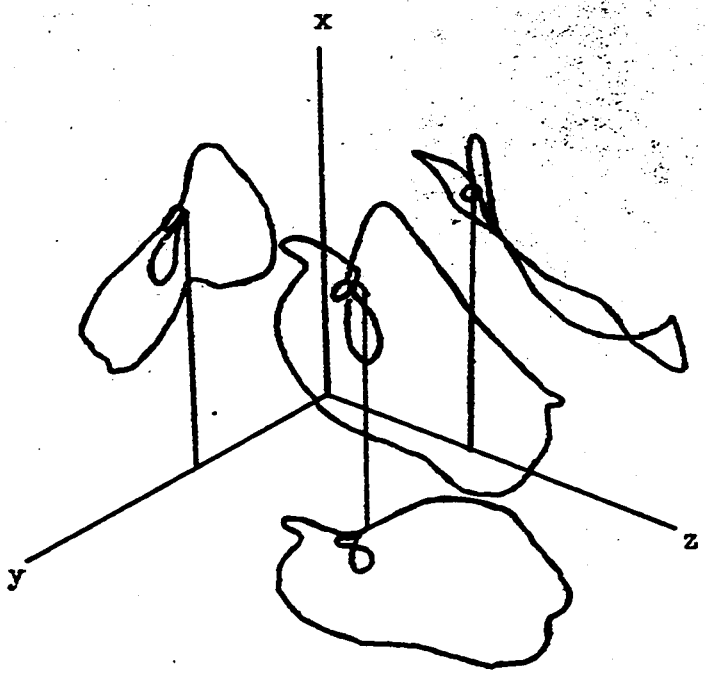

Figure 1.3

Relationship between spatial vectorcardiogram and planar vectorcardiogram

addition, the dipole is considered to remain at the center of the spherical volume conductor at all times and any probes placed on the surface of the sphere are sufficiently distant from the source such that the potential field is not disturbed by the probes.

Such a model is obviously a first approximation[4] since the human torso is an irregular surface, far from being a homogeneous volume, with the heart (dipole) located considerably off center. The potential field is not symmetrical. In addition, the muscular activity of the heart suggests the signal source (SA node), which can be considered a nonlinear negative resistance oscillator, is not stationary during the heat cycle. Furthermore, probes placed on the chest or back near the heart are considerably closer to the signal source than a lead at the extremities of the torso. Though the assumptions and approximations seem quite drastic, and it is easy to question their validity, they are necessary to establish a theory in readily usuable form as a starting point upon which more exact models and theories can be developed.

In three dimensional geometric space, three components are required to describe the heart vector, figure 1.3. Considering one end of the vector as being fixed at the origin of an x, y, z coordinate system the tip of the vector traces out a space curve. ECG theory deals with the projection of the vector onto an axis (lead) in the frontal plane. A projection of the space curve onto the frontal plane yields a vector loop, figure 1.4. ECG theory originally used the Einthoven system of leads (axes) I, II and III, figures 1.2, 1.4 and 1.5. Presently, Goldberger's augmented

---

[4]The heart vector can be considered as the resultant dipole vector of all current sources and sinks in the heart. A generalization of the dipole theory has recently led to a proposed multipole model for electrocardiography (9) which is impractical because of the mathematical expressions that require evaluation.

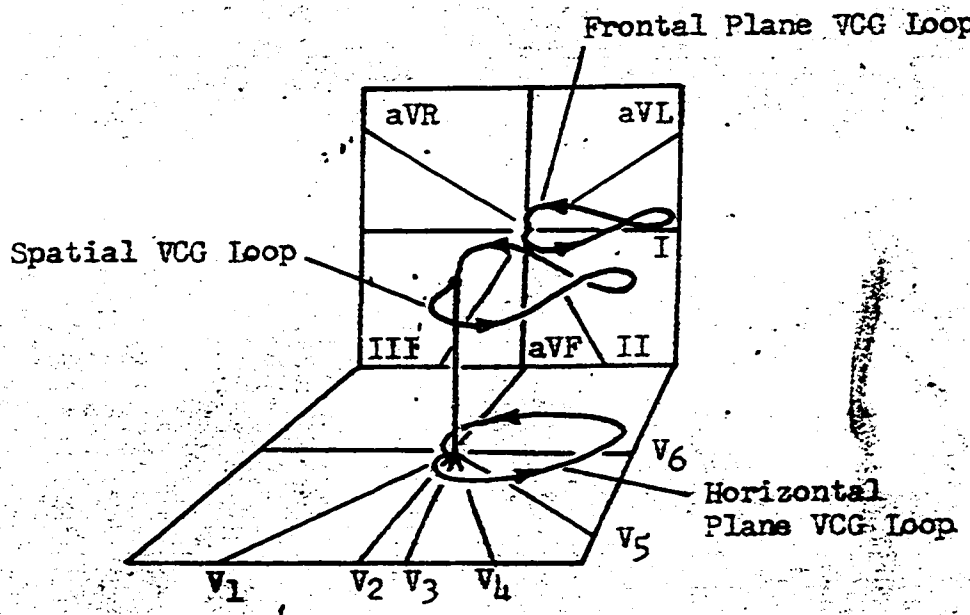

Figure 1.4a

Schematic diagram of vector loop
for QRS interval

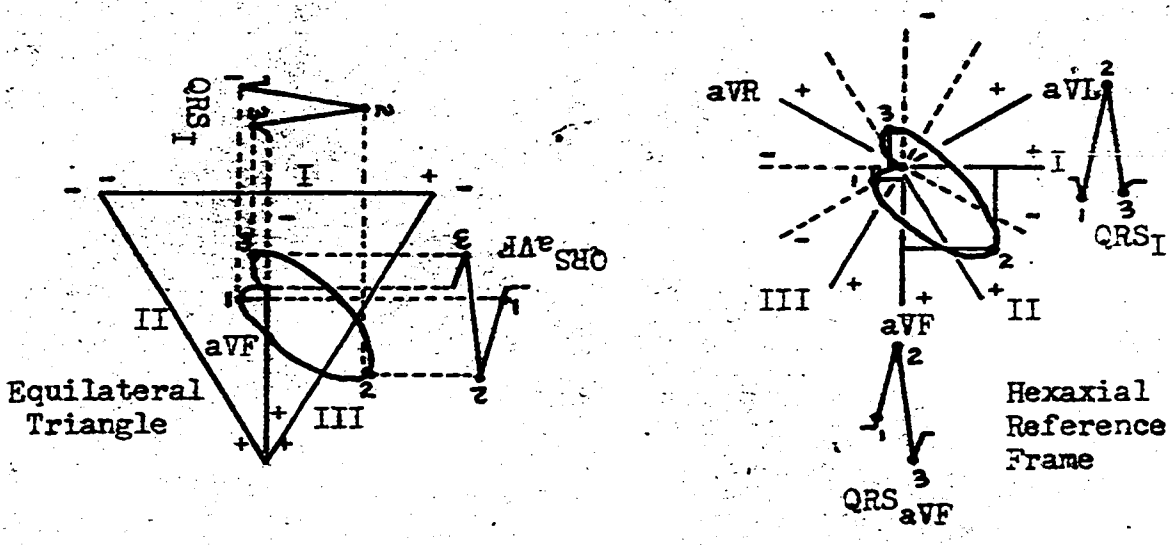

Figure 1.4b

Derivation of the QRS deflections in leads I and aVF using the equilateral triangle and hexaxial reference frames. (In actual practice more than the 3 points indicated would be used)

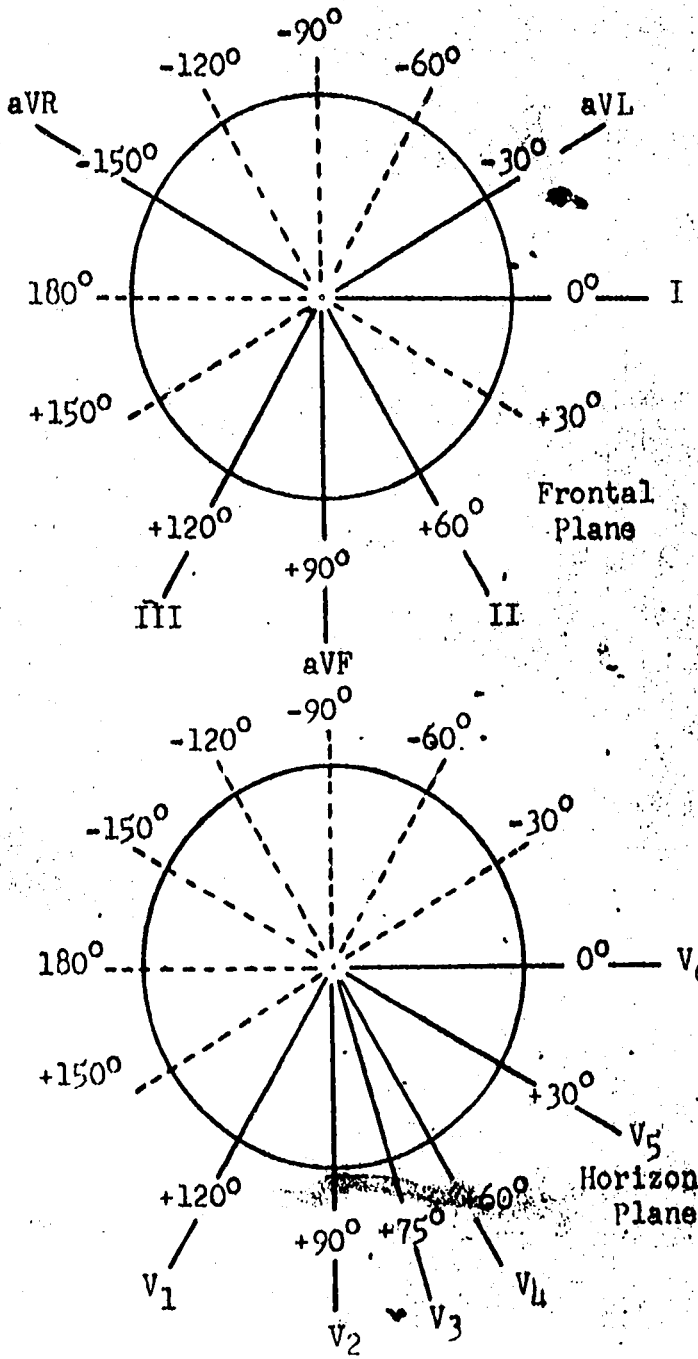

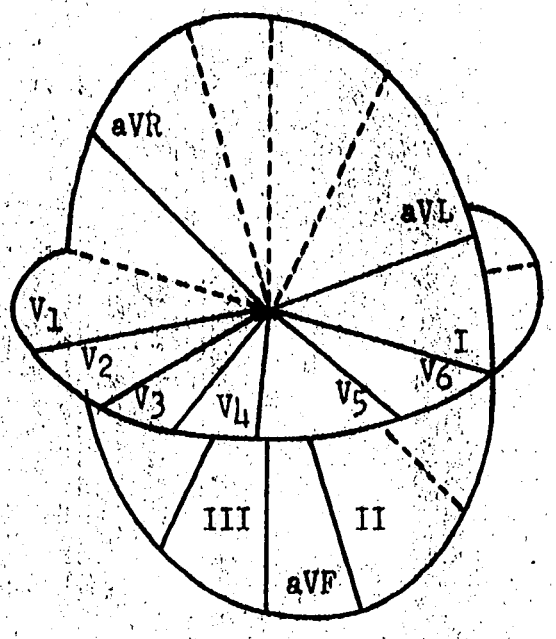

Figure 1.5

The frontal reference frame is formed by the superposition of the lead axes of the bipolar and unipolar limb leads (leads I, II, III, aVR, aVL and aVF) so that the midpoints of the lead axes coincide. The Horizontal reference frame is formed by the lead axes of the unipolar precordial leads (V_1 to V_6). The solid lines indicate the positive half of the lead axes.

leads a VR, a VL and a VF, and the unipolar precordial leads V_1, V_2, V_3, V_4, V_5 and V_6 are also used in clinical work, figures 1.4 and 1.5. The placement of the lead electrodes has become more or less dogmatic until the advent of vectorcardiography. Vectorcardiography evolved from electrocardiography with the application of cathode ray tubes for displaying vector loops. This new display technique spurred the development of new lead systems based on an x, y, z coordinate system and referred to as orthogonal lead systems. One of these, the Frank system,[5] figure 1.6, uses seven electrodes and a resistor weighting network to yield the x, y, z components of the heart vector to a first approximation (5,) (10).

Conventionally, twelve ECG leads, figure 1.7, are recorded for diagnostic purposes (11, 12, 13). The orthogonal x, y, z components could be extracted, but this is a somewhat tedious procedure. Construction of VCG loops from the scalar ECG records is equally tedious, figure 1.8. To form a mental three dimensional picture of the space curve from the twelve ECG leads is a demanding mental exercise. The advent of the VCG technique and suitable orthogonal lead systems enabled the recording of vector loops on the frontal, sagittal, and horizontal planes with the result that a mental three dimensional picture of the locus can be formed from any two of these loops with relative ease as compared to using the twelve conventional ECG leads.

A time scale for the VCG is obtained by modulating the cathode ray tube beam at approximately 400 c.p.s. giving time as parameter along the space curve. The VCG, however, tends to obscure information contained

---

[5] Other "corrected orthogonal lead systems" have been developed by Schmitt, and McFee. In general, orthogonal lead systems were developed from torso model studies to improve on such lead systems as Wilson's equilateral tetrahedron, Grishman's cube lead system, and others.

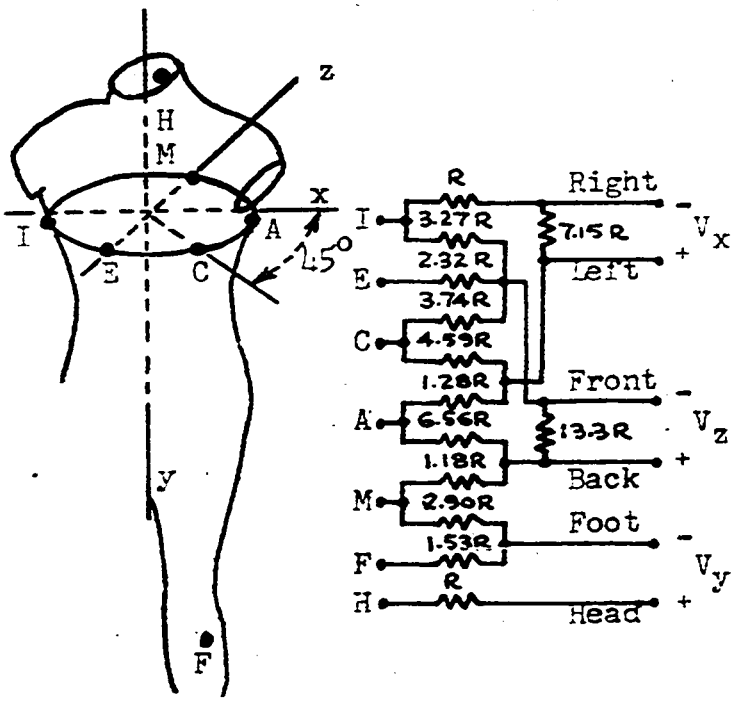

Figure 1.6

Orthogonal lead system due to Frank. On the right is shown the electrical circuit (weighting network) used in recording electrocardiograms and vectorcardiograms with the Frank lead system.

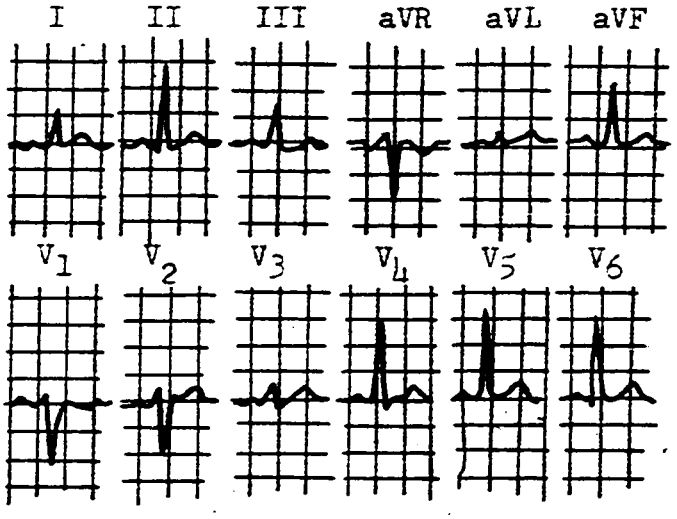

Figure 1.7

12 lead ECG recording conventionally used in clinical practice.

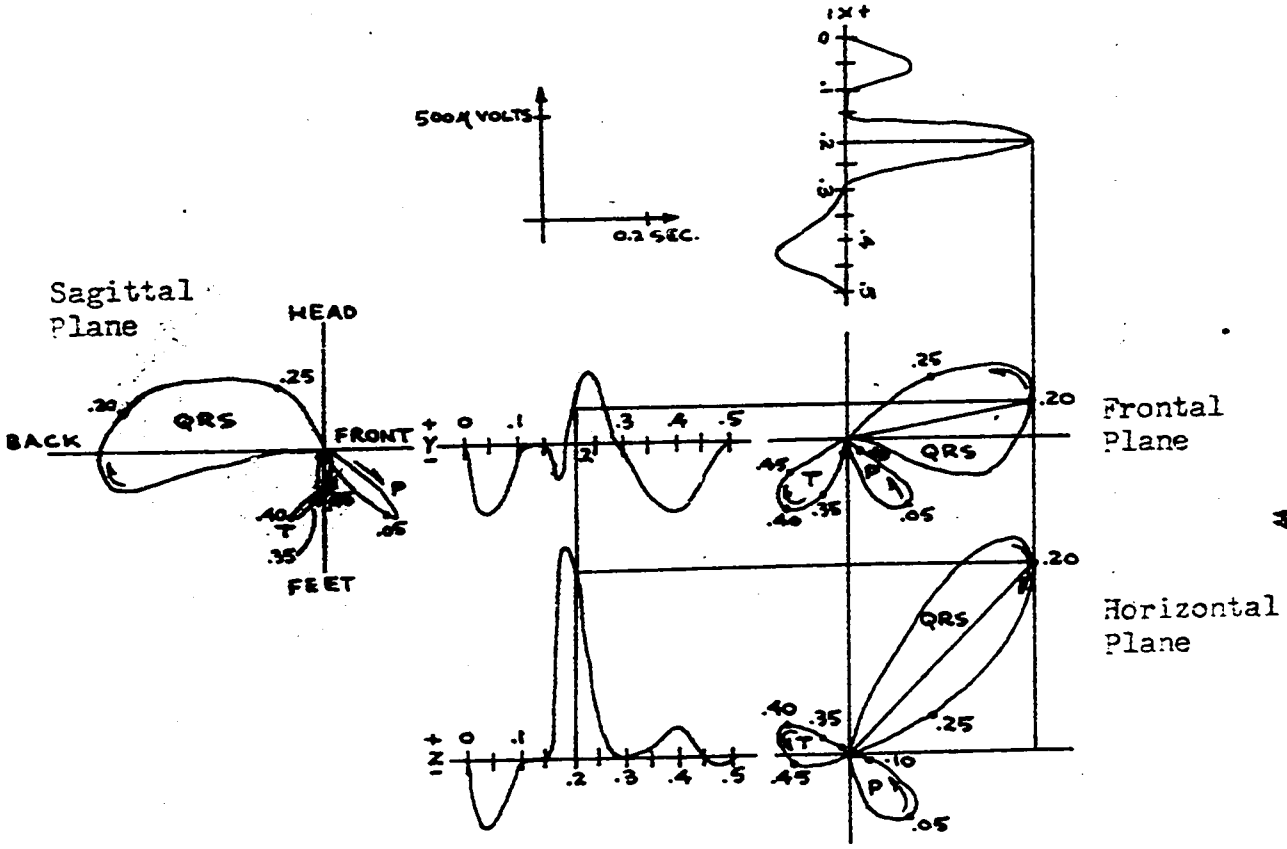

Figure 1.8a

Construction of vector loops from scalar ECG records using orthogonal x,y,z components. The derivation of the frontal and horizontal projection of the instantaneous vector at t = 0.2 seconds is shown. To accurately plot the VCG loops, the indicated projections would have to be carried out at time increments of 0.01 seconds or less. (The scale of the above diagram has been reduced for illustrative purposes.)

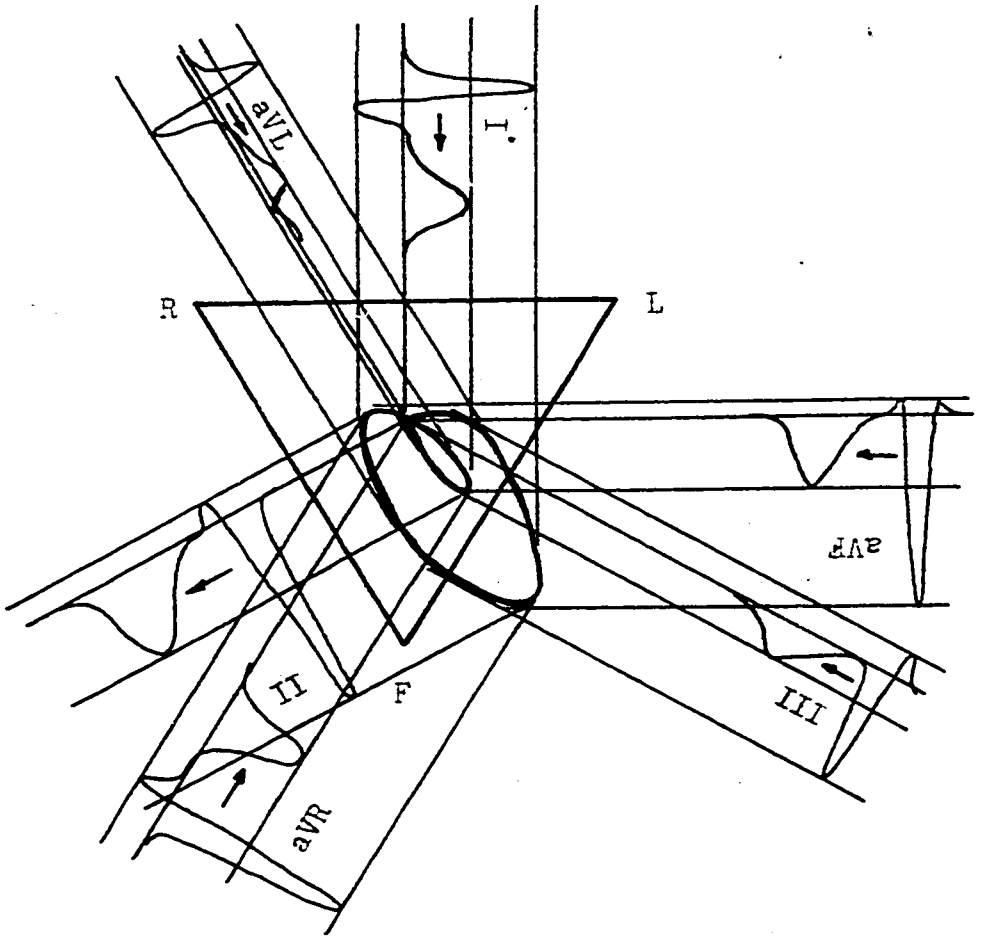

Figure 1.8b

Relationship between the frontal plane vector loop (for the QRS complex and T wave) and leads I, II, III, aVR, aVL and aVF.

in the P and T waves and consequently, the time sequence of events during the heart cycle is not as evident as in the ECG. Furthermore, the VCG provides information for a single heart cycle and so beat to beat variations and discrepancies in rhythym are not available to the observer. Thus, a display using time as one ordinate is preferable to keep the time sequence of events in the heart cycle, beat to beat waveform and rhythym variations clearly in perspective. Obviously, ECG and VCG records are derived from the same source and so contain the same information; this information is simply displayed in a different format, each format having its' advantages and disadvantages.

Since the basic model, as mentioned previously, is a homogeneous spherical volume conductor containing a dipole source at its center is, in a sense, oversimplified, basic ECG theory can be considered essentially emperical. (The model implies that electrical conduction in the body is a linear phenomena). Data has been accumulated over the years on the behaviour of the normal and abnormal heart to the extent that this field appears semi-scientific. However, the interpretation of the ECG still demands the experienced eye of a cardiologist to detect perculiarities in the ECG which often may be quite subtle. The interpretation of the ECG, which is in a sense a pattern recognition technique (14), when correlated with clinical experience, autopsies, and the results of biological experiments and research, has served to advance this discipline. It is perhaps appropriate to mention that considerable work has yet to be done to correlate the work of individuals studying, on the microscopic level, the electrochemical or ionic mechanisms of depolarization and repolarization of isolated heart muscle

fibers by means of microelectrode techniques, and the work of cardiologists observing the effects of heart activity as detected on the body surface and influenced by the intervening tissue and noise generated by other body functions such as respiration and muscle movement. For example, there is at present no generally accepted relation between cell potential and the ECG signal resulting from the activity of a gross collection of cells. In other words, it is still somewhat controversial as to what degree of detail one can distinguish and measure electrically the contributions from various portions or regions of the heart (15, 16).

In view of the comments in the above paragraph, the question could be raised, "Why use computers especially relatively sophisticated and expensive digital computers facilities as some individuals are currently doing?" The following discussion may provide a partial answer.

In an effort to advance the state of the art and establish ECG and VCG analysis and theory, for many years a proven and useful diagnostic tool, on a more qualitative (15), scientific and readily communicated basis, a number of investigators and their associates developed analog instruments as aids in their research. Other workers have resorted to digital computer techniques in their investigations. Computers are thus useful as research tools in spite of the fact that a person, reviewing the current literature, could initially gain the impression that the use of expensive computers are not warranted in investigations relating to electrocardiography and vectorcardiography, the underlying models and theories of which are somewhat empirical.

The development of the vectorcardiography from electrocardiography can be interpreted as an attempt to reduce the number of variables

displayed and a search for the best method of characterizing the heart signal in order to make the record independent of various peculiarities and assumptions. It is an attempt to define a "normal heart" or a common denominator to which all other hearts can be compared. Certainly VCG theory has served to explain the heart vector and its projection on the various leads or planes and thereby unify ECG scalar records and VCG loops. VCG theory has also helped to place in perspective the importance of lead placement, the number of variables required to describe the heart vector and the assumptions made in the basic model. VCG theory is an excellent aid for communicating information to the uninitiated and providing a unifying link between electrocardiography and vectorcardiography.

With the sketchy outline of the basis of electrocardiography and vectorcardiography we will attempt to review the highlights regarding equipment and ideas for methods of display attempted to date, primarily in research work, and discuss advantages and disadvantages where appropriate. A literature search will reveal that there has been numerous attempts to display ECG signals, that is, the heart vector, in a variety of formats by utilizing an automatic analog computing instrument of one sort or another. In a sense, depending on the year an analog device was developed for application to electrocardiography, the state of the art in analog computation and the availability of suitable electronic analog components restricted development in that it was not always possible to readily translate certain operations and ideas on paper into physical electronic hardware.

The analog ECG processing instruments built to date are, compared to digital computers, inflexible from the point of view of programming, that is, they are usually "single purpose". A particular instrument

will display a magnitude curve (17), perform a coordinate transformation on x, y, z, to r, θ, ϕ (18, 19, 20, 21), or effect a rotation of x, y, z, to x', y', z' (22). Such instruments are custom built for specific research projects and generally circuit design problems assume predominance over systems design problems. A simple example is provided by Sayers' magnitude computer (17) in which the design of circuits to achieve squaring and square-rooting operations is relatively more important than the interconnection of circuits into a system that will perform the desired calculations. In the coordinate transformation instrument developed by Park (20), the design of the required modulators (multipliers) using pentagrid tubes (tubes with two control grids) and thereby eliminating the need for transformer coupling is perhaps the single most important consideration.

In considering the possibility of developing an "ECG computer" at the University of Ottawa, attention was devoted to considering a more integrating approach to the instrumentation of a computer research facility for electrocardiography. In view of the inflexibility or "single purpose" restriction of the custom built computers referred to above, it would seem reasonable to assemble an analog computer system utilizing commercially available electronic analog computer components such as chopper stabilized operational amplifiers, Hall effect multipliers, etc. The response of these components, from DC to several hundred cycles is admirably suited for ECG signals. Furthermore, the use of electronic analog components overcomes the frequency response limitations of electromechanical analog components such as resolvers.

Discussions resulted in the proposal[6] to develop an analog computer facility to enable clinical investigation of all possible displays reported to date, namely magnitude of the heart vector, x, y, z, to r, θ, ϕ coordinate transformation, linear velocity (orbit velocity), plus the angular velocity display, with the view that a particular heart disorder may reveal itself more readily from a particular display, and thereby enable diagnosis of the disorder more directly. Such a technique, of course, is based on the conventional method of diagnosis, that is, setting up a one to one correspondence by experience between a particular disorder and a display pattern or characteristic in a dictionary format. The empirical dipole theory and heart vector, is the basis of the underlying theory. Obviously, the total collection of displays contains redundant[7] information. Thus, the problem is to evaluate which displays are best in terms of diagnostic usefulness, keeping in mind that the diagnostic usefulness of a display may be a function of the heart abnormality.

The proposed analog system would be placed in cascade between biological preamplifiers connected to the electrodes on the subject's body surface and a multi-trace real time recorder[8], figure 1.9.

---

[6] The proposal was originated during discussions between Professor G. Glinski, Dr. F. Berkman and the author. See (23) re a proposal for coordinating the instrumentation available at several centres of electrocardiography.

[7] See (24) re an interesting attempt to estimate the amount of information in an ECG signal by means of information theory. Also, see (13) for comments re redundant information in the conventional twelve lead set of ECG signals as compared to the set of three ECG signals obtained using an orthognal lead system. In addition see (29) re further comments on redundancy.

[8] The preamplifiers and multitrace recorders are commercially available and form part of a facility already at Ottawa General Hospital. See Chapter 6 for further details.

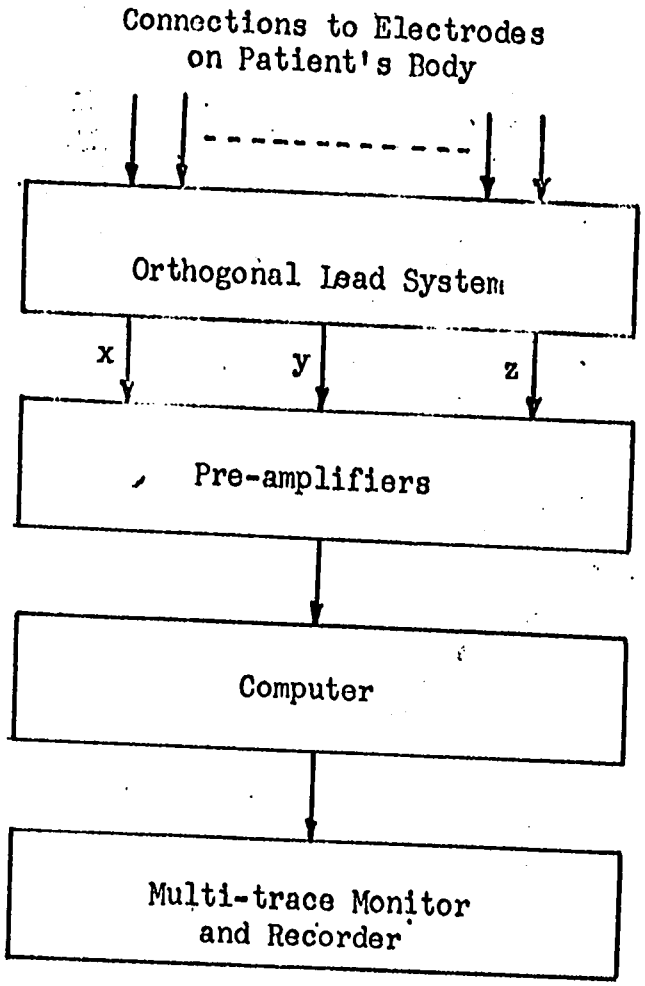

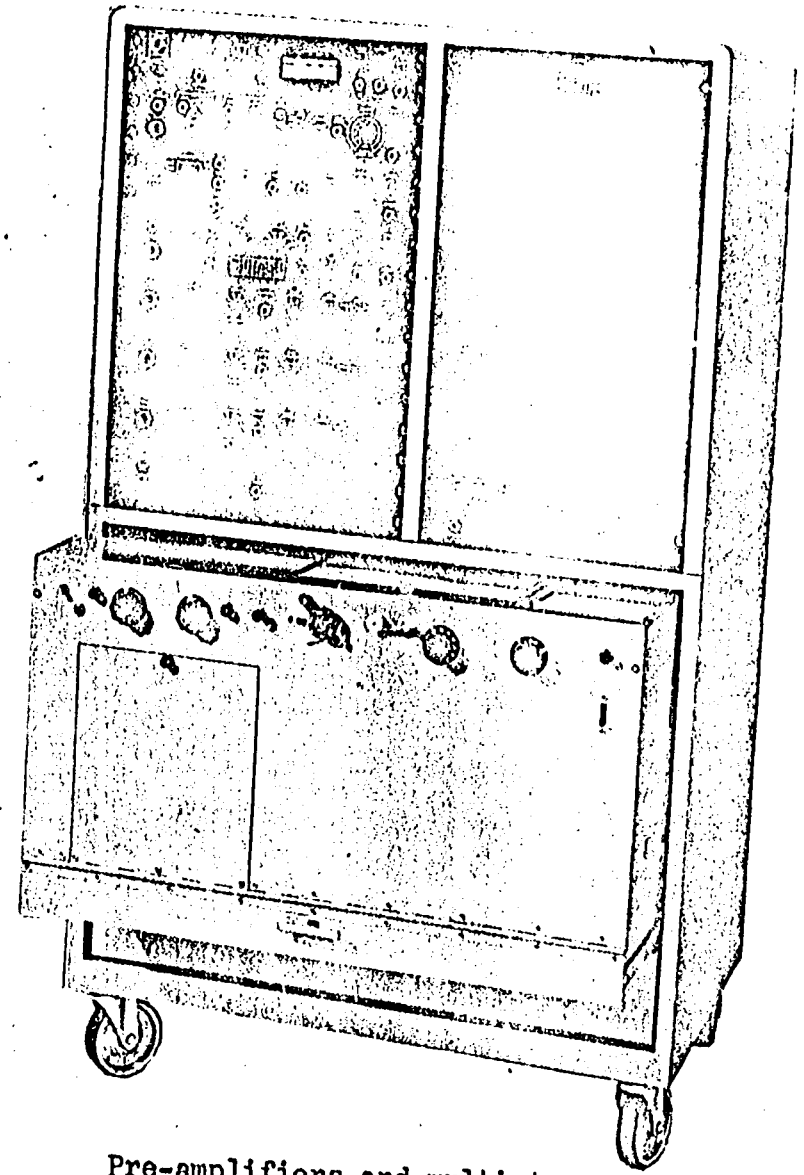

Pre-amplifiers and multi-trace monitor and moving film photographic recorder. (Electronics for Medicine Inc., White Plains, N.Y.)
See Chapter 6 for further details.

Figure 1.9

In such a system, as in current analog computers, the analog components are considered simply as units capable of performing mathematical operations such as addition, subtraction, multiplication by a constant (gain), multiplication of two or more time varying functions, division, differentiation and integration. In contrast to the custom built computers referred to previously, the design of the internal circuitry of the individual analog components to achieve the desired mathematical operation is secondary to the system design. Components would be provided in sufficient number and appropriately arranged so that an ECG technician could insert a prepatched program board to yield one of the displays of immediate interest to the cardiologist. An important requirement of such a system is that any balancing, calibrating, or reprogramming operations can be simply and quickly carried out by an ECG technician with little or no electronic background.

A proposal for such a computer facility involves considerable expense and warrants careful planning. Consequently, this thesis concerns itself with investigating the feasibility of establishing such a facility by: assessing the state of the art re displaying ECG's and VCG's; suggesting possible flow diagrams for the analog computer facility and components best suited for performing the required mathematical operations; investigating related problems such as frequency response required of the components; assessing the value of the displays suggested above using a digital computer; and finally reviewing the application of digital computers (13) and signal analysis concepts used in communications (25).

In chapter 7, a set of displays for a typical ECG record, obtained with the aid of a digital computer, is given. Along with $x(t)$, $y(t)$, $z(t)$, the following displays are given: VCG loops, spherical coordinates

of the heart vecotr, that is, magnitude, azimuth, and elevation, rate of change of magnitude, linear velocity, rate of change of azimuth, rate of change of elevation, and the magnitude of angular velocity. No one has previously reported all of these curves simultaneously. To the author's knowledge, the magnitude of angular velocity curve has previously not been published. Angular velocity has been previously discussed only briefly by Brimberg (26). In this instance the flexibility in programming the digital computer makes it an excellent tool to check out and assess problems associated with generating the desired displays without actually building an analog computer (12, p. 556). In addition, a Fourier analysis was performed on x(t) to obtain a verification of published data. Chapter 8 gives the results along with a discussion.

More recently, digital computers have been used to meet requirements for statistical analysis of ECG data (17) and also for monitoring physiological data (an ECG signal being one portion of the data) transmitted to earth from manned space vehicles (27). Monitoring, in real time, the physiological data transmitted from a space vehicle would not provide sufficient lead time for corrective measures to be initiated to ensure an astronaut's physical safety. Programming the digital computer for these two applications has led to the application of pattern recognition (28) (Chapter 5) concepts and signal analysis concepts (25) as methods for automatically measuring a set of parameters whereby the ECG signal can be characterized. These techniques, if used more extensively, will help to advance ECG and VCG theory.

The signal analysis concept as used in communication engineering and other fields can be considered to be composed of two problems; the

classification problem and the representation problem. Once a signal is described in some definite terms, the classification problem can readily be handled by established statistical methods and processing by digital computers. To effect the classification problem however, the most efficient representation of the signal must first be found. The representation problem consists of attempting to find the most efficient set of parameters whereby an ECG signal can be completely characterized. A Fourier series representation is a possible representation but not necessarily the most efficient. Huggins and Young have demonstrated the feasibility of using a set of orthogonalized exponential functions which form the basis of a multi-dimensional signal space as a method of effecting the representation problem, with an efficiency, in terms of the number of parameters or dimensions in the signal space required to represent the QRS and T portions of the ECG signal, considerably improved over that of a Fourier series representation. This work is reviewed in Chapter 9.

Scher et al (29), in their analysis of ECG signals made use of the factor analysis[9] technique. In studying the ECG's of seventeen normal individuals Scher et al concluded that 95% of all electrocardiographic "information" is accounted for by "three factors", that is there are no significant voltages at the body surface in normal individuals which cannot be discussed in terms of a "three-function system." Huggins and Young carried out analogous procedures in their investigations on ECG signals. However, Scher et al have not attached the same interpretation

---

[9] "Factor analysis is a way of examining mathematically a large number of pieces of information to determine the smallest number of "factors" or independent variables which (in linear combination) can account for all the information." (29, p. 520)

to their results in terms of signal space concepts in the manner that Huggins and Young have done.

Chapter 3 discusses some aspects of present notation and coordinate system conventions. With the increasing effort to apply analog and digital computers to ECG and VCG diagrams, a need for a standardized notation and reference system has arisen. It is misleading and at times difficult to compare the work of various investigators due to the myriad of details that differ from research project to research project as reported in the literature. In any event more care could be taken by researchers to specify their notation and reference conventions more completely when reporting their work in the literature.

As already suggested, programming flexibility is a decided advantage in favour of digital computers provided the available computer has sufficient storage capacity and speed to process the required problem, say the signal analysis problem investigated by Huggins and Young, in reasonable time at reasonable cost. In addition, the consulting services of persons knowledgeable in programming and especially in numerical analysis techniques must be available.

A point that can be mentioned appropriately at this time is that the accuracy to which the cardiologist works in using the ECG record may be appropriate for analog instruments but not for digital computers. Signal format requirements for analog and digital computers are different. The analog computer operates in the continuous time domain.

The frequency response of the analog system must be sufficient to pass all frequency components of the input signal. The digital computer operates in the discrete time domain. Consequently, the ECG signal

recorded in the continuous time domain must be sampled at specified time intervals. The sampling rate must be sufficiently fast, at least twice the highest frequency of interest contained in the input signal, to faithfully represent the analog or continuous time domain signal in the discrete time domain. In the discrete time domain, numerical analysis techniques must be resorted to perform operations such as differentiation and integration.

Analog and/or digital computers now serve as aids in research. Once the use of computers is proven out and accepted in clinical diagnosis, the cardiologist would be released from routine ECG interpretation and thereby could direct his efforts to research or other aspects of his discipline. Furthermore, automatic analysis of the ECG provides information on measurements normally not available or feasible in clinical work because they are tedious or time consuming.

Assuming it is only a matter of time that computers are used more extensively in both ECG research and clinical ECG diagnosis, an analog or digital computer facility need not be physically located in the clinical or research ECG recording room. Medical data sets are now available which enable ECG records to be transmitted over telephone lines to be reproduced for interpretation by a specialist at a distant location (30). Suitably modified, such data sets could transmit ECG records over telephone lines for processing and analysis by a computer. Alternately, a magnetic tape recorder could be used to record ECG signals. The tape recording could then be used to provide the input data to a computer. In the case of a digital computer facility an analog to digital coverter would be required to translate the analog signal into a format suitable for the digital computer. A digital plotting board would enable automatic plotting of

the results of the computer program. Such a system is expensive, but certainly feasible and enables a computer to be rented for short periods of time for ECG signal diagnosis purposes. The ultimate purpose of "digital computer diagnosis" is to assist the cardiologist in making more reliable analysis of data and reduce as much as possible the routine interpretation of analog ECG records.

To conclude this chapter, the unifying or common goal in all the concepts discussed above is the attempt to discover the most advantageous display technique or "best" set of parameters whereby the heart signal can be characterized most efficiently or advantageously.

CHAPTER 2

REVIEW OF THE APPLICATIONS OF ANALOG INSTRUMENTATION IN ELECTROCARDIOGRAPHY

Summary

The following chapter is a review of the most notable contributions reported in the literature concerning the application of "custom built" or single purpose analog instruments for ECG clinical research work. The analog instruments or computers were developed to perform various functions such as evaluate the magnitude of the heart vector, effect a cartesian to spherical coordinate transformation, or perform a coordinate rotation. The purpose of designing the computers, their addvantages and disadvantages and related points of interest are discussed. Reference is also made to a number of related investigations not using electronic analog (or digital) computers.

McFee - A Trigonometric Computer for ECG Applications

One of the first, if not the first, single purpose electronic analog computers developed for processing ECG signals was due to McFee (18)(1950). McFee reported that during a study of the character of the electric field of the heart it became apparent that computers could advantageously be used in the experimental application of ECG theory. The problem was twofold. First, were electronic techniques and components sufficiently well developed to enable the required specification to be met and, secondly, which system of electrode placement should be used? McFee developed an instrument which would effectively transform x, y, to r, e and if two such instruments were combined, an x, y, z to r, e, ϕ coordinate transformation could be achieved, The answer to the second item was investigated by McFee and others in later work.

The ECG theory centered around the concept that the electric fields in the body resulting from the electrochemical activity of the heart could be considered as being caused by a varying electric dipole located at the heart's center and characterized by the "heart vector" was of limited practical value at the time (1950) for several reasons. First, not all persons in the discipline held to the theory, and secondly, the heart vector was tedious to calculate. The more or less dogmatically specified electrode locations which define the leads and thereby the heart vector were a partial reason for this second difficulty which was removed with the acceptance of orthogonal lead systems such as the Frank lead system mentioned in ~~earlier~~ Chapter 1. If a computer were available to process the ECG signals, the calculations related to the heart vector could be accomplished automatically and displayed in graph form thereby eliminating tedious calculations and rendering the heart vector theory experimentally more practical.

Three components, x(t), y(t) and z(t) are sufficient to completely describe the heart vector. However, the waveshape of these components are altered by the orientation of the heart from subject to subject, and there is the possibility that these relatively unimportant changes in the pattern of the signal could obscure information which might indicate a heart abnormality. Also, angular information about the position of the heart vector during the heart cycle is not obvious from the x(t), y(t) and z(t) components.

McFee's instrument established the feasibility of building a computer that would perform the cartesian to spherical coordinate transformation x(t), y(t) and z(t) to r(t), θ(t) and ϕ(t). The magnitude display

$$r(t) = \left| \sqrt{x^2(t) + y^2(t) + z^2(t)} \right| \qquad 2.1$$

should be independent of the anatomical orientation of the subject's heart. ϕ(t) ($-90^\circ \leq \phi \leq +90^\circ$) the latitude angle, and θ(t) ($-180^\circ < \theta < +180^\circ$) the longitude angle, would yield angular information about the heart vector.

In addition to displaying the computer outputs r(t), θ(t) and ϕ(t) as functions of time, McFee also suggested a "heart vector map" presentation, figure 2.1, to be obtained by feeding ϕ(t) and θ(t) to the deflection plates of a cathode ray tube and using r(t) to control the intensity of the electron beam with the time parameter being introduced by modulating the electron beam at a known rate.

The block diagram of McFee's computer is given in figure 2.2. The outputs are given by

$$e_r = k_r \sqrt{e_1^2 + e_2^2} \qquad 2.2$$

$$e_\theta = k_\theta \text{ arc tan } \frac{e_2}{e_1} \qquad 2.3$$

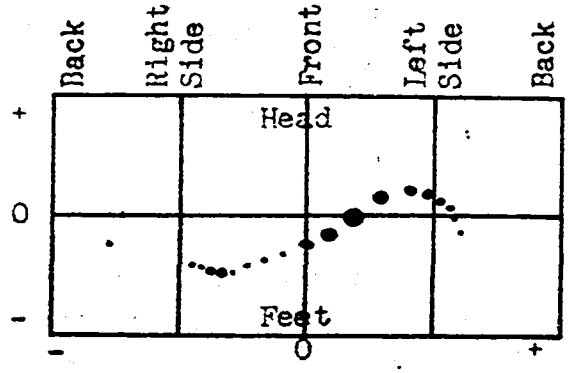

Figure 2.1

Hypothetical heart vector map

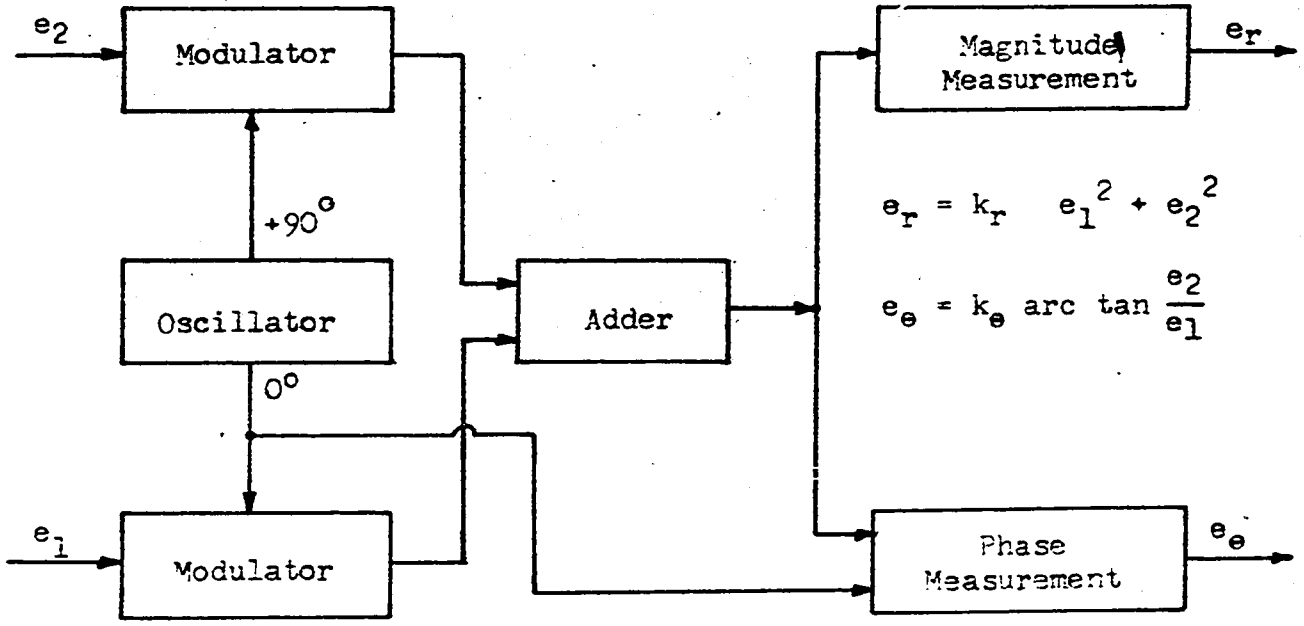

Figure 2.2

Simplified block diagram of McFee's computer

The computer makes use of an analog between equations (2.2) and (2.3) and an equation which gives the phase and magnitude of the sum of two sinusoidal voltage 90° out of phase with each other (31, Chapter 6)

$$V_1 \angle 0 + V_2 \angle 90 = V_1^2 + V_2^2 \angle \arctan V_1/V_2 \qquad 2.4$$

As indicated in the block diagram, e_1 and e_2 are modulated separately by two sine waves supplied by a master oscillator and 90° out of phase with each other. The two signals are added and fed to a detector for obtaining a signal proportional to the amplitude. The phase is determined by comparing the summation of the two signals with an unmodulated output of the oscillator (32). The computer determines e_r and e_θ two thousand times per second with an accuracy of 5%.[1]

A more detailed block diagram, reproduced from (18) in figure 2.3, describes the system in more detail. Interconnection of two instruments would be accomplished as shown in figure 2.4. Since e_r is always positive, e_ϕ will never exceed $\pm$ 90°. In addition to proving the feasibility of building a computer to perform a cartesian to spherical coordinate transformation in an attempt to obtain a magnitude display

$$r(t) = \left|\sqrt{x^2(t) + y^2(t) + z^2(t)}\right| \qquad 2.1$$

which is independent of the coordinate reference system, and thereby independent of the heart orientation, and to obtain angular information, McFee suggested that a coordinate rotation x, y, z, to x', y', z' would possibly be a way of reducing "normal map displays" of his proposed heart vector map to a "standard one".

It may be appropriate at this time to discuss the baseline of the ECG signal in some detail. In figure 2.5 the baseline is indicated and corresponds to the time when the heart is electrically inactive. That is, the

---

[1] 1% accuracy is suggested as a possible limit with careful design.

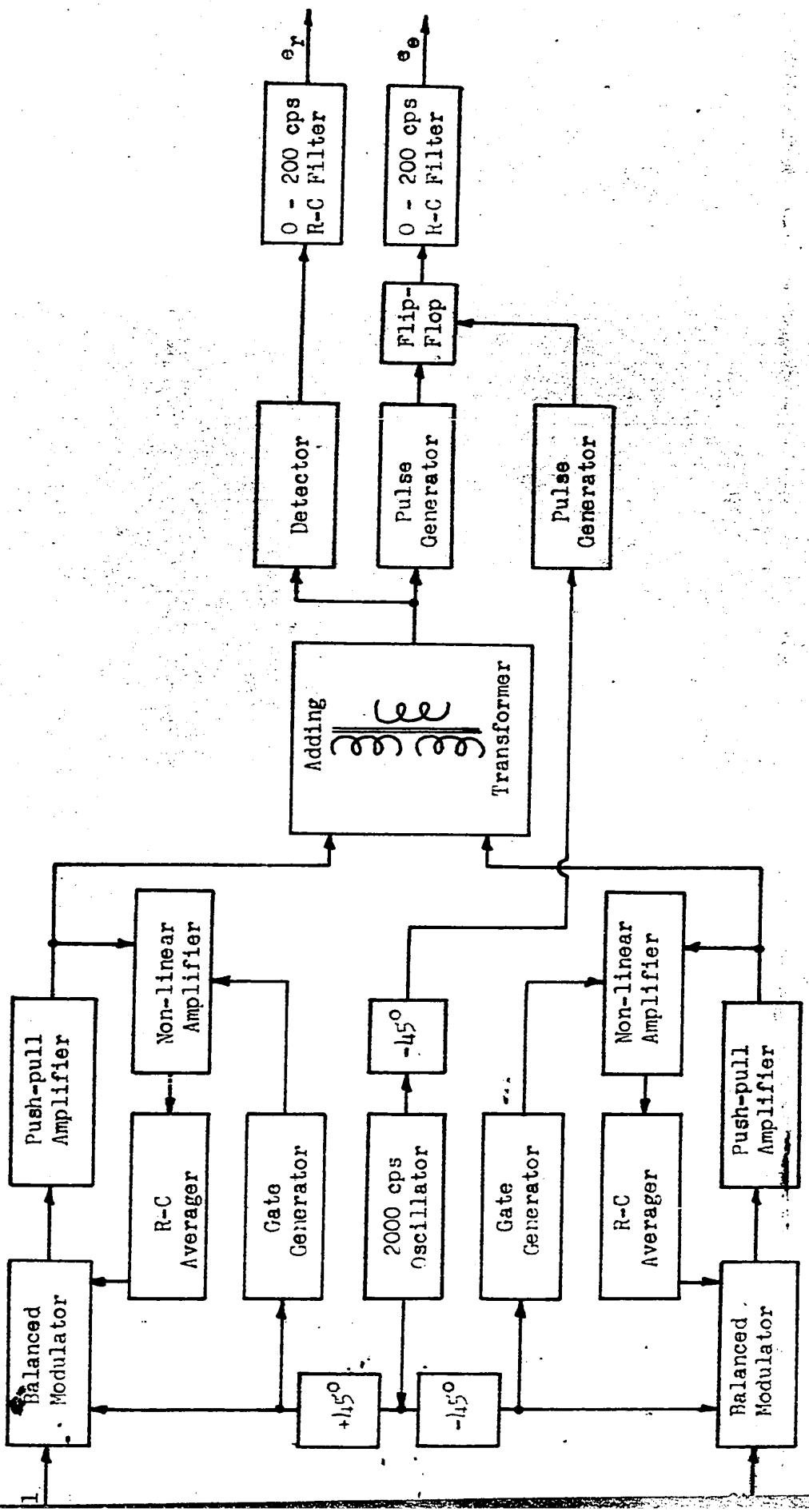

Figure 2.3

Detailed block diagram of McFee's computer.

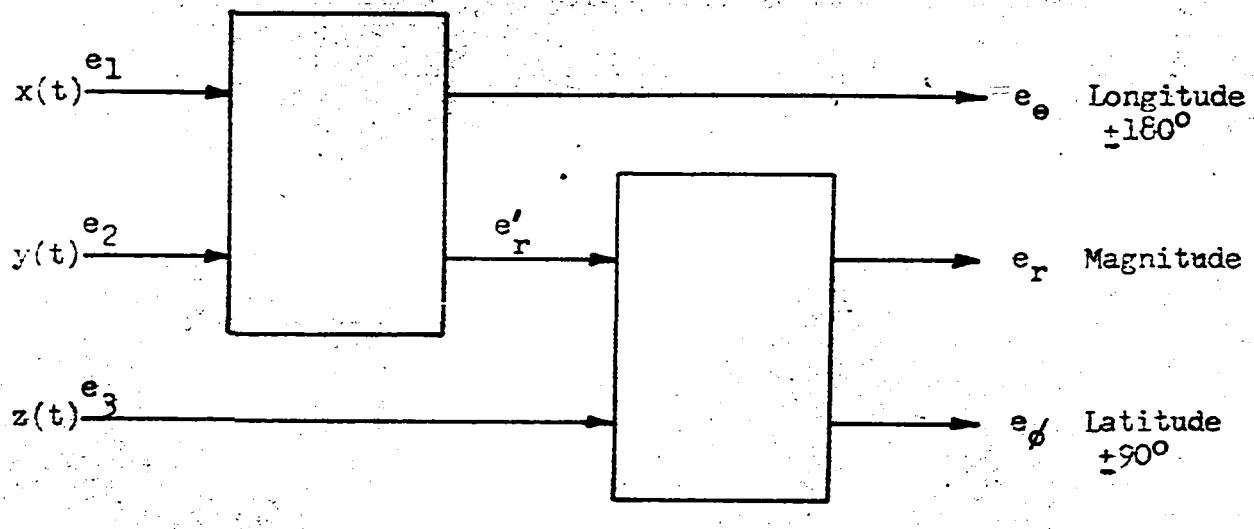

Figure 2.4

Interconnection of two computers to obtain spherical coordinate transformation

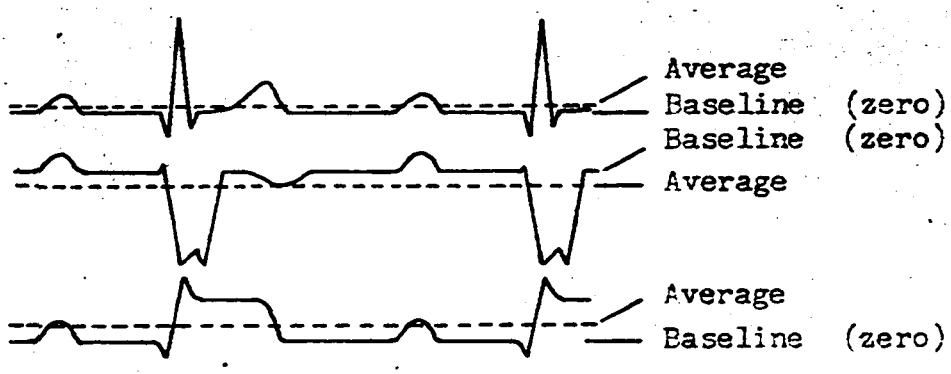

Figure 2.5

Baseline and average levels for various ECG signals

x(t), y(t) and z(t) components of the heart vector are zero[2]. In McFee's computer, a baseline clamper is provided to make the outputs of the modulators zero when the input signals are at their baseline level[3]. If the pickup electrodes are connected to an ac amplifier, the input to the modulator differs from zero by the difference between the baseline level and the average level. For the case of dc amplifiers, a non zero input to the modulators results from unbalanced electrolytic potential differences at the pick up electrodes (See also 20, p. 34).

Sayers - A Spatial Magnitude Electrocardiograph

Sayers (17) (1954) developed an electronic analog computer as an aid in studying the magnitude display of the heart vector[4]. Although the magnitude of the heart vector can be visualized from VCG displays, the VCG gives time as a parameter along the vector loop. Thus, the time sequencing of events in a heart cycle, especially around the origin of the VCG, is not as evident as in displays which are recorded as functions of ~~time~~ time, such as x(t), y(t) and z(t), the components of the heart vector. Also, due to the variation in writing rate of the VCG, a time scale adequate for the QRS interval, is inadequate for the remainder of the cycle. In addition

---

[2]In the VCG, the baseline corresponds to the origin of the vector loop.

[3]McFee suggests the use of such clampers for automatically centering VCG displays.

[4]Provision was also made for obtaining the ventricular gradient (12, 5.12) obtained by integrating, with respect to time, the magnitude function. The ventricular gradient has physical meaning as related to the total unbalanced charge developed in the body due to the electrical activity of the heart, that is, the polarization and depolarization phenomena. Ventricular gradient has meaning only when related to the electrical activity over the duration of a complete heart beat. There is some controversy as to the meaning and dimensions of the ventricular gradient (that is, volt-second or amp-second) resulting from conflict of opinion whether current or potential is the fundamental quantity recorded in an ECG.

to the loss of detail in the VCG around its origin, only one heart beat is recorded thus precluding the study of disturbances in the heart rate or rhythm. It is worthwhile to repeat that the origin of the VCG corresponds to the baseline of the ECG, that is, the resting potential or isoelectric interval. Displays recorded as a function of time are often referred to as linear or scalar cardiograms. Thus, to obtain a magnitude display as a function of time, Sayers developed a computer, the block diagram of which is reporduced in figure 2.6. The three input signals x(t), y(t) and z(t) are amplified, squared separately and then summed. The square root of the sum is then evaluated and recorded. The square root of the sum may also be integrated if required. Reference (17) describes the circuitry in detail.

Some comments about the squaring and square root circuits are appropriate. The squaring circuit (33, 34) makes use of the multiplication law

$$i_p = k_1 + k_2 e_{g1} + k_3 (e_{g1})^2 \qquad (2.5)$$

where i_p is the plate current and e_{g1} is grid signal of a vacuum tube. If a pentode is used and the input signal e_{in} is applied to the suppressor grid and a fraction of e_{in} is applied to the grid then the relation becomes

$$i_p = k e_{g1} e_{g3} \qquad (2.6)$$

where e_{g1} and e_{g3} are the voltages applied to the grid and suppressed grid respectively. Under the condition that a pair of pentodes sharing a common load is used, figure 2.7, the plate current is given by

$$i_p = k_1 + k_4 e_{in}^2 \qquad (2.7)$$

where the pentodes are driven push-pull to eliminate odd power terms. The circuit is tested and balanced by using a push-pull sine wave input so that

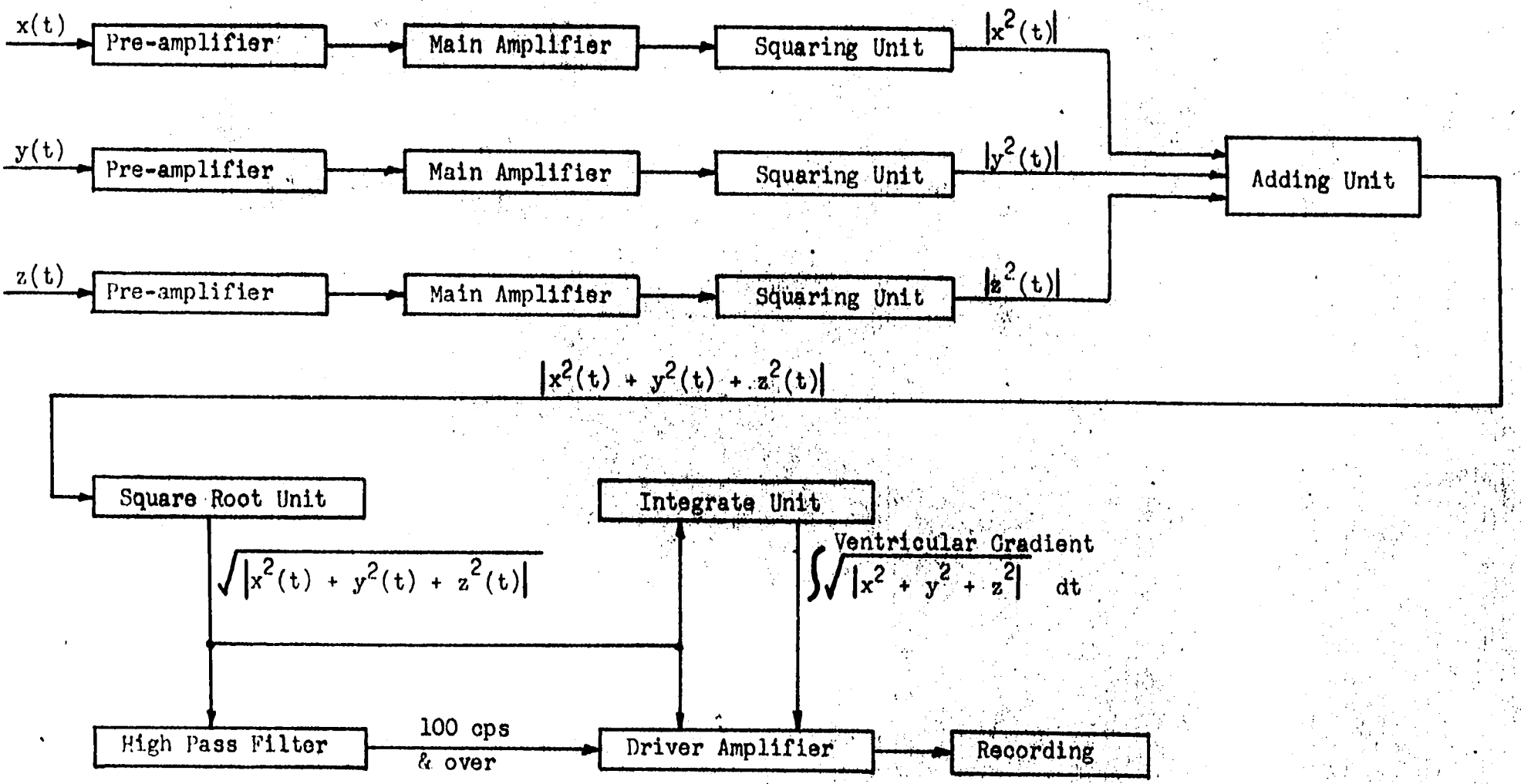

Figure 2.6

Block diagram of Sayers' computer
(see notes on following page)

Figure 2.6 (cont'd)

Notes:

Pre-amplifiers	- designed for high in-phase rejection ratio - use 6SU7 tubes in push-pull configuration (2 stages)
Main Amplifiers	- provided with fine gain control - use 6SL7 tubes in push-pull configuration (2 stages)
Squaring Unit	- push-pull fed - see figure 2.7 for circuit
Adding Unit	- triple input anode follower configuration - uses 6AC7 tube
Square Root Unit	- square root characteristic synthesized with multiple segments using diode network
Integrate Unit	- manually operated feedback amplifier - uses 6SL7 tube

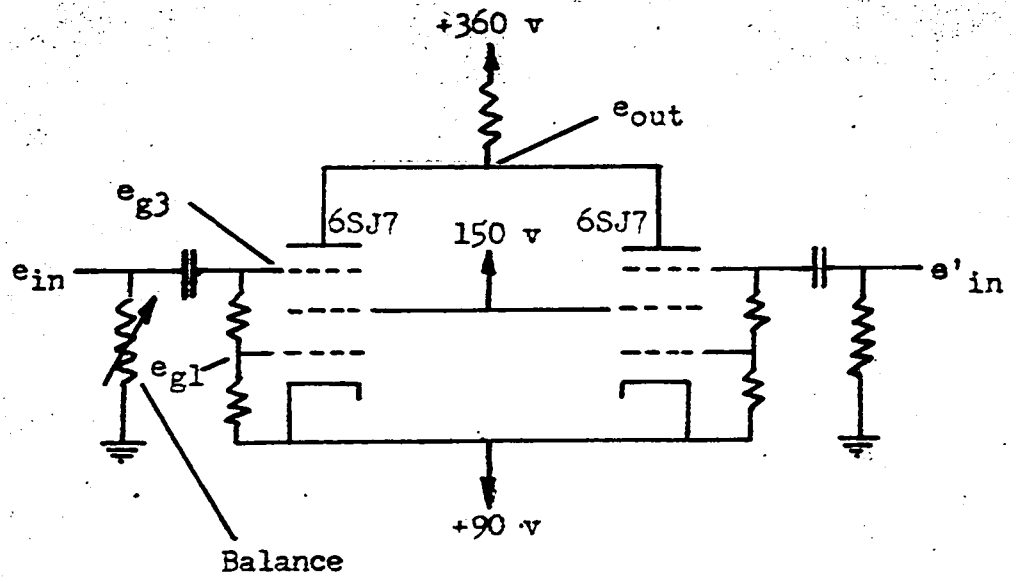

Figure 2.7

Squaring circuit used in Sayers' computer

the output, neglecting dc components, becomes a double frequency sine wave according to

$$\sin^2 wt = \tfrac{1}{2}(1 - \cos 2\,wt) \qquad (2.6)$$

The square root is obtained by generating a semi-parabolic input-output characteristic synthesized in segments by using a set of appropriately biased diodes connected in parallel. Only the positive portion of the input-output characteristic is required since the input is derived from a squaring process which always gives a positive output.

The accuracy of the instrument depends on the least accurate process in the computer. The squaring and square rooting operations are the least accurate, with square rooting being the most critical. The accuracy of the square rooting unit is a variable quantity since the desired characteristic is made up of a finite number of segments and since the higher the input signal is, the less percentage distortion it will suffer due to the fact that the slope of the square root curve decreases with increasing input signal. The input zero level must be carefully set as small errors in the zero setting can result in large output errors, especially for low signal levels. Sayers quotes an accuracy of the order of 10% for near maximum input signals with the accuracy decreasing considerably as the maximum usable signal level is reached, the accuracy being determined by the square rooting operation. He considers this sufficient when variations in the ECG due to the subjects attitude and respiration are taken into account.

The time constant of the apparatus is 0.2 sec and the upper frequency limit is 10 K cps. Sayers does not comment on problems regarding the difference between the ECG signal baseline (zero) and the average or dc component of the signal. The circuitry is ac coupled and it would thus

seem that the dc component has not been taken into consideration in generating the magnitude display.

Dower, Moore, Park, Poole and Yuan - A New Computer for Three-Dimensional Electrocardiography

A computer to effect a coordinate transformation from x, y, z to r θ, ϕ was developed (19, 20, 21)(1955) by the above mentioned group at the University of British Columbia. The initial stage of development (20) resulted in a two dimensional computer comparable to McFee's except for the manner in which the multiplication (modulation) was performed. Multiplication in McFee's computer was performed in a circuit using tubes with a single control grid and transformer coupling, that is, in a balanced modulator. The computer developed at the University of British Columbia used a multiplier designed around pentagrid tubes, that is, tubes with two control grids, and thereby eliminated the need for transformer coupling. The second stage of development (21) resulted in a three dimensional computer which achieves the cartesian to spherical coordinate transformation in a simpler manner than resorting to McFee's suggestion of combining a pair of two-dimensional computers. The resulting computer, the block diagram of which is shown in figure 2.8, is capable of an accuracy of approximately 5%. The computer input can readily be modified to operate from any four-electrode lead system.

Automatic calibration and stabilizing features were incorporated enabling unskilled personnel to operate the device. Clamping circuits ensure a zero output corresponding to the baseline or zero level which indicates the portion of the cycle during which the heart is electrically quiet. The clamping, or gated feedback circuit, attempts to compensate for interfering signals due to muscle movement, respiration, amplifier and multiplier drift, and the fact that the ECG signal has a dc component, by

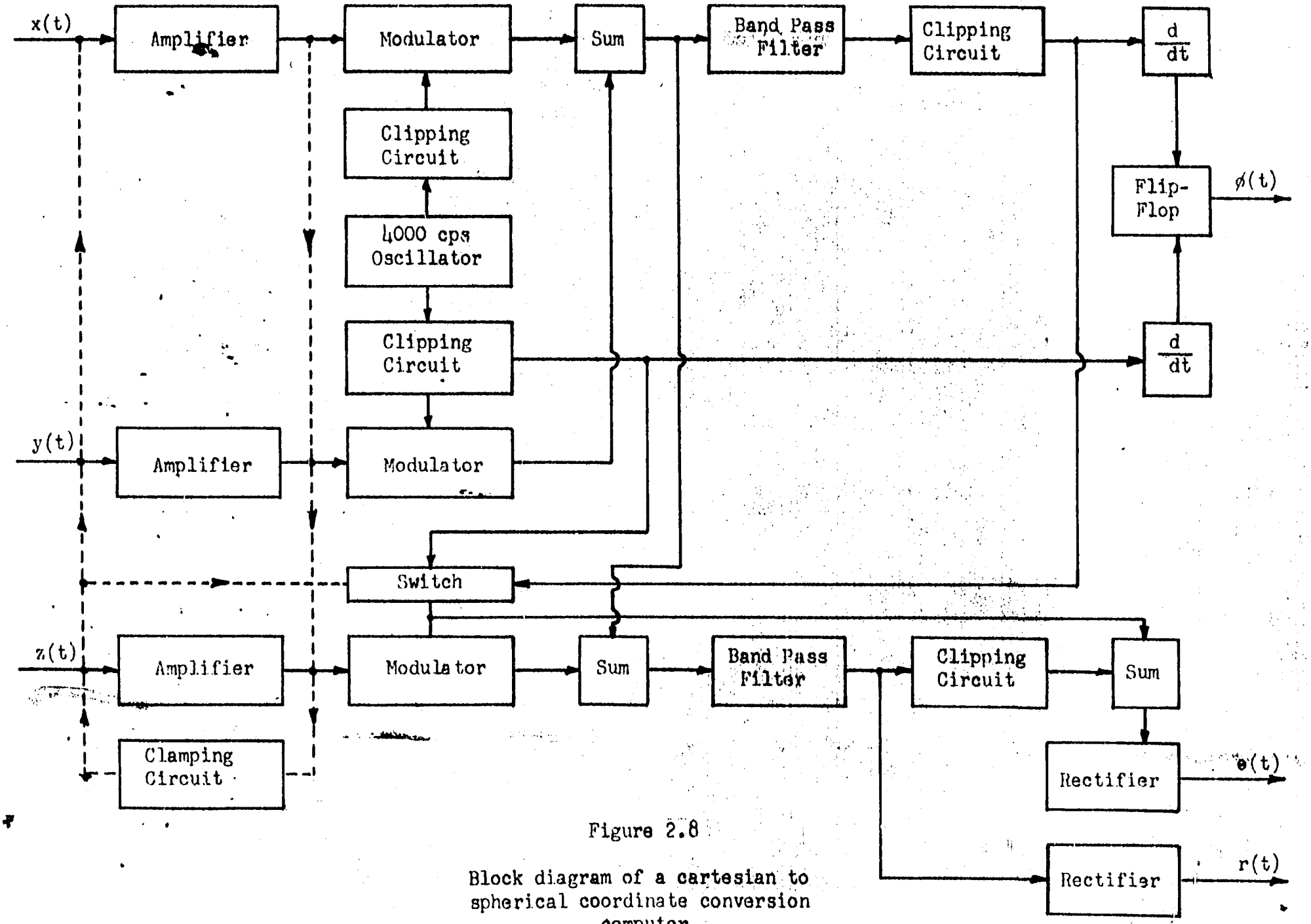

Figure 2.8

Block diagram of a cartesian to spherical coordinate conversion computer

automatically rebalancing the system once during each heart beat.

De Cote and Horwath - An Electronic Computer for Electrocardiography

De Cote and Horwath (35)(1956) developed a computer to evaluate a function of the form

$$\int_{t_1}^{t_2} \left[x^2(t) + y^2(t) + z^2(t)\right] dt \qquad (2.9)$$

using electronic data handling techniques. This integral is useful in the study of depolarization and repolarization of the myocardium (heart muscle tissue). The computation is tedious to perform, however, with the computer it is feasible to evaluate the integral for a volume of cases that would never be attempted manually.

A block diagram of this "cardiac vector integrator" is given in figure 2.9. Each of the three input signals is amplified and converted into a modulated pulse train, the pulse modulators being fed from a common free-running blocking oscillator to ensure proper time phasing for the three channels. The rectified output of the modulators is fed to the squaring circuit. The output of the three squaring circuits is summed in a summing amplifier and fed to an integration circuit.

The squaring circuit uses five diodes in a voltage divider circuit to obtain a six-line approximation to a parabolic response curve. It operates on each pulse individually to produce a new envelope whose amplitude is proportional to the square of the input waveform. The theoretical accuracy of the instrument as calculated for a triangular wave input signal of maximum operating amplitude is 3%, that is, the integral of the square of a triangular waveform will be within 3%. As the percentage accuracy of a squaring circuit increases for decreasing input voltages, 3% is the minimum error to be expected.

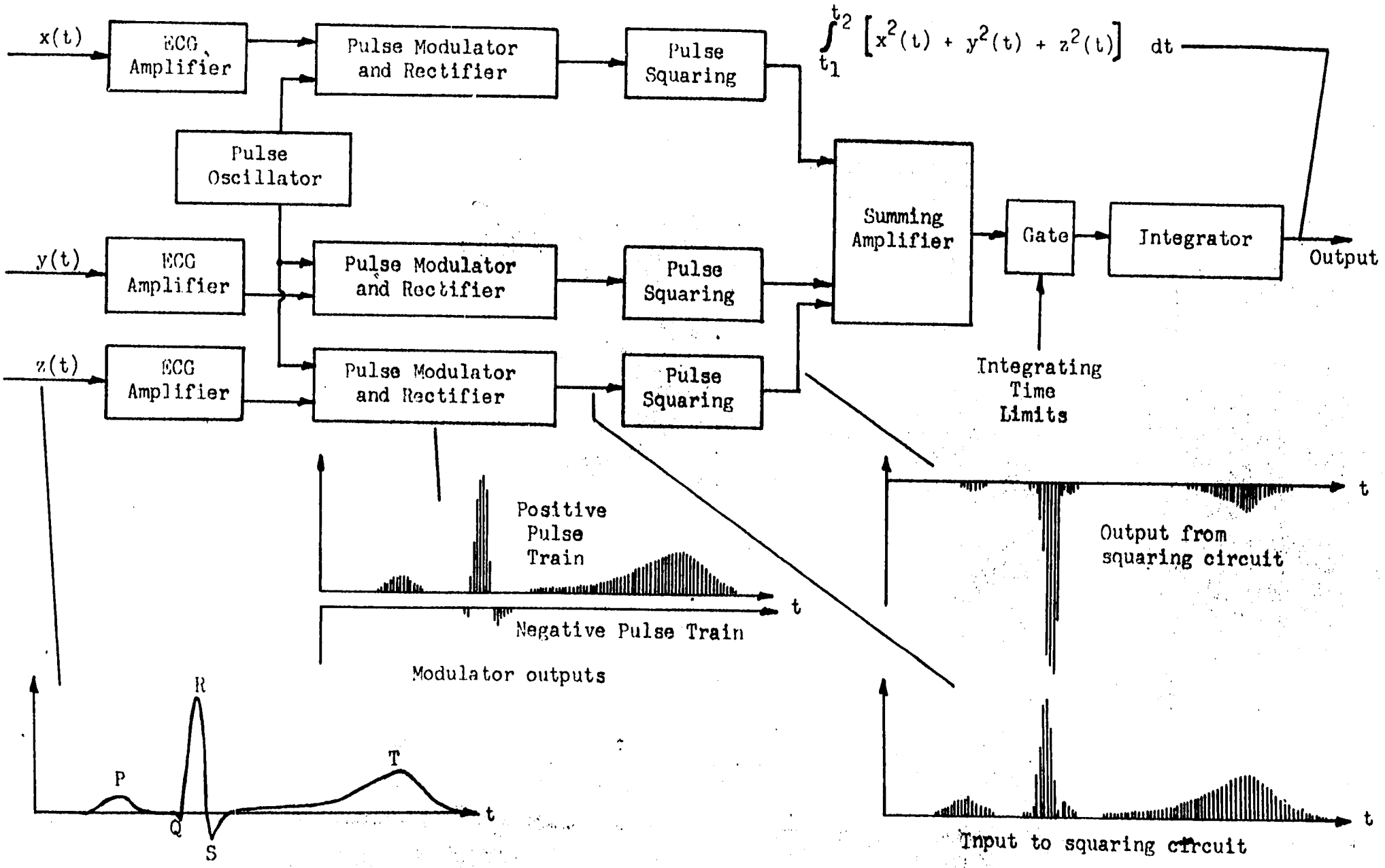

Typical ECG input signal

Figure 2.9

Block diagram of a computer designed to evaluate $\int_{t_1}^{t_2} [x^2(t) + y^2(t) + z^2(t)]\ dt$

McFee, Parungao and Mueller - An Electronic Coordinate Transformer for Electrocardiography

A computer to effect a coordinate transformation, or more properly, a coordinate rotation from x, y, z to x', y', z' was developed by McFee, Parungao and Mueller (22)(1961). To the author's knowledge, this is the most recent instrument developed to perform the coordinate rotation, the first instrument dating back to 1953 (36).[5] The rotation of coordinates represents another approach to the problem of eliminating apparent differences in electrocardiograms of normal subjects resulting from the orientation of the heart. McFee et al suggest that the problem of identifying diagnostic details obscured by waveform changes due to variations in heart orientation is analagous in some ways to the problem of detecting weak signals in noise.

The block diagram of the resolver is shown in figure 2.10, and the system has been designed according to the following equations.

$$\left.\begin{aligned} x' &= k(x \cos \theta - z \sin \theta) \\ y' &= k(y) \\ z' &= k(z \cos \theta + x \sin \theta) \end{aligned}\right\} \qquad (2.10)$$

$$\left.\begin{aligned} x'' &= k(x') \\ y'' &= k(y' \cos \phi - z' \sin \phi) \\ z'' &= k(z' \cos \phi + y' \sin \phi) \end{aligned}\right\} \quad -90^\circ \leq \phi \leq 90^\circ \qquad (2.11)$$

$$\left.\begin{aligned} x''' &= k(x'' \cos \delta - y'' \sin \delta) \\ y''' &= k(y'' \cos \delta + x'' \sin \delta) \\ z''' &= k(z'') \end{aligned}\right\} \qquad (2.12)$$

The θ, ϕ and δ knobs are adjusted appropriately to rotate the frame of reference to the desired new position x''', y''', z''' with respect to x, y, z by "minimizing" the output of one channel. The system has been designed around the sine-cosine potentiometers as indicated in figure 2.10.

---

[5] See also (37) for work reporting on coordinate rotation using a coordinate resolver of the Schmitt type.

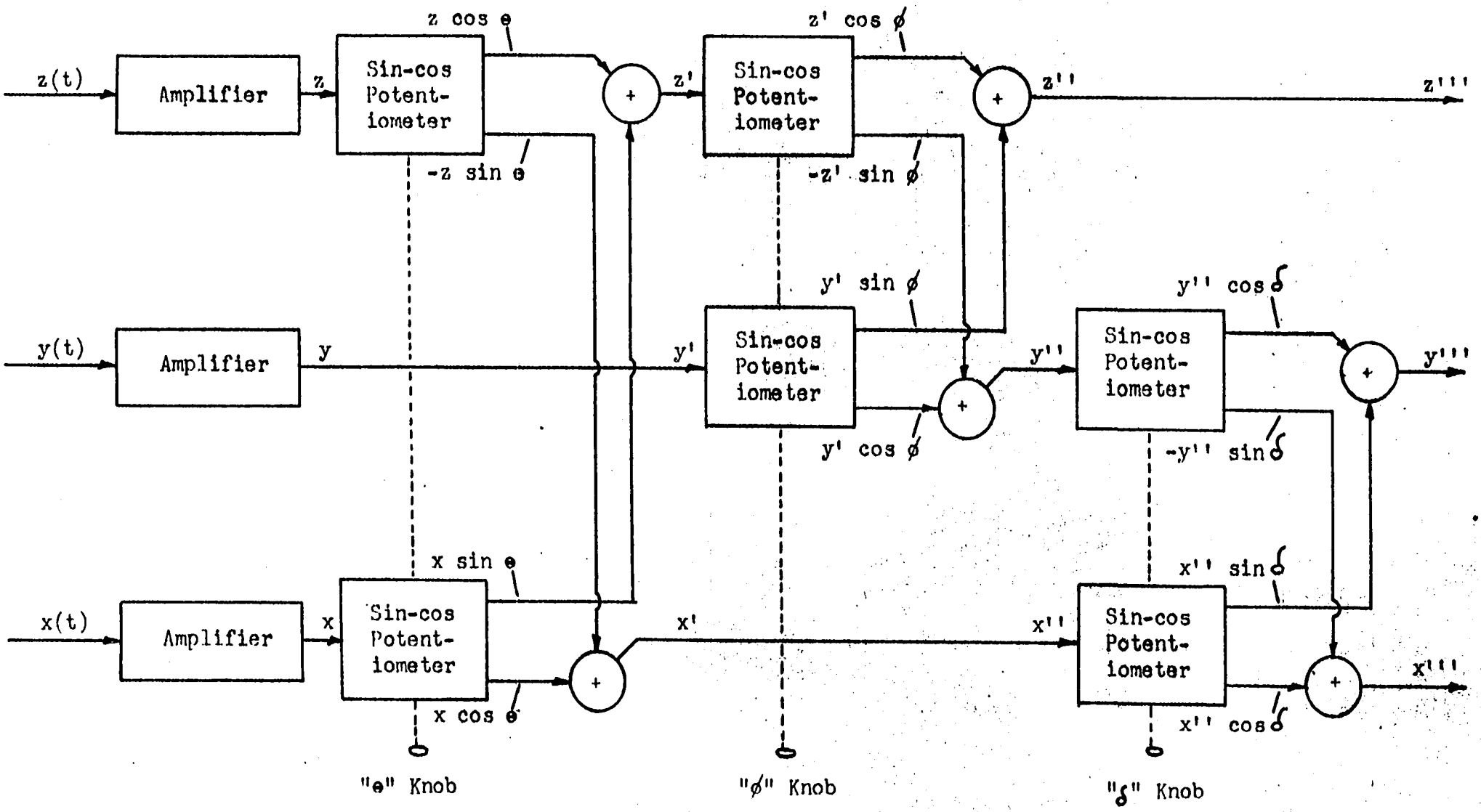

Figure 2.10

Block diagram of a computer designed to effect a coordinate rotation

Investigations Using Other Than Electronic Analog (or Digital) Computers

Abildskov, Ingerson and Hisey (36)(1956) were possibly the first group to report on clinical observations of the cartesian to spherical coordinate transformation. Following the work and suggestions of McFee (16), Frank (7), Mayer et al (17, 39), Abildskov et al recorded x(t), y(t) and z(t) simultaneously and calculated the spherical coordinate transformation, for 57 subjects, using an IBM card punch calculator. Figure 3.6 illustrates the coordinate convention and equations used. The recordings were taken using two methods of electrode placement, namely the equilateral tetrahedron system and a system based on the work of McFee and Johnston (40). Abildskov et al, in discussing and verifying the accuracy of their work regarding such items as the time phasing of the cartesian components, indicate that VCG loops constructed for the QRS interval using the calculated spherical components reporduced the actual VCG loops recorded with considerable precision. This comparison was possible only for the QRS interval due to the characteristic of VCG loops previously mentioned in that information near the origin is difficult to identify. Mention was made of the fact that when the magnitude curve was small in amplitude, the curves giving angular orientation information were somewhat unreliable. This was possibly due to slight baseline drift, in the original scalar cartesian recordings, which could influence the apparent angles significantly. Among other conclusions arrived at, Abildskov et al claim that features of clinical significance found in abnormal x(t), y(t), z(t) records were represented in easily recognizable form in the spherical coordinate transformation records.

It is of interest to note that Abildskov et al suggest other displays such as rate of change of magnitude and orientation and subjecting the derivatives of the cartesian components to the same manipulations used to

obtain the magnitude and orientation traces to obtain vector derivatives. Such analyses were not carried out by this group due to limitations inherent in taking derivatives of curves plotted from a limited number of points. However, the suggestion made was that the displays be obtained by appropriately processing (by computer) the cartesian components directly.

In spite of the significant contribution made by this group, they suggest considerable further study is required to establish the most significant measurements and methods of analysis for ECG signals.[6] In an attempt to give a partial numerical description of the spatial magnitude curve, Abilaskov et al measured the period of the QRS complex (between points 10% off maximum deflection), the kurtosis ratio (maximum amplitude/width), the skewness factor $\left(\frac{\text{rise time - fall time}}{\text{rise time + fall time}}\right)$, the areas of the QRS and T waves and their ratios, and in the magnitude curves which exhibited notches, the ratio of depth of notch to maximum amplitude.

Another investigation of interest was carried out by Hellerstein and Hamlin (41)(1960). Their investigation was concerned with a study of the QRS interval of the spatial vectorcardiogram, spatial magnitude and spatial velocity cardiograms of the normal dog, and the correlation of these displays with the scalar ECG, the cross-sectional anatomy of the heart and the activation process. In the initial study the magnitude and velocity were calculated from the x, y, z components of the heart vector as measured from the appropriate VCG. The magnitude curve was calculated using the relation

$$M = \sqrt{x^2 + y^2 + z^2} \qquad (2.13)$$

for each instant of time, See figure 2.11. The velocity curve, the

---

[6] A more general interpretation of this suggestion would point the way to quite different concepts in methods of analyzing ECG signals. The work on the application of signal analysis concepts to be discussed in Chapter 3 serves as an example.

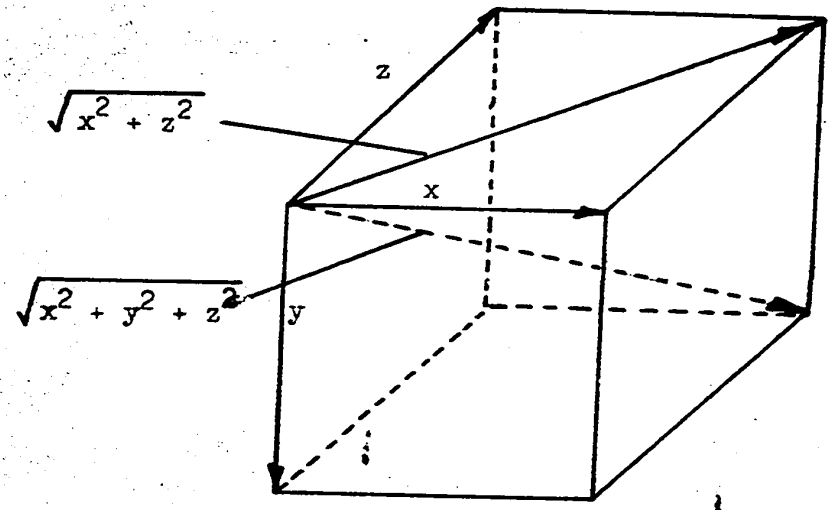

Figure 2.11

Magnitude of an instantaneous vector.

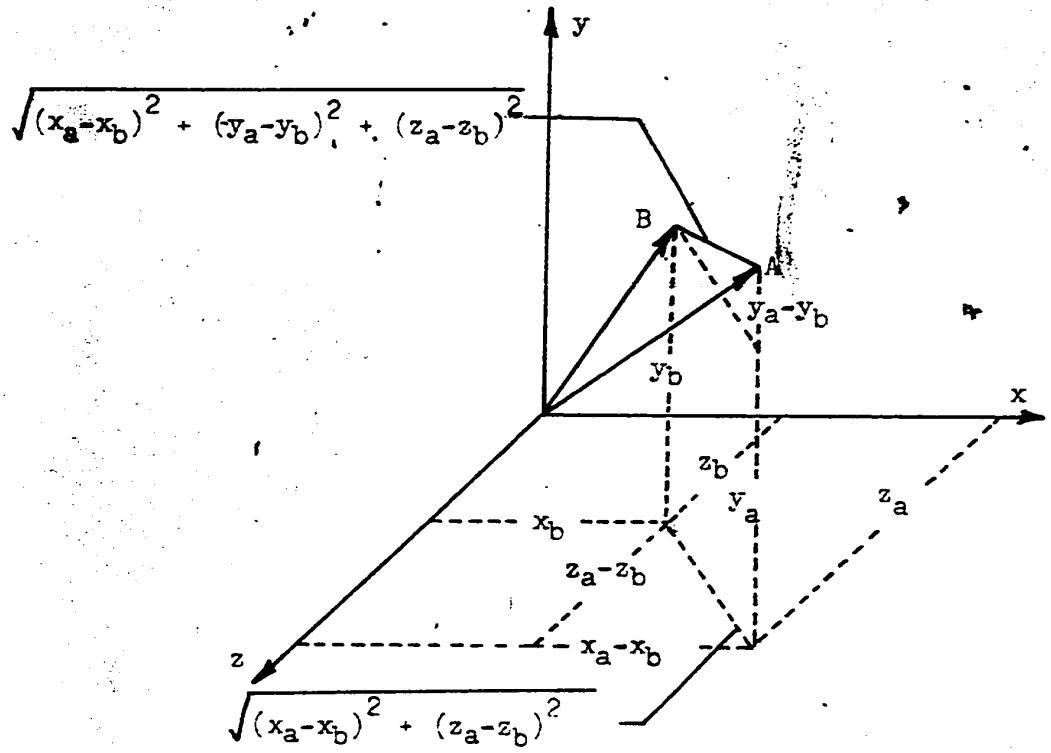

Figure 2.12

Velocity of spatial displacement per unit of time of two consecutive vectors.

spatial displacement between the termini of consecutive vectors per unit of time, was obtained by measuring the projection of the vectors formed by the termini of consecutive vectors on the three coordinate planes, figure 2.12, and evaluating

$$V = \sqrt{(x_a-x_b)^2 + (y_a-y_b)^2 + (z_a-z_b)^2} \qquad (2.14)$$

which is equivalent to

$$V = \sqrt{\left(\frac{dx}{dt}\right)^2 + \left(\frac{dy}{dt}\right)^2 + \left(\frac{dz}{dt}\right)^2} \qquad (2.15)$$

(x_a-x_b), $y_a-y_b)$ and (z_a-z_b) represent x, y and z or the change in x, y and z respectively per unit of time. Subsequent to the initial study an analog computer was constructed which performed the necessary functions for obtaining the magnitude and velocity curves electronically. Details of the computer are not given but an example of the magnitude and velocity curves, recorded simultaneously, was given (41, p. 1060).

CHAPTER 3

NOTATION AND COORDINATE SYSTEM CONVENTIONS IN ELECTROCARDIOGRAPHY AND VECTORCARDIOGRAPHY.

Summary

The following chapter discusses a number of points relating to the established convention and coordinate systems and to those presently in use by relatively restricted groups of investigators. The general techniques and methods of approach currently used in ECG and VCG research meet with good acceptance among the various investigators. Differences in details, the individual investigator likely being biased by his immediate research problem or equipment, however, at times makes it difficult to compare the results of different workers and creates confusion in that errors or misinterpretations are readily made. These differences arise primarily because of the somewhat varied notation and definition of coordinate systems in use. Advantages, disadvantages and comparisons are given in the following discussions where appropriate. Various criticisms are made and suggestions given in order to establish some degree of consistency in work that may follow. An effort has been made to incorporate suggestions and criticisms given in the literature.

In electrocardiography and vectorcardiography there is a lack of uniformity of notation as used by various authors. This tends to create confusion in that errors or misinterpretations are readily made. A discussion regarding coordinate system and notation is thus in order if consistency is to be maintained on this project. Suggestions made in subsequent paragraphs are recommendations for a standard convention for work at Ottawa General Hospital and University of Ottawa until such time as the conventions in the field of vectorcardiography are sufficiently well established and a standard orthogonal lead system is chosen. In regard to lead systems, the Frank lead system currently seems the best.

The usual point of departure is Einthoven's well established frontal plane convention in electrocardiography, Figure 1.2. This is the most firmly fixed convention and so cannot be changed. No one has questioned Einthoven's convention and historically, as well as practically, it would seem best not to. The advent of vectorcardiography has led to a collection of conventions similar in principle but somewhat varied with respect to details. Whether a cartesian, spherical, or other coordinate system is used, a higher degree of standardization of notation among investigators in this relatively new field of vectorcardiography would be desireable.

As already mentioned, the Frank system of electrode placement currently seems the best, since, of the lead systems proposed to date, it yields close agreement between spatial vectorcardiographic loops recorded directly and those reconstructed from temporal electrocardiograms (1, ~~302~~ 42, ~~303~~ 43). In this work, the Frank system will be used with the modification that Helm's suggestions (~~305~~ 44) will be followed with respect to the point of view taken for observing the frontal, transverse (horizontal) and sagittal

vectorcardiographic planes, and notation with respect to measuring angles in these planes, figures 3.3a and 3.3b.

Figure 3.1 shows the x, y, z coordinate reference axes as used by Frank (1, 42). This is a right handed cartesian coordinate system. The observers' position for viewing the vectorcardiographic planes, figure 3.2, however, does not correspond to that used in either of the two systems proposed by Helm.

Einthoven's convention requires a clockwise direction of rotation for a positive angle with the reference or zero degree axis corresponding to the (subject's) left end of the x axis, that is, lead I in Einthoven's equilateral triangle scheme. Helm made his proposals in order that Einthoven's frontal plane convention be retained in each of the 3 vectorcardiographic planes and so obtain a uniform convention for measuring angles on each of the 3 planes, keeping in mind, that trigonometric sign should be preserved. Helm's suggestions correct discrepancies in oscilloscopic views advocated and preferred by the Committee in Electrocardiography and Vectorcardiography of the American Heart Association and obtain symmetry of presentation (45).

TABLE 3.1

Observer's position for viewing vectorcardiographic planes
(Subject is assumed to be upright)

System / Vectorcardiographic plane	Frank Figure 3.1 and 3.2	Left Handed System Helm Figure 3.3a	Right Handed System Helm Figure 3.3b
Frontal xy	Front aspect of subject	front	front
Sagittal xy	Left aspect of subject	right	left
Transverse xz (Horizontal)	Superior aspect of subject	superior	inferior

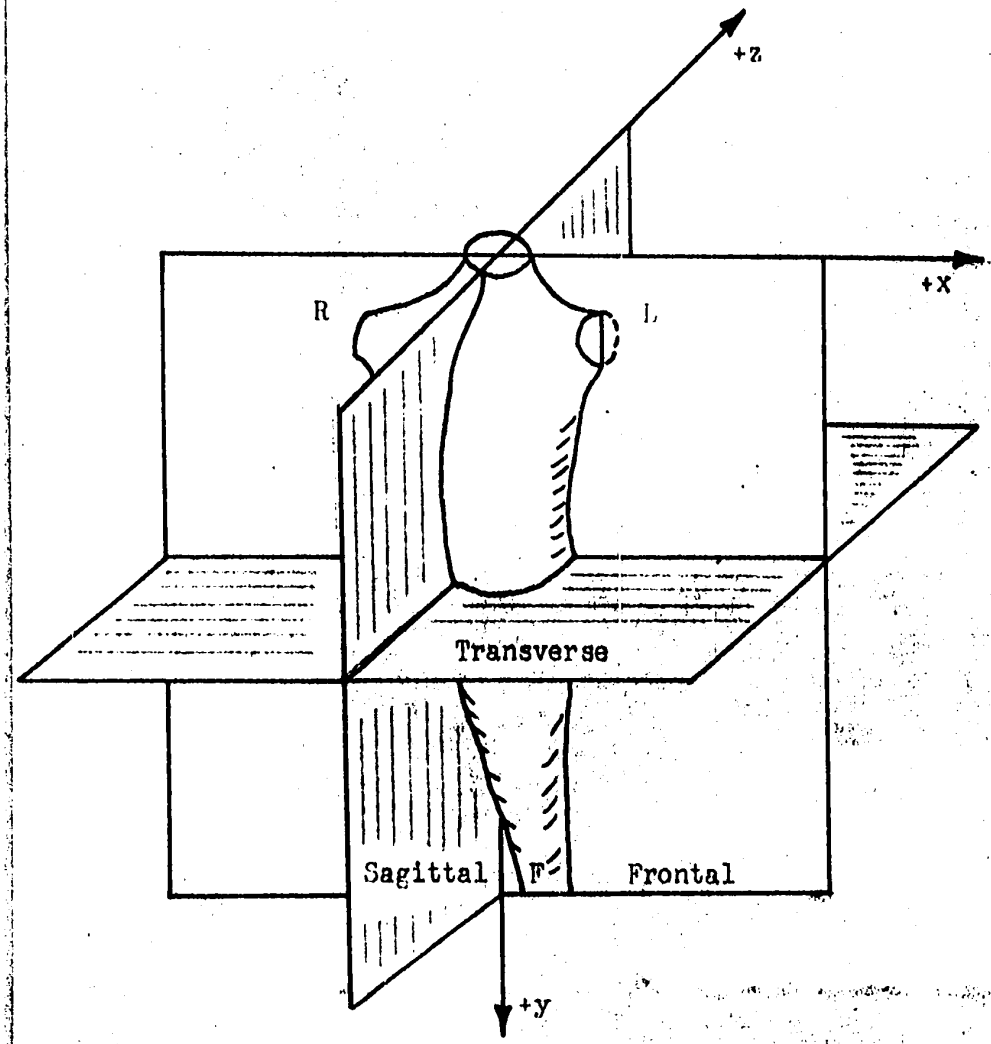

Figure 3.1

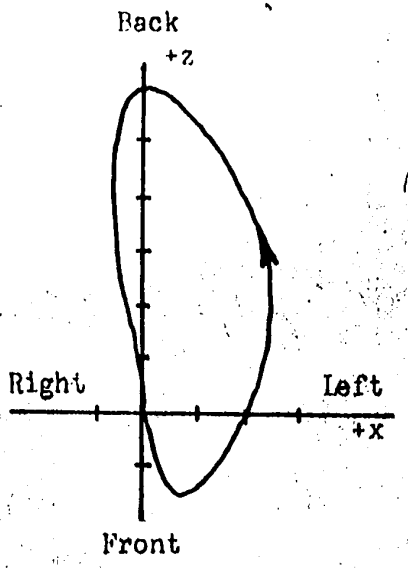

(Superior) Transverse Plane

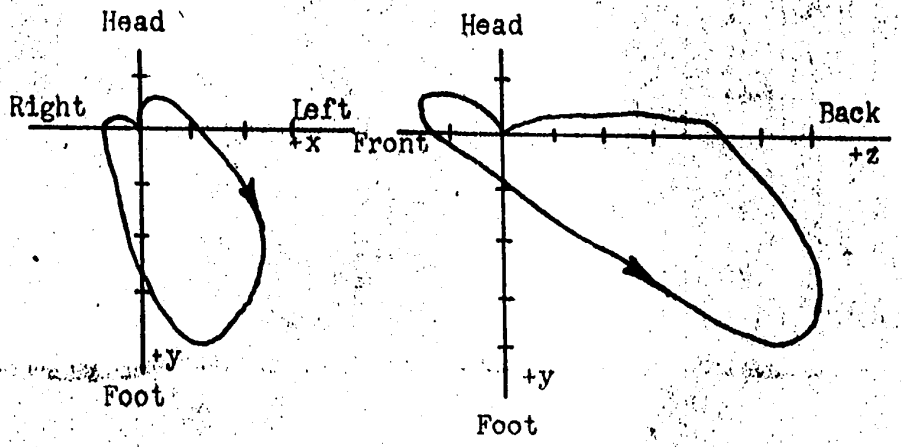

Frontal Plane (Left) Sagittal Plane

Figure 3.2

The system shown in figure 3.3a is left handed, the one shown in figure 3.3b is right handed. Since the Frank system of electrode placement is defined with respect to a right handed coordinate system, figure 3.1, and since a right handed system is conventionally used by engineers and scientists, it would seem reasonable to adopt the convention of figure 3.3b.

This suggestion, as seen by comparing columns 1 and 3 of Table 3.1, requires that the transverse (horizontal) plane viewed by Frank by observing the superior aspect of the upright subject, should instead be viewed by observing the inferior aspect of the upright subject. The positions taken by Frank to observe the xy and zy planes (frontal and sagittal planes respectively), correspond to those taken by Helm in the system of figure 3.3b.

It should perhaps be emphasized that a right handed system is convenient from the point of view that initial consultations with persons not associated with some aspect of cardiology, will not suffer from errors arising from the seemingly similar conventions, a closer inspection of which will show they are in fact somewhat dissimilar.

It is appropriate to mention at this point that confusion often arises when the term "horizontal plane" is used in referring to the xz or transverse plane since the subject may be in an upright, prone or supine position. "Sagittal plane" can be misleading unless qualified by "left" or "right". Often, upon inspecting the definition of the reference system used in a particular publication, one finds that the information given is incomplete, and inappropriately or insufficiently specified. Figure 3.4 shows one example where the definition of angles in spherical coordinates is unclear unless the figure is carefully studied.

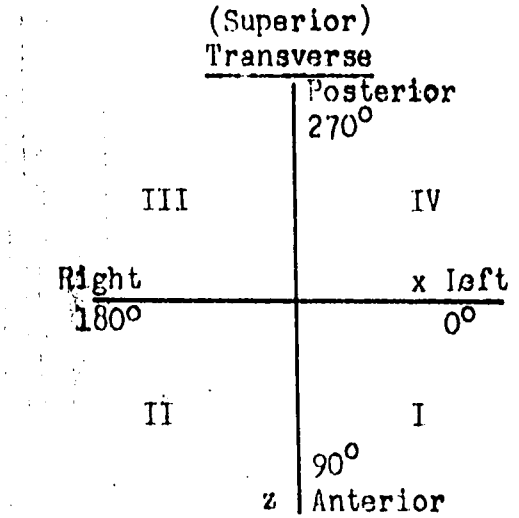

xz Plane
(Horizontal)

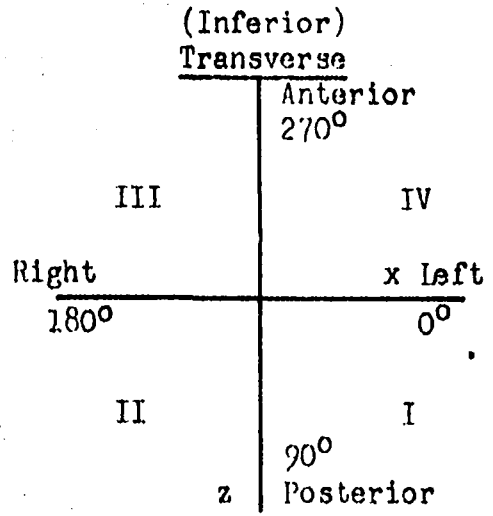

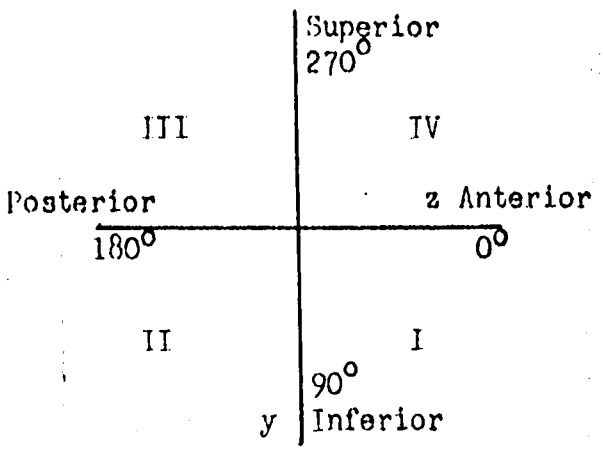

zy Plane

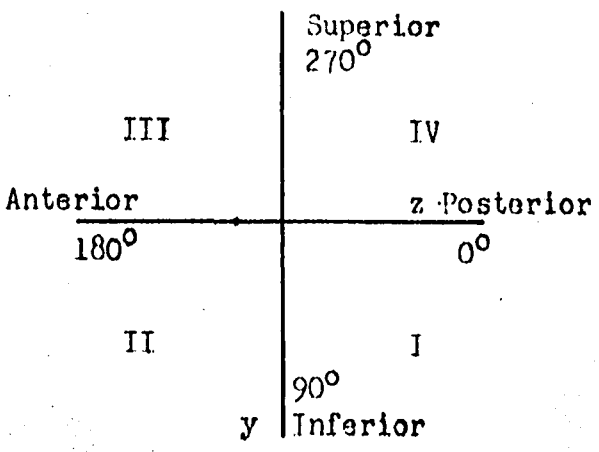

As mentioned previously, Einthoven's frontal plane is the usual point of departure in discussions on notation in electrocardiography. In vectorcardiography, Einthoven's convention in the frontal or xy plane is retained and the definition of the direction of the z axis gives rise to the left (z anterior) or right (z posterior) handed system. Thus, uniformity in defining the z axis must be established. Nonuniformity in conventions is also evident in spherical coordinate systems recently introduced in the literature. A review of the notation used by Dower et al (~~3.7~~ 19), figure 3.5, Abildskov et al (~~3.8~~ 38), figure 3.6, Brinberg (26), Pipberger (12), figure 3.7, and figure 3.8 (1, p. 96, figure 7.3) will illustrate this statement. (see also figure A.3 in the Appendix).

Dower et al, and Abildskov et al, in their work on cartesian to spherical coordinate transformations, have used a right handed system. However, their definition of azimuth ϕ, and elevation θ, differs from that of Brinberg, and Pipberger. A check of figure 3.8 shows the system illustrated to be left handed, assuming +x, +y and +z are left, down, and anterior respectively as implied by the reference lines from which the angles are measured in the frontal, horizontal (transverse) and sagittal planes.

Abildskov et al take the xy frontal plane as corresponding to the equatorial plane of a sphere in which the azimuth (longitude) angle is measured. Elevation (latitude) is the angle measured with respect to the equatorial plane (complement of the angle to the z axis in this case). Dower et al follow a similar convention except in taking a polar or colatitude angle in place of a latitude angle.[1] This definition of angles

---

[1] See Appendix for definition of spherical coordinate and spherical polar coordinates.

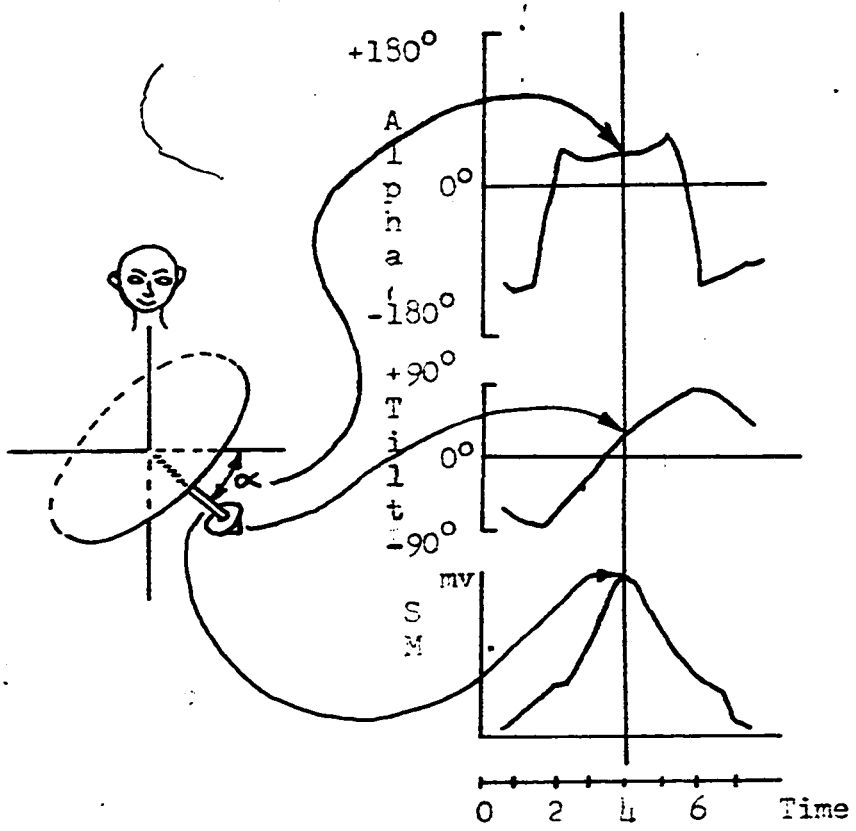

Figure 3.4

Vector shown is in posterior hemisphere
at t = 4

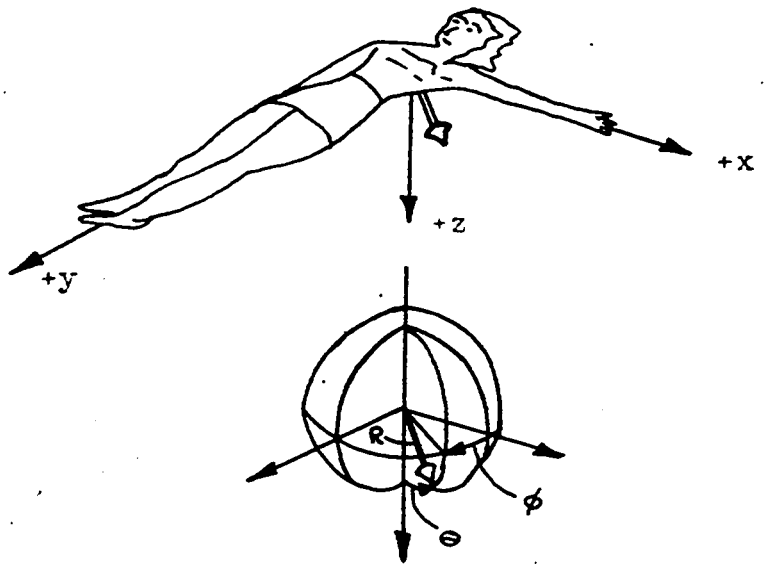

Figure 3.5

Vector shown is in posterior hemisphere

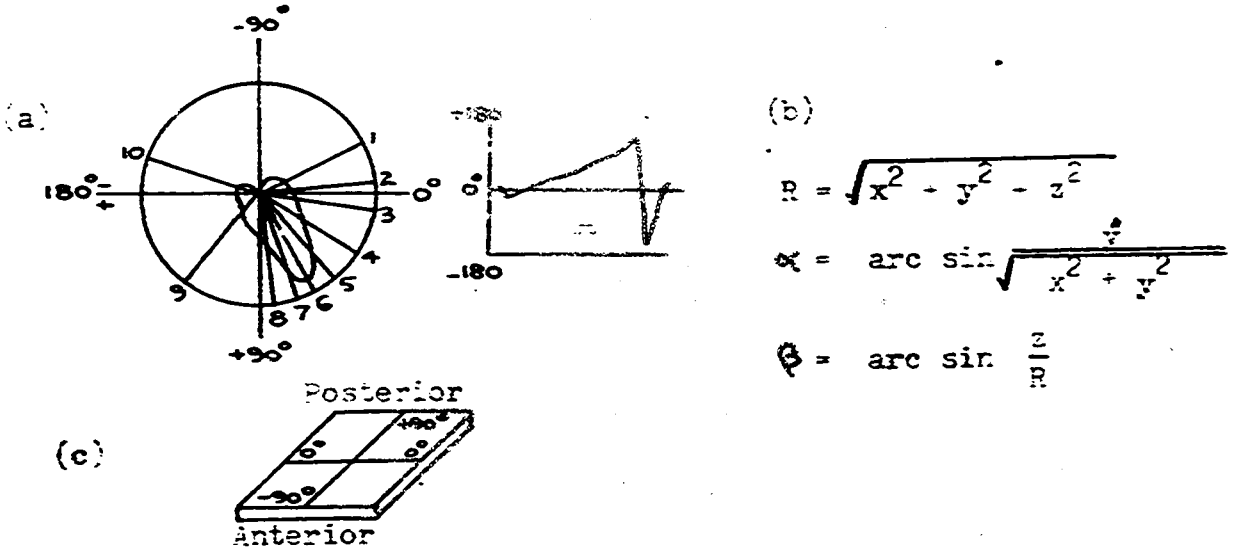

Figure 3.6

Scales employed to indicate orientation of vectors

(a) A diagrammatic frontal plane projection of a QRS loop at the center of a circle in which the angular scale is illustrated. Ten points at equal time intervals illustrate the changing orientation of vectors during ventricular depolarization.

(b) These ten points are plotted with time on the abscissa and an angular scale of -180° to $+180^{\circ}$ on the ordinate. With this angular scale $+180^{\circ}$ and -180° represent the same point, so that a linear time-scale plot contains an instantaneous "step" between the two values.

(c) The method of representing angles about an anteroposterior axis is illustrated. Vectors directed posteriorly lie between 0° and $+90^{\circ}$ while those directed anteriorly lie between 0° and -90°.

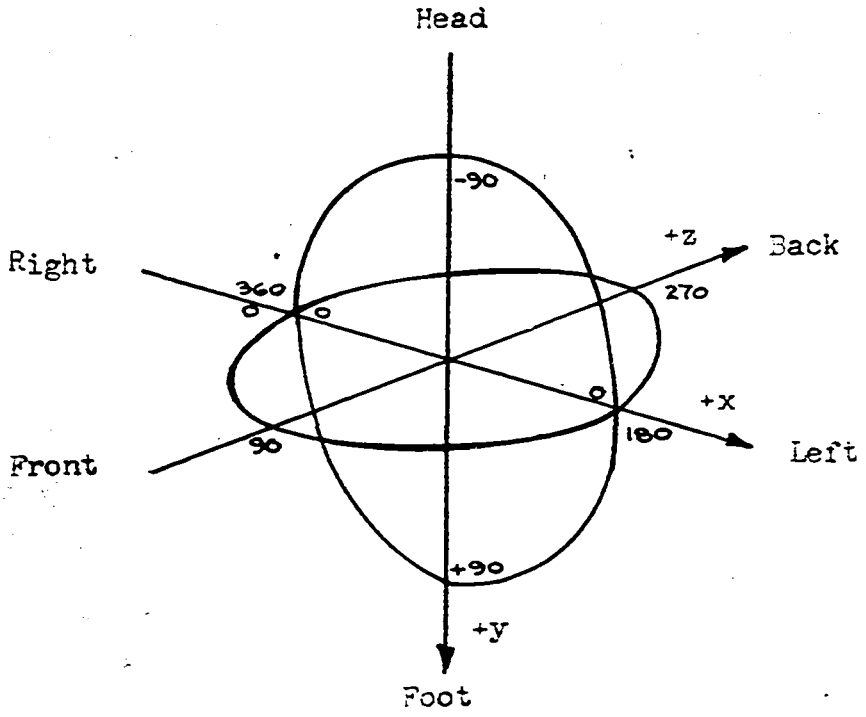

Figure 3.7

On the azimuth scale, 90° indicates the subject's front, 180° his left side, 270° the back, and 360° his right side. Positive values on the elevation scale are below and negative values above the equator.

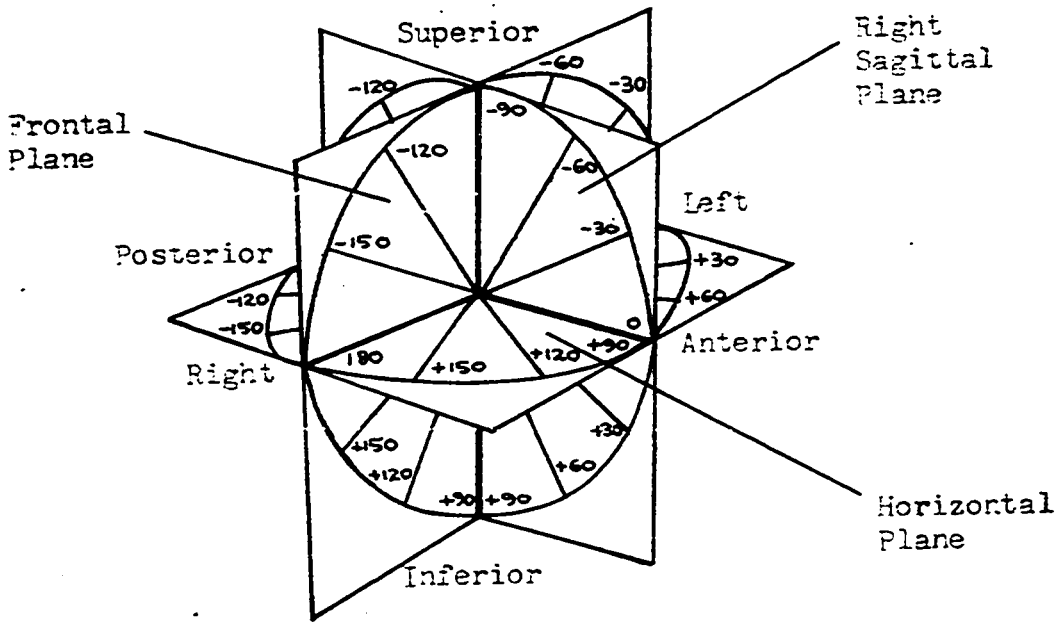

Figure 3.8

Reference frames for the horizontal, right sagittal, and frontal projections of vectorcardiographic loops. The three planar reference frames are depicted as if viewed from the right anterior. Note that the 0° axis is situated to the left in the horizontal and frontal reference frames and anteriorly in the right sagittal plane.

is taken so that the azimuth angle corresponds to Einthoven's definition of frontal angle α. Brinberg and Pipberger, however, were apparently not concerned with retention of the frontal angle α established by Einthoven since they take the xz transverse (horizontal) plane as corresponding to the equatorial plane in which to measure the azimuth (longitude) angle. Elevation (latitude) is then measured with respect to the xz transverse plane (complement of the angle to the y axis). For measuring azimuth, Pipberger, figure 3.7, uses 0° to indicate the subject's right side corresponding to the negative x axis. Normally, one would use 0° to indicate the subject's left side corresponding to the positive x axis.

Finally, it is worthwhile to mention that when reading Brinberg's text, one should keep in mind the distinction between plane trigonometry and spherical trigonometry. In the transformation of the cartesian coordinates of a heart vector to spherical coordinates or spherical polar coordinates, all definitions and calculations are based on plane trigonometry. Brinberg has occasion to measure the distance between two points on the surface of a sphere, joined by a great circle, (spherical distance) in terms of angular measure. The position of the two points, corresponding to two instantaneous heart vector positions, are specified and referred to in terms of longitude and latitude. The longitude and latitude of the two instantaneous heart vector positions can be calculated from cartesian coordinate positions by means of plane trigonometry. However, the measurement made by Brinberg on the surface of the sphere is based on the principles of spherical trigonometry (~~3.10~~ 46).

CHAPTER 4

PROPOSAL FOR A GENERALIZED ELECTRONIC ANALOG COMPUTER FOR ECG AND VCG CLINICAL RESEARCH

Summary

The following chapter[1] shows some block diagrams for the interconnection of electronic analog computer components to form a generalized analog computer capable of obtaining various displays of interest. The term generalized analog computer is meant to refer to an assembly of commercially available electronic components supplied in sufficient number and type and with suitable balancing, calibration, and programming features to enable the desired displays to be obtained. As suggested in Chapter 1, the computer would fit between the preamplifiers connected to the lead system and real time recorders. A discussion of some of the problems re effecting the technically more difficult analog operations, such as differentiation, squaring, square rooting, and multiplication of two time varying functions, with a sufficient degree of accuracy and at reasonable cost, is also included. The operations of summing, subtracting, multiplication by a constant, etc. will not be discussed since these operations are achieved relatively simply and inexpensively and are sufficiently well described in texts on analog computation.

Magnitude and Linear Velocity

The block diagram for obtaining the magnitude curve $|\underline{r}(t)|$ and the rate of change of magnitude $\frac{d|\underline{r}(t)|}{dt}$ is given in figure 4.1, where x(t), y(t) and z(t) are the input signals from an orthogonal lead system. The input amplifiers would provide sufficient gain to amplify x(t), y(t) and z(t) to the appropriate level for the squaring circuit input. The squaring circuits must be capable of accepting positive and negative amplitudes with respect to the ECG signal baseline and produce an output signal proportional to the square of the input. The outputs of the squaring circuits are then added by a three input adder and the sum fed to a square root circuit, the outputs of which yields the magnitude curve $|\underline{r}(t)|$. By providing a differentiator, the rate of change of magnitude could be obtained. Referring to Chapter 7, figure 12, the curve of $\frac{d|\underline{r}(t)|}{dt}$, obtained using a digital computer, exhibits a rise time of the order of 2 milliseconds. Applying the emperical law (47)

$$\text{Bandwidth} \times \text{Rise time} = 0.35 \text{ to } 0.45 \qquad (4.1)$$

gives an indication of the frequency response required of the analog components. A 2 millisecond rise time indicates that a bandwidth of at least 175 cps is required to ensure the presence of the higher frequency components of the $\frac{d|\underline{r}(t)|}{dt}$ waveform. Inspection of figures 1 to 3 in Chapter 7 indicates that the fastest rise time in x(t), y(t) or z(t) is of the order of 4 millisecond, which corresponds to a bandwidth of approximately 90 cps.

The block diagram of figure 4.1 can be modified by inserting analog differentiators at points a, b and c to yield figure 4.2, thereby permitting the linear velocity curve $|\underline{v}(t)|$ and component velocities $v_x(t)$, $v_y(t)$ and $v_z(t)$ to be recorded. To effect this modification, consideration

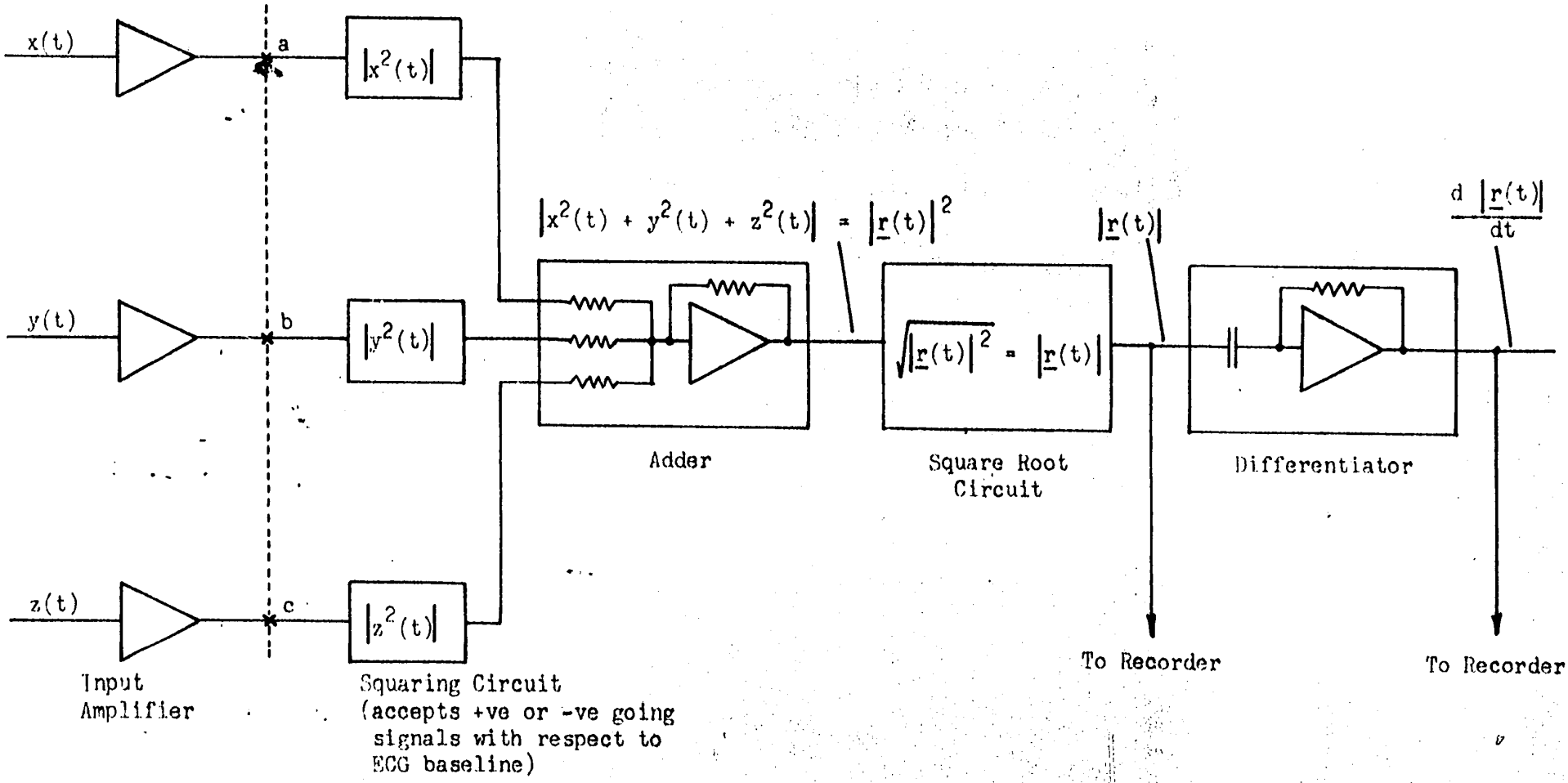

Figure 4.1

Block diagram for magnitude and rate of change of magnitude computer

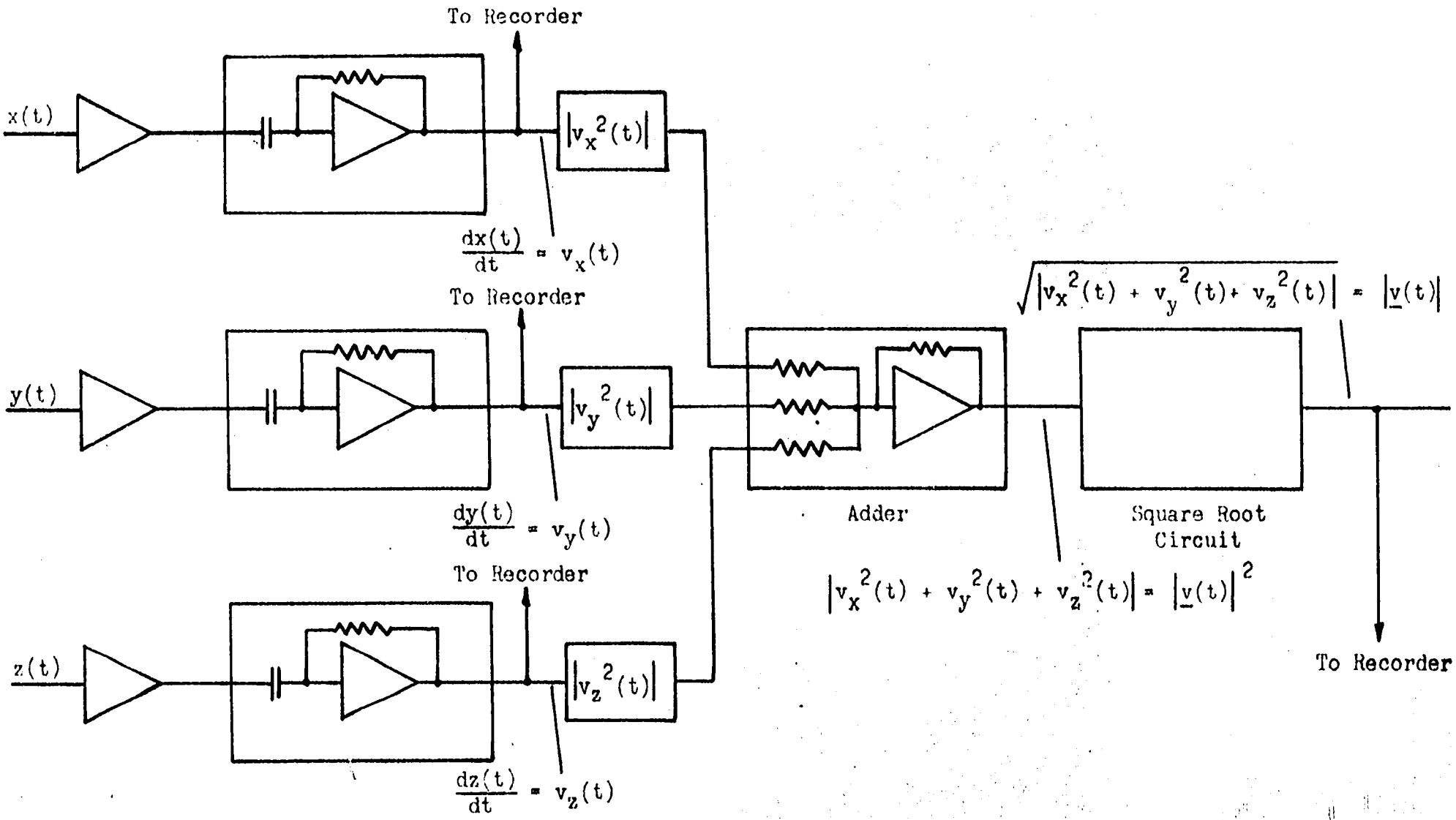

Figure 4.2

Block diagram for linear velocity computer

would have to be given to adjusting the gain of the input amplifier and/or ensuring the differentiator output provides sufficient signal amplitude for the squaring circuit. Figures 4.1 and 4.2 indicate how a collection of 3 amplifiers, 3 squaring devices, 1 adder, 1 square rooting device and 3 differentiators could be interconnected into two different systems to yield a number of displays.

Cartesian to Spherical Coordinate Transformation

In establishing cartesian to polar coordinate transformations, the equations

$$r = \sqrt{x^2 + y^2} \qquad (4.2)$$

$$\theta = \arctan \frac{x}{y} \qquad (4.3)$$

could be established directly on an analog computer. However, r and θ are more conveniently obtained by the implicit solution of the equations

$$-x \cos \theta + y \cos \theta = 0 \qquad (4.4)$$

$$x \cos \theta + y \sin \theta = r \qquad (4.5)$$

which are equivalent (48, p. 336) to the transformation equations (4.2) and (4.3). The direct solution of (4.3) by approximating the inverse trigonometric function by a series approximation leads to loss of accuracy. Implicit solution allows feedback techniques to be used and thereby the possibility of obtaining better accuracy.[2] However, (4.4) and (4.5) could involve the computation of a small difference of two large terms so the possibility of large percentage errors should be considered.

A completely electronic cartesian to polar coordinate converting system

---

[2]Accuracies attainable with vector servo electromechanical devices are of the order of ½ to 1% in amplitude of the radius vector r and 0.5° in angle.

(4.9) is shown in figure 4.4. Such a system avoids the use of electromechanical resolvers which have limited bandwidth. The system is based on the equations[3]

$$r = x_1 \cos \alpha - y_1 \sin \alpha \qquad (4.6)$$

$$0 = x_1 \sin \alpha - y_1 \cos \alpha \qquad (4.7)$$

Figure 4.3 shows the coordinate system. Referring to figure 4.4, the conversion is achieved by multiplying x_1 and $-y_1$ by the two outputs of a circuit loop which generates the appropriate trigonometric functions. Both products are then combined and applied to a high gain amplifier. A portion of the output of the amplifier is integrated to yield a voltage proportional to the angle α. Another portion of the output of the amplifier is applied at two points to the trigonometric function generating loop. At one point in the loop, the amplifier output is multiplied by the output of a phase inverting amplifier and the resulting product is integrated to yield a voltage proportional to $\cos \alpha$. The voltage proportional to $\cos \alpha$ is one of the loop outputs and is used to multiply $-y_1$. This voltage is also used to multiply the voltage applied to the loop at the second of the two input points. This latter product voltage is integrated and applied to the phase reversing amplifier output from which the second circuit loop output voltage proportional to $\sin \alpha$ is obtained. The voltage proportional to $\sin \alpha$ is used to multiply x_1.

To understand the operation of the circuit loop of figure 4.5, assume that the output of the phase inverter is proportional to $\frac{d^2y}{d\alpha^2}$ and so the loop equation is

$$-y = \frac{d^2y}{d\alpha^2} \qquad (4.8$$

---

[3](4.6) is equivalent to $r = x_1\left(\frac{x_1}{r}\right) + y_1\left(\frac{y_1}{r}\right) = \frac{r^2}{r}$. To obtain equation (4.7), multiply $x_1 = r \cos \alpha$ and $y_1 = r \sin \alpha$ by $\sin \alpha$ and $-\cos \alpha$ respectively and add to get $x_1 \sin \alpha - y_1 \cos \alpha = x_1\left(\frac{y_1}{r}\right) - y_1\left(\frac{x_1}{r}\right) = 0$

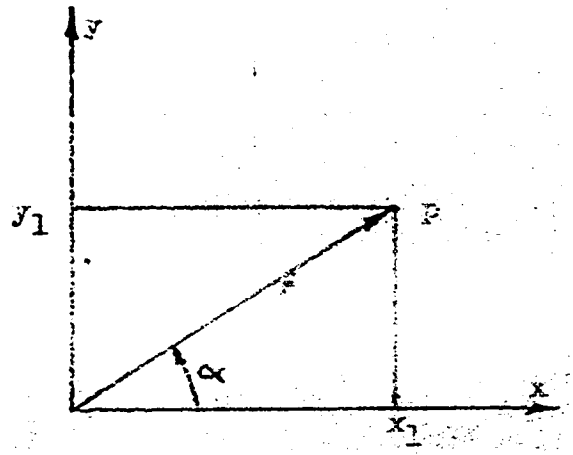

Figure 4.3

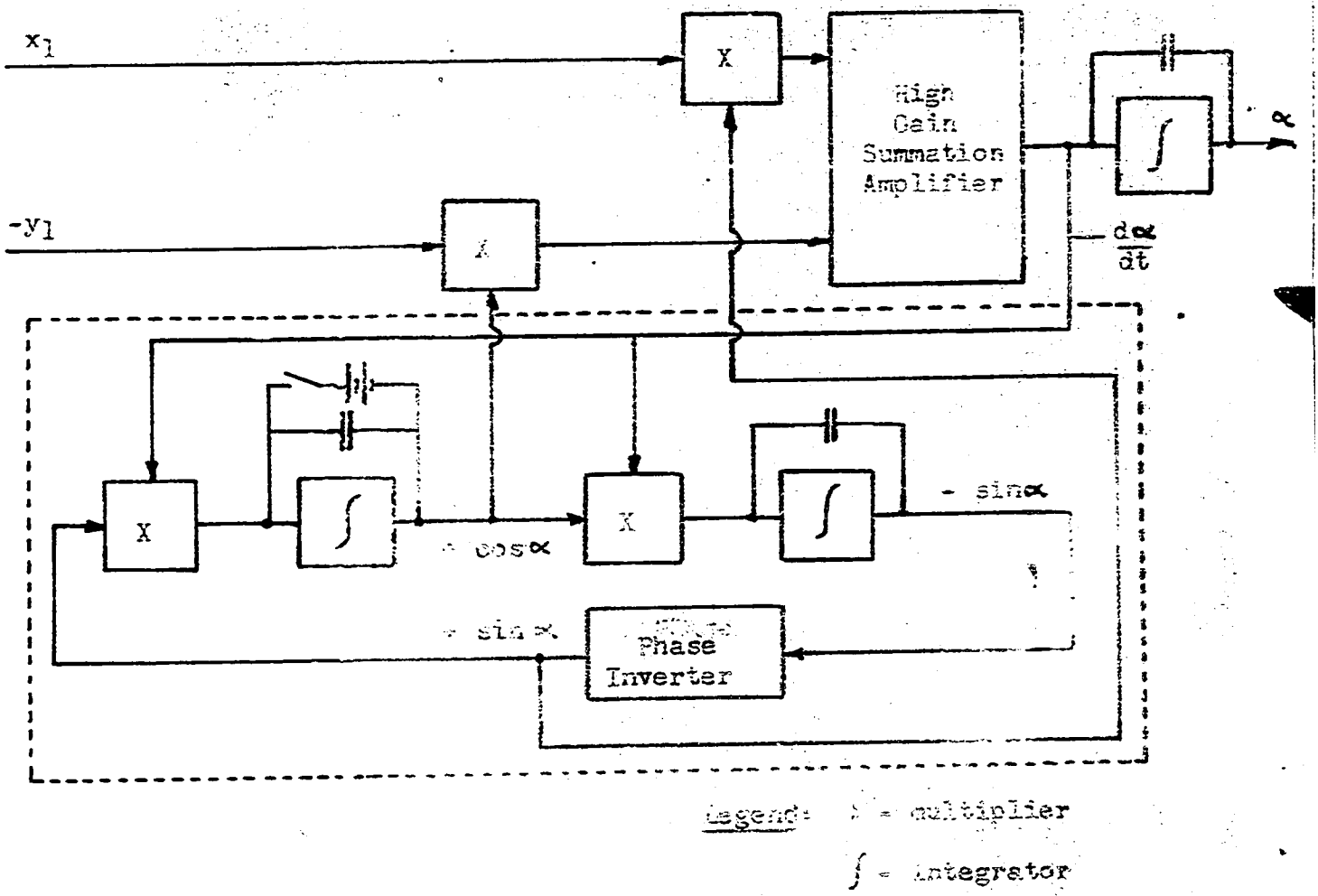

Figure 4.4

Solution of the equation $x_1 \sin\alpha - y_1 \cos\alpha = 0$
See figure 4.5 for further details re circuit loop enclosed by the dotted line.

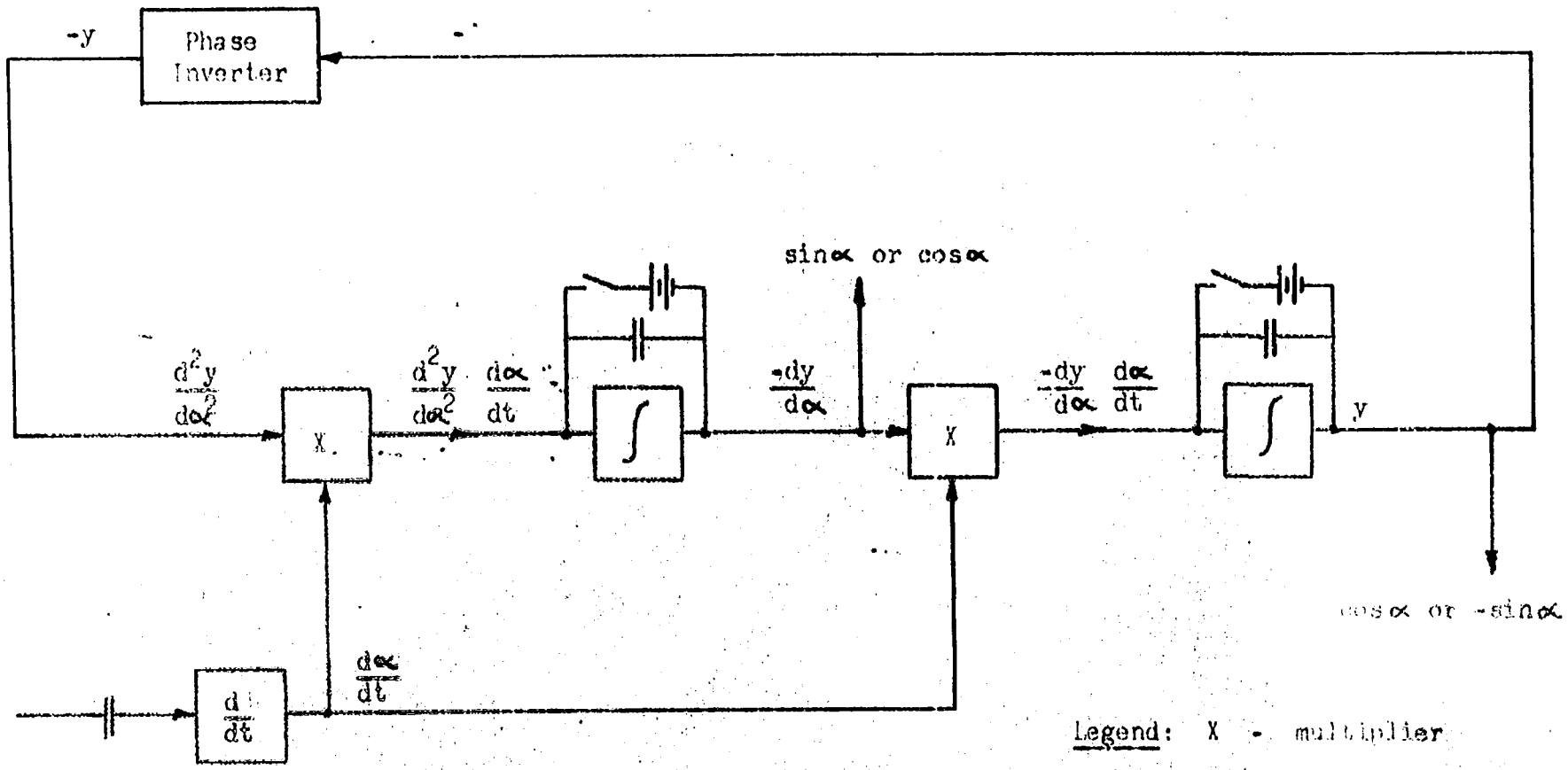

Legend: X - multiplier

$\int$ - integrator

$\frac{d}{dt}$ - differentiator

Figure 4.5

Circuit loop for generating trigonometric functions

which has the solution

$$y = c_1 \cos \alpha + c_2 \sin \alpha \qquad (4.9)$$

where c_1 and c_2 are determined by initial conditions. If the second integrator feedback capacitor is charged then $y = \cos \alpha$, if the first is charged, $y = -\sin \alpha$. The operation of the loop is similar to that of an integrating servo system. Assume that the system is initially balanced, that is, the outputs from input multipliers substantially cancel each other, then a change in either of the input voltages x_1 or $-y_1$ causes a voltage to appear at the output of the high gain amplifier. This voltage is applied to the multipliers in the loop and causes changes in the two loop output voltages. These two loop output voltages change as the system is balanced again. For this condition

$$x \sin \alpha - y_1 \cos \alpha = 0 \qquad (4.7)$$

and the two loop output voltages, which multiply the input voltages x_1 and $-y_1$ in figure 4.4, are respectively proportional to $\sin \alpha$ and $\cos \alpha$. Thus, the system provides voltages proportional to α, $\cos \alpha$ and $\sin \alpha$. In order to evaluate r as per equation (4.6), the system of figure 4.6 would be required.

To obtain a cartesian to spherical coordinate system conversion, figure 4.7, two systems of figure 4.4 and 4.6 would have to be interconnected as indicated in figure 4.8. That is, if to one system of figure 4.4. voltages proportional to z_p and $-\rho$ are applied, voltages proportional to e, cos e and sin e are produced. To a second system of figure 4.4 voltages proportional to x_p and $-y_p$ are applied and voltages proportional to ϕ, $\sin \phi$, $\cos \phi$ are produced. Now

$$x_p \cos \phi + y_p \sin \phi = \rho \qquad (4.10)$$

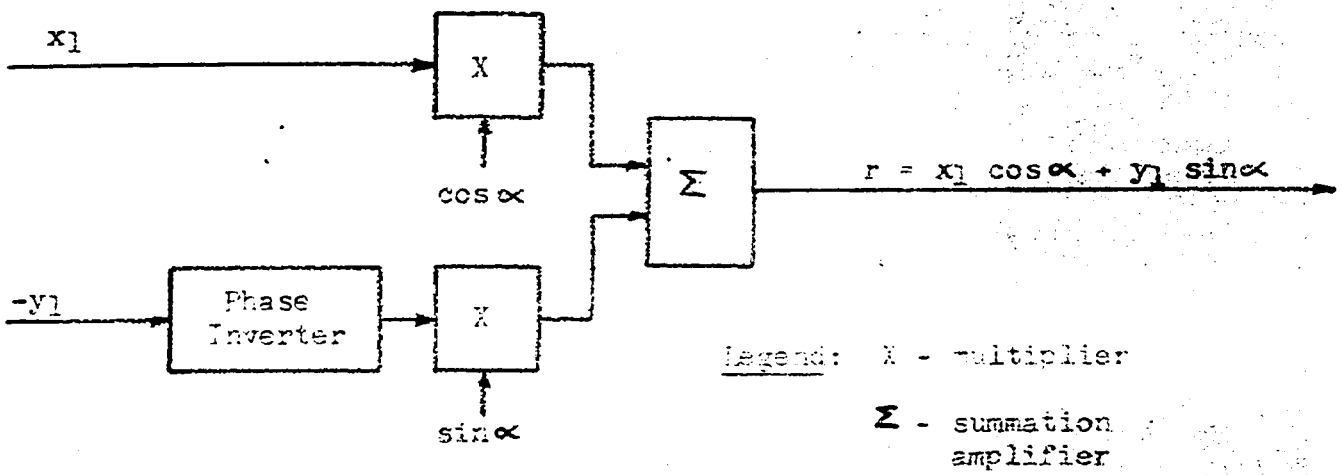

Figure 4.6

Block diagram of system designed to obtain a voltage proportional to the magnitude r

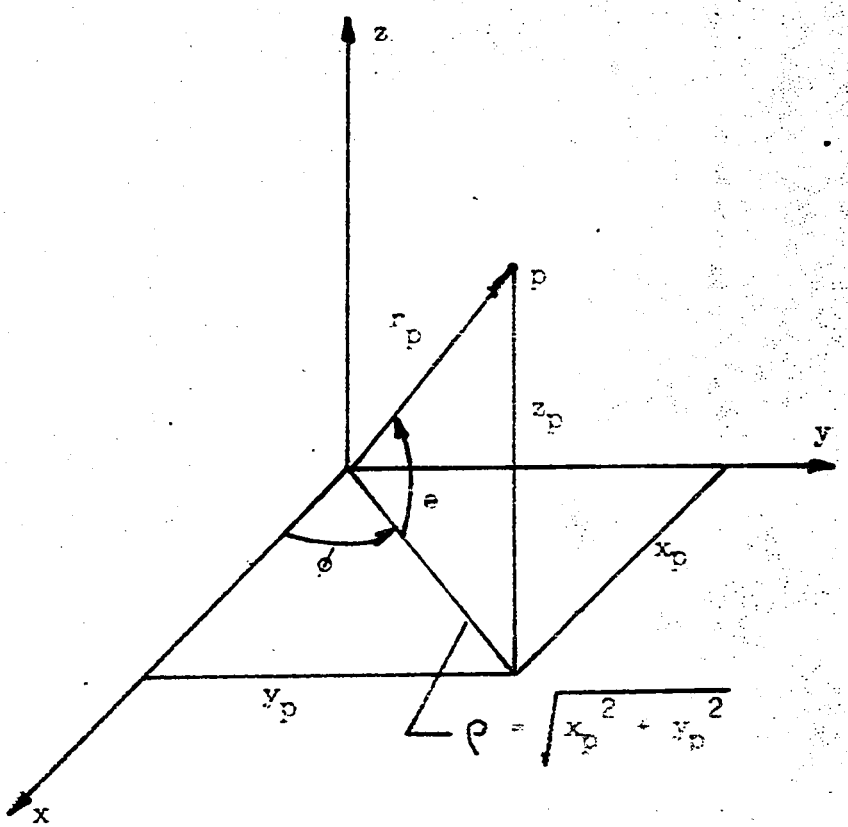

Figure 4.7

Three dimensional coordinate system indicating cartesian and spherical coordinates

$$\cos\theta = \frac{e_p}{r_p} \qquad \sin\theta = \frac{f}{r_p} \qquad (4.11)$$

so that θ and r_p may be obtained by incorporating the system of figure 4.6 as shown in figure 4.8. Notice that in figure 4.6, $\frac{dx}{dt}$ is available at the input to the circuit loop so that $\frac{de}{dt}$ and $\frac{d\phi}{dt}$ are available in the system shown in figure 4.8. This suggests that the $\frac{de}{dt}$ and $\frac{d\phi}{dt}$ signals could be tapped off via buffer amplifiers and fed individually to two squaring devices plus an adder and square rooting device to yield the magnitude of the angular velocity given by $\sqrt{\left(\frac{de}{dt}\right)^2 + \left(\frac{de}{dt}\right)^2}$ (see appendix).

Mathematical Operations and Devices Required for Analog Computation

The mathematical operations required to establish the systems illustrated in figures 4.1, 4.2 and 4.8 are: addition, phase inversion, multiplication by a constant (gain), integration, differentiation, squaring, square-rooting and multiplication of two continuously varying functions of time. The operations of addition, phase inversion, multiplication by a constant and integration using operational amplifiers, figure 4.9, are perhaps technically the easiest to accomplish, and as details on these operations may be found in any good text on analog computation (48, 50, 51, 52), they will not be discussed. The operations of differentiation, squaring, square-rooting and multiplication of two functions of time are technically more difficult to accomplish and therefore deserve some attention.

The two perhaps most primary considerations relating to the performance of the devices effecting the desired mathematical operations are bandwidth and accuracy. For the purposes of displaying and processing signals, a bandwidth of several hundred cycles and an accuracy of [illegible]

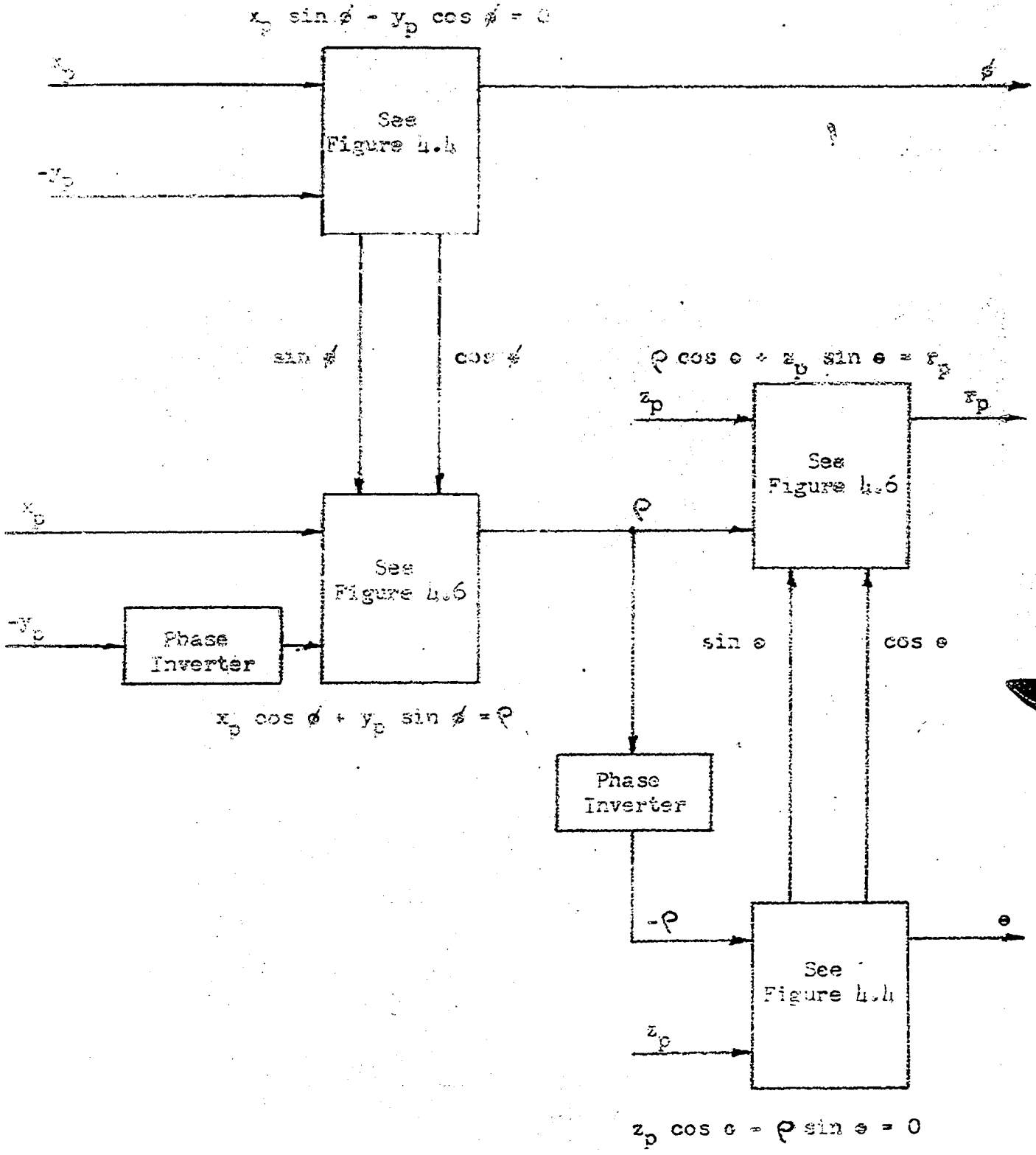

Figure 4.8a

Interconnection of system shown in figures 4.4 and 4.6 to give cartesian to spherical coordinate transformation. See figure 4.8b for a more detailed block diagram.

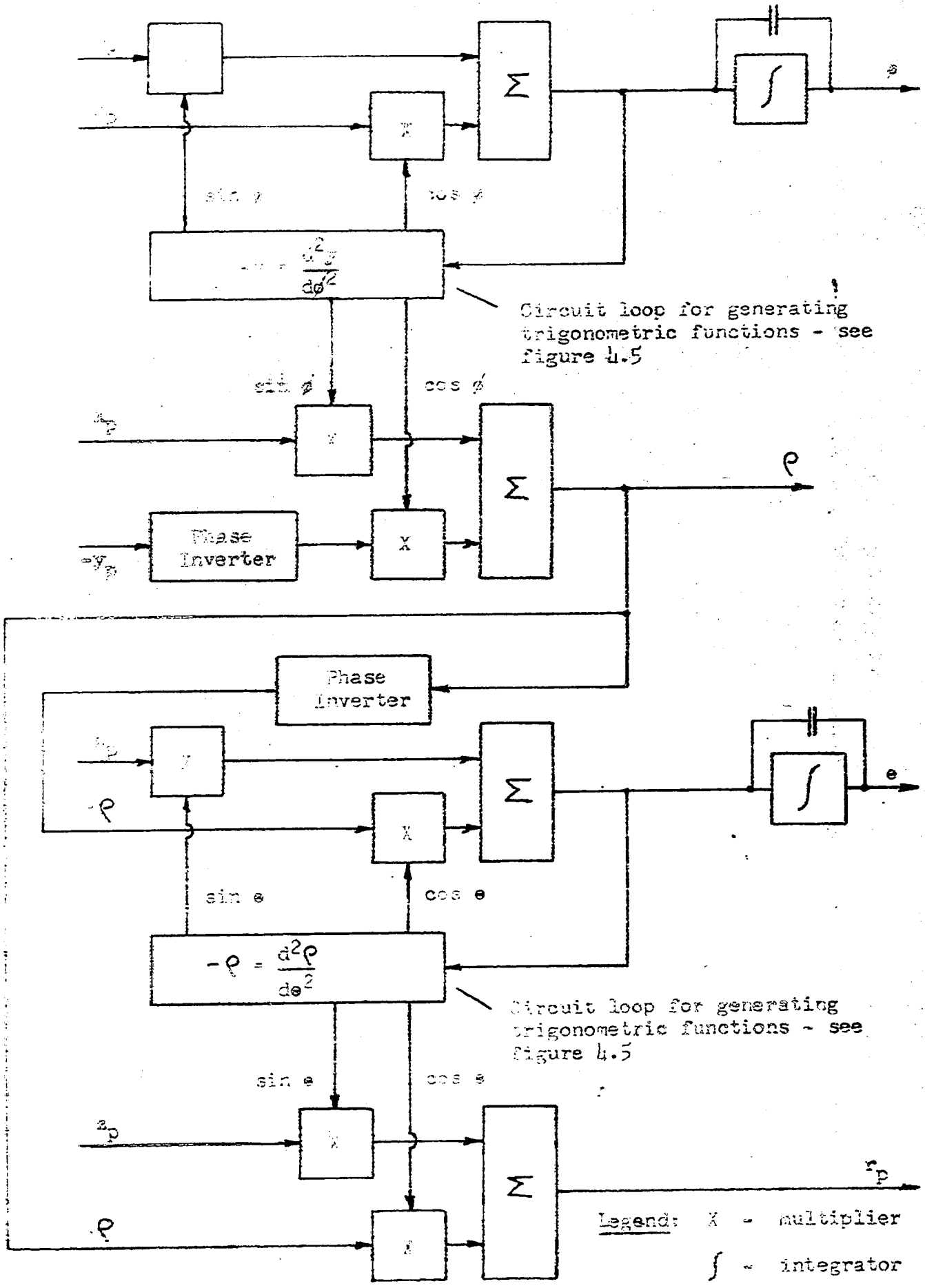

Figure 4.3b

System for cartesian to spherical coordinate transformation

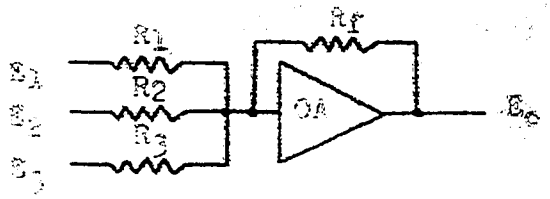

Addition

$$E_o \cong -R_f \sum \frac{E_i}{R_i}$$

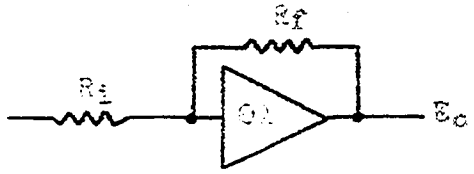

Phase inversion

$$E_o = -E_i; \quad R_f = R_i$$

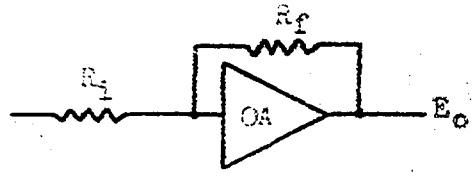

Multiplication by a constant

$$E_o = -E_i \frac{R_f}{R_i}$$

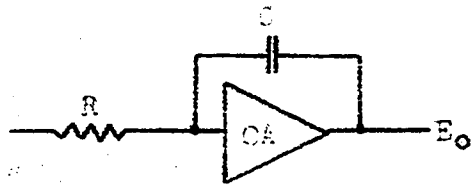

Integration

$$E_o \cong -\frac{1}{RCs} E_i$$

Legend: OA - Operational Amplifier

Figure 4.9

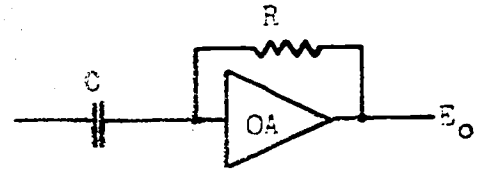

Differentiation

$$E_o \cong -RCsE_i$$

Legend: OA - Operational Amplifier

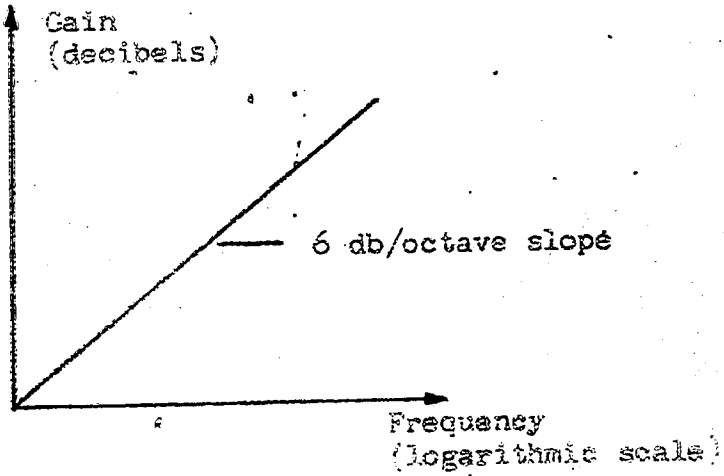

Figure 4.10

...t is sufficient for initial research investigations. The problem of bandwidth and accuracy are mentioned at various points throughout this report.

To illustrate the comment that the operations of differentiation etc. are conceptually more difficult to accomplish than addition, etc., figure ... indicates a practical configuration for a differentiator using an operational amplifier. A configuration used by Langner and Geselowitz (53) for differentiating ECG signals is shown in figure 4.11. The purpose of their investigation was to demonstrate how the first derivative of the ECG signal emphasizes the higher frequency components of the ECG signal. Stroman (51) gives a number of illustrations of the ECG signal and its first derivative, recorded simultaneously, for both normal and abnormal heart conditions. The diagnostic usefulness of using this display technique has yet to be established.

The difficulty in performing analog differentiation (48; 52, p. 106, ..., 15) arises primarily from the fact that the frequency characteristics of an ideal differentiator must increase with frequency at 6 db/octave and so leads to noise corruption of the differentiated signal, that is, the high frequency components of the signal and noise are enhanced relative to the low frequencies. In practice, a 6 db/octave slope cannot be maintained indefinitely. It can be difficult to stabilize a differentiation circuit with respect to spurious oscillations[4] and there exists the problem of over-

---

[4] Note that the circuits in figures 4.9, 4.10 and 4.11 consist of high ... operational amplifiers with feedback between output and input and consequently are subject to the instability problems associated with feedback systems unless the proper design procedures are followed to ensure stability, that is, freedom from loop oscillation.

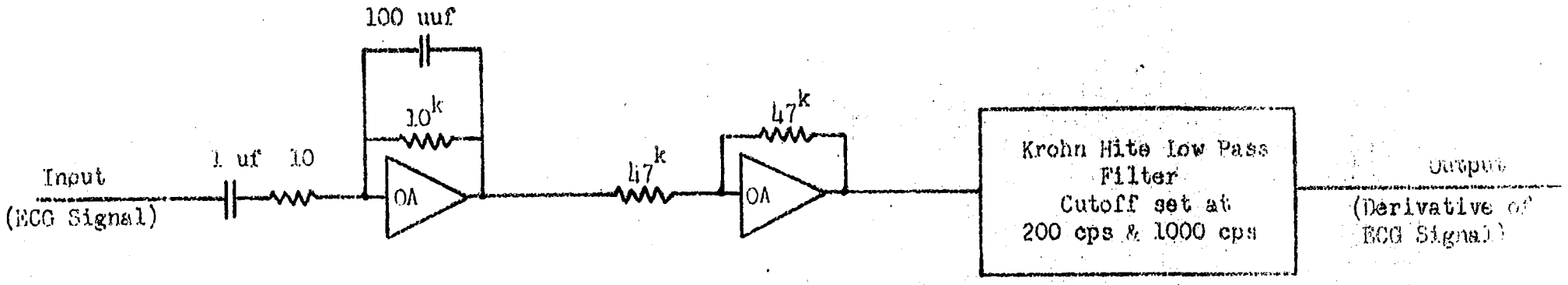

Legend: OA = Operational Amplifier

Figure 4.11

Electronic circuit for obtaining the first derivative of an ECG signal. The second amplifier is used to reinvert the signal (phase inverter).

loading the amplifier of the differentiator if the input waveform changes very rapidly, that is, has discontinuities or near discontinuities. The sensitivity of the differentiator to noise can render the output unintelligible. Thus, a practical differentiator must be designed on a compromise basis in that the higher frequencies must be filtered to reduce the noise transmission to a sufficient degree so that intelligible results are obtained. Langner and Geselowitz illustrate the effect of passing the derivative of an ECG signal through a variable passband low pass filter, Figure 4.11, set at a cutoff frequency of 200 cps and 1000 cps (53, figure 7, p. 224) in order to indicate the difficulty in interpretting the derivative as the degree of noise corruption increases with increasing cutoff frequency of the filter.

The configurations indicated in figures 4.9 and 4.10 can be considered as special cases of figure 4.12. The ratio $\frac{Z_f}{Z_i}$ is the transfer function of the network. To obtain a square or square-rooting characteristic the ratio $\frac{Z_f}{Z_i}$ must be a nonlinear transfer function. It is possible to approximate nonlinear functions with straight line segments using networks consisting of a number of branches made up of a fixed or variable resistor and an appropriately biased diode. Such networks are often referred to as diode function generators since they are capable of generating a wide variety of nonlinear functions (48,50,51). The accuracy of such networks depends, among other things, on the number of straight line segments used to approximate the desired function. The networks can be used at frequencies of up to 10 to 20 KC. A biased-diode network designed to yield a square or square-root characteristic in conjunction with an operational amplifier can be referred to as a fixed purpose diode function generator.

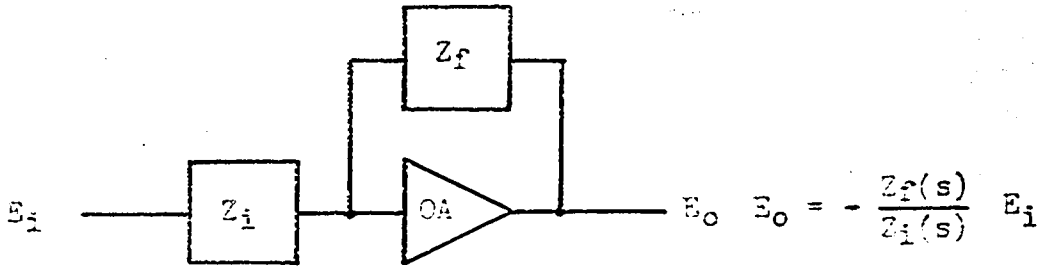

Legend: OA - Operational Amplifier

Figure 4.12

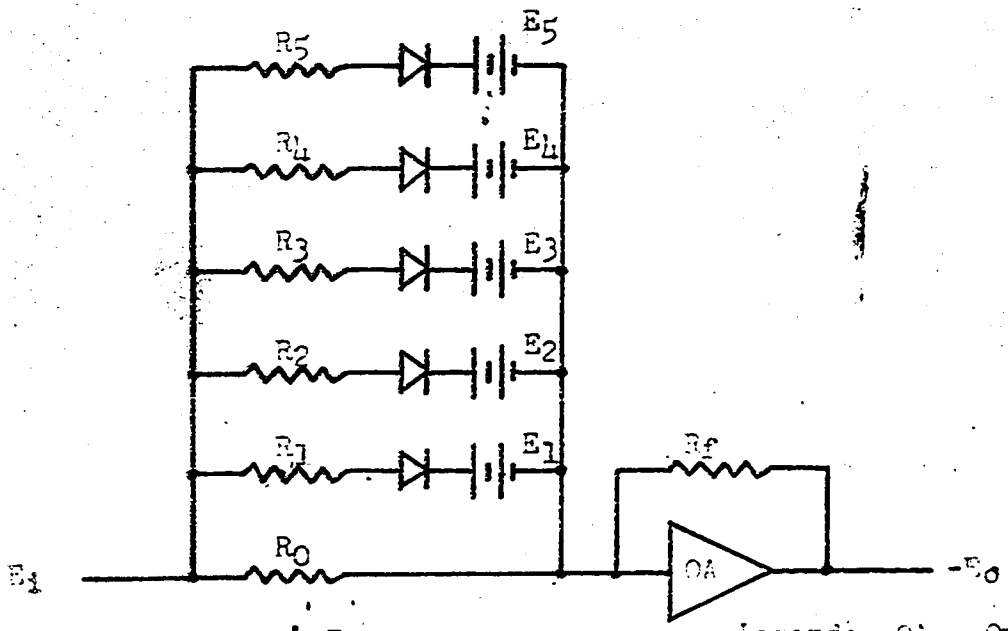

Legend: OA - Operational Amplifier

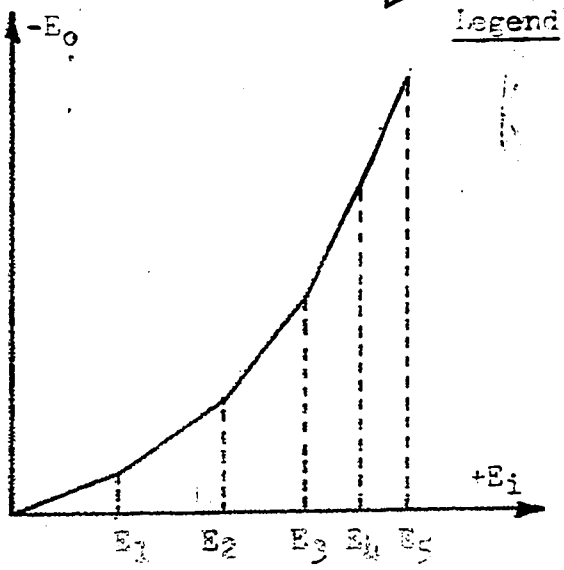

Figure 4.13

Biased-diode squaring circuit and transfer function

Figure 4.13 shows a biased-diode squaring circuit and its parabloic or square law curve function. Such a circuit is capable of approximating a square law curve to within ±1% with 5 straight line segments and less than ±0.1% with 15 segments. The input impedance Z_i in figure 4.13 is seen to consist of 6 parallel branches. Five of these branches contain diodes which are biased by batteries E_1 to E_5 of progressively increasing voltage. For low values of E_i, current flows only through R_O and the output voltage $E_o = -\frac{R_f}{R_O} E_i$. When the input voltage E_i exceeds E_1, current flows through R_1 as well as R_O so that $E_o = -R_f(\frac{1}{R_1} + \frac{1}{R_O}) E_i$. As the input voltage is increased more and more diodes conduct yielding the parabolic transfer function of figure 4.13. The biased-diodes can be thought of as voltage sensitive switches which cause the resistors R_1 to R_5 to be switched into a parallel arrangement at a predetermined threshold set by the bias voltages E_1 to E_5. In a commercially available biased-diode squaring circuit, the batteries are replaced by a single bias or reference voltage source and a resistor divider network. With present day high back-resistance silicon semiconductor diodes, biased-diode squaring circuits can be packaged in a compact volume.[5] For example, one commercially available electronic multiplier which consists of two biased-diode squaring networks (excluding external operational amplifiers and reference voltage sources), each of which is made up of 8 resistor/biased-diode branches in parallel, occupies a volume of the order of 15 cubic inches.[6]

---

[5] See Chapter 2 (also 56) for an example of the application of biased-diode networks using vacuum tube diodes to obtain a square-root characteristic. Also see Chapter 2 and (33,34) for circuits that have been developed to yield square-law characteristics by using the approximately parabolic plate-current versus grid voltage transfer characteristic of certain vacuum tubes.

[6] See circuitry between dotted lines in figure 4.17 and discussion below on quarter-square type multipliers.

In addition to using biased-diode networks to synthesize a nonlinear transfer function, say a square law characteristic, it is also possible to make use of the nonlinear voltage-current relationship

$$i = k\, e^{n} \qquad (4.12)$$

of silicone carbide varistors.[7] A typical configuration using a silicone carbide varistor as part of the input impedance is shown in figure 4.14(50). By suitably adjusting R_a and R_b a wide variety of nonlinear functions can be obtained. The varistor could also be used as part of the feedback impedance. Referring to equation 4.12, the constant k depends upon the resistivity and dimensions of the particular varistor whereas the exponent n depends upon manufacturing process factors and can be made to be as high as 7. Varistor units can be designed to operate over a wide variety of voltage and current ranges.

An analog computer component that has been designed using silicon carbide varistors is commerically available under the trade name of Quadratron[8](57). The Quadratron is basically a varistor squaring unit which has been compensated for various errors inherent in the varistor itself, namely; inaccuracy of the exponent n in equation 4.12, large negative temperature coefficient, a slight rectification error, and the apparent inability of varistor manufacturers to produce a unit sufficiently consistent in its various characteristics. The device can be used with external operational amplifiers in approximately 15 different configurations to obtain such nonlinear functions such as a square-law curve, square-root

---

[7] "Varistor" is derived from "variable resistor" and refers to voltage sensitive resistors manufactured from resistive materials exhibiting nonlinear voltage-current characteristics. Varistors using silicone carbide as the nonlinear material are useful for analog computer applications and are known under various trade names such as Thyrite resistors and Metrosil resistors.

[8] Douglas Aircraft Company, El Segundo, California. Quadratron - from the latin "quadrare" - to square, and "tron" as in "electron".

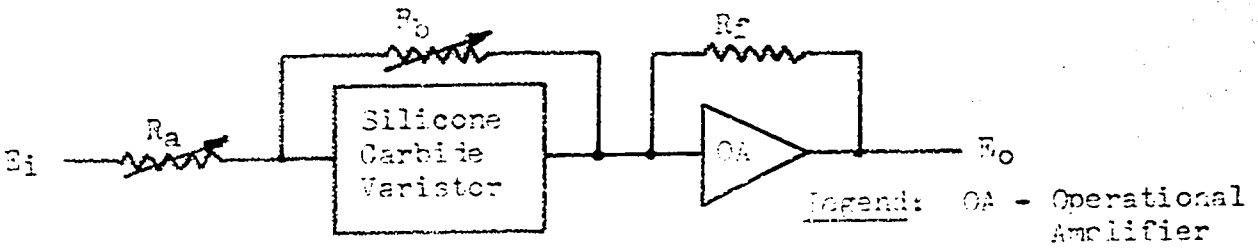

Figure 4.14

Nonlinear function generator using silicone carbide varistor

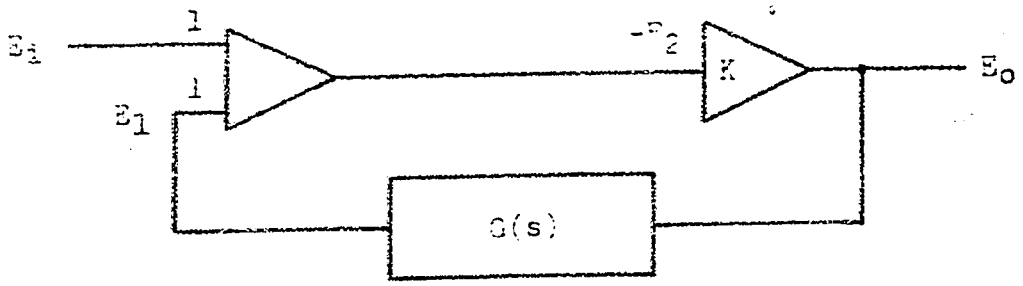

Figure 4.15

Use of the operational amplifier to obtain the reciprocal of a given transfer function

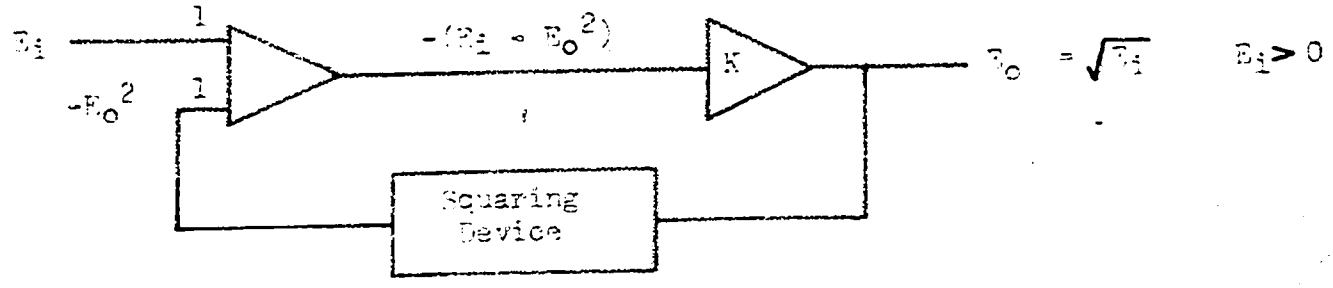

Figure 4.16

Use of the operational amplifier to obtain a square root characteristic given a device obeying a square-law characteristic.

characteristic, sine function, cosine function, tangent function, hyperbolic cosine and tangent functions, multiplication, division, variable exponent, etc. The Quadratron frequency response is given in terms of the frequency at which measurable phase shift appears which is 400 cps for the squaring operation and 50 cps for the square rooting operation. The maximum squaring error is claimed to be 0.2% at maximum input voltage.

At this point, it is worthwhile to take note of the fact that a high gain operational amplifier can be used to obtain the reciprocal of a transfer function of a given device or network by connecting the given device or network in the feedback path of the operational amplifier as shown in figure 4.15 (58). This can be shown by writing the following equations

$$E_i + E_1 = -E_2 \qquad (4.13)$$

$$-K E_2 = E_o \qquad (4.14)$$

$$E_1 = G(s) E_o \qquad (4.15)$$

and solving these equations to obtain the overall transfer function E_o/E_i, that is,

$$\frac{E_o}{E_i} = \frac{1}{\frac{1}{K} + G(s)} \qquad (4.16)$$

where K is the gain of the operational amplifier and G(s) is the transfer function of the given device. For $K \gg\gg 1$, equation 4.16 may usually be approximated by

$$\frac{E_o}{E_i} = -\frac{1}{G(s)} \qquad (4.17)$$

Thus, a differentiator may be obtained by connecting an integrator in the feedback path of the circuit shown in figure 4.15. Similarly, a square-root characteristic may be obtained by using a device with a square law

characteristic in the feedback path. For example (34,51), in figure 4.15 if the element G(s) is a squaring device then, referring to figure 4.16, the following equation holds

$$E_o = K(E_i - E_o^2) \qquad (4.18)$$

or rearranging

$$E_o(1 + K E_o) = KE_i \qquad (4.19)$$

Thus, for $K >> 1$, equation 4.18 may be approximated by

$$E_o^2 \cong E_i \qquad (4.20)$$

or

$$E_o \cong \sqrt{E_i} \qquad E_i > 0 \qquad (4.21)$$

It should be noted that the establishment of the dc level of the input waveform to a square-root-extracting circuit is very important since at the start of the waveform an error of 1% of the peak amplitude will result in a 10% error in the output (34, p.691).

The operation of instantaneously multiplying two continuously varying functions of time[9] can be achieved in a number of ways without resorting to schemes employing oscillators and associated mixing or modulating devices after the manner of McFee(18) and Park(20, see also 19 and 21), or without employing electromechanical devices, photoelectric devices, cathode ray tubes, etc. One of the currently more popular techniques makes use of the well known quarter-square identity

$$\frac{(x + y)^2 - (x - y)^2}{4} = xy \qquad (4.22)$$

---

[9]See (59) for a classification list of a wide variety of analog multipliers according to their accuracy and bandwidth and a listing of their most important features.

where x and y are the two time functions to be multiplied. The block diagram of a typical commercially available electronic multiplier[10] of the quarter-square type is shown in figure 4.17(60). This particular multiplier (consisting of the circuitry between the dotted lines in figure 4.17) is made up essentially of two biased-diode squaring networks and must be used in conjunction with operational amplifiers and a reference voltage source to effect multiplication as per the identity equation 4.22. Referring to figure 4.17, the two input voltages x and y are applied to the input summing networks of the multiplier in two polarities via two external inverting amplifiers. The voltage polarities applied to the positive summing network result in a voltage proportional to $(x + y)$ regardless of whether x and y are positive or negative, while those applied to the negative summing network result in $(x - y)$. The diodes in the input summing network form absolute-value circuits which limit each resultant voltage to positive only for the x channel and negative only for the y channel. Following the input summing and absolute value circuits ~~and~~ are the biased-diode squaring networks which are the heart of the multiplier. One network is designed to operate only with positive input voltages and the other only with negative input voltages. These networks are identical except for the polarity of the diode connections and bias voltages. Each network consists of 8 resistor and biased-diode branches plus a resistor branch all in parallel and approximates the square-law characteristic $+(x + y)^2$ or $-(x - y)^2$. The outputs of the two squaring networks are summed and then converted to the proper output voltage range by the external output amplifier (which also changes the sign, that is, inverts the output signal).

---

[10] Donner Scientific Co., Concord, California. Model 3732 Electronic Multiplier.

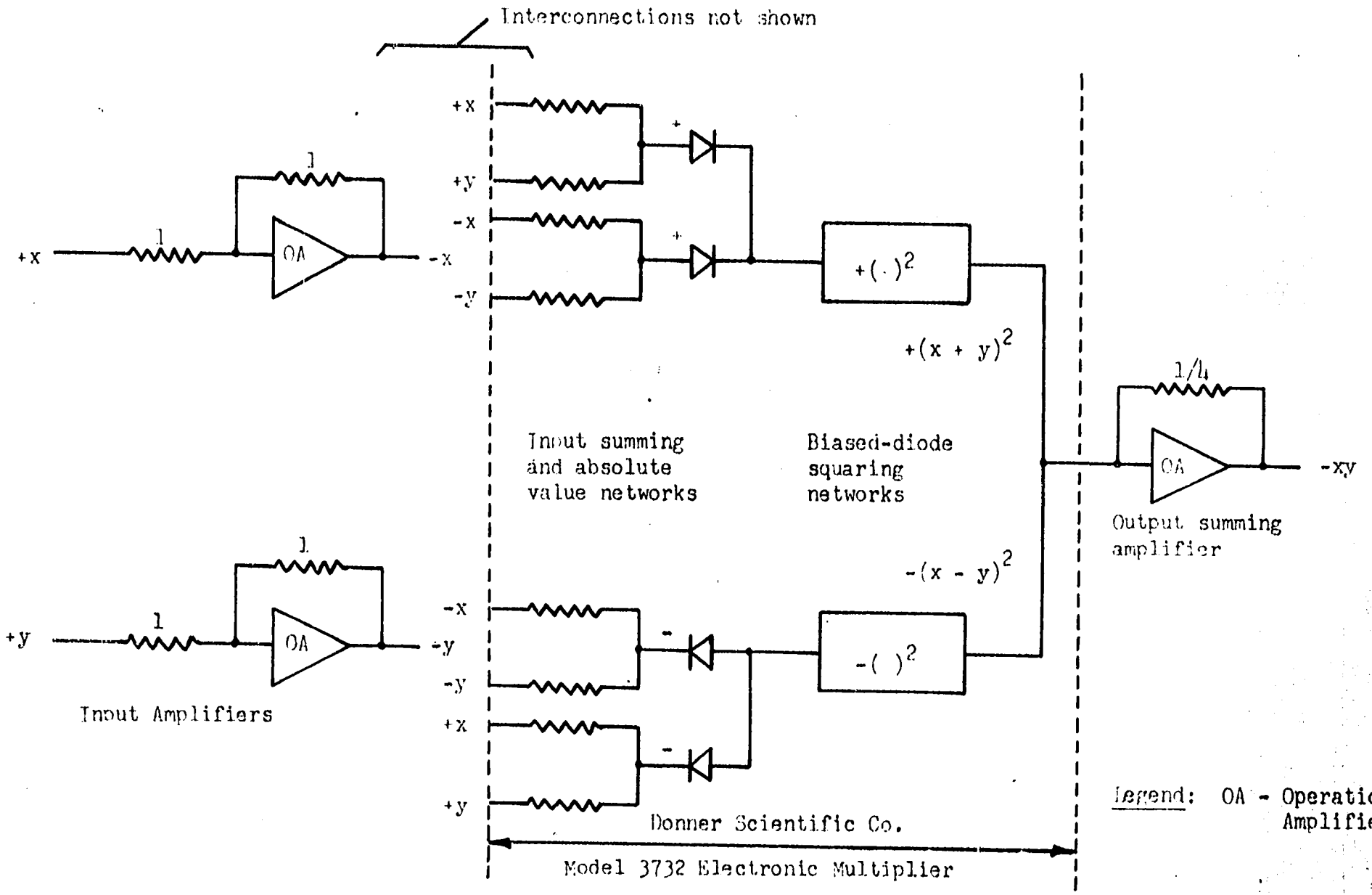

Figure 4.17

Quarter-square multiplier

It should be noted that this multiplier is a four-quadrant multiplier, that is, the output is unrestricted as to the sign (polarity) of the input signals x and y. With this type of multiplier, accuracies of the order of 0.5% and a bandwidth of up to 20 kc can be achieved. Squaring and square-rooting can be of course performed with this "multiplier" by appropriately interconnecting the squaring networks with external operational amplifiers and reference voltage sources such that configurations similar to those in figures 4.13 and 4.16 are obtained. The "multiplier" is available in models for use with either tube type or transistorized operational amplifiers.

Recall that the Quadratron mentioned earlier is basically a varistor squaring unit. It is possible to use a pair of Quadratrons with 3 external operational amplifiers to obtain a multiplier based on a variation of the quarter-square identity (57). The Quatratron, however, has a bandwidth somewhat less than that obtainable with biased-diode squaring networks.

Another purely electronic multiplier which is capable of four quadrant operation makes use of the Hall effect. (61,62,63). Whenever current carriers are subjected to a magnetic field perpendicular to the direction of their motion a transverse potential difference (Hall voltage) is observed, figure 4.18. The Hall voltage V_y is given by

$$V_y = R_h \frac{I_x B_z}{t} \qquad (4.23)$$

where I_x is the applied current, B_z the applied electric field, R_h the Hall constant characteristic of the material, and t the thickness of the wafer. The effect of the Hall electric field is to annul the deflecting force of the magnetic field enabling the current carriers to pass through the material. Commercially available Hall elements are made from wafers

of semiconductor material (germanium or silicon) or intermetallic compounds (indium arsenide or indium antimonide). A simplified block diagram of a Hall effect multiplier is shown in figure 4.19. The Hall element is mounted in the air gap of an electromagnet core. Current I_x is passed through the Hall element while current I_z is passed through the electromagnet coil to create the magnetic field B_z. The resulting Hall voltage V_y appears across two opposite faces of the wafer and is mutually perpendicular to I_x and B_z. With Hall effect multipliers, properly compensated for various sources of error in the Hall element itself, and in the Hall element--magnetic circuit combination (62,63), accuracies of the order of 0.5% and a bandwidth of 500 cps can be achieved.

The foregoing material indicates the feasibility of designing an analog computer system using commercially available analog computer components and mentions problems that have been overcome and some that remain in analog computer technology. In designing the system, consideration would have to be given to providing baseline clamping, automatic calibrating and balancing features[11] along with the provision of programming or patching facilities to enable systems of the type illustrated in figures 4.1, 4.2 and 4.8 to be set up quickly by an ECG clinical technician. Such an analog facility would enable a variety of displays to be studies and provide the possibility of effecting other displays by suitably expanding the number and type of analog components in the system. For example, in addition to the systems shown in figures 4.1, 4.2, 4.8, the incorporation of an x,y,z to x',y',z' coordinate conversion system might be of value to a researcher. In Chapter

---

[11] See (64) for a discussion of the design of a preamplifier for an ECG monitoring system and an analysis of the 60 cps interference problem. Also see (65) for a description of the design of an electronic heart beat simulator.

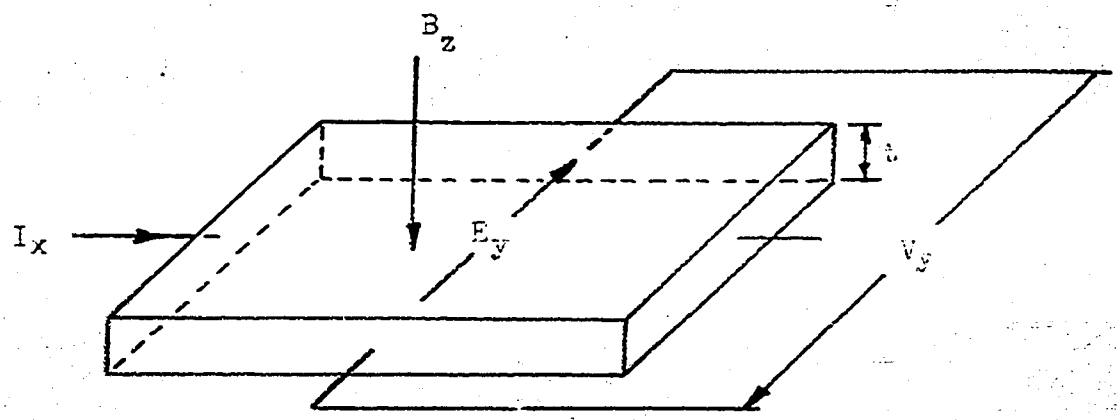

Figure 4.18

Basic Hall effect

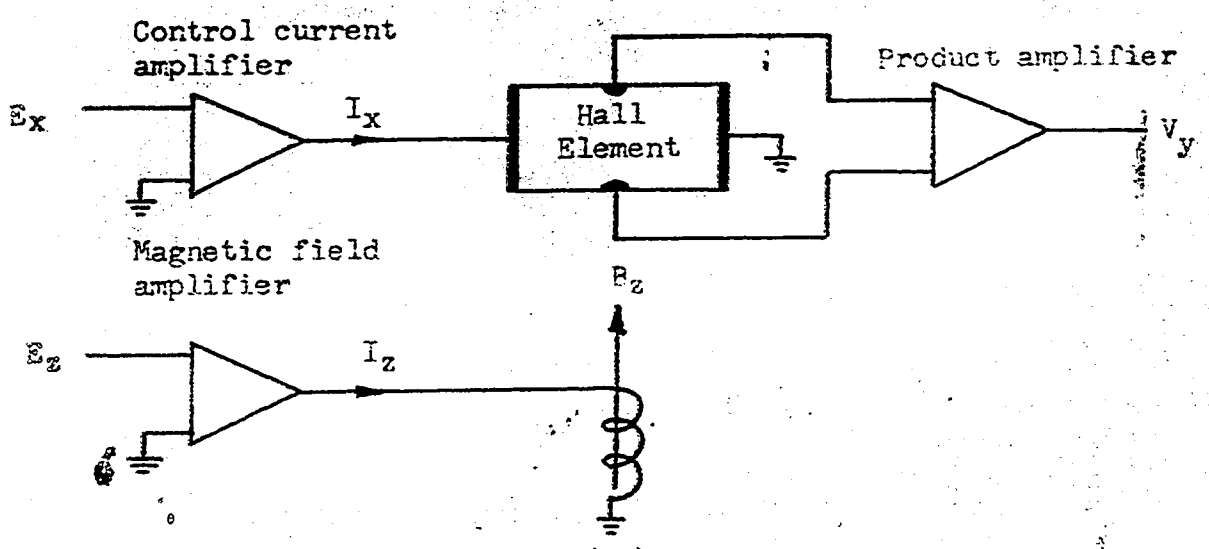

Figure 4.19

Simple block diagram of Hall effect multiplier

8, a brief reference is given regarding the use of analog computation in studies dealing with the power spectrum and correlation functions of the ECG signal. For example, to obtain the power spectrum, a variable bandwidth filter and a device to perform a squaring operation are required. Thus, if the researcher desired to study the power spectrum of the ECG signal, he could readily do so by suitably adding to (if required) and programming his collection of analog computer components.

Finally, it is worthwhile to mention at this point, that if a satisfactory representation of an ECG signal can be obtained using exponentials as discussed in Chapter 9, analog instrumentation techniques are available whereby a simple electrical filter networks (orthonormal filter) may be synthesized to form an equivalent signal generator which will generate the required exponentials individually and then form the sum yielding the approximating ECG signal which can then be compared to the original ECG signal in order to evaluate the accuracy of the representation.

CHAPTER 5

REVIEW OF APPLICATIONS OF DIGITAL COMPUTERS IN ELECTROCARDIOGRAPHY

Summary

The following chapter is a review of some of the applications of digital computer techniques to ECG clinical and research work. The object of the application and various points of interest are mentioned. The attempt to find the "best" representation or display of an ECG signal implies a choice is made with respect to some criterion. This is briefly discussed along with classifying measured ECG parameters using the likelihood ratio. Chapter 6 will contain complementary information on items such as establishment of the baseline, smoothing of input data, etc. The use of the digital computer in work related to signal analysis concepts referred to in Chapter 1 will be mentioned in Chapter 9.

The first report (1959), to the author's knowledge, concerned with the application of digital computer techniques for processing ECG signals was due to Pipberger et al (66, 67). This initial work concerned itself with establishing a recording, monitoring, and analog-digital conversion facility suitable for recording ECG signals, translating, and storing these signals in appropriate format for digital computer processing. Such a facility would enable ECG signals to be stored on magnetic tape in any desired volume and period of time. The facility records, using a corrected orthogonal 3-lead system (Schmitt SVSC III; Frank system used in later work), the x, y, z ECG signals simultaneously on separate FM channels on magnetic tape. Fidelity of the signals with respect to accuracy, dynamic range and frequency response is maintained at a higher degree than is possible with single-channel direct-writing instruments commonly used. Retrieval of specific signals for purposes of comparison or further processing by a digital computer is readily achieved. Such a facility enables a quantitative and objective analysis to be made with the advantage that the analysis will not reflect the inaccuracies inherent due to variations in interpretations made by different observers.

Once the data has been stored and is readily retrieved in appropriate format, it is possible to take advantage of the flexible programming feature of digital computers, as compared to special purpose analog computers, to perform various mathematical analyses, keeping in mind the speed and capacity of the computer could provide limitations in some problems. The consulting services of personnel knowledgeable in the details of programming, numerical analysis, statistics, etc. are required.

Pipberger et al state that "The diagnosis of heart disease from an electrocardiogram is largely emperical, and although a great deal of work

has been done, it appears desirable to increase the number and variety of records studied for the purpose of setting more accurate limits for normality and abnormality." (1, p. 168; 3, p. 21; 8, p. 360; 68, p. 156). A "variety of records", obtained at the University of Ottawa using a digital computer, is presented in Chapter 7.

One of the reasons for developing the facility was to satisfy the need for investigating and evaluating new criteria for analyzing ECG signals by using the flexibility of programming provided by a digital computer. "The need for new criteria for analyzing" is termed the "representation problem" in the signal analysis concepts referred to in Chapter 1 and discussed in Chapter 9.

References (66) and (67) give a detailed description of the facility, the block diagram of which is reproduced in figure 5.1. The facility can be expanded to allow for processing phonocardiograms (PCG), ballistocardiograms (BCG), electrencephalograms (EEG), electromyograms (EMG), etc. The ECG was chosen, however, since it seems to lend itself more readily to mathematical analysis than other electrophysiologic waveforms and because of its wide use and acceptance.

After recording x, y, z on the analog tape recorder along with patient identification information on the voice channel, an operator at the control unit can monitor and select the desired interval of a cycle or cycles of the x, y, z ECG signals. The selected interval of analog voltages is then converted into binary digits in the analog-digital converter. The binary digits are delivered to the "digital write" unit for re-recording on the digital magnetic tape in a format suitable for the digital computer (IBM 7044). Once the appropriate interval of analog voltage has been selected by operator, the remainder of the process is completely automatic.

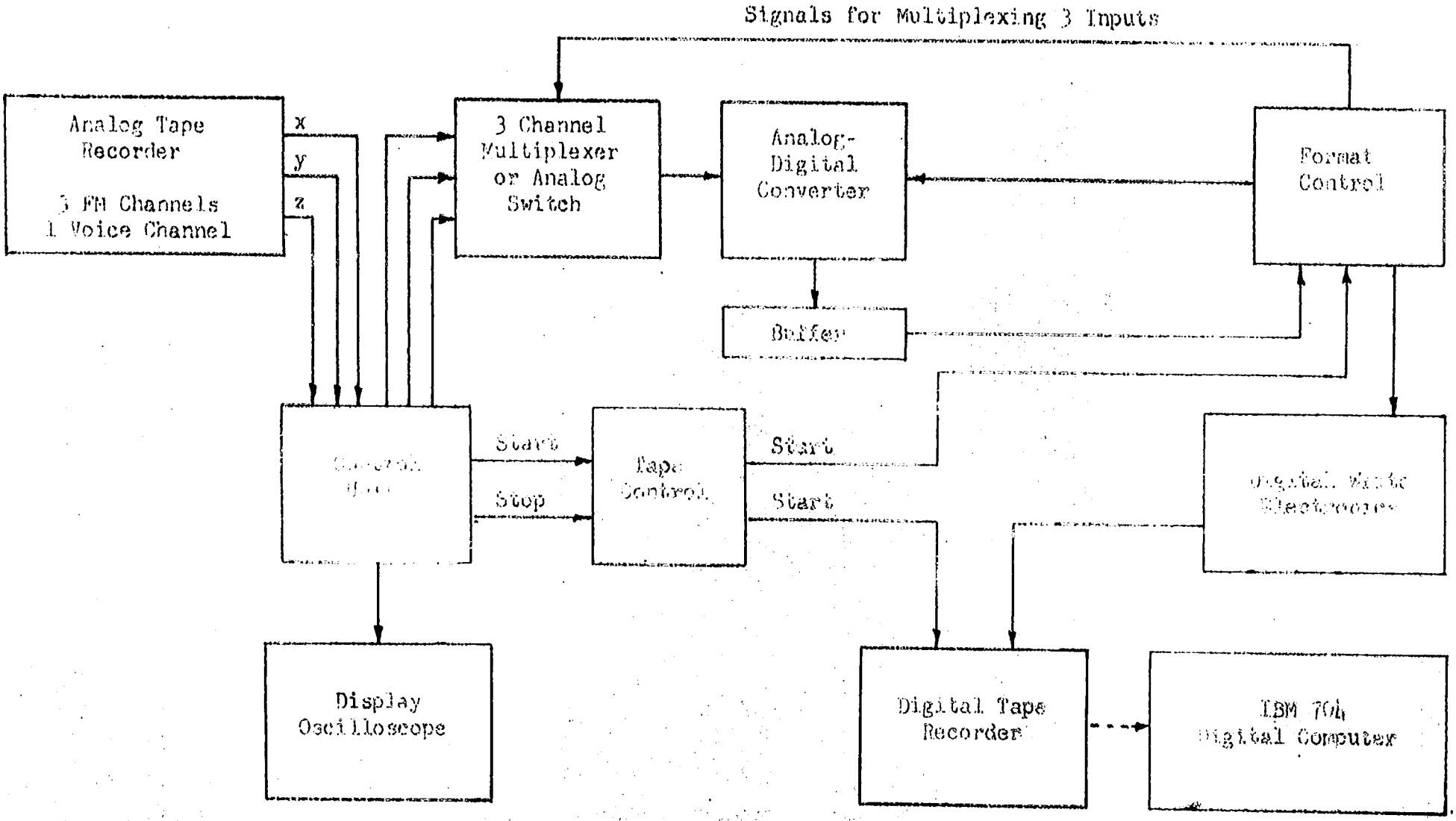

Figure 5.1

Block diagram for analog-digital conversion equipment for electrocardiograms

In the application of digital computers to electrocardiography there are two methods of approach. The first approach is well presented by Caceres (1962) in a short paper (11, see also appendix in 71). He emphasizes that for computer outputs to be of use, the program must be based on definitions which have been developed, accepted and proven useful for clinical work over the past half century, irregardless of the level of empericism involved. Consequently, the primary task lies with the physician in that he possesses the detailed knowledge of cardiology. He must provide the computer programmer with a detailed organization of those steps in his logic which he subconciously carries out in interpreting ECG "patterns". This approach of simulating the pattern recognition technique of the human mind is perhaps a short range point of view in that this may not be the best criterion for analyzing ECG signals, but, it is very practical in the sense that it can be correlated with developments achieved over a half century of effort. The second approach is that of developing new criteria for analyzing ECG signals. Caceres recognizes this approach as the one that might be followed by technical personnel, following the logical procedure of physical sciences, without the guidance of the practicing physician. This approach is more of a long range point of view in which the ECG signals would be studied to determine the most easily measured parameters or determine a whole spectra of variables upon which statistical analysis techniques could be used. This approach requires time for study and creative research. An example of such an approach using signal analysis concepts is discussed in Chapter 9. Caceres' differentiation between "practicing physician" and "technical personnel" is perhaps somewhat unclear. Certainly, for the second approach (carried on

"without the guidance of the practicing physician") to be useful, "technical personnel" should be interpreted as including personnel knowledgeable in biophysical concepts who could consult as required with personnel knowledgeable in mathematics, electronic engineering, computer programming and other disciplines.

The balance of this chapter will concern itself mostly with a review of the literature re the application of digital computers first to develop "pattern recognition programs" and subsequently to obtain "a variety of records" as discussed above.

The recent literature (1961 to date) on pattern recognition techniques is due mainly to two groups, namely Pipberger et al (~~5-11~~ 69, 11), and Caceres et al (~~5-6~~ 70). The work performed at University of Ottawa (Chapter 7) did not require the use of pattern recognition methods since the input data for the digital computer was prepared manually from measurements taken from an enlarged ECG record, ~~i.e.~~ that is, automatic analog-digital conversion equipment was not used.

Pipberger et al (11), having developed an automatic recording and analog-digital conversion system, considered the problem of developing a wave recognition or pattern recognition program prior to carrying out other analyses. A pattern recognition program was developed around the computation of the spatial velocity whereby a threshold was established to define the onset and end of the P wave and QRS complex, and the end of the T wave, the clinically significant time points.

First, the digitized x, y, z signals were filtered (Chapter 6) to eliminate noise due to 60 cps interference and muscle tremor. The filtering was only an intermediate step. Once the required time points were

determined, the unfiltered x, y, z signals were used in subsequent processing. Technically poor tracings were used to ensure the program would be useful even with clinical recordings taken under unfavourable conditions.

The filtered x, y, z signals were used to calculate the spatial velocity $V = \frac{1}{\Delta t}\sqrt{\Delta x^2 + \Delta y^2 + \Delta z^2}$. A threshold of 3 u volts/m sec (3 mv/sec) was chosen since this threshold was exceeded only during the P and T waves, and QRS complex and not during the TP, PR or ST intervals. The program logic was arranged such that the spatial velocity maxima during the QRS complex were determined. From the first maximum, calculations of V were carried on in both the forward and backward direction until the 3 uv/ms threshold was reached and thereby the onset and end of the QRS complex obtained. The end of the P wave was identified next by working backward from the QRS onset till the threshold was exceeded. A P wave was assumed not to exist if the threshold was not exceeded. After establishing the P wave onset, the end of the T wave was determined by working back from the end of the record. The onset of the T wave was not located as it is poorly defined and consequently not used in clinical work. (Computation time for the pattern recognition process using an IBM 704 computer was 15 seconds). Allowing for the limits of visual accuracy and beat-to-beat variations in wave duration, the comparison of computed and visual (on an enlarged record) time measurements yielded close agreement in all but 1.3% of the measurements made on 395 records. Pipberger (11) discusses the disagreements and suggests that refinements in the program logic could take the disagreements into account. The filtering did not noticeably affect the time determinations.

Caceres et al (~~5.6~~ 70) have described their work in developing a pattern recognition program in much more detail (28, ~~5.8~~ 71) than Pipberger et al. In developing the logic for the program, (LGP-30 computer) considerable attention was paid to allowing for pattern changes arising from changes in electrode positioning, and from normal to abnormal heart conditions, etc. The various waves can have peaks of varying amplitudes either positive, negative, diphasic, or even completely absent, figure 5.2 In order to isolate one heart cycle a repeatable reference common to all patterns is required. It was determined that the slope between the peak of the R wave and the peak of the S wave is the maximum negative slope and common to all waveforms. Consequently, the first derivative (slope) of the ECG was used to locate the maximum negative slope and thereby determine the reference point enabling one heart beat to be isolated. Caceres et al did not use an orthognal lead system in obtaining their records. (Lead II and V3 were used). Recalling the use of the spatial velocity by Pipberger et al, it is perhaps worthwhile to note that had an orthogonal lead system been used by Caceres et al, the derivatives of the x, y, z signals would correspond to the components of spatial velocity in the x, y, z directions respectively. To filter out the noise in the records, the data was smoothed by fitting a nine point least squares parabola (Chapter 6) to the data.

Briefly, once the data were smoothed, and the reference point determined, the program followed through a logical procedure which enables clinically pertinent amplitudes and time intervals to be determined. The recognition sequence first locates the Q, R and S wave peaks. Next, the P wave peak, onset of P wave, and baseline are determined. Finally, the T wave peak is determined along with the onsets and ends of the P, Q, R, S and T waves and the results of the recognition sequence printed out on an electric

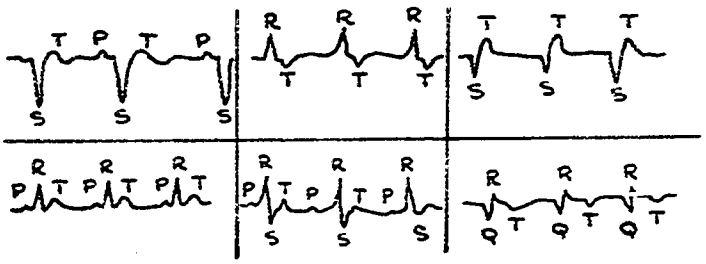

Figure 5.2

Examples of some ECG signal waveforms

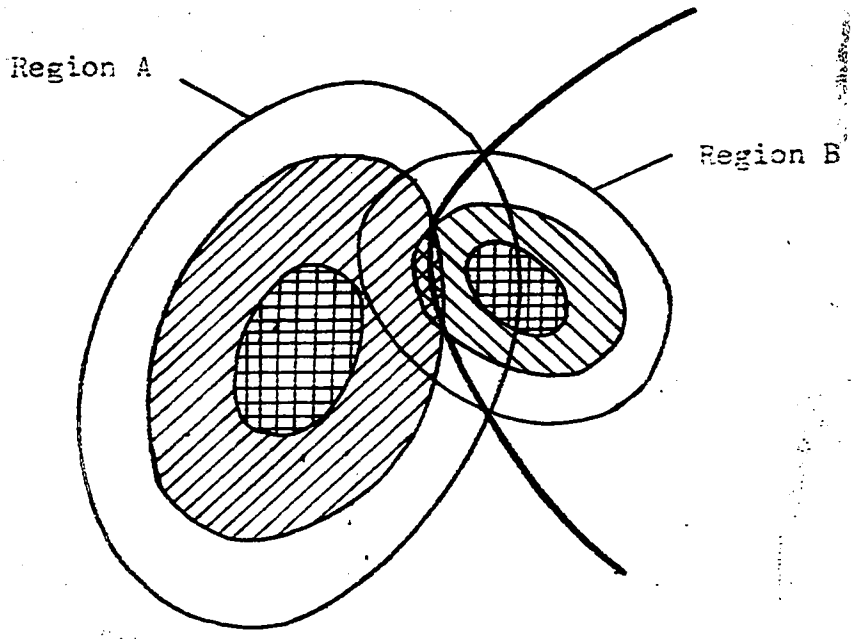

Figure 5.3

Separation of two overlapping ranges of spatial vectors on the basis of their frequency density distribution.

typewriter. Appendices 1 and 2 of (28) list and describe the rules and definitions used for measurements and the logic of recognition.

Having developed the pattern recognition program Caceres et al used multi-dimensional probability density functions to perform, using the digital computer, statistical analyses on the measured parameters in order to characterize and permit classification of the ECG records into normal and abnormal categories. Previously, the statistical analyses had been carried out using measurements manually derived from ECG, BCG, PCG, and AP (arterial-pulse) records (5~~-7~~, 5~~-10~~a, 5~~-10~~6). The pattern recognition program enables measurements on the ECG to be obtained automatically. In future work, Caseres et al intend to develop pattern recognition programs for the other types of cardiac recordings.

Caseres et al, and Pipberger et al make use of a likelihood-ratio test in their programs for statistical analyses of various parameters. Statistical analysis is a tool for use with the "classification" problem in the signal analysis concepts referred to in Chapter 1.

To digress briefly from the main theme of this chapter, this investigation is primarily concerned with the "representation" problem in that attention is being focused on reviewing the methods and techniques currently in use in clinical and research work in the display or representation of ECG signals. The evaluation of which method of representation is optimal or best is not attempted. The classification problem is of secondary interest and consequently little attention is devoted to statistical analysis methods. The "best representation" implies that a choice has been made with respect to some criterion. The criterion for choosing the parameters of wave amplitudes ratios, durations, etc. is that of diagnostic usefulness

in clinical work. Using another criterion, these parameters may not be the best. Thus, the "representation" problem consists of two complementary parts, namely, finding the best representation with respect to a specific criterion. The classification problem may or may not play a role in the evaluation of the representation.

In spite of the fact that the "classification" problem and statistical analysis are of secondary interest, it is worthwhile to discuss the likelihood ratio briefly. Once the distribution of pertinent parameters has been described in terms of means, variances, and covariances, the problem arising in diagnostic classification can be explained with reference to figure 5.3. The goal in classification is the differentiation between normal and abnormal.

Figure 5.3 shows two overlapping ranges of, say, spatial vectors, together with the probability density distribution. The ranges of spatial vectors are typically three-dimensional ellipsoids. The concentration of spatial vectors decreases with increasing distance from the mean in the center of the ranges (indicated by shading in figure 5.3). The position of a spatial vector to be classified is given with respect to its distance from the means and the density of the distribution at the position. A vector that occurs in the region of overlap may be equidistance from the two means but the probability of its belonging to one of the two groups may be greater due to the fact that the distribution density at the point is not the same for both cases. The use of the likelihood-ratio test enables the classification to be effected on the basis of the frequency density-distribution functions. In figure 5.3, the two ranges are shown as being separated by a curved surface (indicated by a heavy solid line) based on the relative frequency density distributions. For an unknown case, the probability of the spatial vector belonging to region B is

greater when it falls on the concave side of the separating surface. On the convex side, the probability of belonging to region B is lower than that of belonging to region A. Obviously, the optional parameters will be those that give the best separation between normal and abnormal.

Returning to the main theme of our chapter now, the work of Pipberger et al, following the initial pattern recognition program development phase, covers a more broad spectrum than that of Caceres et al (5-4, 13). In addition, to statistical analyses performed on the spatial ventricular gradient, and polar and instantaneous vectors (5-12, Chapter 2 - Footnote [1], 5-15) Pipberger et al reported on work falling under the "variety of records" classification mentioned earlier. For example, spatial magnitude, orientation (azimuth and elevation) and velocity curves were calculated (IBM 7090 computer)(12, 13, 5-15) and plotted by means of a digital X-Y plotter. Pipberger gives one illustration of the curves for the QRS interval which exhibits a specific abnormality. He does not qualify why the P and T waves were neglected in spite of the fact that polar vectors (see below) for the P and T loops were obtained along with the QRS polar vector.

In addition to the spatial magnitude etc., Pipberger et al investigated polar vectors and eigenvectors which are related to the coordinate rotation concepts (see Chapter 2 re coordinate resolvers) developed from the observation that the VCG loop in three-dimensional space is essentially planar for the QRS complex in normal subjects, figure 5.4. The polar vector[1]

---

[1]The polar vector in three dimensional space is equivalent to Einthoven's manifest QRS vector in the frontal plane which has been shown to be of diagnostic value.

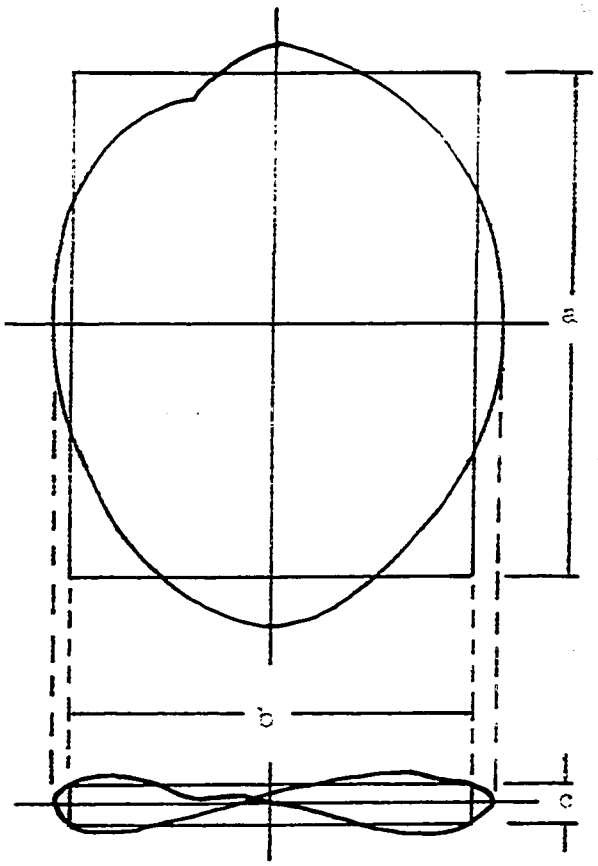

Figure 5.4

Diagrammatic representation of a QRS loop in "broadside" projection (upper diagram). The projection in the lower diagram is obtained after rotation of the QRS loop by 90° which results in an "edgewise" view. The mutually perpendicular axes a, b, and c represent three eigenvectors forming and orthogonal reference frame based on the spatial orientation and configuration of the loop. Eigenvector c is identical with the polar vector, which is perpendicular to the QRS plane.

which is perpendicular to the QRS vector loop, characterizes the orientation of the plane. The configuration of the loop is characterized by three mutually perpendicular "eigenvectors" which form an orthogonal reference system based on the spatial orientation of the QRS vector loop rather than on body axes. Two of the eigenvectors, figure 5.4, give an indication of the length and width of the vector loops, and the third gives an indication of the deviations from the QRS plane.. This latter eigenvector is identical to the polar vector.

The optimal fit between the vector loop and a plane is obtained by choosing the plane which has the smallest mean square deviation from the loop. This procedure, used in factor analysis, is known as the eigenvalue or eigenvector problem. The solution consists of three extreme values of mean square deviations, the eigenvalues, with three corresponding eigenvectors. The advantage of such an analysis is that the results are independent of extraneous factors such as heart orientation and body build.

Finally, in a short paper (5.16 → 77), von der Groeben et al describe the details of programming a digital computer to effect the cartesian to spherical coordinate transformation for the QRS interval, figure 3.5. This work represents an extension of previous work by von der Groeben on spherical coordinate transformations obtained by using tables and graphical methods (5.17 → 78, 5.18 → 79, 5.19 → 80).

Another investigation of interest is that due to Okajima, Stark, Whipple and Yasui (5.20 → 81, 5.21 → 82) dealing with a new approach involving pattern recognition techniques. The study uses a digital computer program employing a multiple adaptive matched filter system in an attempt to simulate human interpretation of ECG's more closely as compared to the

programs developed by Caceres et al, and Pipberger et al as discussed earlier in this chapter. Caceres et al and Pipberger et al have restricted their programs to automatically measuring a few preselected features or parameters of the ECG signal. By using multiple adaptive matched filters in a pattern recognition and classification program, Okajima et al, attempt to simulate the human recognition and diagnostic process more closely by attempting to consider the fact that a human is capable of focusing attention (distorting the information metric) on a small detail which would ordinarily be ignored by any system using a fixed number of parameters. In effect, the new approach to the pattern classification process provides for the generation of new dimensions.

CHAPTER 6

PREPARATION OF ELECTROCARDIOGRAPHIC DATA FOR PROCESSING BY DIGITAL COMPUTER

Summary

The following chapter describes and comments on the pertinent features of the recording equipment used to obtain an electrocardiogram recording, the enlarging, and digitizing of this analog record. The establishment of a baseline and the smoothing of the record is considered. Mention is made of the accuracy and repeatability of the data where possible. In order that this chapter serve as a reference for future work, as many details as possible have been given.

The electrocardiograph strip chart record is an analog record and so does not lend itself for direct presentation to a digital computer input. Furthermore, although measurements can be made on the ECG waveform to a sufficient accuracy for clinical purposes, (that is, for qualitative analysis), the degree of accuracy is not sufficient if the data is to be processed by a digital computer and useable results obtained (that is, for quantitative analysis) (14, p. 22; ~~6.6~~ 83). Consequently, the analog information must be converted to a format appropriate for use with the digital computer.

The x, y, and z components of the heart vector were simultaneously recorded as functions of time using an Electronics for Medicine cathode ray oscilloscope monitoring and recording equipment. This equipment is provided with two cathode ray tubes; one for monitoring on a 12 cm high screen and one for recording the display on 12 cm wide photosensitive paper. The recording CRT is a two gun tube. One gun produces the display of up to seven traces plus a baseline in conjunction with an electronic switch operating at 24,000 cycles/sec. The second gun produces the timing lines. Time lines may be spaced at 1, 0.2, 0.1, 0.04 and 0.02 sec.. Paper speeds of 2.5, 25 and 75 mm/sec are available.

Figure 6.1 shows a recording taken at a paper speed of 75 mm/sec. with timing lines at 40 m sec. intervals. The recording shows considerable 60 cycles/sec. interference and a rather wide trace width. Though this is not the best quality of record obtainable, this recording will illustrate the details which will have to be given careful and patient attention to make the preparation of the data into digital format as expedient as possible. One heart beat (cycle) was picked from such a record and a slide (reduced by approximately 0.8) mounted between glass plates was obtained. With the aid of a slide projector, an image of

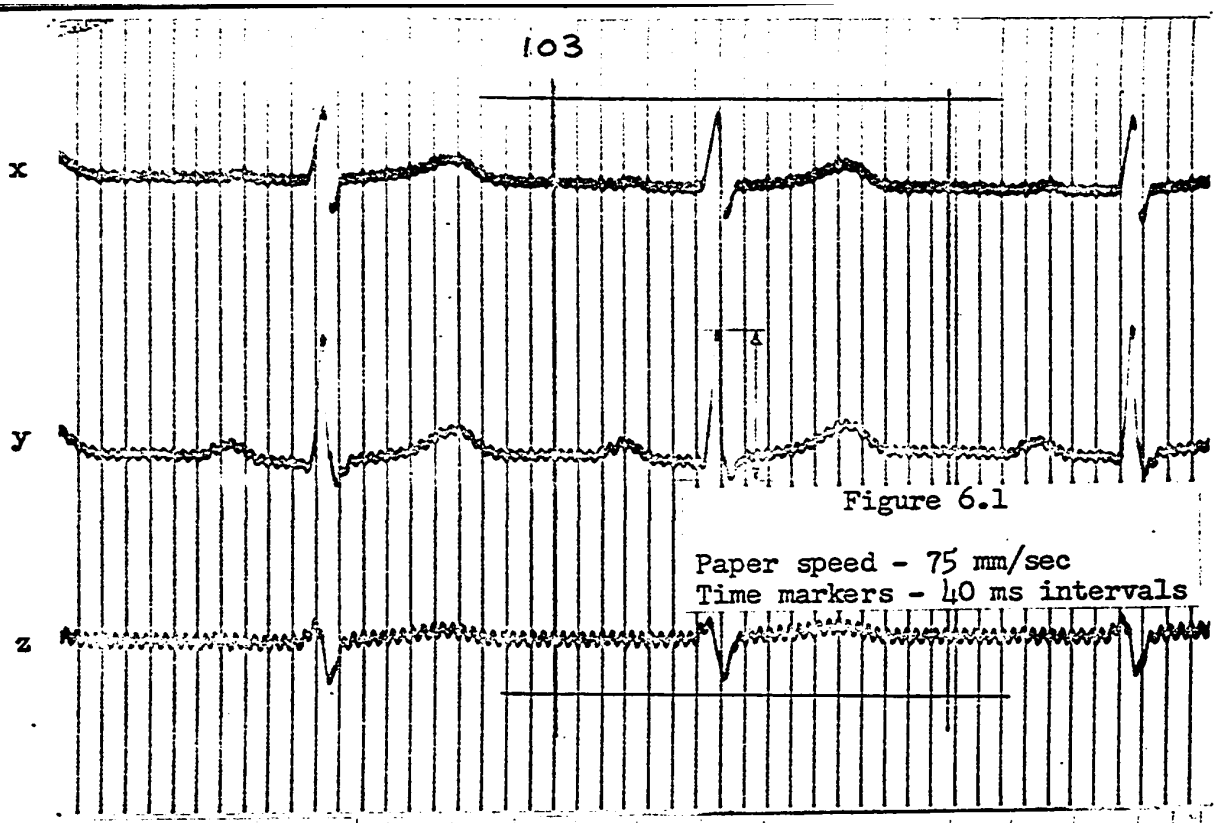

Figure 6.1

Paper speed - 75 mm/sec
Time markers - 40 ms intervals

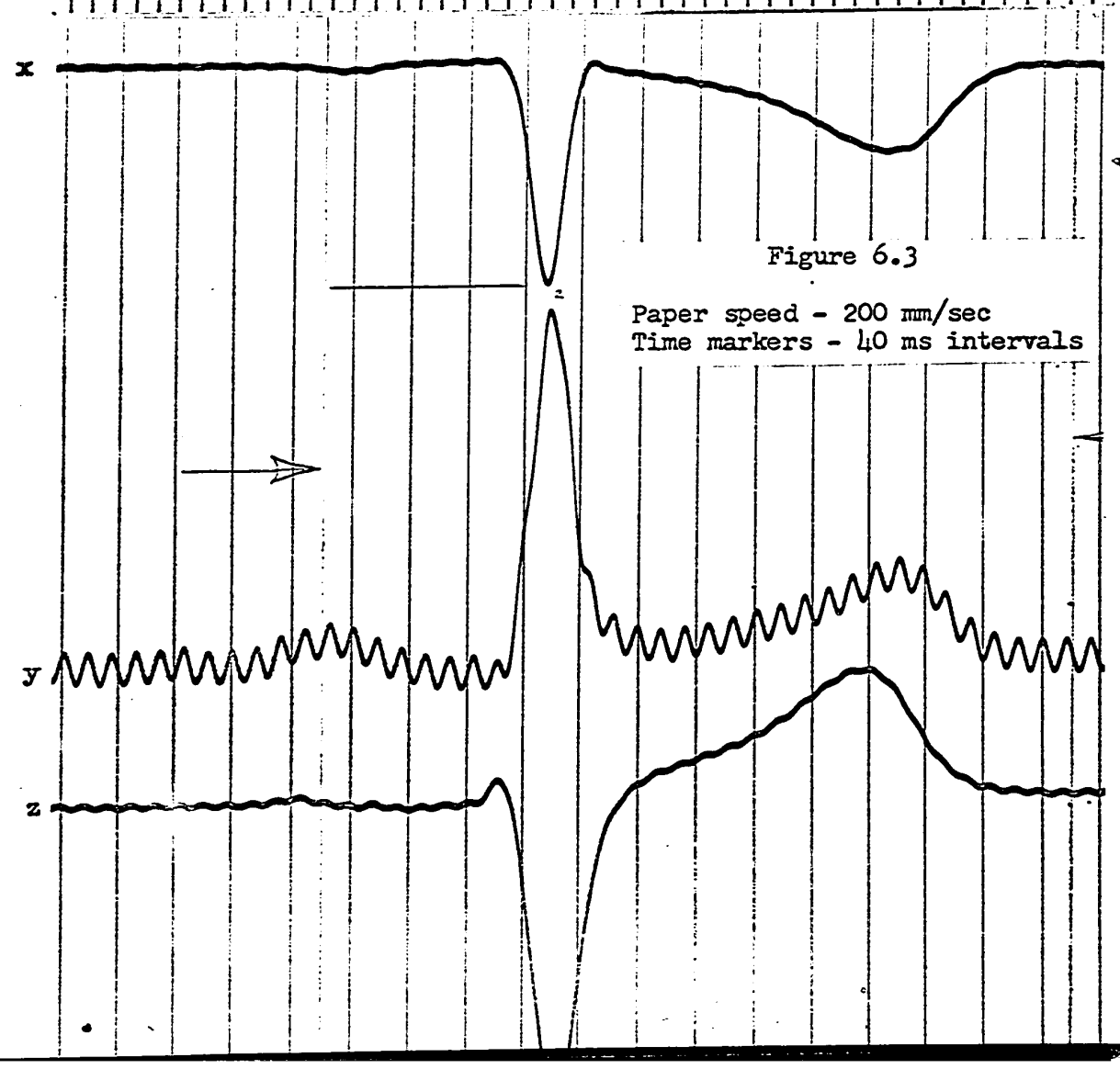

Figure 6.3

Paper speed - 200 mm/sec
Time markers - 40 ms intervals

Figure 6.2

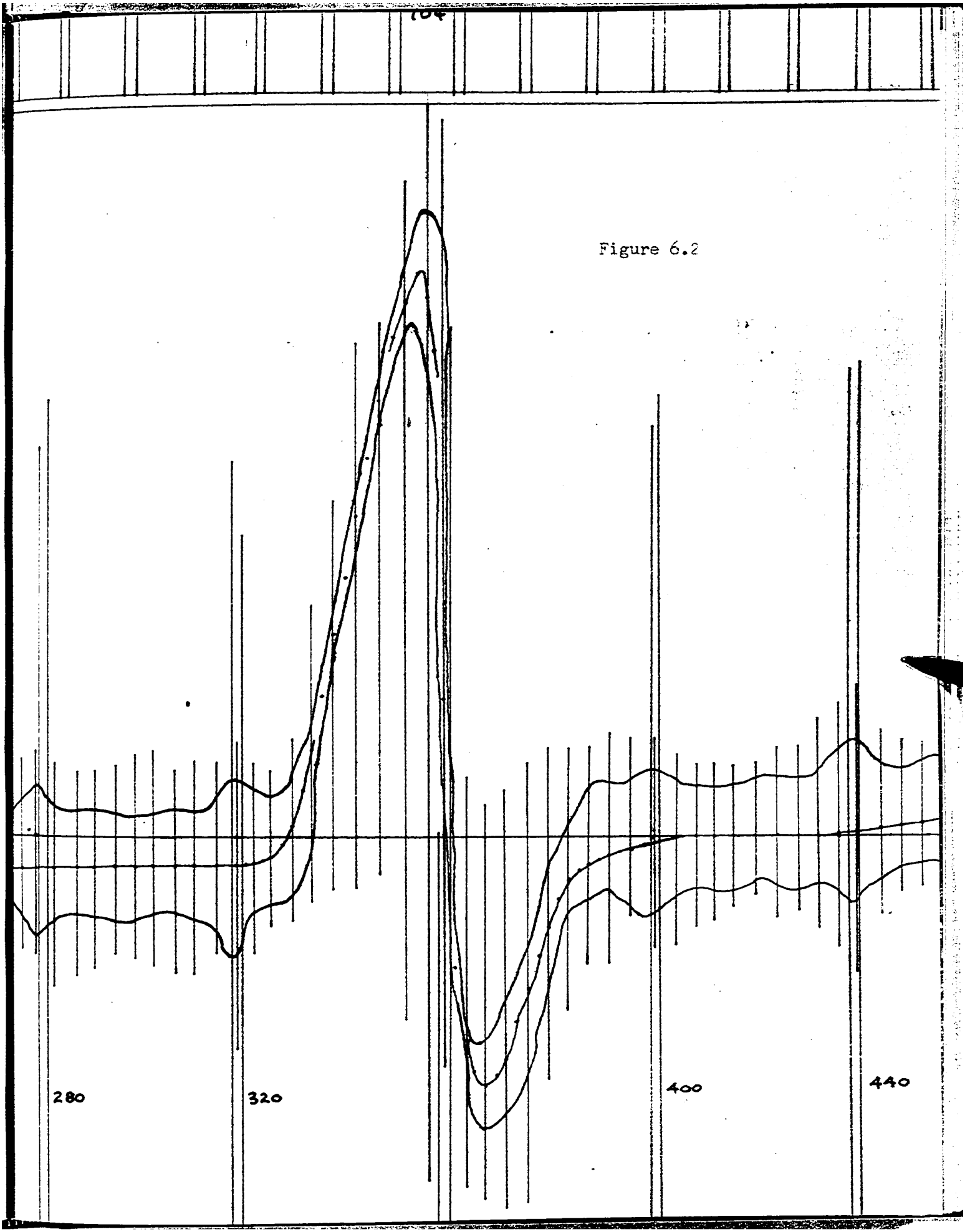

approximately 15 times magnification over the original record was traced onto a 42" X 52" sheet of tracing paper. This procedure enabled the 40 m sec timing intervals (approximately 40 mm wide) to be subdivided into 10 parts and amplitude measurements made every 4 m sec (4 mm spacing) for the P and T waves, and 2 m sec (2 mm spacing) for the QRS complex, using a scale graduated in mm. A portion of the enlarged x component is shown full size in figure 6.2.

The enlarged tracing modulated with 60 cycles/sec (2½ cycles per 40 m sec interval) interference was smoothed manually. This was done by sketching in the centerline of the trace width and simultaneously smoothing out the 60 cycles/sec ripple. The smoothing process retains the essential attributes of the waveform and eliminates (filters) the ripple and noise. Figure 6.2 illustrates the necessity for discriminate focusing of the display, commensurate with trace intensity, to allow enlarging without obtaining a trace that is impractically wide or of insufficient darkness. Figure 6.3 shows a record taken with an improved and more versatile Electronics for Medicine multi-trace cathode ray monitor and recorder. The paper speed used was 200 mm/sec. Figure 4 shows a portion of the x component of figure 6.3 in full size after approximately 6 times magnification and indicates the improvement in trace darkness and trace width resulting from improved focusing and intensity control.

The baseline for each of the 3 traces was established by determining the center line of the trace width during the interval between the end of the T wave and the onset of the P wave for two such intervals one beat (cycle) apart (14, Appendix 1, p. 26; 5.6, Appendix 1, p. 361; 5.12, p. 131). The center lines were then connected with a straight line. (sighting along the trace from the edge of the paper is helpful in establishing the base-

line.) From the baseline, amplitude measurements were made at time intervals of 2 m sec and 4 m sec as mentioned above. The region between the T and P waves corresponds to the interval when the heart is electrically quiet (region of least voltage fluctuations) and so establishes the isoelectric point of a vectorcardiogram and the origin of the xyz coordinate system. The amplitude measurements were recorded in the form of a numerical table in a format expedient for punching IBM cards. The beginning of the heart beat was taken at the onset of the P wave. (t = 180 on graphs in Chapter 7).

The data was remeasured on two separate occasions. The repeatability of the measurements was within 0.5 mm except for 17 out of a total of 423 amplitude measurements (141 samples per trace). Of these 17 points, only 2 points, both on the maximum slope of a QRS complex, exceeded a 2 mm discrepancy. (The discrepancy was 4.5 mm). These discrepancies in the repeatability of the data have negligible effect on the essential character of the waveform.

The percent precision to which an amplitude measurement can be made will vary with the magnitude of the sample. The measurements made during the P and T waves are precise to about 1 part in 20 or 5% and those made during the QRS interval are precise to about 1 part in 100 or 1%. The overall precision of the data is approximately 3% (weighted root mean square deviation error (~~6.7~~ 8.4)).

The enlargement from which figure ~~4~~ 6.4 was taken was obtained through a local reproduction firm. A semi-transparent sheet of Herculene film (Keuffel and Esser) with a 10 to the inch grid overlaid over such an enlargement would eliminate the tedium and drawing errors associated with retracing a projected slide and subdividing the time intervals, etc. Once a baseline is defined and the time calibration lines on the enlargement

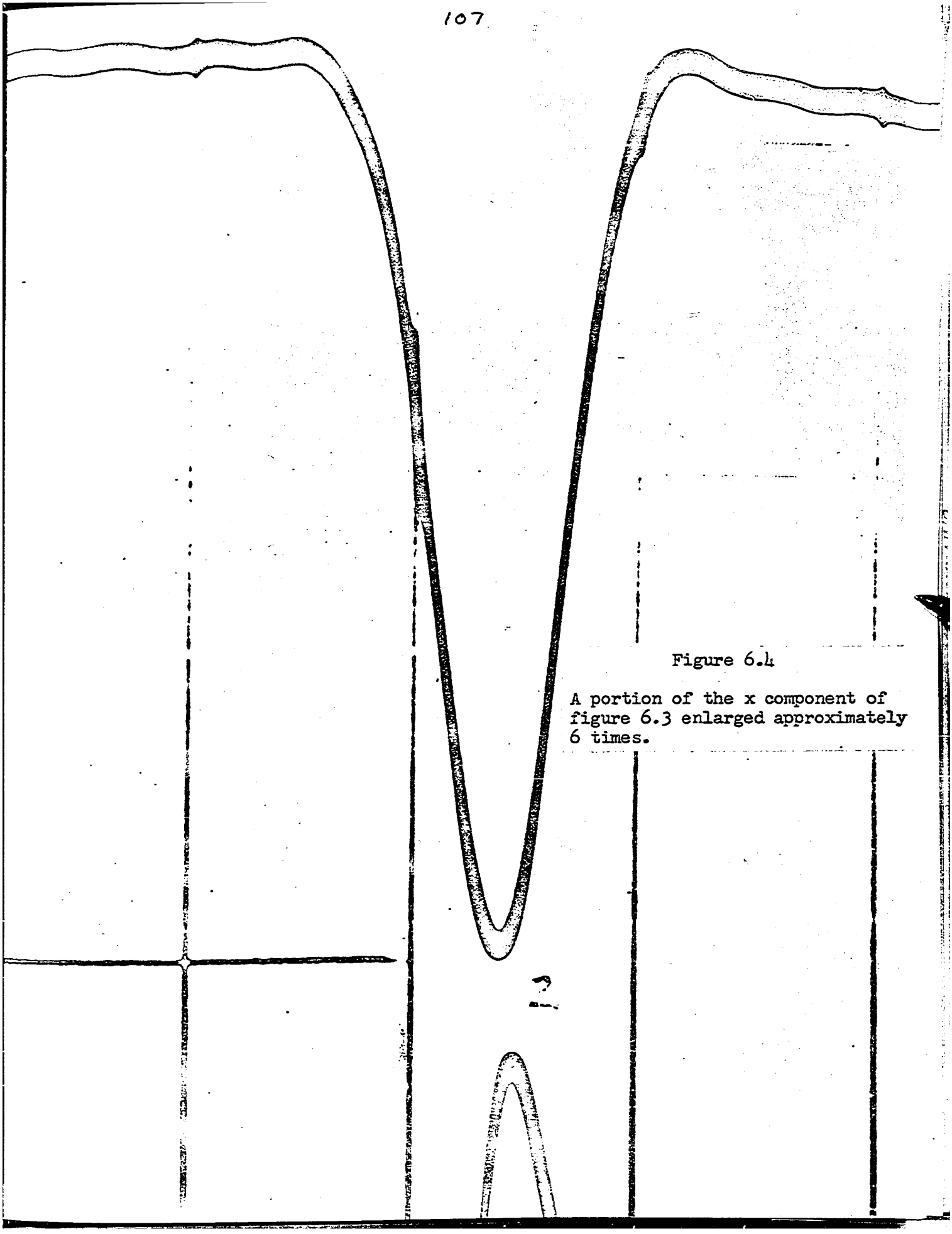

Figure 6.4

A portion of the x component of figure 6.3 enlarged approximately 6 times.

are a convenient distance apart, say 2", readings could be made directly from the overlaid grid at 2 m sec intervals. All drawing procedures would thus be eliminated. With time lines at a 4" separation, readings could be made at 1 m sec intervals. A two man team of one reader and one recorder would expedite the process of digitizing. The above manual technique is inexpensive in that costly equipment is not required but it suffers from the disadvantage of being tedious and time consuming.

The manual procedure is prohibited if a large number of subjects is to be examined. In this case the digitizing process should be performed automatically using commercially available analog-digital converters. A flow chart of an automatic digitizing system might appear as in figure ~~5~~ 6.5. The ECG leads attached to the subject would feed a 3 channel (a 4th channel is advisable for recording subject history and identification information) FM magnetic tape recorder. Suitable amplification or coupling circuits would be provided between the leads and the recorder. The magnetic tape record could then be transported (or transmitted over telephone lines) to an analog-digital converter and a digital computer facility for processing. Careful attention would be required in the design of the interfaces between the ECG leads and tape recorder, recorder and converter, converter and computer. The output of the computer could be plotted automatically on a digital plotting board (13) or cathode ray tube display (~~6.0~~ 85).

Recent workers have performed the digitizing process using analog-digital converters to a claimed accuracy of 1 part in 1000. Sampling rates of up to 1000 samples/sec have been used. Typically, a normal heat may beat from 60 to 100 times/minutes. With samples taken at 1 m sec intervals, 1000 to 600 samples would be required per heart beat for each lead.

The use of an analog-digital converter requires that a smoothing pro-

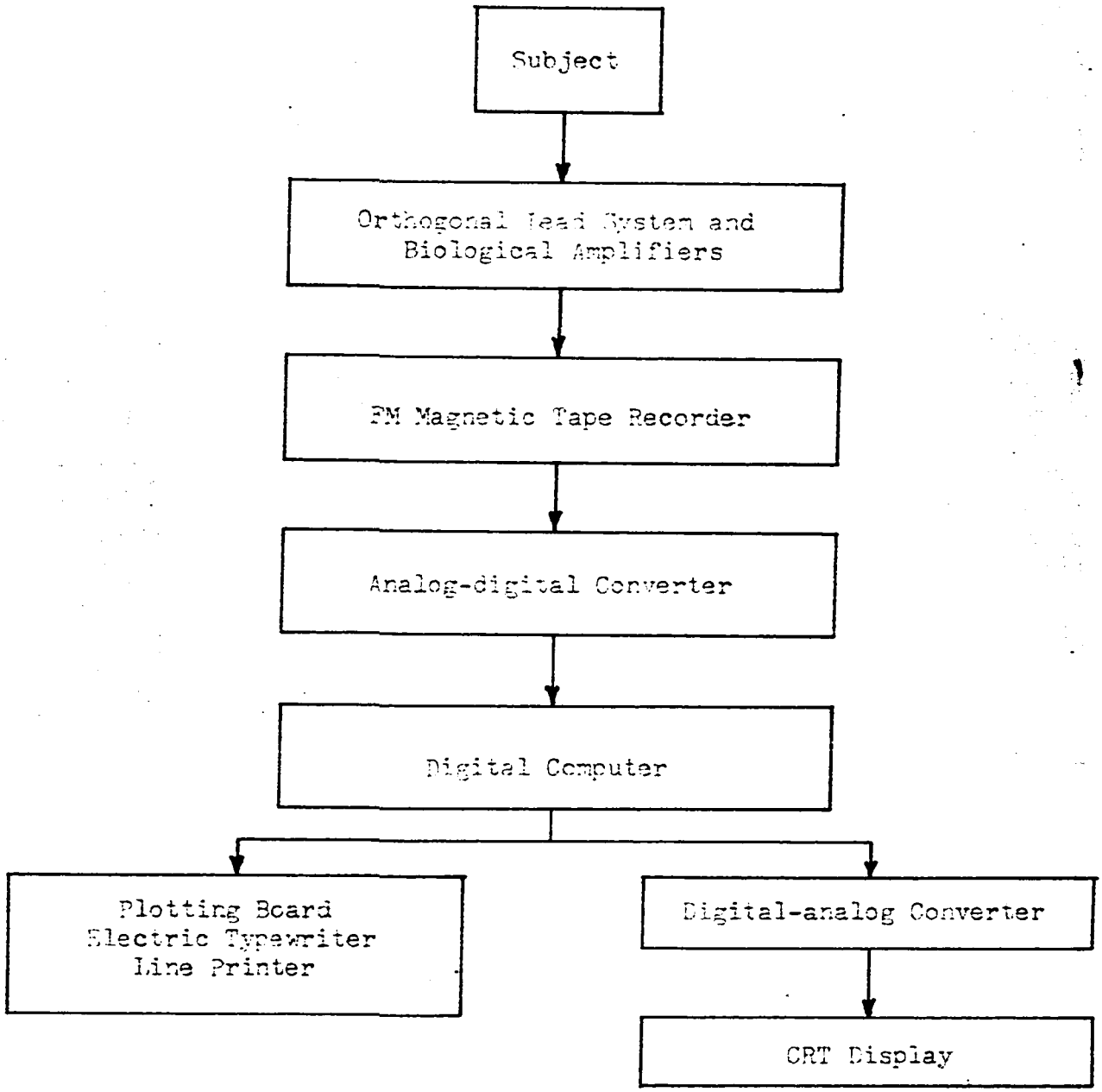

Figure 6.5

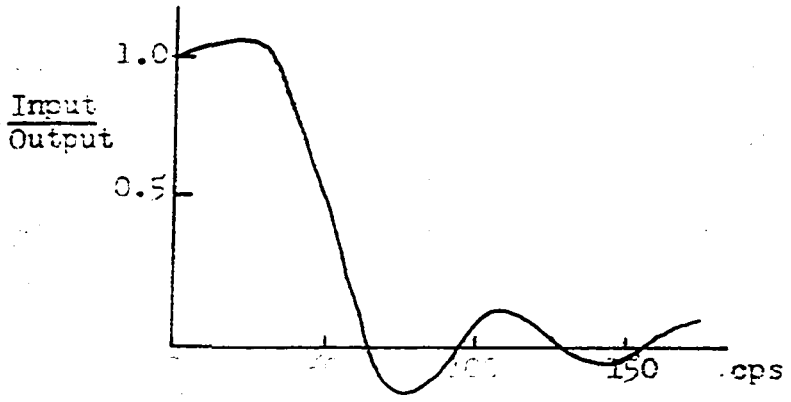

Figure 6.6

cess be carried out as the initial step in a computer program in order to eliminate 60 cycle/sec ripple and noise and retain only the essential character of the waveform in subsequent processing. Caceres et al (28, ~~5.106~~ 74) used nine point least-square parabolic smoothing (sampling rate 625/sec and digitized to 1 in 1000.) The parabola is defined so as to minimize the mean square difference between the parabola and the ECG samples at the corresponding points. In choosing the number of samples to which a parabola is to be fitted, a compromise between elimination of noise and retaining the essential attributes of the waveform ~~smoothing~~ (signal degradation) must be made. That is, the degree of smoothing increases as more ECG samples are taken in determining the parabola which best fits the samples and the degradation of the data increases with an increase in the number of points taken. The value of the parabola at the center point is retained for the smoothed data. This smoothing technique has the advantage that once the coefficients of the parabola $y = a_o + a_1x + a_2x^2$) have been obtained, the first and second derivatives are readily determined ($\frac{d^2y}{dx^2} = 2a_2$) from these coefficients. The choice of using a least squares parabolic smoothing over that of a moving average smoothing was made by Caceres et al since they found that for the same degree of smoothing, the moving average did not eliminate as much background noise as desired without degrading the signal. Pipberger et al (11) used a moving average smoothing or filtering process (see figure ~~6~~ 6.6) (sampling rate 1000/sec, digitizing accuracy not quoted). For every time point, the computer evaluates an average over the samples within a certain time interval and so achieves a smoothing, that is, eliminates higher frequencies. As the number of averaged samples increases, a point is reached where averaging over a longer interval results in severe signal degradation in that the amplitudes and characteristic peaks of the signal are attenuated (12, p. 556). Their determination of the frequency spectrum

of the ECG signal and noise indicated the signal to noise ratio was high below and low above 60 cycles/sec. An essential part of the noise resulted from 60 cycles/sec and its higher harmonics. As a result of the filtering, 60 cycles/sec and higher frequencies were effectively filtered out. The filtered signal was used for determination of time intervals during the heart cycle. Such a filtered signal would not be appropriate for any high-fidelity ECG studies. Pipberger et al retained the original unfiltered ECG signal in all further analyses to ensure the presence of high frequency components which might have been suppressed by the filter.

CHAPTER 7

A COLLECTION OF DISPLAYS OF ELECTROCARDIOGRAPHIC SIGNALS FOR ONE SUBJECT

Summary

The following chapter[1] presents the results of processing x(t), y(t), z(t) on an IBM 650 computer facility at the University of Ottawa to obtain the cartesian to spherical coordinate transformation, rate of change of magnitude, rate of change of angles, linear velocity, and angular velocity of the heart vector. To the author's knowledge, no one has reported all the above curves simultaneously for one subject. Furthermore, angular velocity has been discussed only briefly by Brinberg (26).

[1] As suggested in the summary of Chapter 4, it may be helpful for the reader to review the material in the Appendix, if he has not already done so, before reading this chapter.

In most of the recent literature reporting on spherical coordinate transformations, velocity and magnitude curves etc. obtained using digital techniques, only the QRS complex is discussed and the P and T waves are disregarded with no direct justification for this restriction being mentioned. (for example, see 12, 16 and 5, 76). Possibly, one could imply from this that the P and T waves are relatively uninteresting in comparison to the QRS complex, or that the accuracy of measurements and calculations deteriorates in the P and T wave intervals. In their work on applying signal theory to the ECG signal, Huggins and Young restrict themselves to the QRS and T intervals but qualify their point of view by noting that the P, QRS and T intervals each correspond to distinctly independent events in each cycle of heart activity (7, 86, p. 91).

Huggins and Young were interested mainly in obtaining an efficient, discrete set of parameters to characterize the main attributes of an ECG waveform in a manner that lends itself for processing and statistical evaluation on a digital computer. As their work is the first attempt at applying signal theory to ECG waveforms, their point of view in restricting themselves to the QRS and T intervals is justified, if only because they attempt to qualify their point of view.

The calculations performed to obtain the curves described below were carried out over one complete heart beat[2] for two reasons. Firstly, the curves will provide a basis for evaluating the usefulness of the desired displays and give quantitative information in evaluating design details for an analog computer system. Secondly, the author, because

---

[2]The problem of whether to consider the complete heart cycle or restrict one's attention to a portion of it is a fairly good example of the controversial nature of many aspects of ECG and VCG theory.

of his limited background in the field of ECG and VCG theory and related topics, cannot justify restricting calculations to a specific interval of the ECG signal. Intuitively, it would seem reasonable to treat one complete heart cycle until the restriction to a particular interval can be unquestionably qualified.

After preparation of the original ECG analog record as described in Chapter 6, the data was punched onto IBM cards and processed by an IBM 650 computer using appropriate programs. The x(t), y(t), z(t) components of the heart vector (Frank lead system) are shown in figures 1, 2 and 3 respectively. Selecting the components of the heart vector in pairs, the VCG loops were plotted[3] and are shown in figures 4, 5 and 6.

Spherical Coordinates

Figures 7, 8 and 9 show the magnitude $|r(t)|$, the elevation (latitude)[4] $\theta(t)$, and the azimuth (longitude) $\phi(t)$ respectively of the heart vector as obtained by performing a cartesian to spherical coordinate transformation. Figures 10 and 11 show the azimuth $\alpha(t)$ and elevation $\beta(t)$ respectively as per the convention used by Abildskov[5] (see Chapter 3 and figure A.3 of the Appendix). It is interesting to note that $\alpha(t)$

---

[3]The P and T loops were plotted using samples taken at 20 millisecond intervals and the QRS loop was plotted using samples taken at 2 millisecond intervals, that is, from t = 180 to t = 320 and t = 420 to t = 660, 20 millisecond intervals were used and from t = 330 to t = 388, 2 millisecond intervals were used.

[4]Figure 8a is a plot of the colatitiude or polar angle $\theta_p(t)$ with respect to the y axis.

[5]Figure 10a shows $\alpha(t)$ plotted using a scale running from 0° to 360° continuously rather than 0° to ± 180° as per Abildskov's convention. In figure 10a, 0°(360°) indicates the positive x axis (left), 90° the positive y axis (feet), 180° the negative x axis (right), and 270° the negative y axis (head). The discontinuities at t = 334 and 454 correspond to the frontal plane VCG crossing the positive x axis (y = 0). Figure 11a is a plot of the colatitude or polar angle $\beta_p(t)$ with respect to the z axis.

is a monotonically increasing function over the greater portion of the heart cycle.

It is perhaps worthwhile to compare $\theta(t)$ and $\phi(t)$ with the vector loops plotted from $x(t)$, $y(t)$ and $z(t)$. First of all, it should be mentioned that comparison during the P and T waves around the isoelectric point or origin of the VCG is difficult. Comparison is relatively easy during the QRS interval primarily because the QRS interval is traced out relatively faster and has a greater amplitude than the P and T intervals. Consequently, the time parameter cannot be indicated during the P and T intervals with a precision comparable to that during the QRS interval. Secondly, large errors in angle for very small vectors in the region of the isoelectric point of the VCG are possible. For example, observe the curves for azimuth and elevation, figures 8, 9, 10 and 11, at approximately $t = 660$ towards the end of the T wave where $x(t)$, $y(t)$ and $z(t)$ are approaching zero, figures 1, 2, 3. In future cartesian to spherical coordinate transformation programs written for the digital computer, some attention should be devoted to establishing a threshold for $x(t)$, $y(t)$ and $z(t)$ below which the azimuth and elevation would not be computed.

Consider now $\phi(t)$, figure 9, and compare it with the inferior horizontal VCG loop, figure 6, Starting at $t = 180$ to $t = 200$, $x \simeq 0$ and $z \simeq 0$ so that ϕ is 0°. From $t = 200$ to $t = 240$, z is negative and ϕ changes from 0° to -155° indicating that the heart vector is in the anterior hemisphere (with respect to the frontal plane). Between $t = 240$ and $t = 300$, ϕ remains at approximately -155°. At $t \simeq 318$ the heart vector sweeps across the negative x axis and into the posterior hemisphere. The crossing of the negative x axis creates a discontinuity

in $\phi(t)$ as the scale changes from -180° to $+180^{\circ}$. As the QRS complex initiates, ϕ sweeps from nearly $+180^{\circ}$ at $t \simeq 318$ to 0° at $t \simeq 348$ indicating that the heart vector has swept across the positive x axis at $t \simeq 348$ and again entered the anterior hemisphere. At $t \simeq 360$, figure 9 shows a finite jump corresponding to the rapid fall in amplitude of the QRS complex. At $t \simeq 396$, ϕ again sweeps the negative x axis creating a discontinuity in $\phi(t)$ as discussed above and stays constant at $+90^{\circ}$ in the posterior hemisphere between $t = 404$ and $t = 432$ since $x = 0$ (figure 1) during this interval. ϕ then tapers off to approximately $+30^{\circ}$ during the T wave maximum. The T wave appears as a narrow loop on the VCG's and in the inferior horizontal plane VCG loop has a mean orientation of the order of $+30^{\circ}$.

Consider now $\theta(t)$, figure 8, and compare it with the frontal and left sagittal VCG loops, figures 4 and 5. Starting at $t = 180$, $x = 0$, $z = 0$ and y is positive so that θ is $+90^{\circ}$ below the equatorial (horizontal) plane. Between $t = 220$ and $t = 240$ y changes from positive to negative and correspondingly θ goes negative indicating the heart vector is above the equatorial plane. Between $t = 240$ and $t = 320$ y is negative and θ equals approximately -60°. As the QRS interval approaches, θ crosses to the positive region at $t \simeq 334$ indicating the heart vector is now below the equatorial plane, reaches a value of approximately $+60^{\circ}$ at the peak of the QRS complex, and returns to the negative region at $t \simeq 362$. The heart vector then remains above the equatorial plane until $t \simeq 454$ at which time it drops below the equatorial plane and retains an orientation such that θ levels off at approximately $+50^{\circ}$ during the T wave maximum. The T wave appears as a narrow loop on the VCG's.

Rate of Change of Magnitude

The first derivative[6] or rate of change of $|r(t)| = \frac{d|r(t)|}{dt}$ is shown in figure 12 as calculated using the equation

$$\frac{d|r(t)|}{dt} = \frac{x(t)v_x(t) + y(t)v_y(t) + z(t)v_z(t)}{\sqrt{x^2(t) + y^2(t) + z^2(t)}} \qquad (7.1)$$

This is the slope of the magnitude curve $|r(t)|$, figure 7, and should not be confused with the magnitude of linear velocity shown in figure 16 and calculated using the equation.

$$v(t) = \sqrt{v^2_x(t) + v^2_y(t) + v^2_z(t)} \qquad (7.2)$$

In comparing $|r(t)|$, figure 7, and $\frac{d|r(t)|}{dt}$, figure 12, it is interesting to note the notch in $|r(t)|$ at $t \simeq 362$ is sharply accentuated in $\frac{d|r(t)|}{dt}$, that is, note the sharp negative impulse in $\frac{d|r(t)|}{dt}$ corresponding to the notch in $|r(t)|$. One can readily compare the slope of $|r(t)|$ with $\frac{d|r(t)|}{dt}$ by recalling that the derivative of a function can be considered in terms of the slope of the tangent to the curve at a given point. Thus, for a maximum or a minimum in $|r(t)|$, or if $|r(t)|$ equals a constant value, the tangent to $|r(t)|$ is horizontal and so $\frac{d|r(t)|}{dt} = 0$. For example compare $t \simeq 232$, $t \simeq 356$, $t \simeq 570$ in figures 7 and 12. If $r(t)$ is approaching a constant, $t \simeq 360$ to $t \simeq 300$ in figure 7, then $\frac{d|r(t)|}{dt}$ approaches zero. Also, if the slope of $r(t)$ is positive then $\frac{d|r(t)|}{dt}$ is positive. Similarly, if the slope of

---

6See (87) for the first, and to the author's knowledge, the only published records of the rate of change of magnitude of the heart vector. Abilskov et al obtained the recordings using a special purpose analog instrument built to effect a cartesian to spherical coordinate transformation and perform a differentiation of the magnitude curve. The system frequency response was stated to be 300 cps.

$|r(t)|$ is negative, then $\frac{d|r(t)|}{dt}$ is negative.

Figure 12a indicates the rate of change of magnitude for the QRS interval as calculated from

$$\frac{\Delta|r(t)|}{t} = \frac{|r(t_{i+1})| - |r(t_i)|}{\Delta t} \qquad \Delta t = t_{i+1} - t_i \quad (7.3)$$

where Δt corresponds to the sampling interval and t_i and t_{i+1} the time of occurance of two successive samples. A comparison of figures 12 and 12a indicate that $\frac{d|r(t)|}{dt}$ is somewhat smoothed in comparison to $\frac{\Delta|r(t)|}{t}$. The smoothing in $\frac{d|r(t)|}{dt}$ comes about from the fact that $v_x(t)$, $v_y(t)$ and $v_z(t)$ in equation 7.1 where calculated from x(t), y(t) and z(t) using a Lagrangian interpolation polynomial in the numerical differentiation process (see next section).

Magnitude of Linear Velocity

The first derivative or rate of change of the components of the heart vector[7], that is $\frac{d\,x(t)}{dt} = v_x(t)$, $\frac{d\,y(t)}{dt} = v_y(t)$ and $\frac{d\,z(t)}{dt} = v_z(t)$ are shown in figures 13, 14 and 15 respectively. Figure 16 shows the magnitude of the linear velocity vector

$$|v(t)| = \left|\sqrt{v_x^2(t) + v_z^2(t) + v_z^2(t)}\right| \qquad (7.2)$$

where $v_x(t)$, $v_y(t)$, $v_z(t)$ are the components of the velocity vector in the x, y. z directions respectively. The linear velocity represents the change in spatial displacement between the termini of consecutive heart vectors per unit of time (7.5). The direction of the velocity

[7] See (7.4) for an interesting new approach to studying cardiac electrical activity by means of the magnetocardiogram (MCG) which has the form of the first derivative of the electrocardiogram. Work is currently in progress at the Department of Electrical Engineering, University of Ottawa investigating the feasibility of detecting the magne[illegible] field of the heart by means of a Hall element mounted in the air[illegible] of a high permeability magnetic circuit.

vector is tangential to the spatial vector loop in the direction of motion at the instant in question. In other words, $|v(t)|$ can be considered as the speed (magnitude of velocity) at which the terminus of the heart vector traces out the spatial vector loop or space curve. The units of velocity in figures 13 to 16 are in millivolts/second.

The components of the velocity vector $v_x(t)$, $v_y(t)$, $v_z(t)$ were calculated from x(t), y(t) and z(t) using the Lagrangian method of numerical differentiation (7.5, p. 64; 7.6, p. 85 and p. 93; 7.7). One can readily compare the slope of x(t) with $v_x(t)$, etc. in the same way that the slope of $|r(t)|$ was compared to $\frac{d\,|r(t)|}{dt}$. Figure 13a indicates the rate of change of x(t) for the QRS interval as calculated from

$$\frac{\Delta x(t)}{\Delta t} = \frac{x(t_{i+1}) - x(t_i)}{\Delta t} \qquad \Delta t = t_{i+1} - t_i \qquad (7.4)$$

Recalling the discussion relating to equation 7.3 and comparing figures 13 and 13a one notes that $v_x(t)$ indicates some smoothing in comparison to $\frac{\Delta x(t)}{\Delta t}$ as a result of the Lagrangian numerical differentiation process. The comparisons also indicate that $\frac{\Delta x(t)}{\Delta t}$ and $\frac{\Delta |r(t)|}{\Delta t}$ are reasonable approximations for the first derivatives of x(t) and r(t) respectively. The evaluation of the derivatives by means of equations 7.3 and 7.4 can be considered as an "emperical" calculation in comparison to the evaluation of the derivatives by means of the Lagrangian numerical differentiation method.

To illustrate the difficulty in obtaining higher order derivatives, figure 13b indicates an attempt to obtain the second derivative of x(t) for the QRS interval by evaluating

$$a_x(t) = \frac{\Delta v_x(t)}{\Delta t} = \frac{v_x(t_i + 1) - v_x(t_i)}{\Delta t} \qquad \Delta t = t_i + 1 - t_i \quad (7.5)$$

$a_x(t)$ is the x component of the linear acceleration vector, the magnitude of which could be evaluated from

$$|a(t)| = \left|\sqrt{a_x^2(t) \quad a_y^2(t) + a_z^2(t)}\right| \quad (7.6)$$

The acceleration vector gives the rate of change of (linear) velocity and has the units of millivolts/sec^2. Figure 13b illustrates how taking successive derivatives of a function tends to accentuate the noise in the function differentiated. This could be overcome by smoothing the function to be differentiated prior to carrying out the next higher order differentiation. Thus, to evaluate $a_x(t)$, attention would have to be devoted to smoothing $v_x(t)$ (89, p. 64; 92).

Rate of Change of Angles and Magnitude of Angular Velocity

The rate of change of the azimuth and elevation angles $\frac{\Delta\theta(t)}{\Delta t}$, $\frac{\Delta\phi(t)}{\Delta t}$, $\frac{\Delta\alpha(t)}{\Delta t}$ and $\frac{\Delta\beta(t)}{\Delta t}$ in degrees millisecond are shown in figures 17, 18, 19 and 20 respectively as calculated from the equations

$$\frac{\Delta\theta(t)}{\Delta t} = \frac{\theta(t_i + 1) - \theta(t_i)}{\Delta t} \qquad \Delta t = t_i + 1 - t_i \quad (7.7)$$

$$\frac{\Delta\phi(t)}{\Delta t} = \frac{\phi(t_i + 1) - \phi(t_i)}{\Delta t} \quad (7.8)$$

$$\frac{\Delta\alpha(t)}{\Delta t} = \frac{\alpha(t_i + 1) - \alpha(t_i)}{\Delta t} \quad (7.9)$$

$$\frac{\Delta\beta(t)}{\Delta t} = \frac{\beta(t_i + 1) - \beta(t_i)}{\Delta t} \quad (7.10)$$

These equations are analagous to equations 7.3 and 7.4 which indicate the "emperical" calculation of the first derivative of $x(t)$ and $|r(t)|$ respectively. The discussion above relating to equations 7.3 and 7.4 has indicated that evaluation of the first derivative by "emperical" calculation gives a reasonably good approximation for the first derivative when compared to the evaluation by means of the Lagrangian numerical differentiation method. Thus, it is not unreasonable to use equations 7.7 to 7.10 to evaluate the first derivatives of the azimuth and elevation angles.

The magnitude of angular velocity[8] as calculated by

$$|w(t)| = \left| \sqrt{\left(\frac{\Delta\theta(t)}{\Delta t}\right)^2 + \left(\frac{\Delta\phi(t)}{\Delta t}\right)^2} \right| \qquad (7.11)$$

is shown in figure 21. The units of $w(t)$ are degrees/millisecond. The linear velocity (millivolts/sec) can be thought of as an "orbit Velocity" of a point (terminus of heart vector) tracing out a space curve. In contrast, considering the heart vector now as a "line generator" (one end of the line being at the origin of the reference axes and the other being the terminus tracing out the space curve or spatial vector loop), the magnitude of angular velocity is a measure of the angular speed at which the "line generator" changes its orientation per time unit.

To the author's knowledge, the only mention of the angular velocity of the heart vector in the literature is due to Brimberg (26, p. 44). Brimberg gives only a definition of angular velocity and a brief discussion. Consequently, the results plotted in figures 18 to 21 are probably the first quantitative data obtained on the rates of change of azimuth and

---

[8]The suggestion to obtain the angular velocity in this investigation is due to Dr. F. Berkman.

elevation angles and the magnitude of the angular velocity of the heart vector. The diagnostic usefulness of these displays has yet to be established.

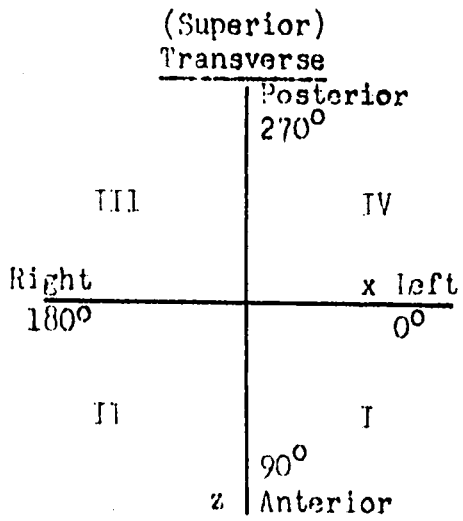

xz Plane
(Horizontal)

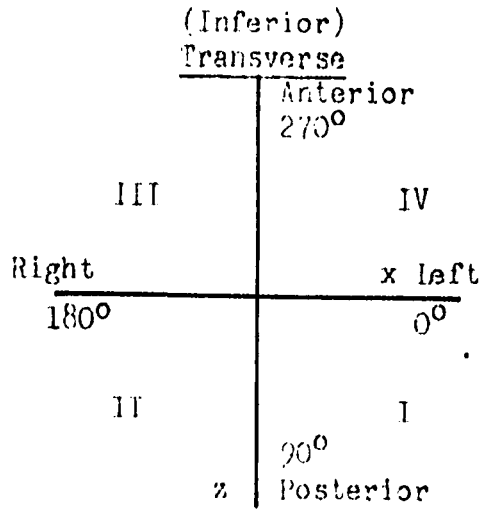

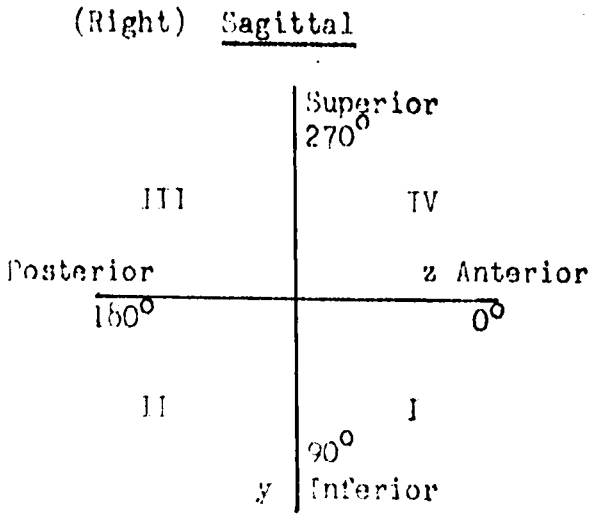

zy Plane

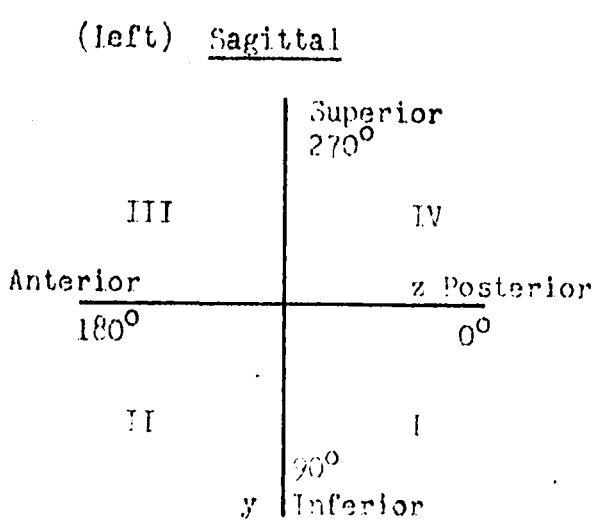

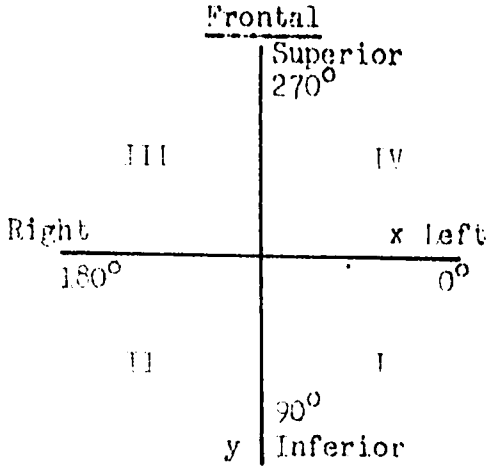

Figure 3.3a

xy Plane

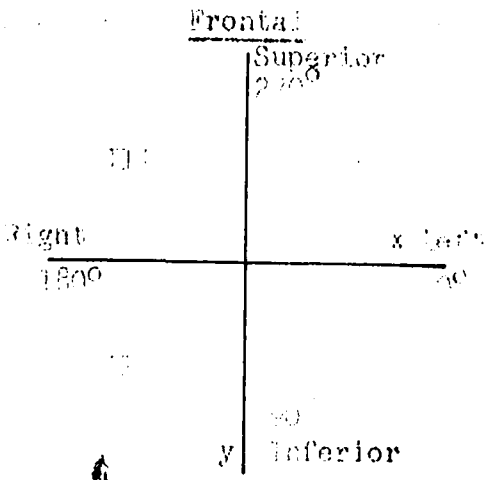

Figure 3.3b

Figures 3.3a and 3.3b are reproduced from reference (44) with additions given in parentheses.
The frontal, sagittal, and transverse planes are represented by the symbols xy, zy, xz, in order that the first term of the paired symbol might designate the reference axis of the respective planes for measuring angles in the clockwise direction.

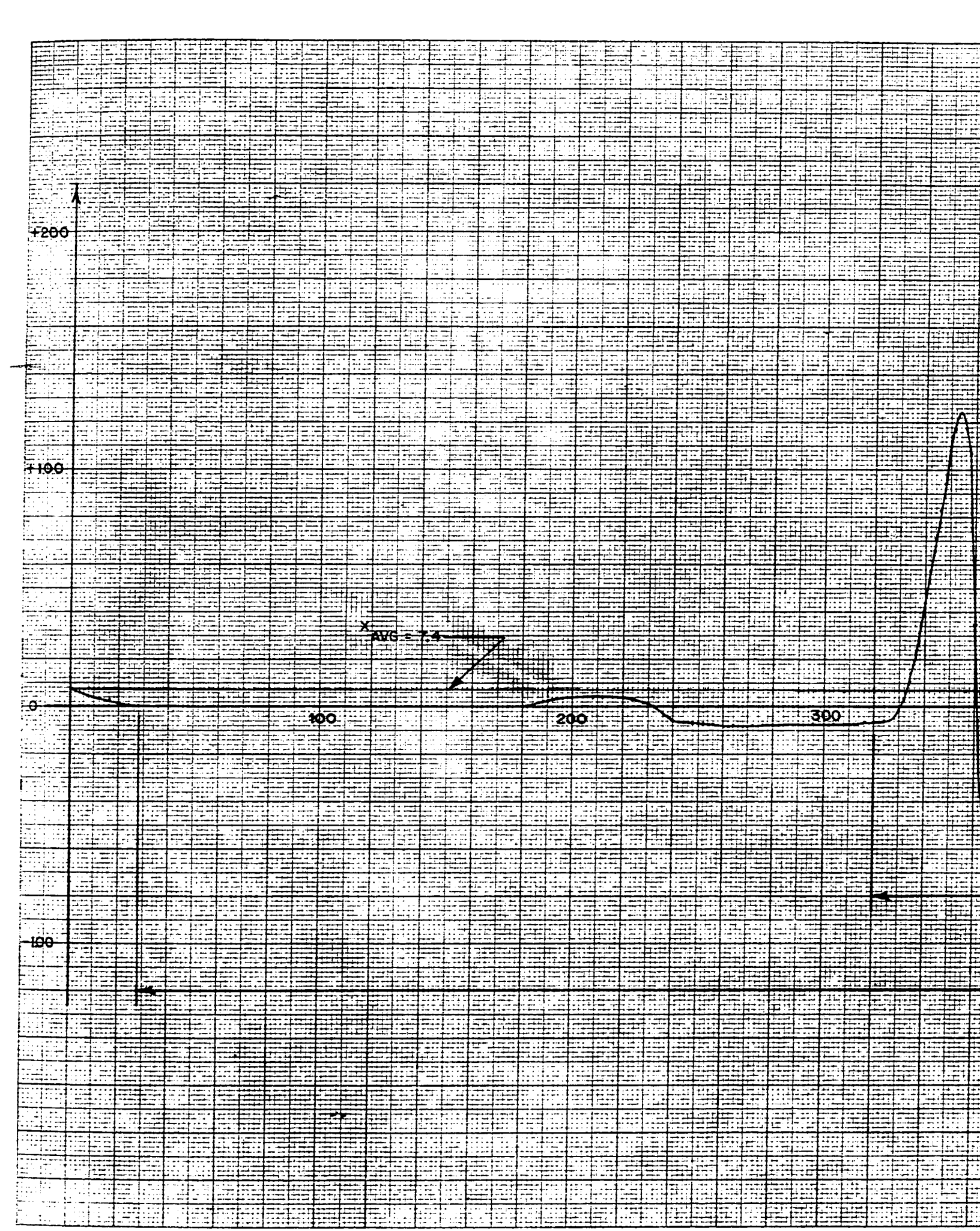
+200
+100
0
-100
100
200
300
X
AVG = 7.4

FIGURE 1

$x(t)$

VERTICAL SCALE 150 = 1 MILLIVOLT

HORIZ. SCALE – 1 CM = 20 MILLISECONDS

PERIOD OF ONE CYCLE = 640 M S

* INTERVALS USED FOR FOURIER ANALYSIS

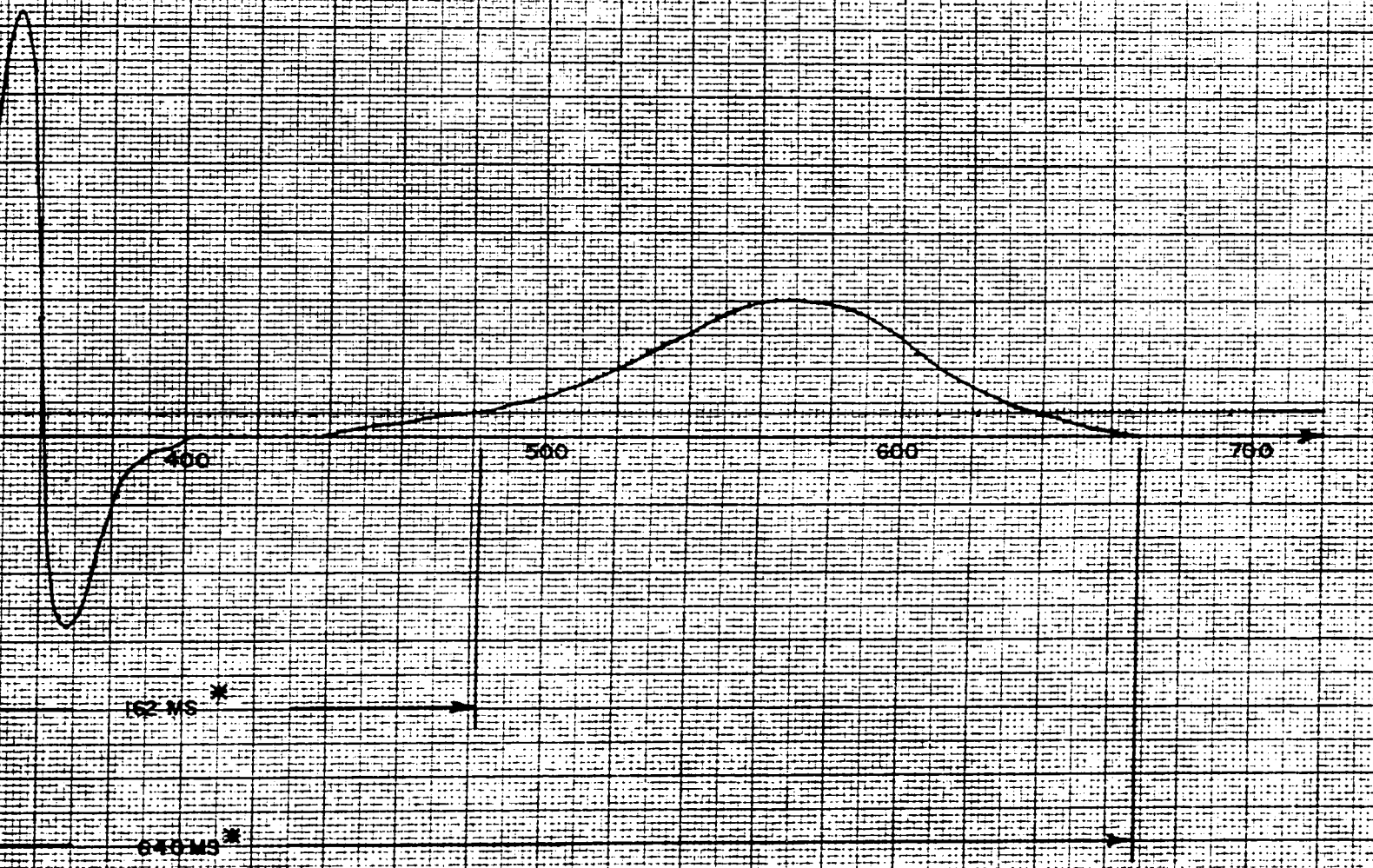

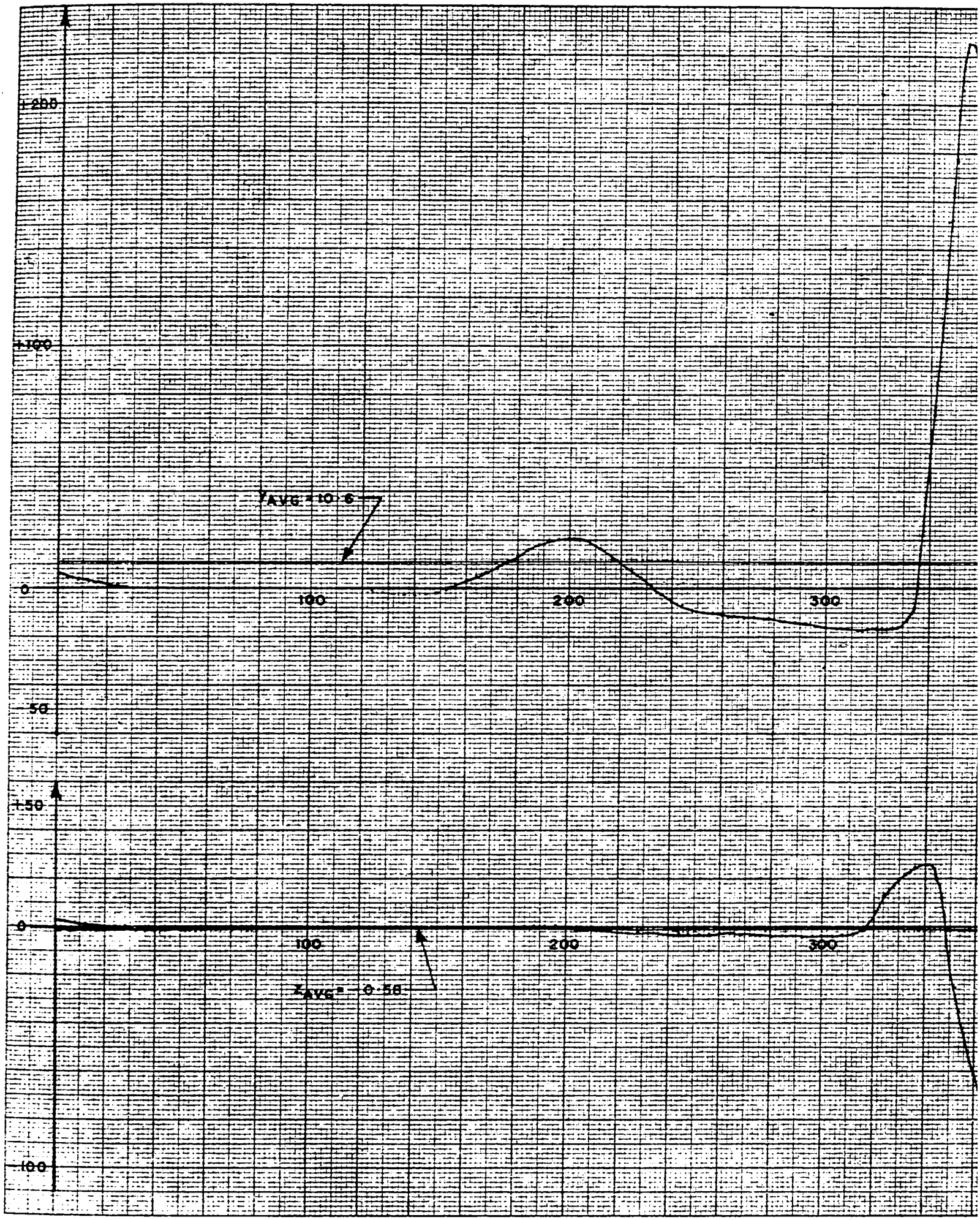
+200
+100
Y_{AVG} = 10·6
0
100
200
300
-50
+50
0
100
200
300
Z_{AVG} = -0·58
-100

FIGURE 2

Y (t)

VERTICAL SCALE — 150 = 1 MILLIVOLT

HORIZ SCALE — 1CM = 20 MILLISECONDS

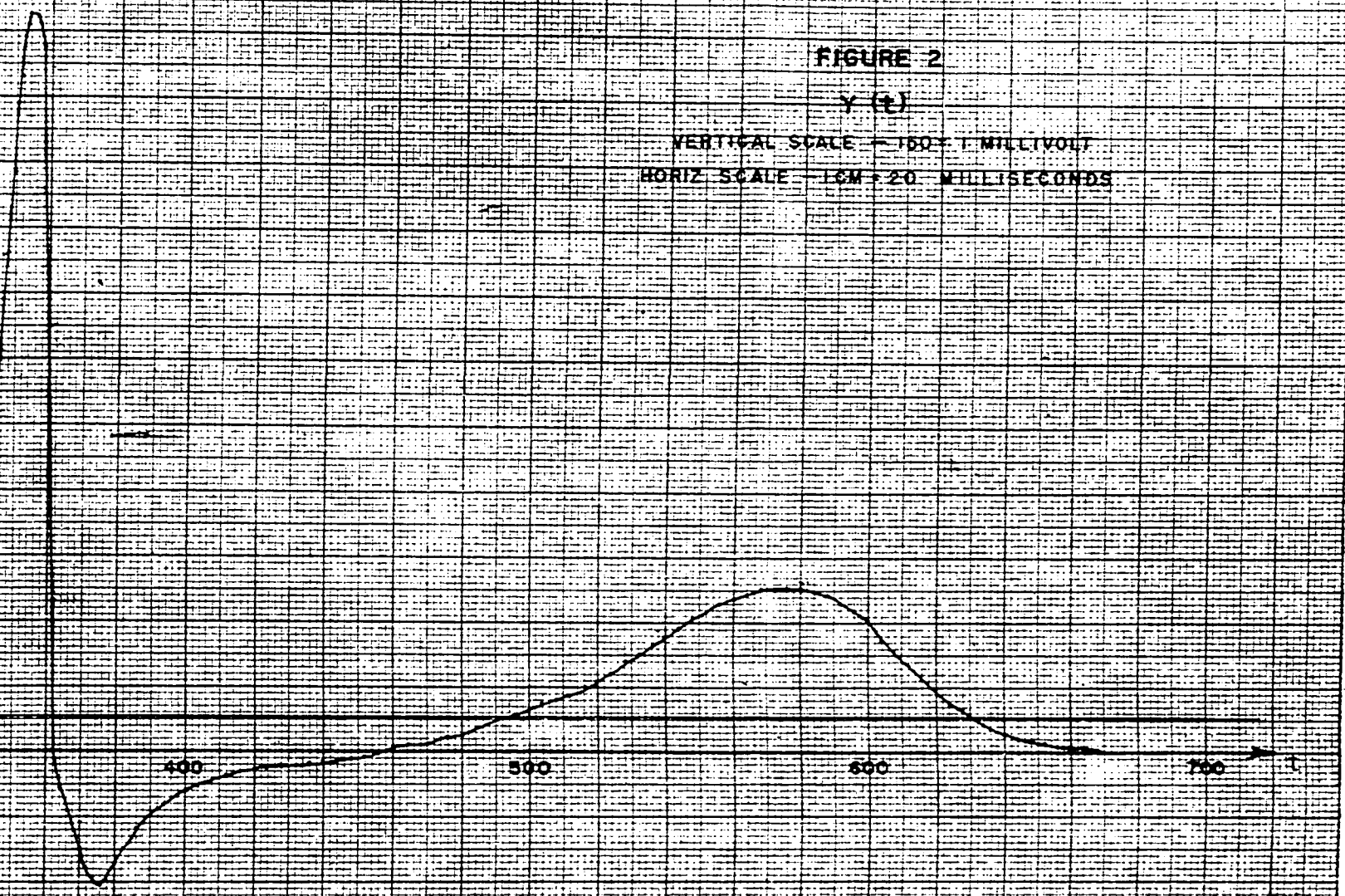

FIGURE 3

Z (t)

VERTICAL SCALE — 150 = 1 MILLIVOLT

HORIZ SCALE — 1CM = 20 MILLISECONDS

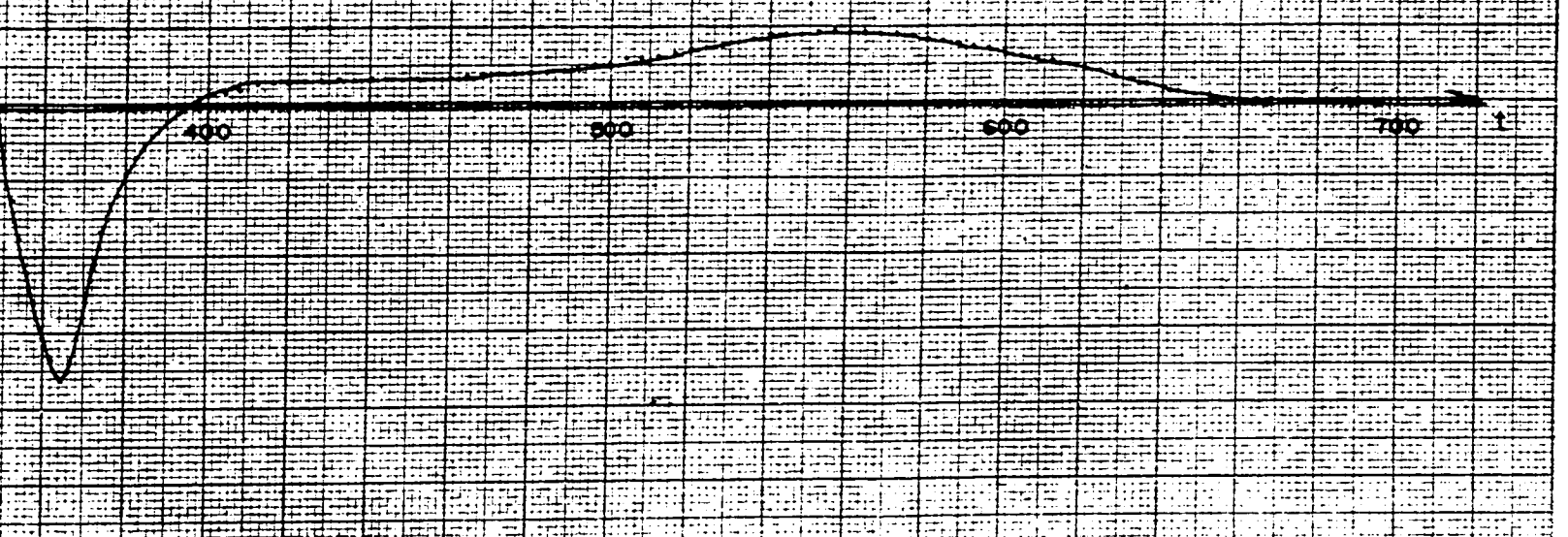

FIGURE 4

FRONTAL PLANE VCG

VERTICAL SCALE = 150 = 1 MILLIVOLT

HORIZ SCALE = 150 = 1 MILLIVOLT

TIME SCALE = MILLISECONDS

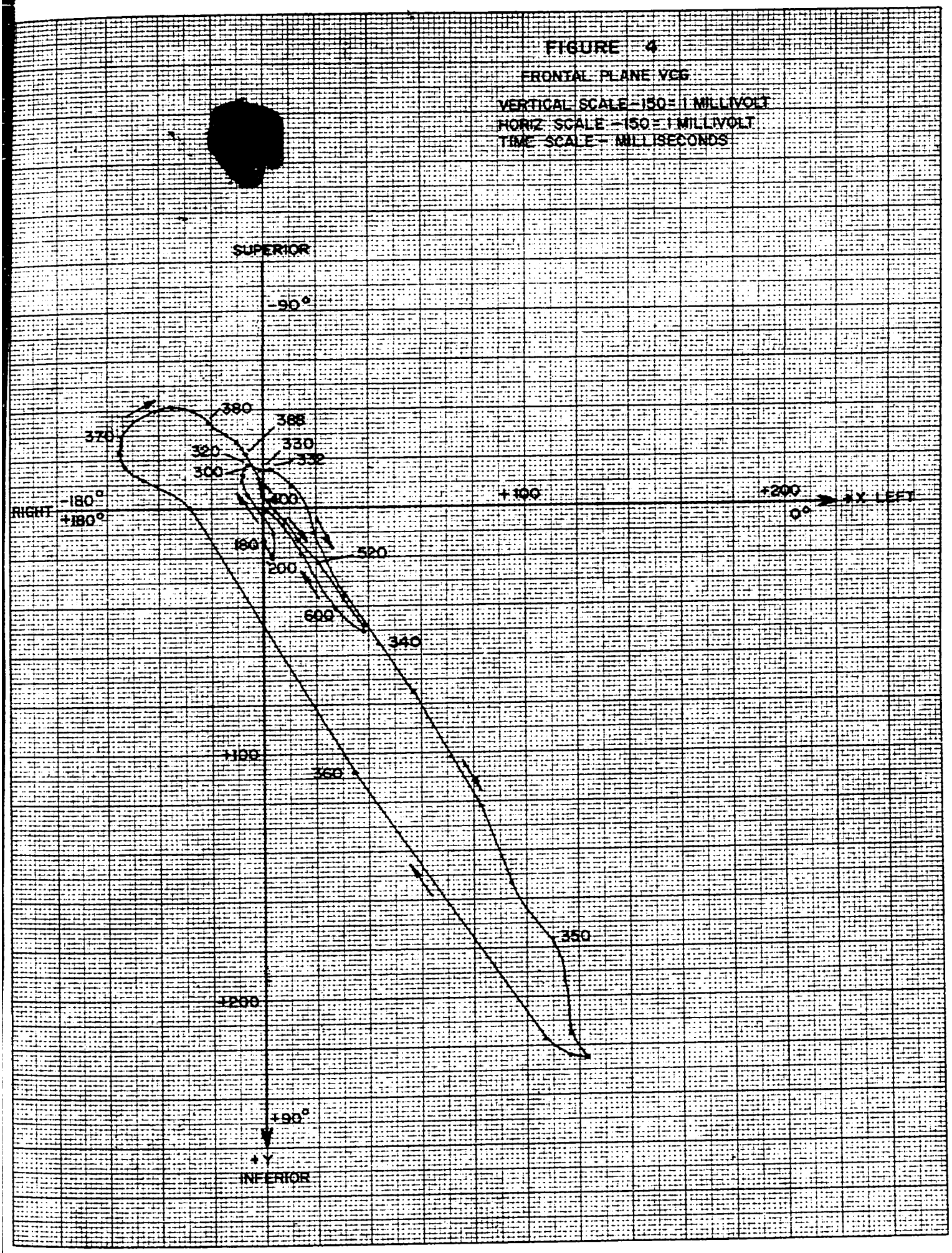

FIGURE 5

LEFT SAGITTAL PLANE VCG
VERTICAL SCALE - 150 = 1 MILLIVOLT
HORIZ SCALE - 150 = 1 MILLIVOLT
TIME SCALE - MILLISECONDS

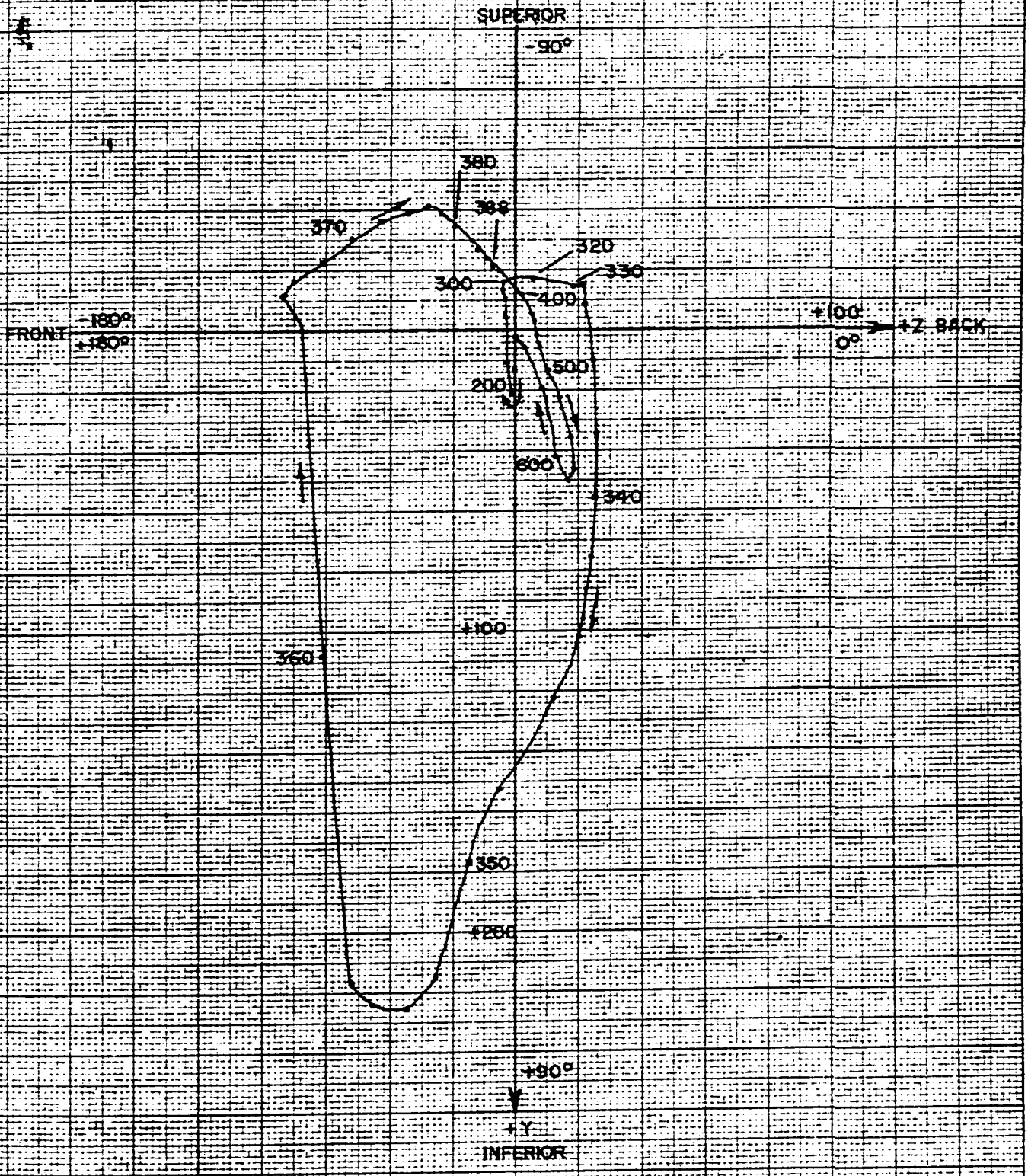

FIGURE 6

INFERIOR HORIZONTAL PLANE VCG

VERTICAL SCALE — 150 = 1 MILLIVOLT
HORIZ SCALE — 150 = 1 MILLIVOLT
TIME SCALE — MILLISECONDS

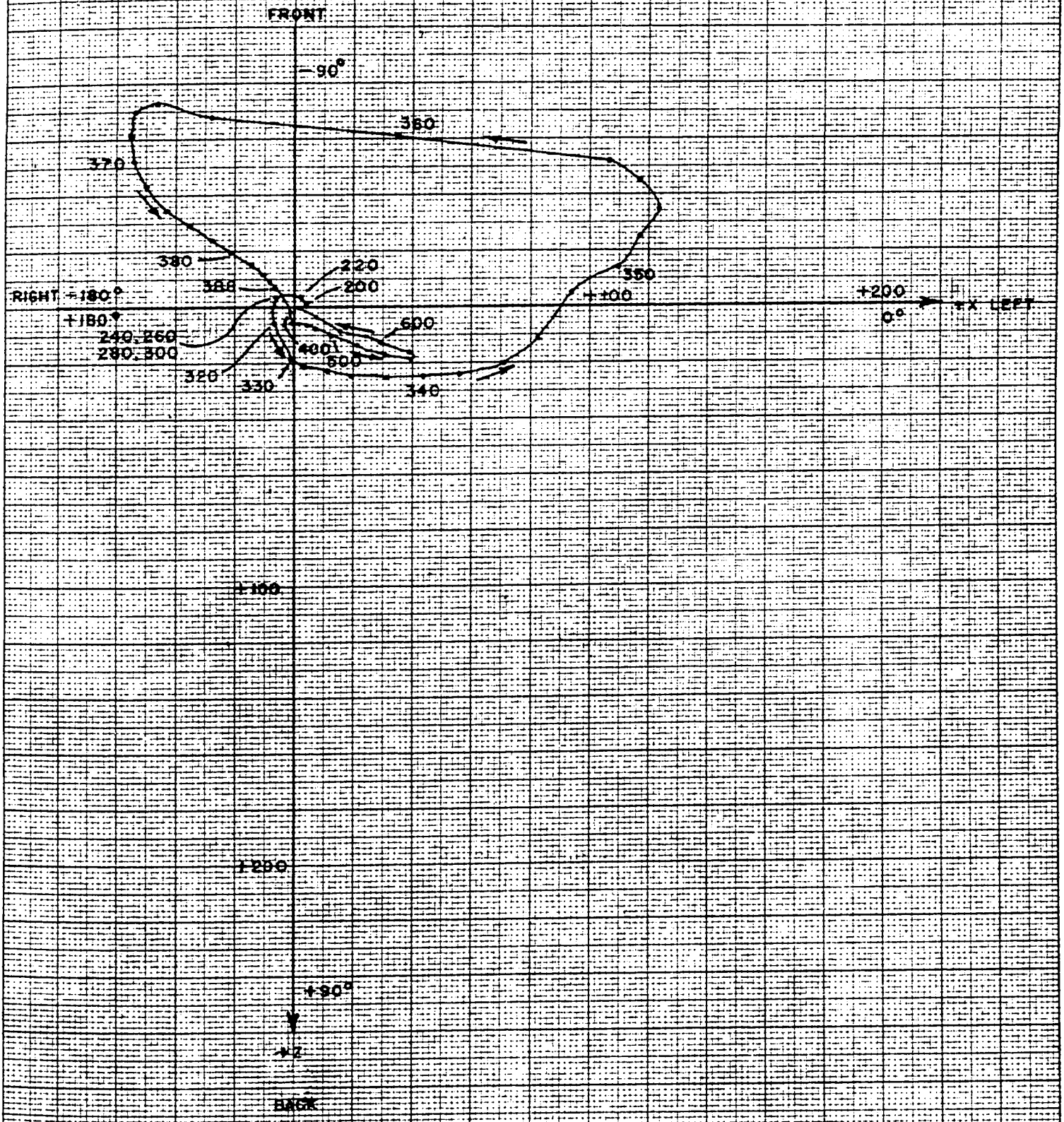

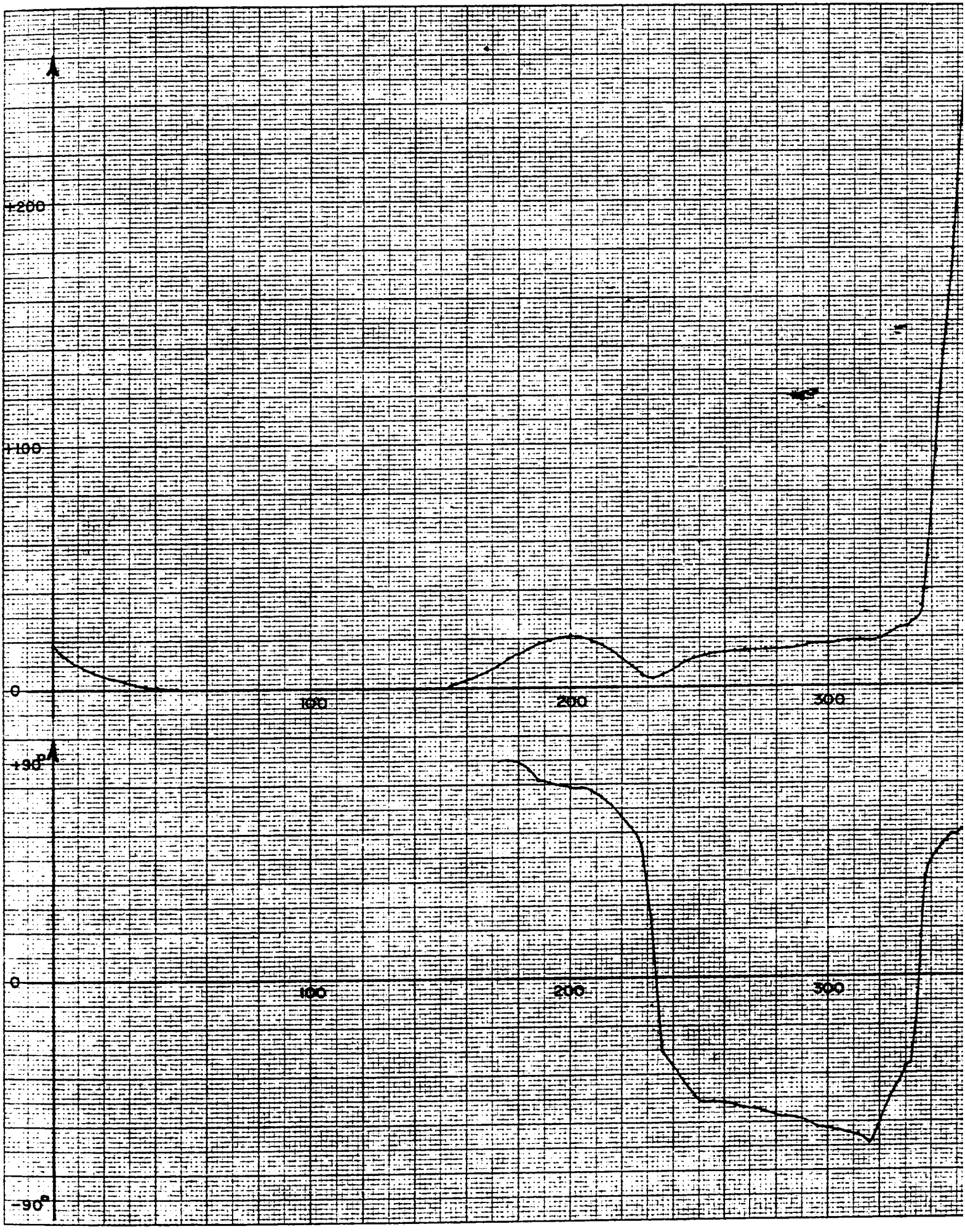
+200
+100
0
100
200
300
+90°
0
100
200
300
-90°

FIGURE 7

$$|r(t)| = \left|\sqrt{x^2(t) + y^2(t) + z^2(t)}\right|$$

VERTICAL SCALE = 150 = 1 MILLIVOLT
HORIZ SCALE = 1 CM = 20 MILLISECONDS

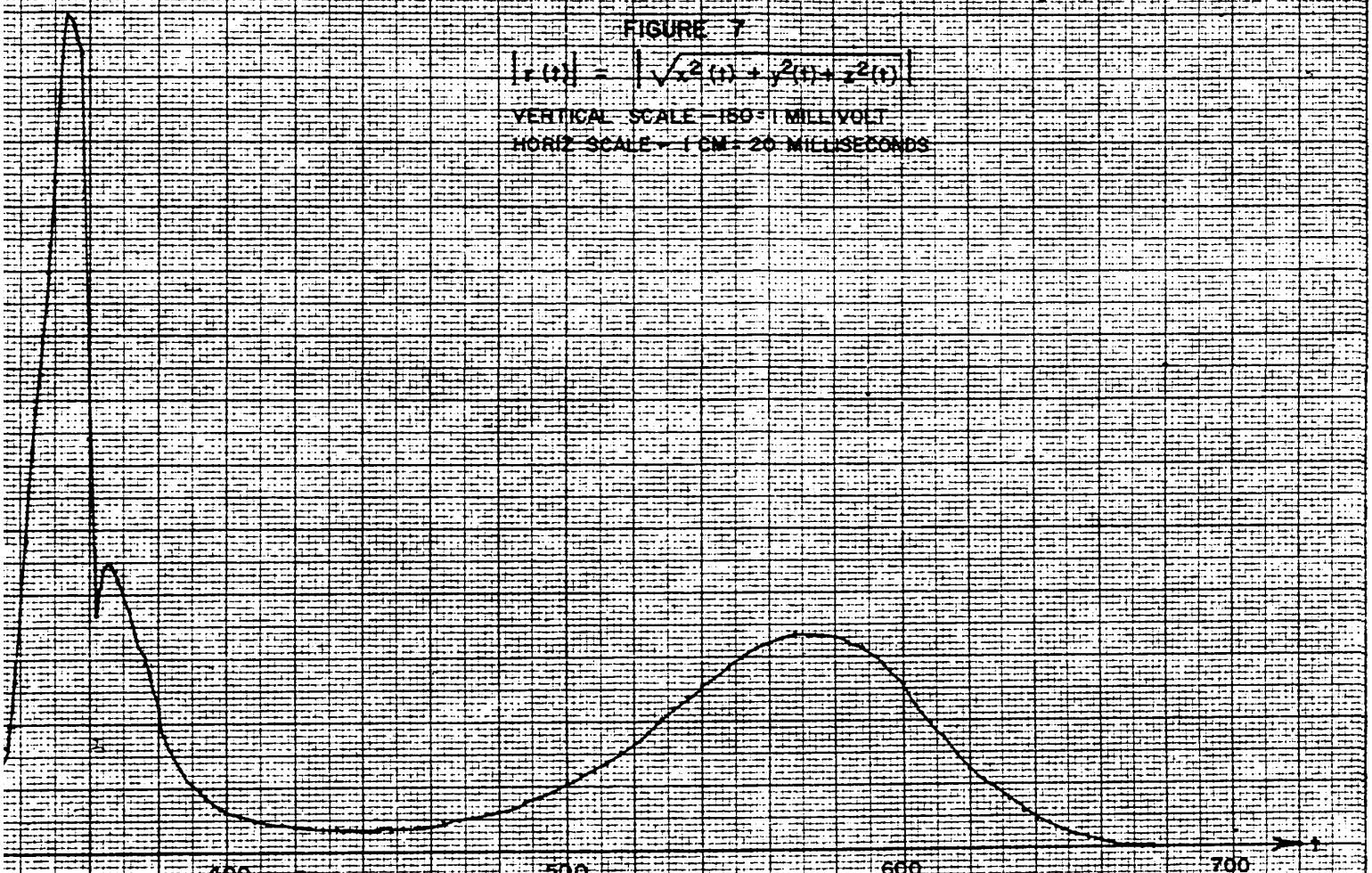

FIGURE 8

$\theta(t)$

VERTICAL SCALE = 1 CM = 20°
HORIZ SCALE = 1 CM = 20 MILLISECONDS

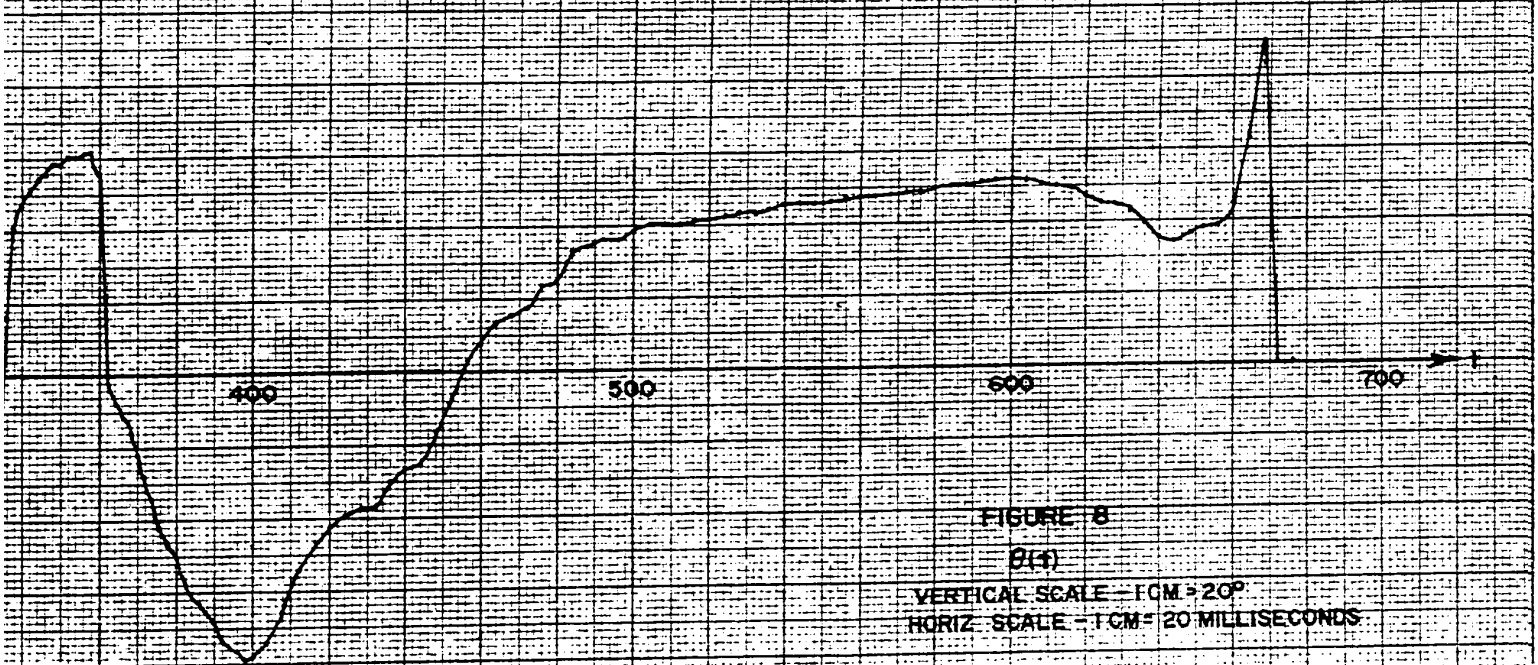

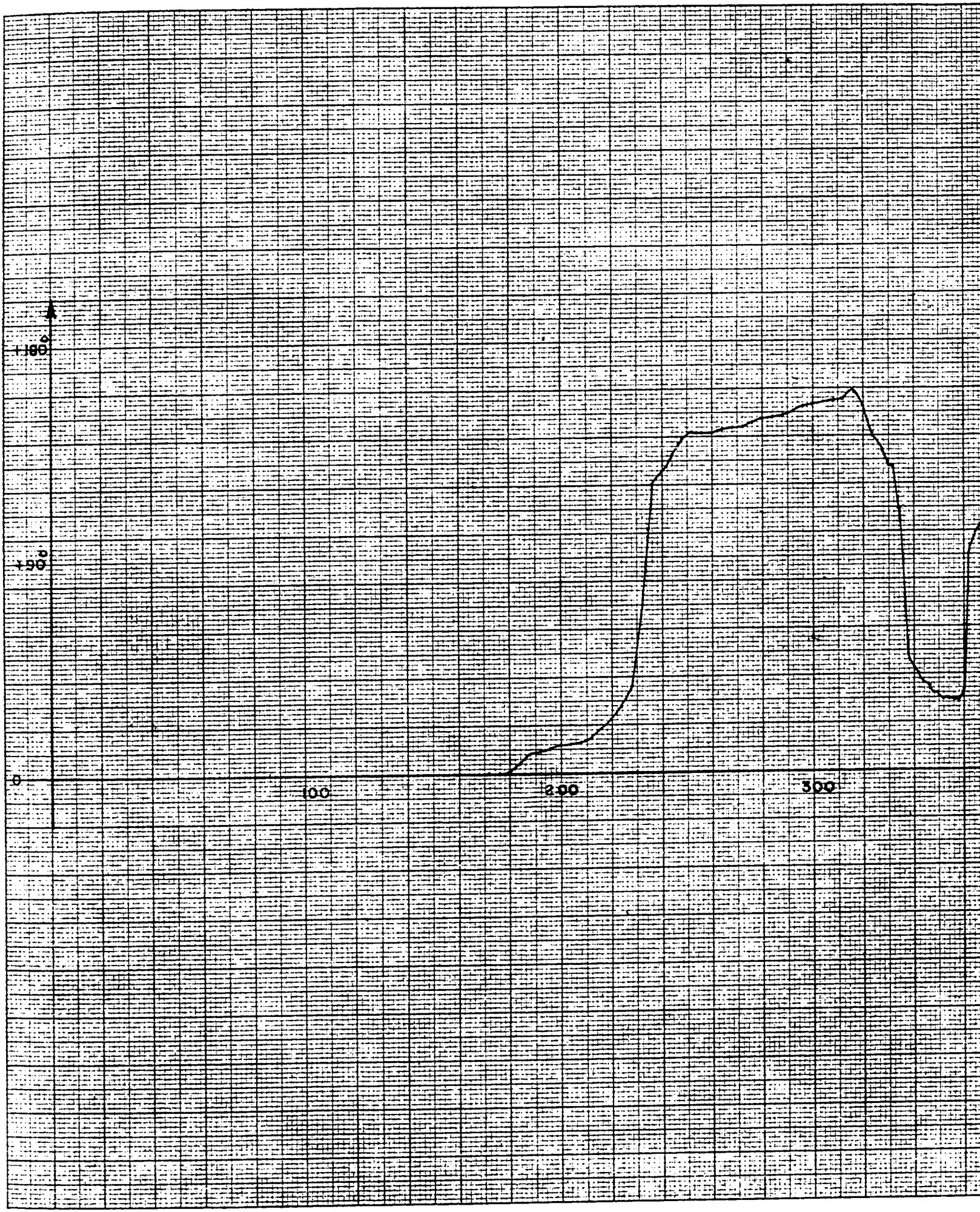
+180°
+90°
0
100
200
300

FIGURE 8a

$\theta_0(t)$

VERTICAL SCALE - 1CM = 20°

HORIZ SCALE = 1CM = 20 MILLISECONDS

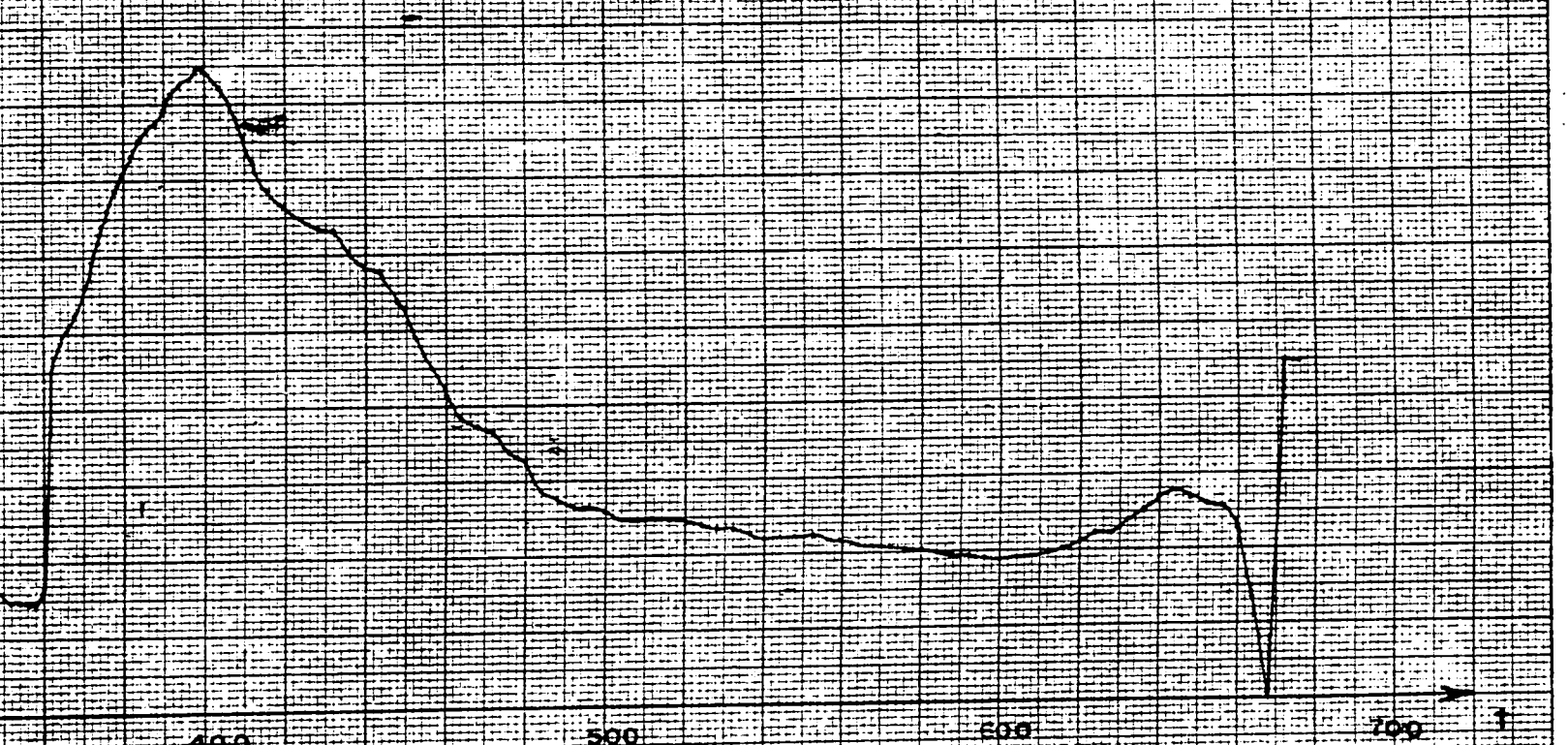

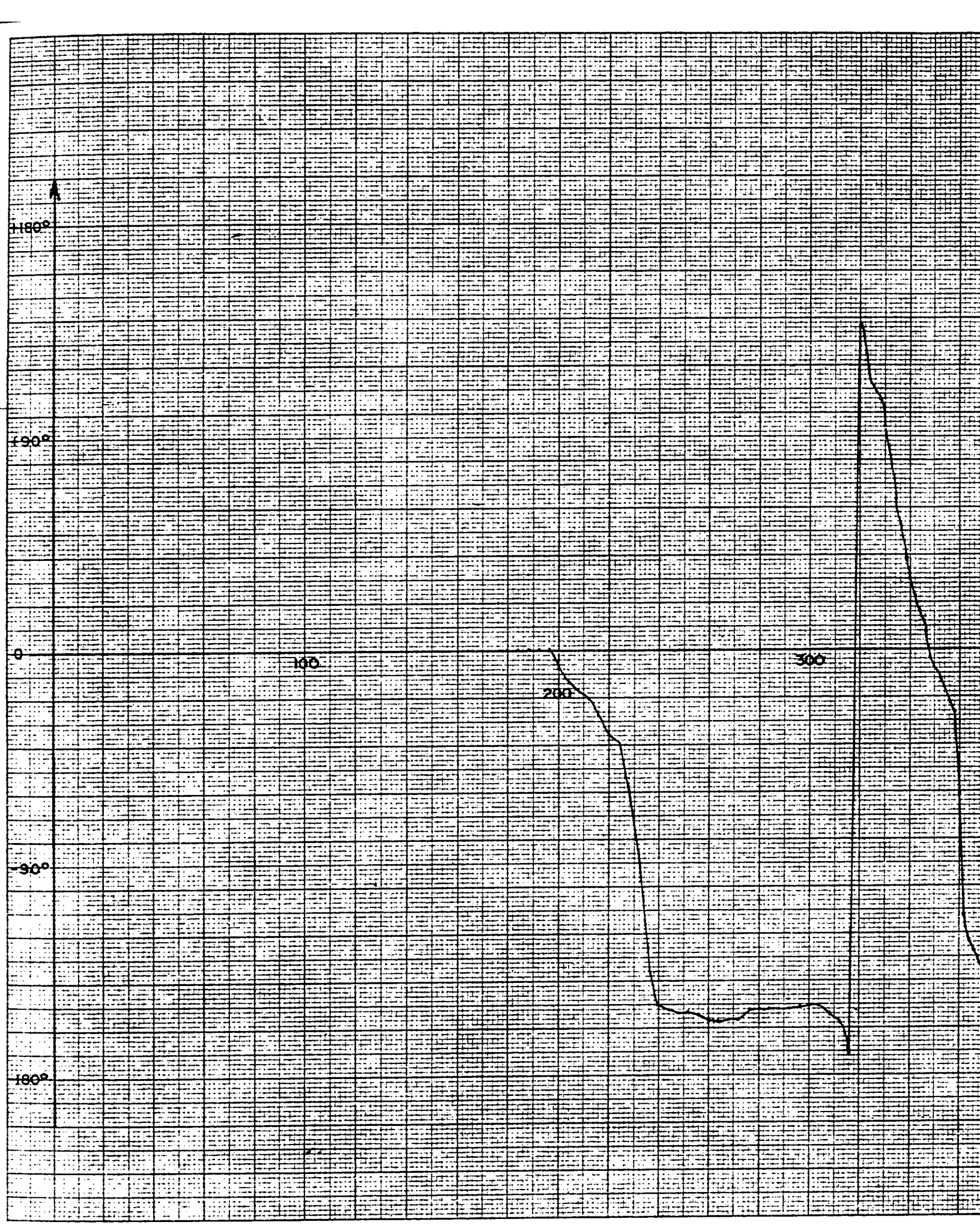
+180°
+90°
0
100
200
300
-90°
-180°

FIGURE 9

$\phi(t)$

VERTICAL SCALE - 1CM = 20°

HORIZ SCALE - 1CM = 20 MILLISECONDS

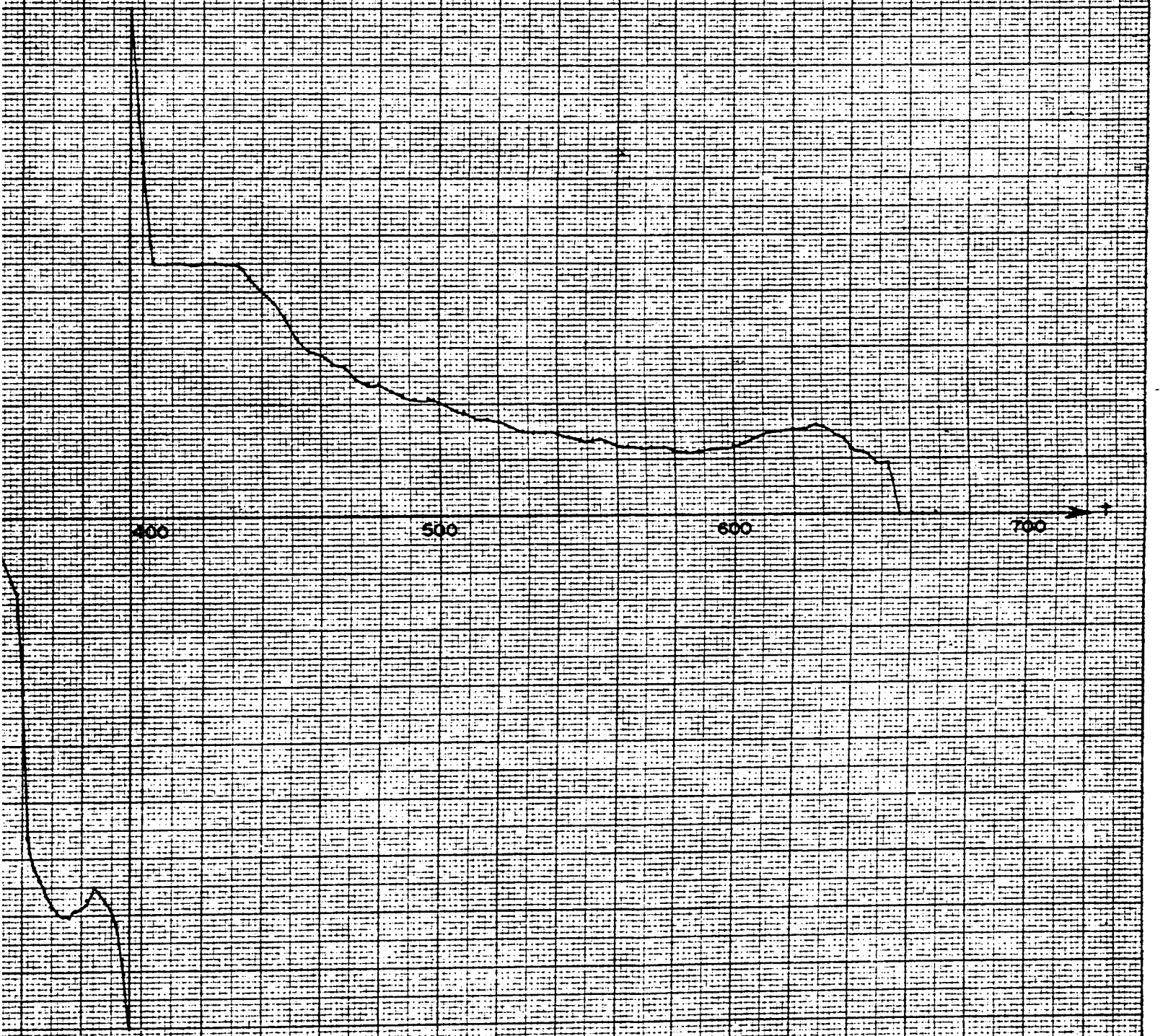

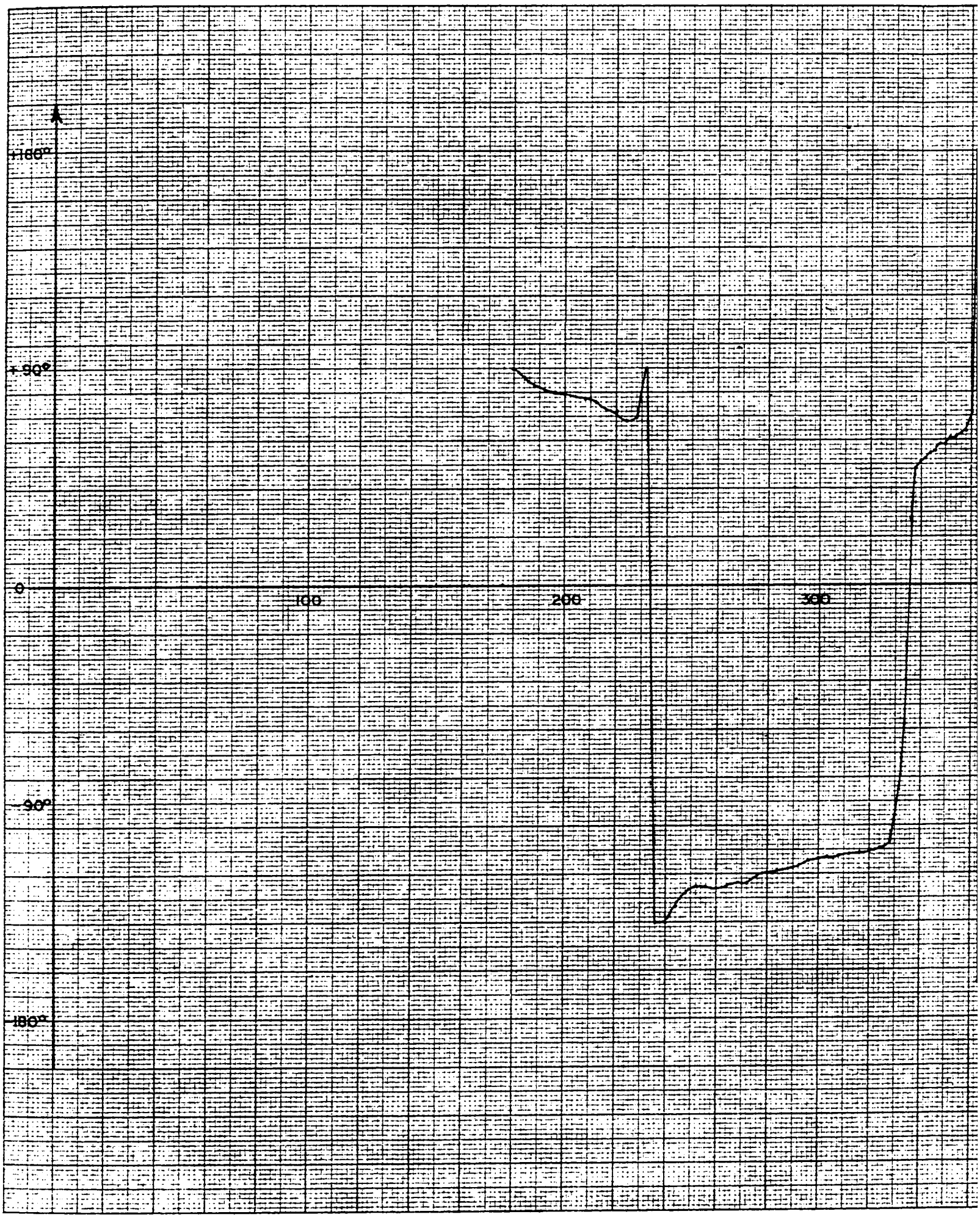
+180°
+90°
0
100
200
300
-90°
-180°

FIGURE 10

α (+)

VERTICAL SCALE = 1 CM = 20°

HORIZ SCALE = 1 CM = 20 MILLISECONDS

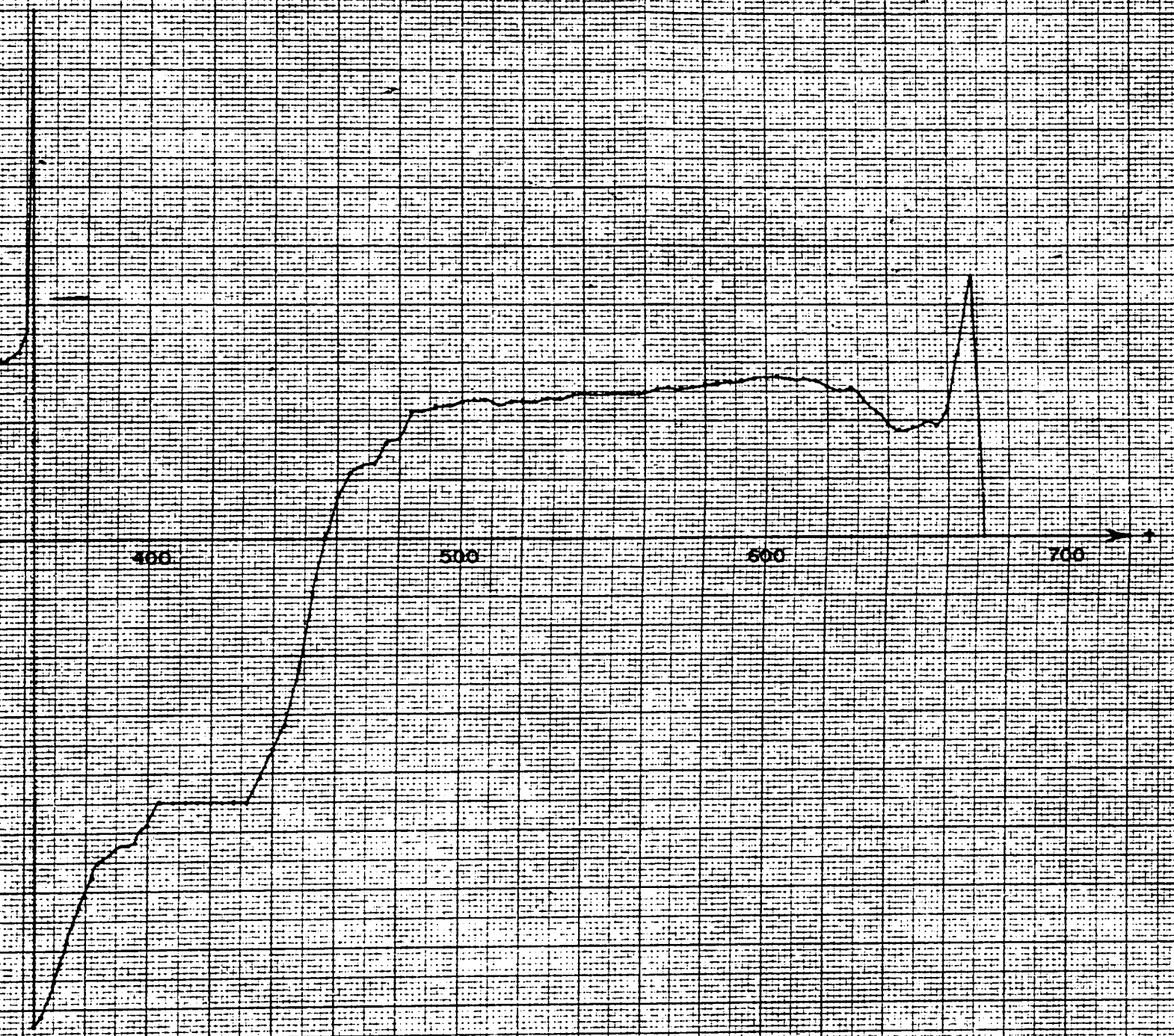

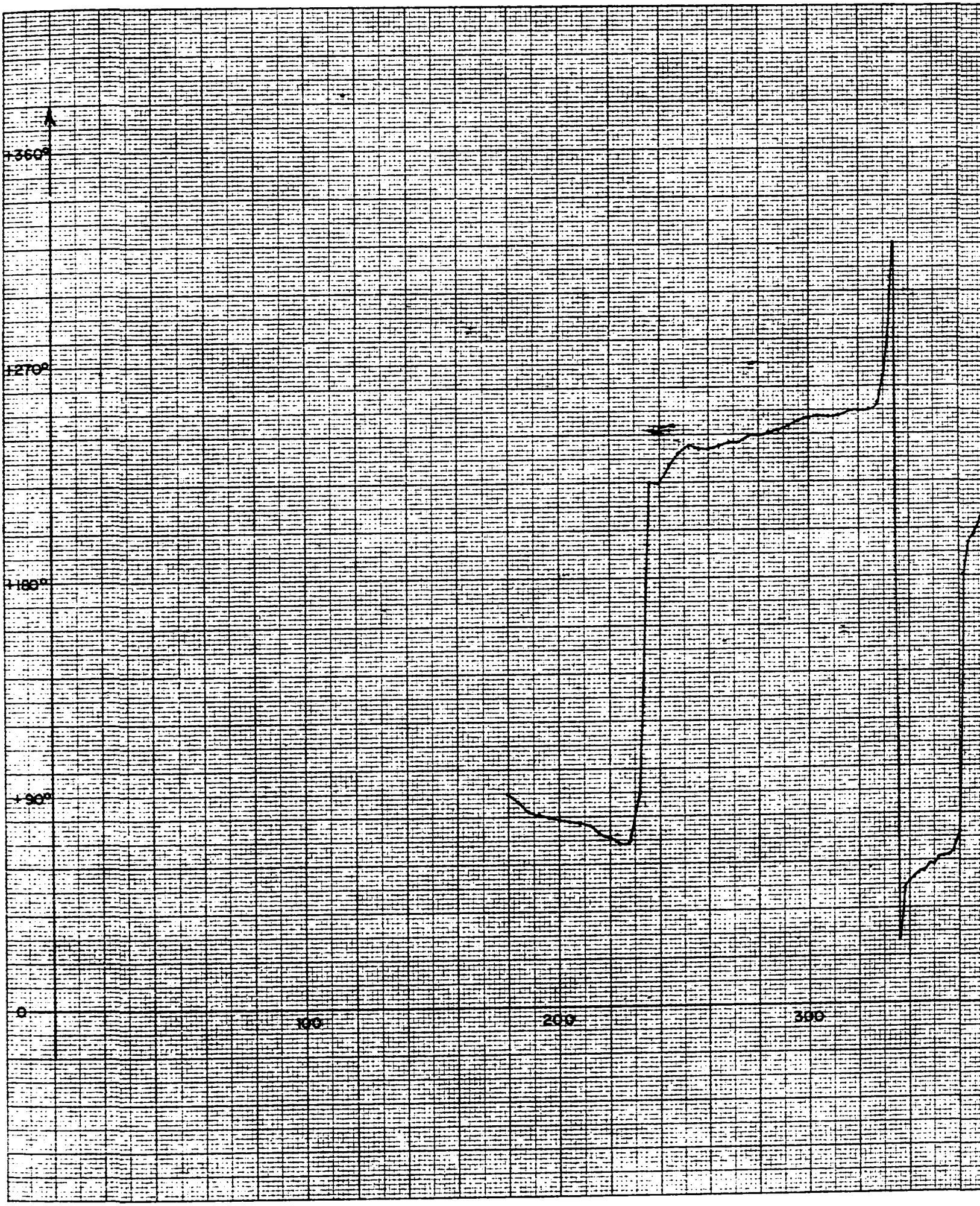
+360°
+270°
+180°
+90°
0
100
200
300

FIGURE 10a

α (t)

VERTICAL SCALE – 1CM = 20°

HORIZ. SCALE – 1CM = 20 MILLISECONDS

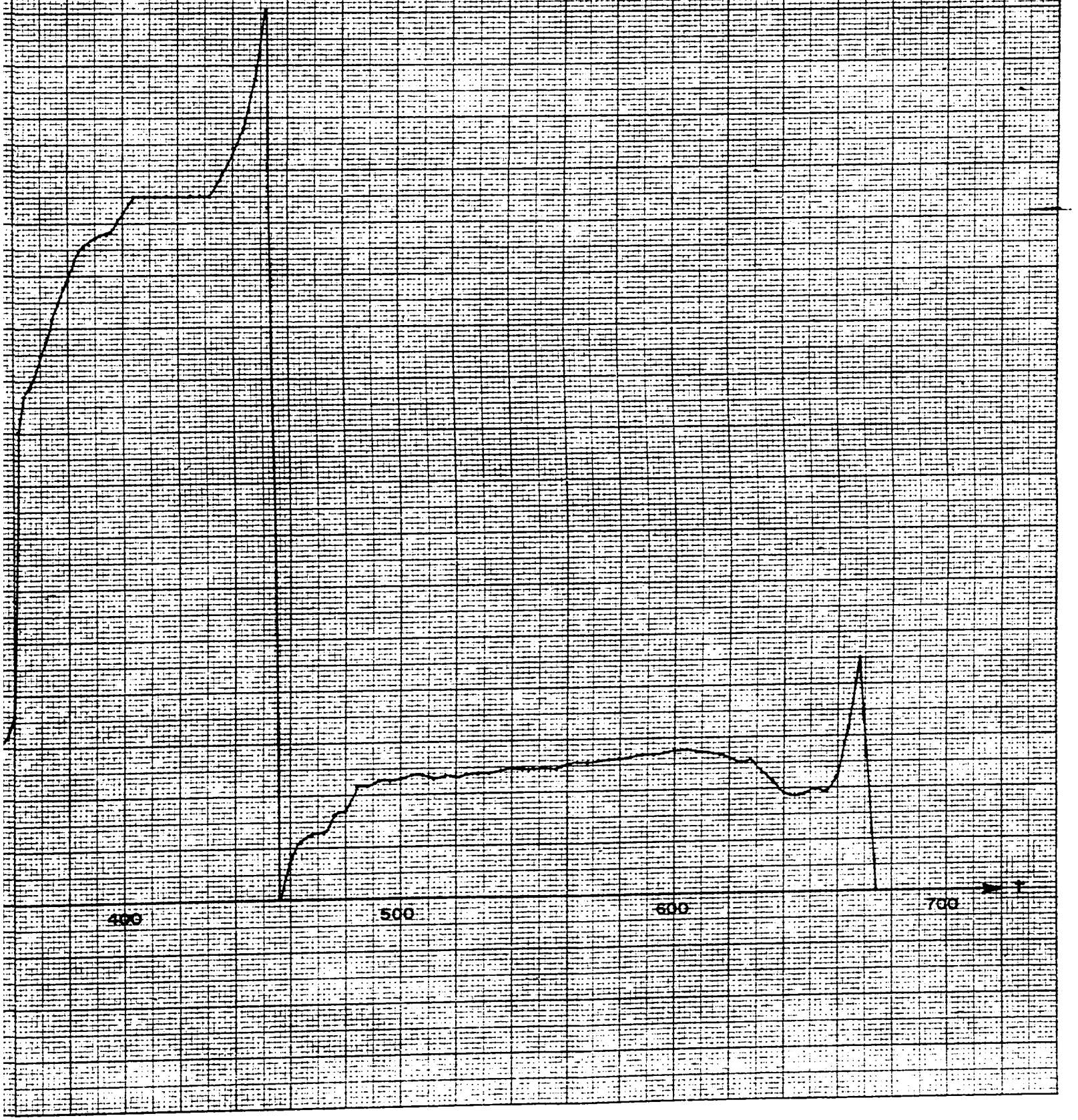

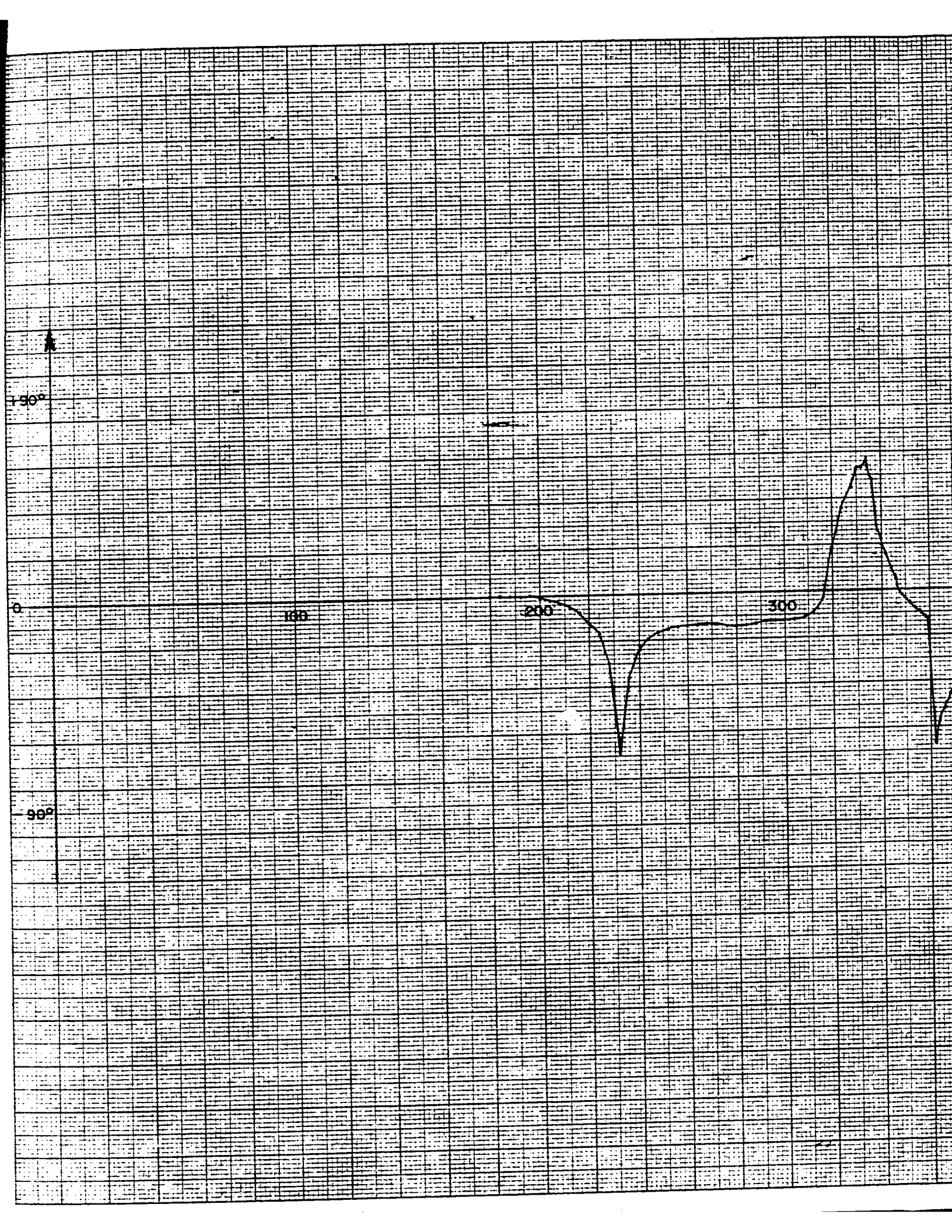
+90°
0
100
200
300
-90°

FIGURE 11

β (t)

VERTICAL SCALE – 1CM = 20°

HORIZ SCALE – 1CM = 20 MILLISECONDS

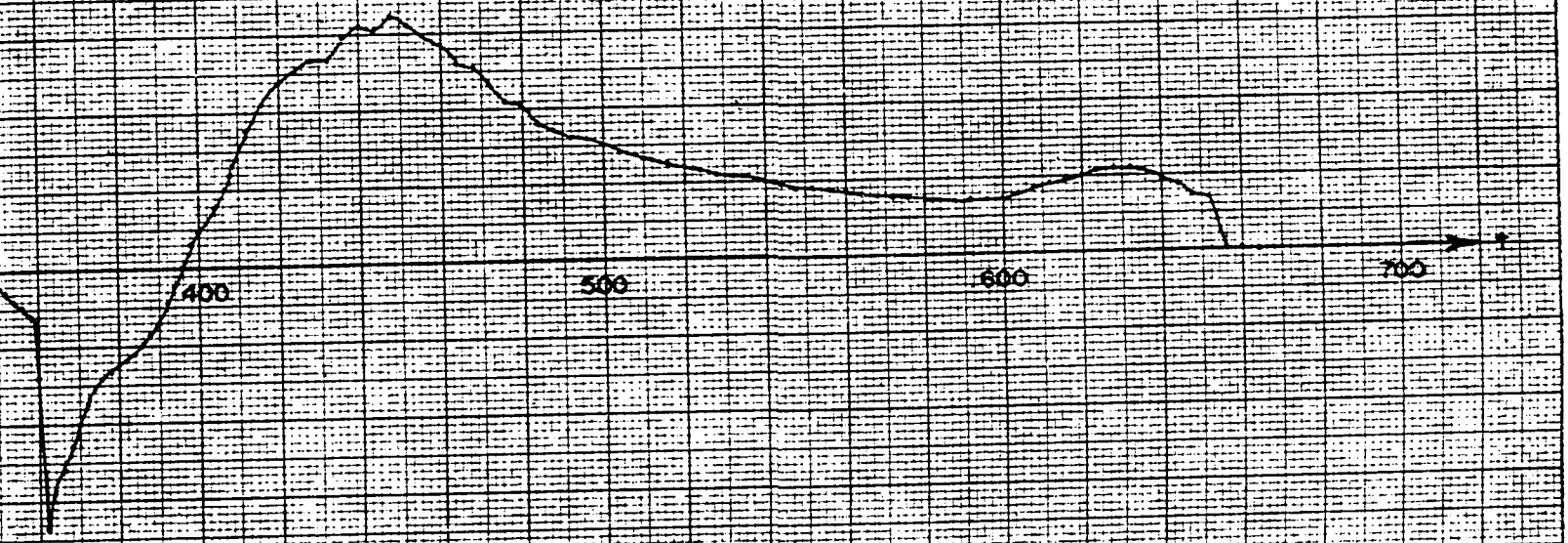

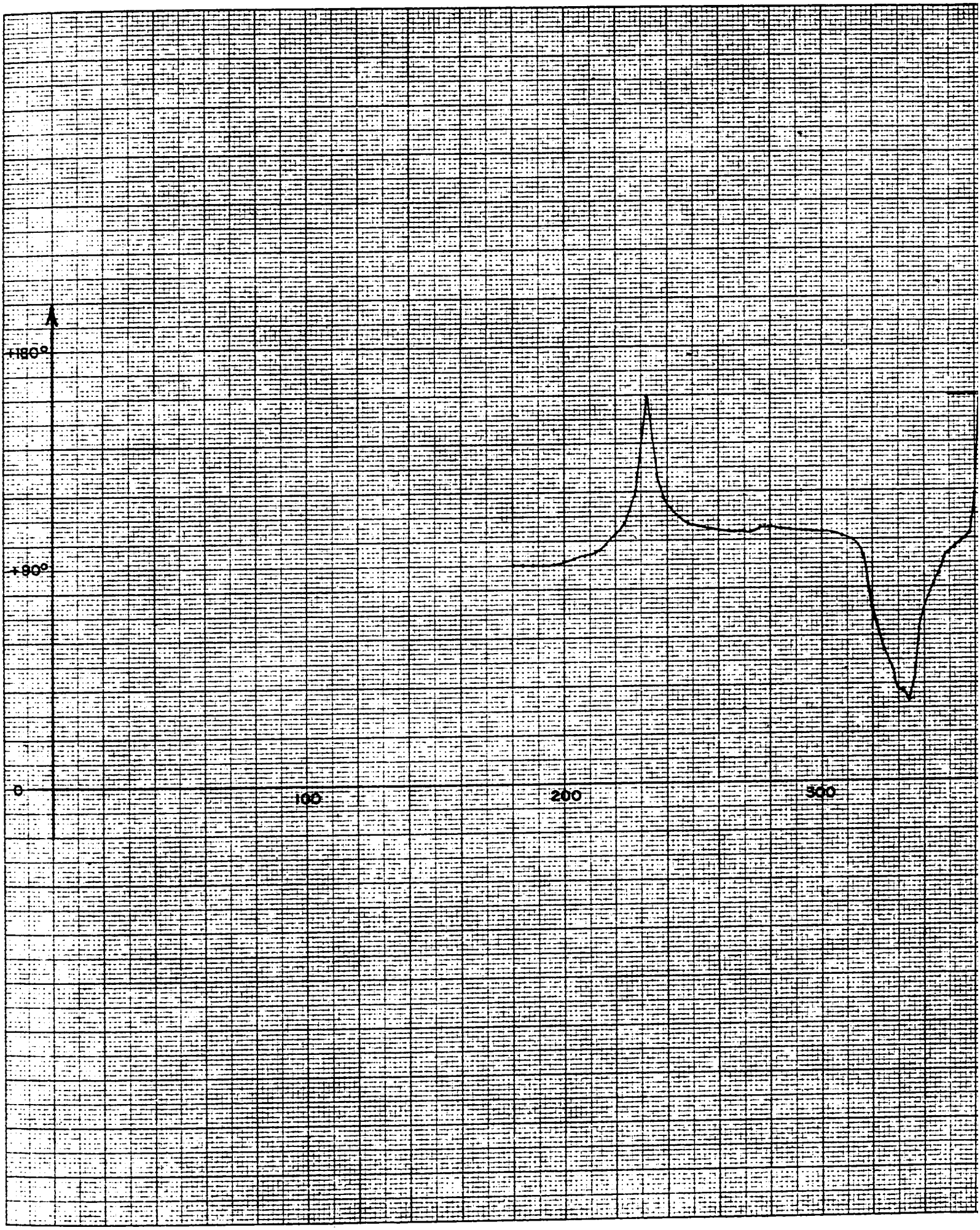
+180°
+90°
0
100
200
300

FIGURE IIa

$\beta_p(t)$

VERTICAL SCALE – 1CM = 20°

HORIZ SCALE – 1CM = 20 MILLISECONDS

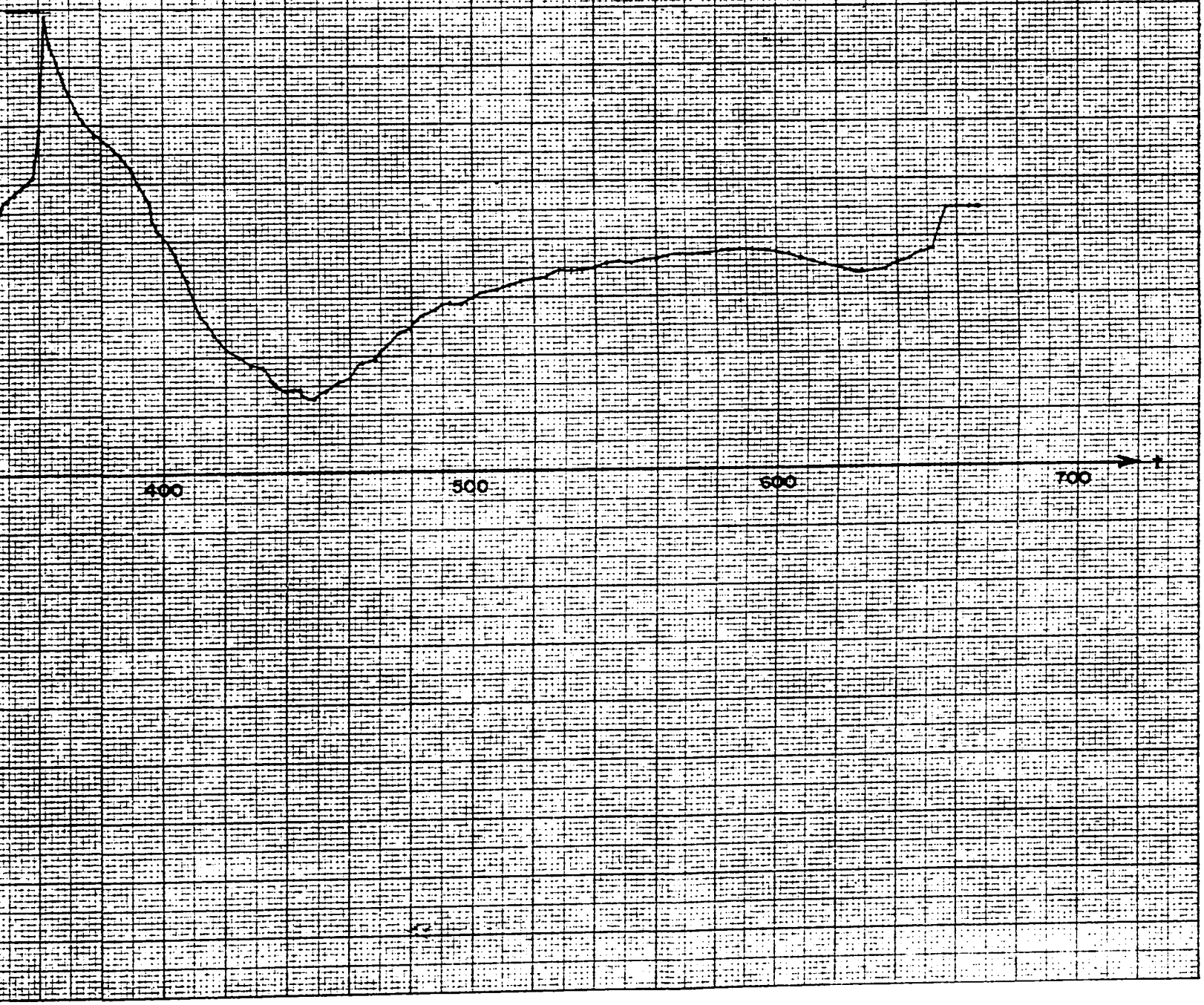

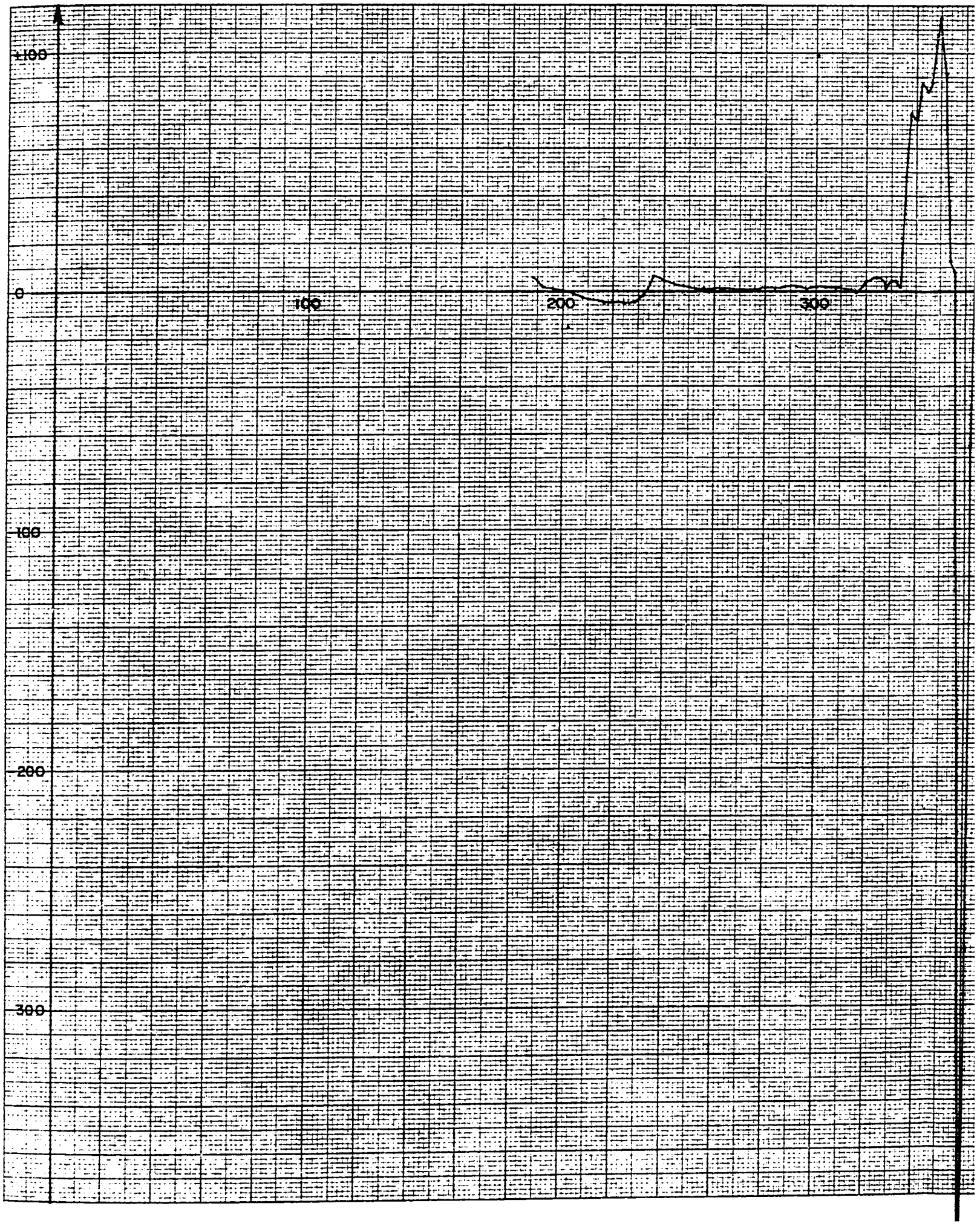
+100
0
100
200
300
-100
-200
-300

FIGURE 12

$\left| \frac{d}{dt} r(t) \right|$

VERTICAL SCALE — 1CM = 20 MILLIVOLTS/SEC
HORIZ SCALE — 1CM = 20 MILLISECONDS

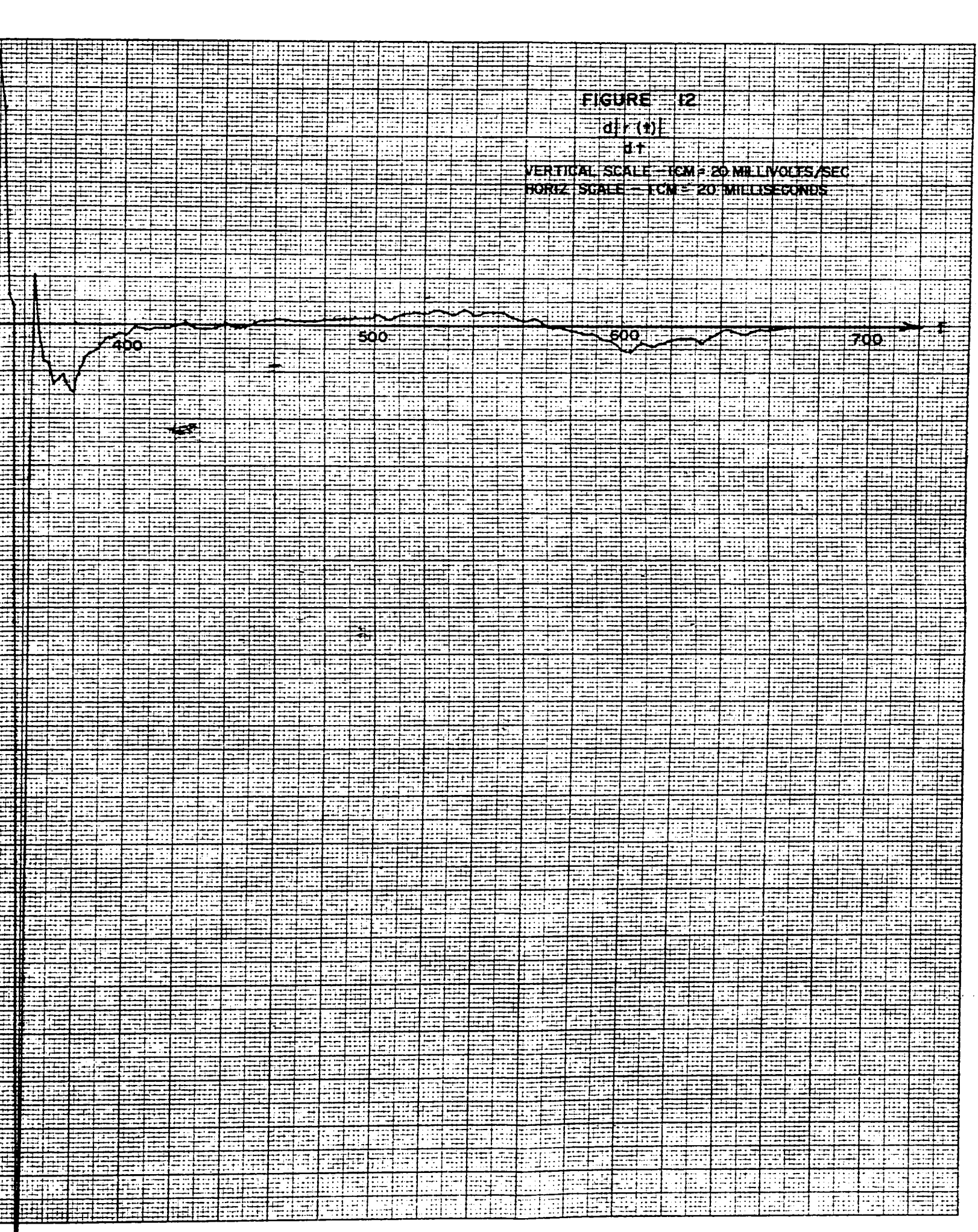

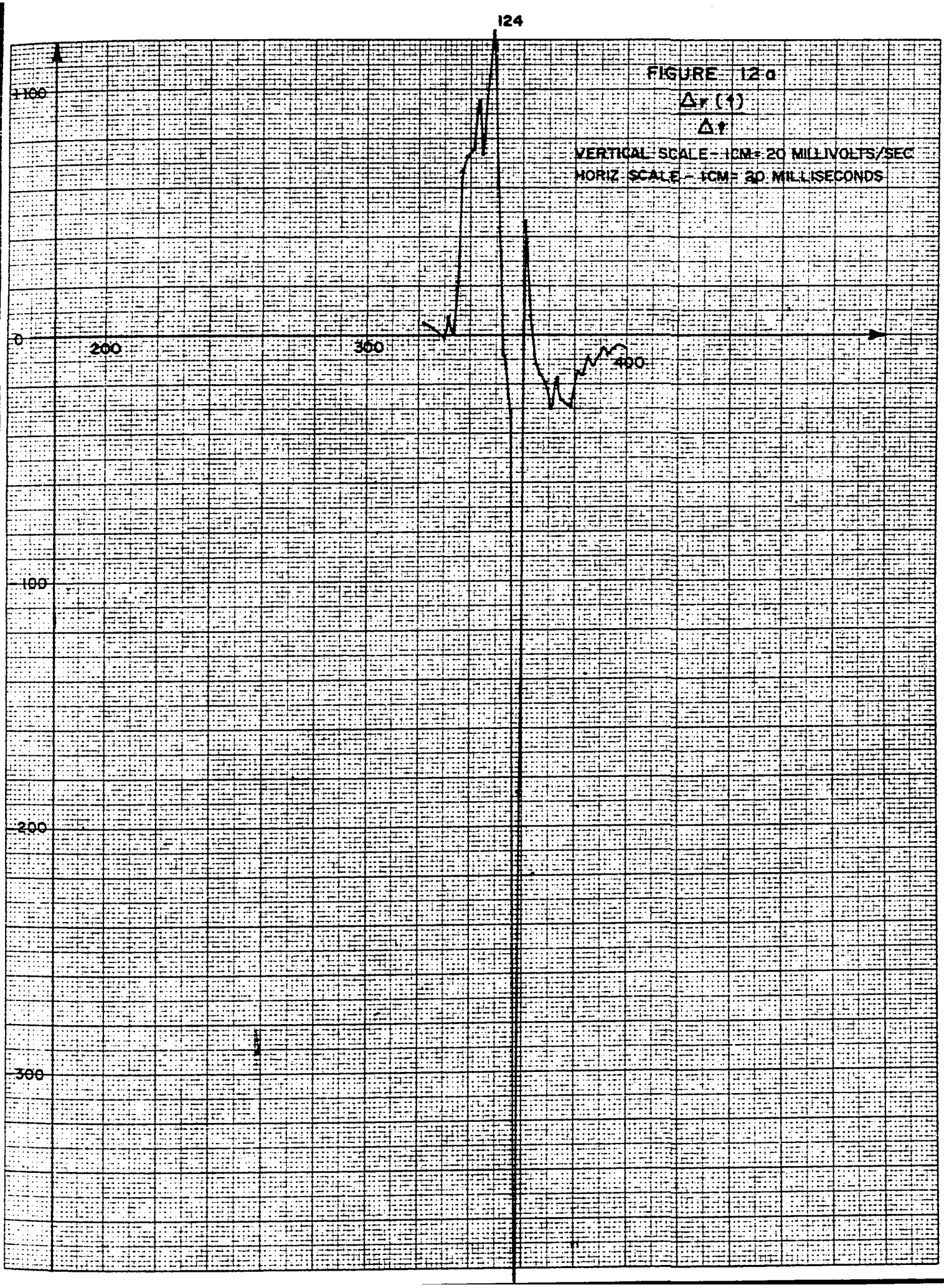
FIGURE 12a
Δr (t)
Δt
VERTICAL SCALE - 1CM = 20 MILLIVOLTS/SEC
HORIZ. SCALE - 1CM = 20 MILLISECONDS
100
0
200
300
400
100
200
300

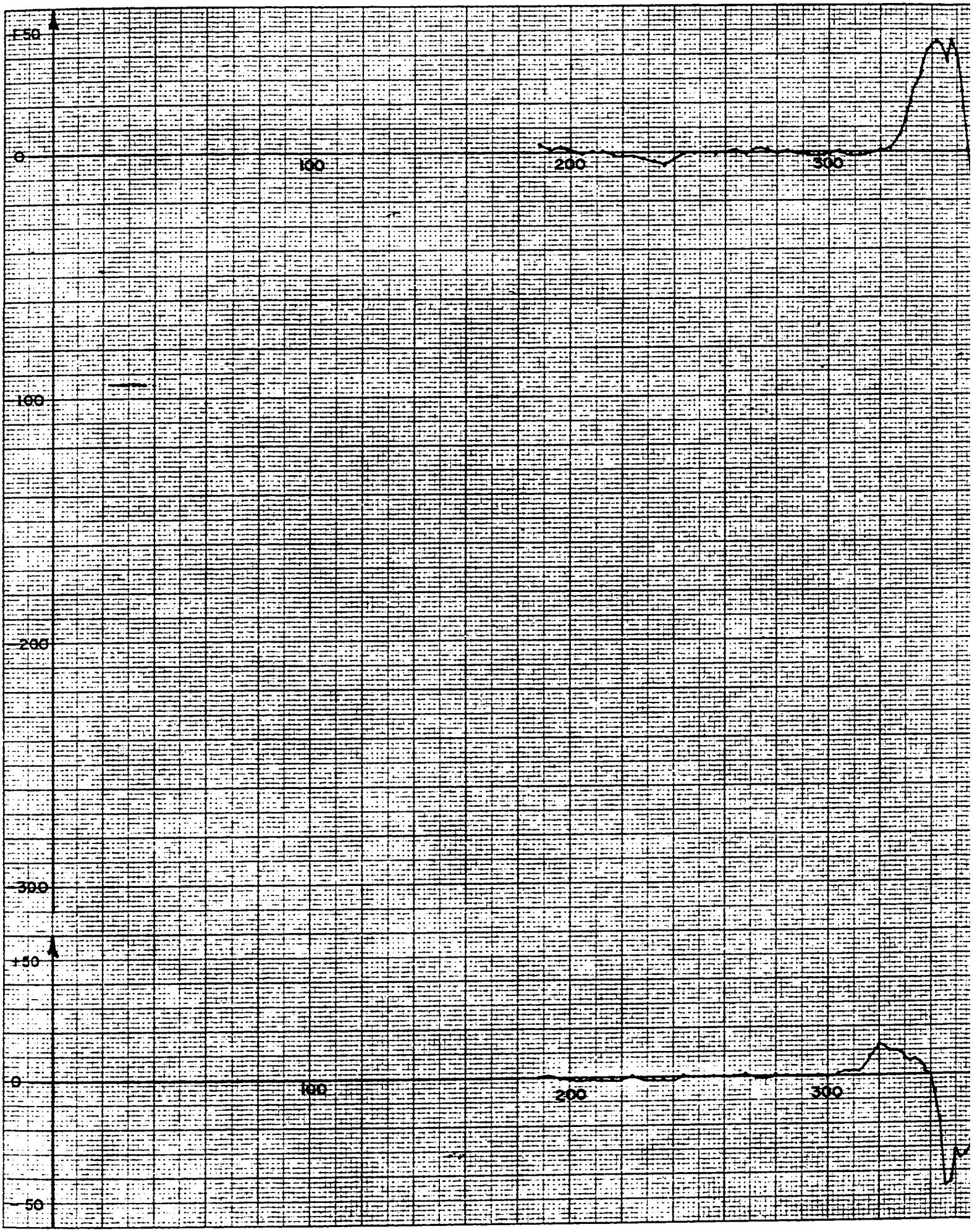
+50
0
100
200
300
-100
-200
-300
+50
0
100
200
300
-50

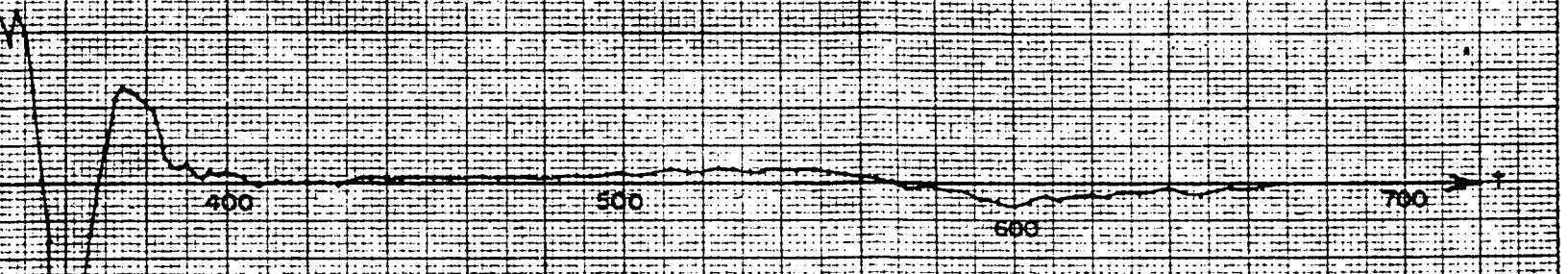

FIGURE 13

$$\frac{dx(t)}{dt} = v_x(t)$$

VERTICAL SCALE - 1CM = 20 MILLIVOLTS/SEC
HORIZ SCALE - 1CM = 20 MILLISECONDS

FIGURE 15

$$\frac{dz(t)}{dt} = v_z(t)$$

VERTICAL SCALE - 1CM = 20 MILLIVOLTS/SEC
HORIZ SCALE - 1CM = 20 MILLISECONDS

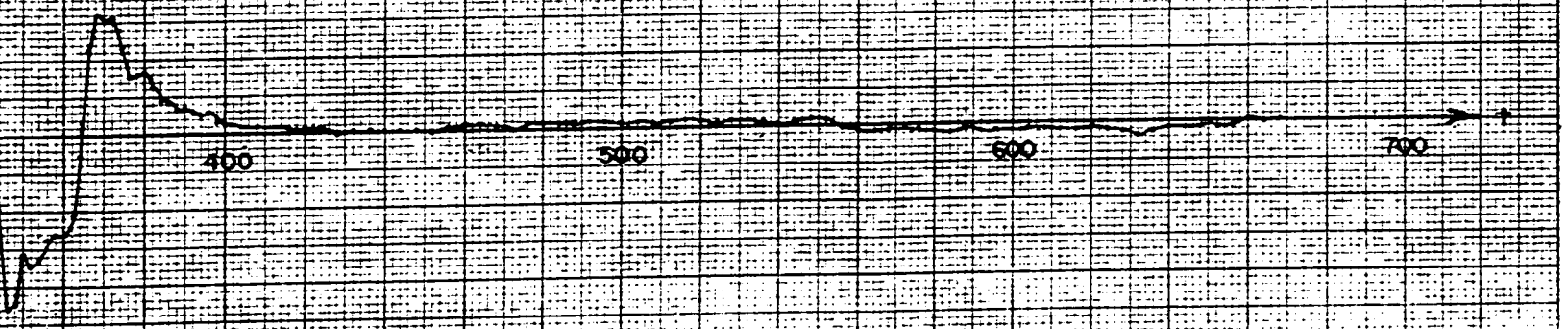

FIGURE 13a

$\frac{\Delta X(t)}{\Delta t}$

VERTICAL SCALE = 1 CM = 20 MILLIVOLTS/SEC
HORIZ SCALE = 1 CM = 20 MILLISECONDS

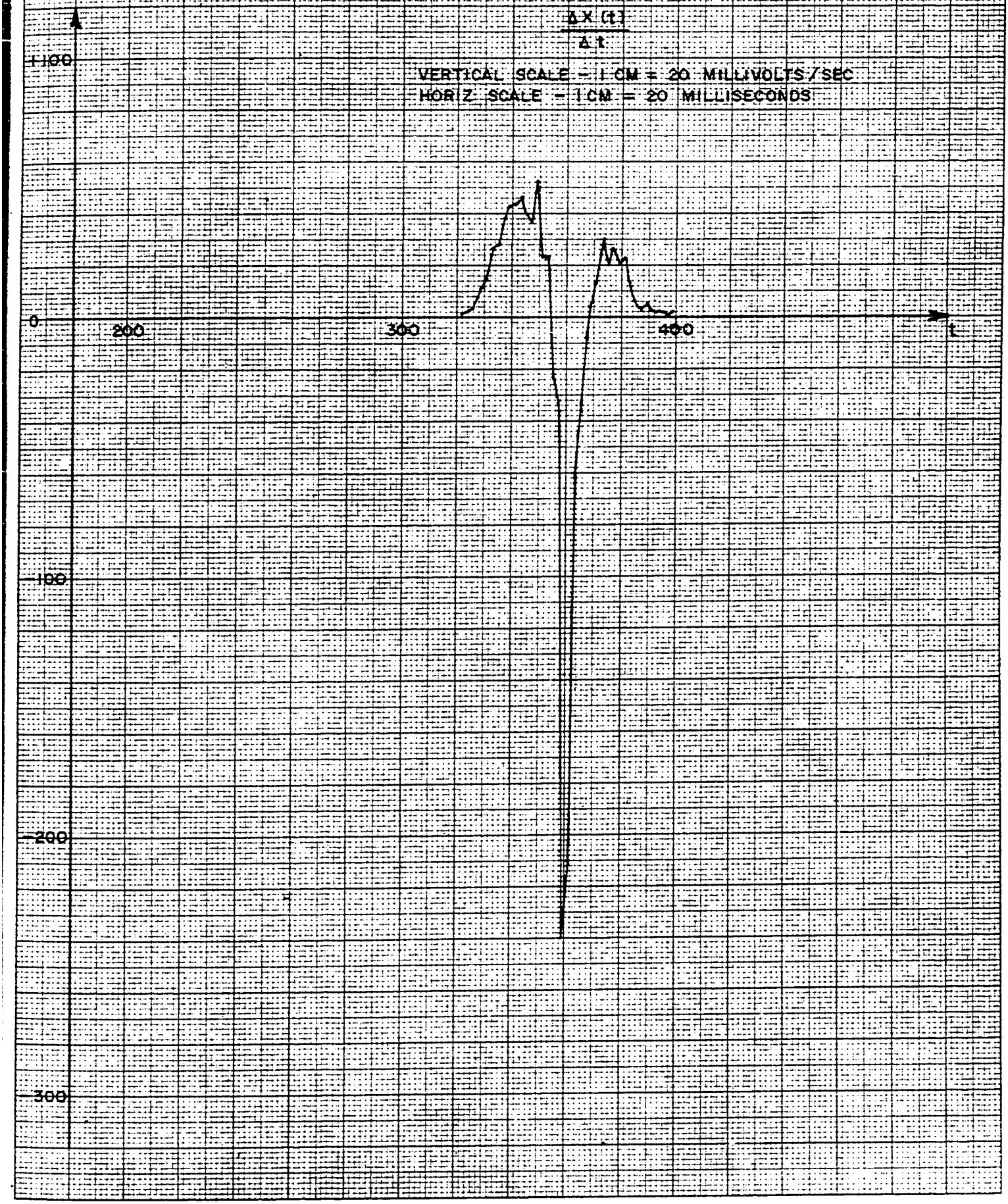

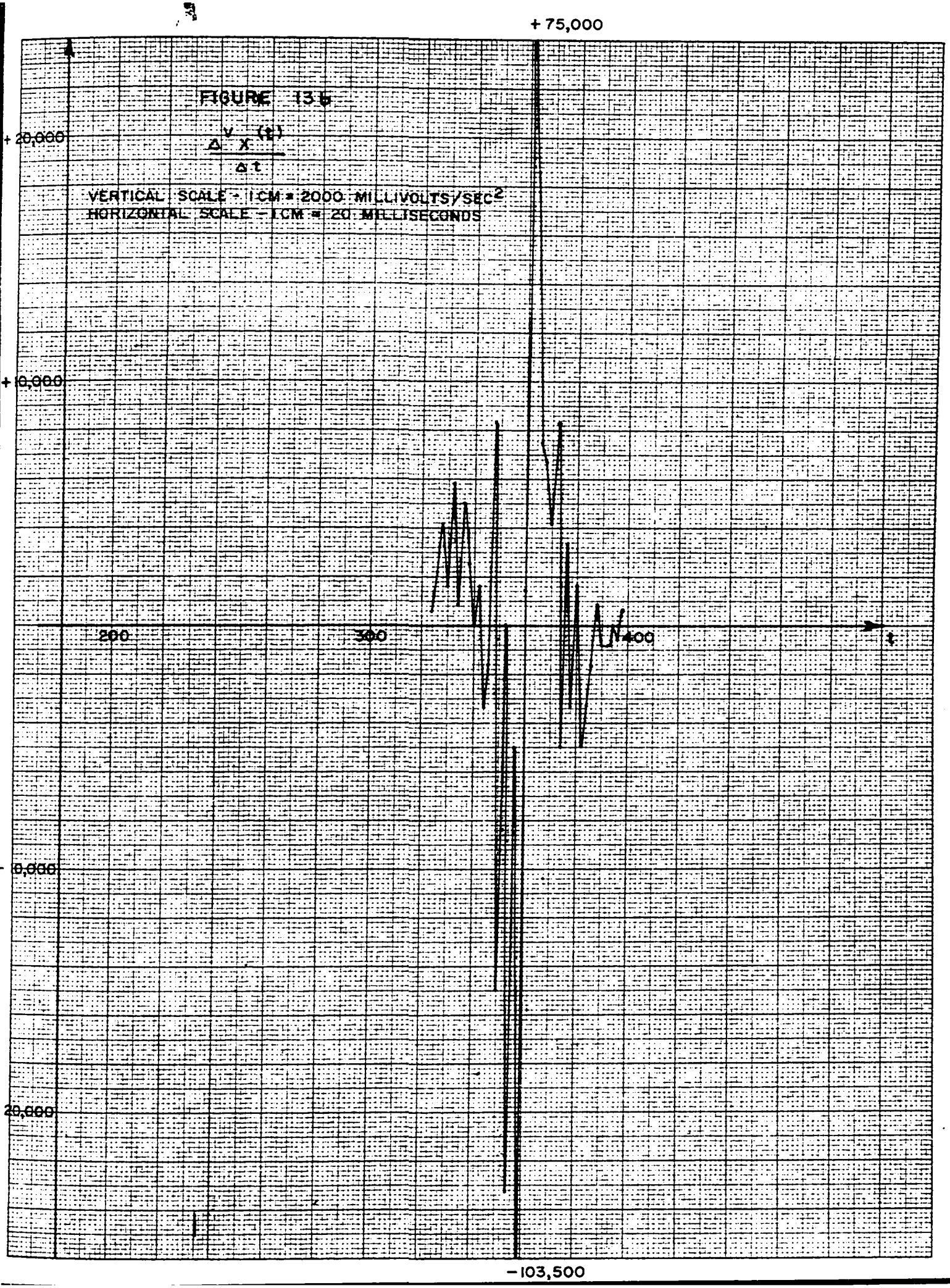
+ 75,000
FIGURE 13b
$\frac{\Delta V_x(t)}{\Delta t}$
VERTICAL SCALE - 1 CM = 2000 MILLIVOLTS/SEC^2
HORIZONTAL SCALE - 1 CM = 20 MILLISECONDS
+ 20,000
+ 10,000
0,000
- 20,000
200
300
400
t
- 103,500

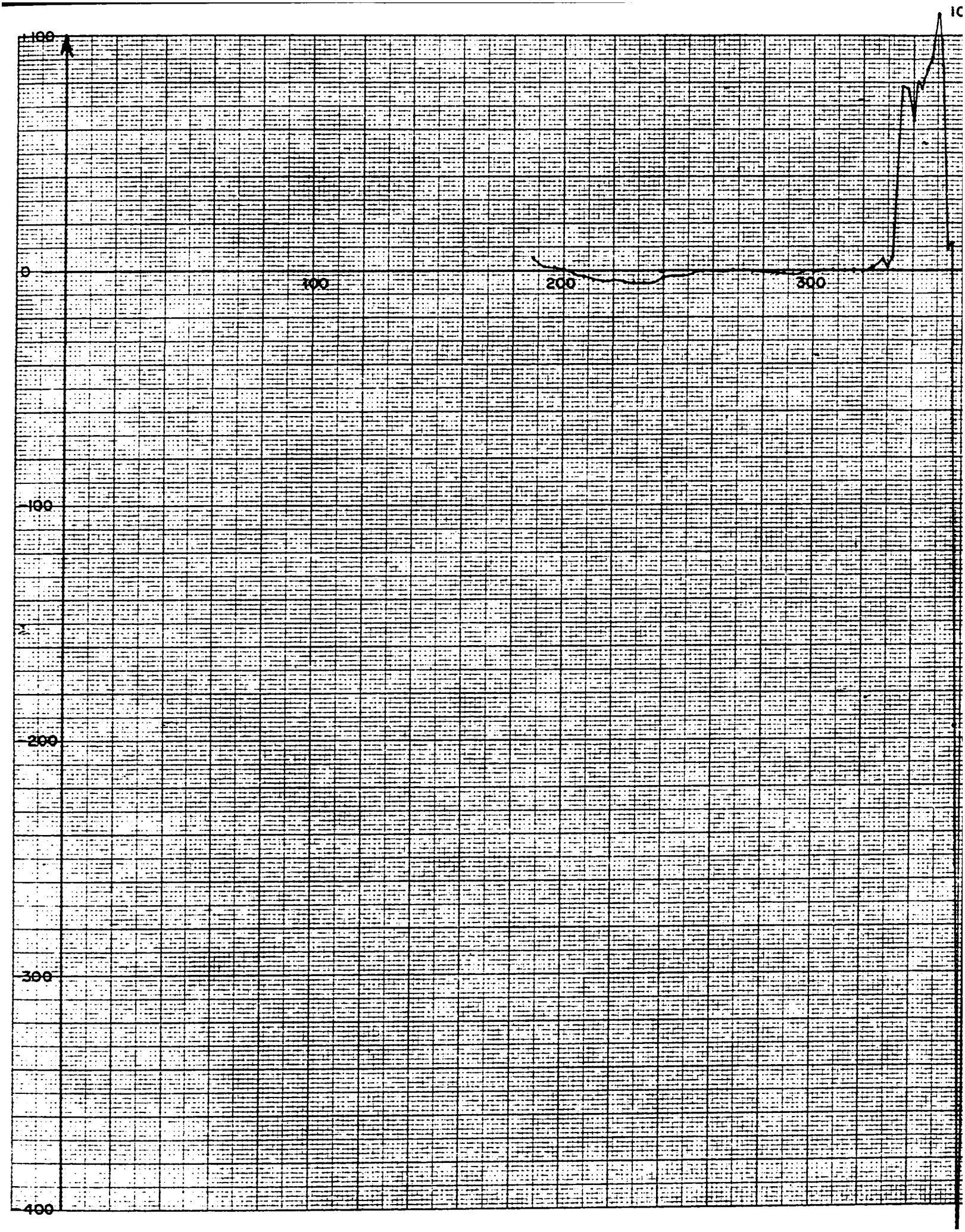
+100
0
100
200
300
-100
-200
-300
-400

FIGURE 14

$$\frac{dy(t)}{dt} = v_y(t)$$

VERTICAL SCALE – 1 CM = 20 MILLIVOLTS/SEC
HORIZ SCALE – 1 CM = 20 MILLISECONDS

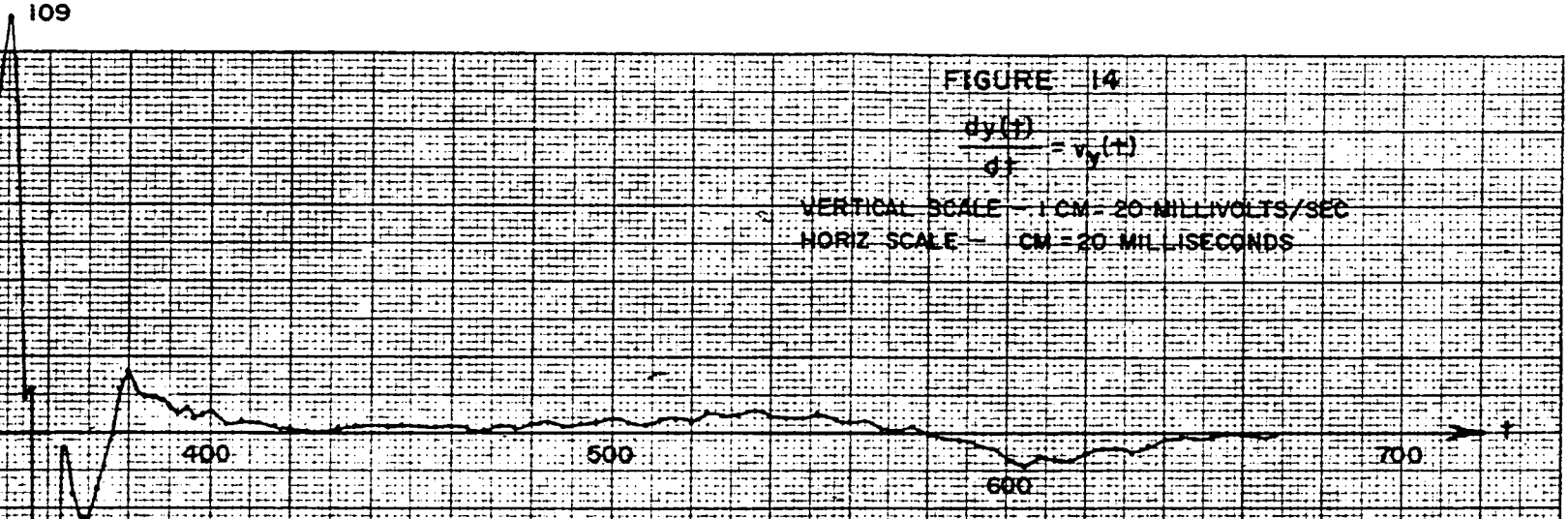

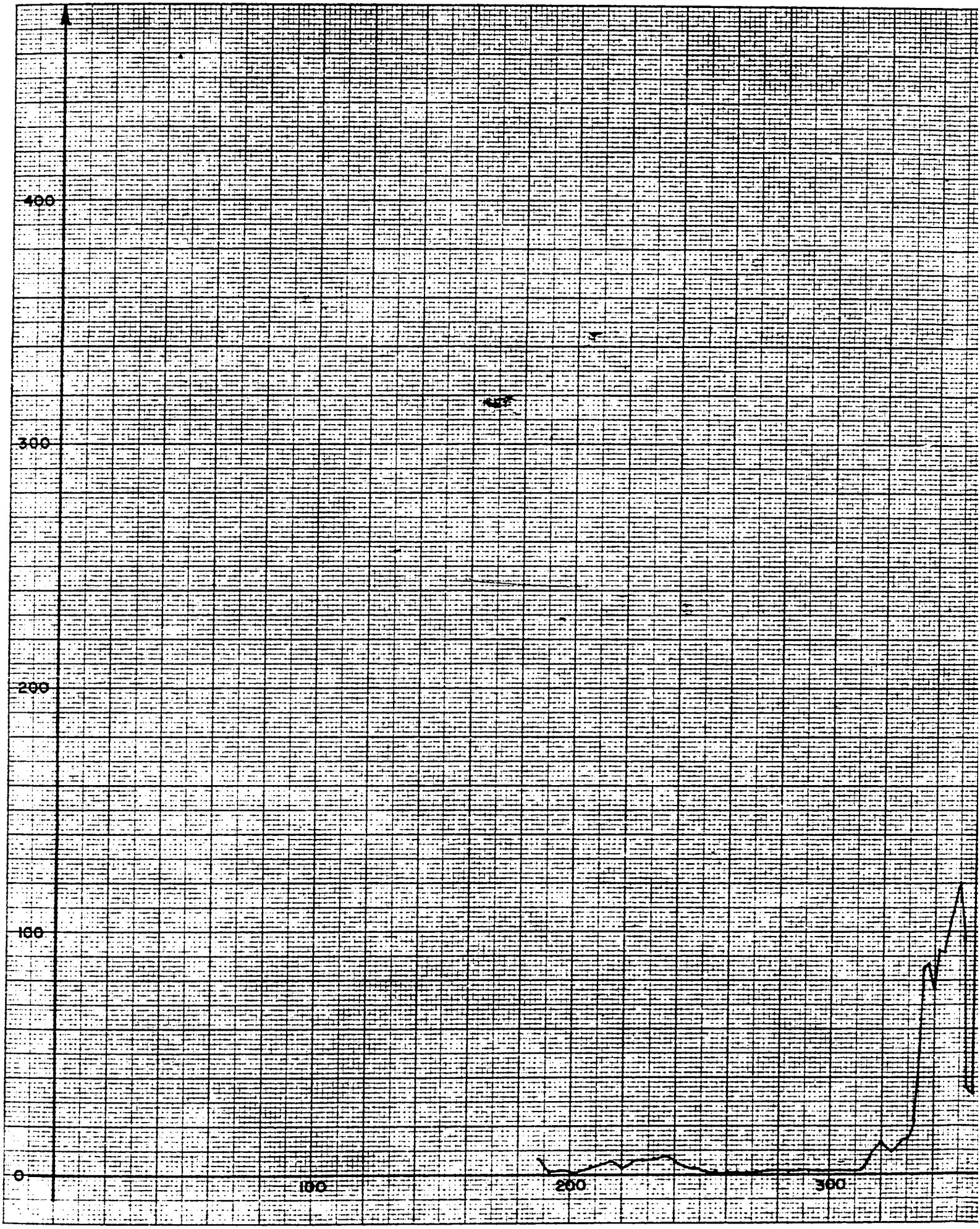
400
300
200
100
0
100
200
300

FIGURE 16

$$|v(t)| = \sqrt{v_x^2(t) + v_y^2(t) + v_z^2(t)}$$

VERTICAL SCALE = 1CM = 20 MILLIVOLTS/SEC

HORIZ. SCALE = 1CM = 20 MILLISECONDS

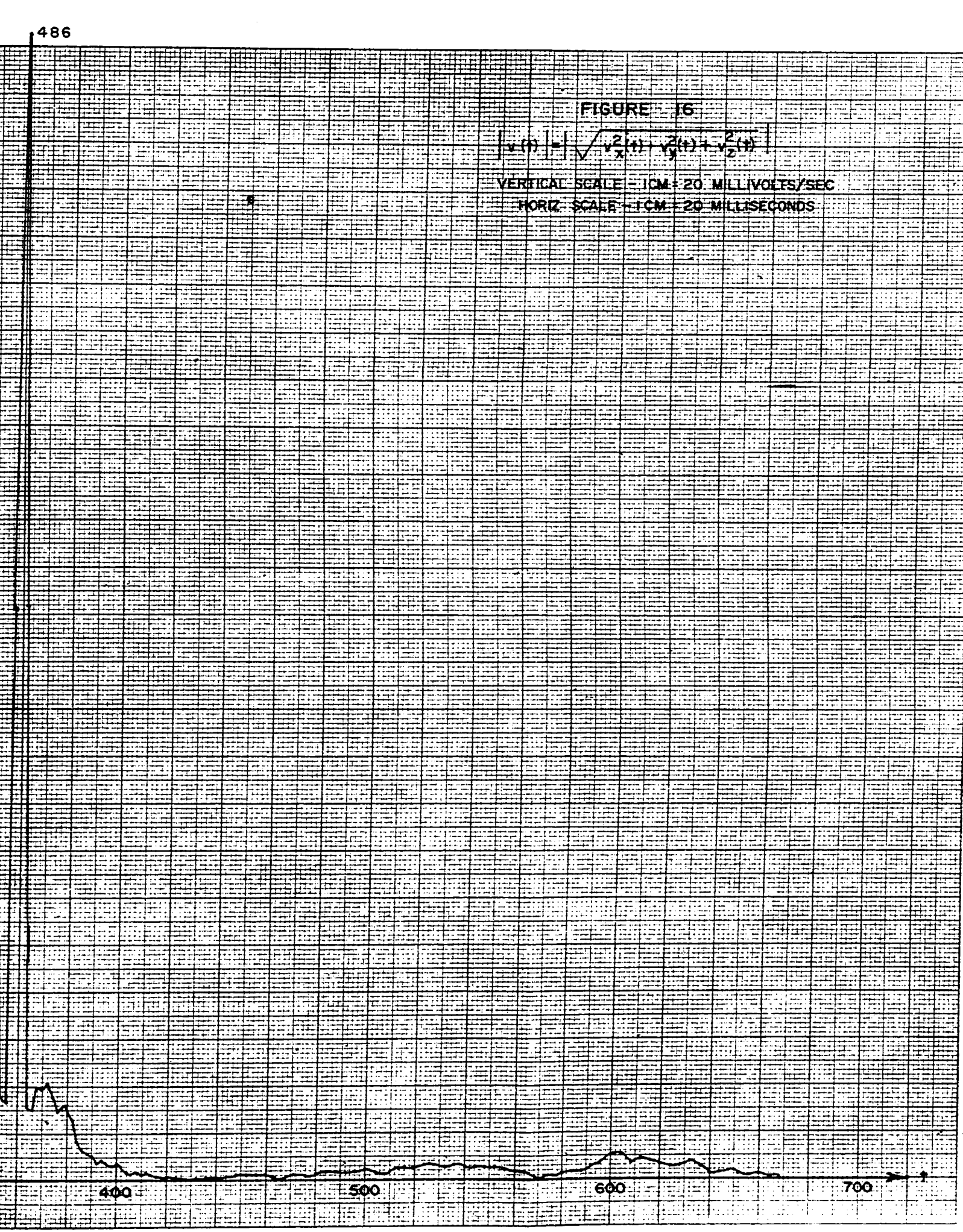

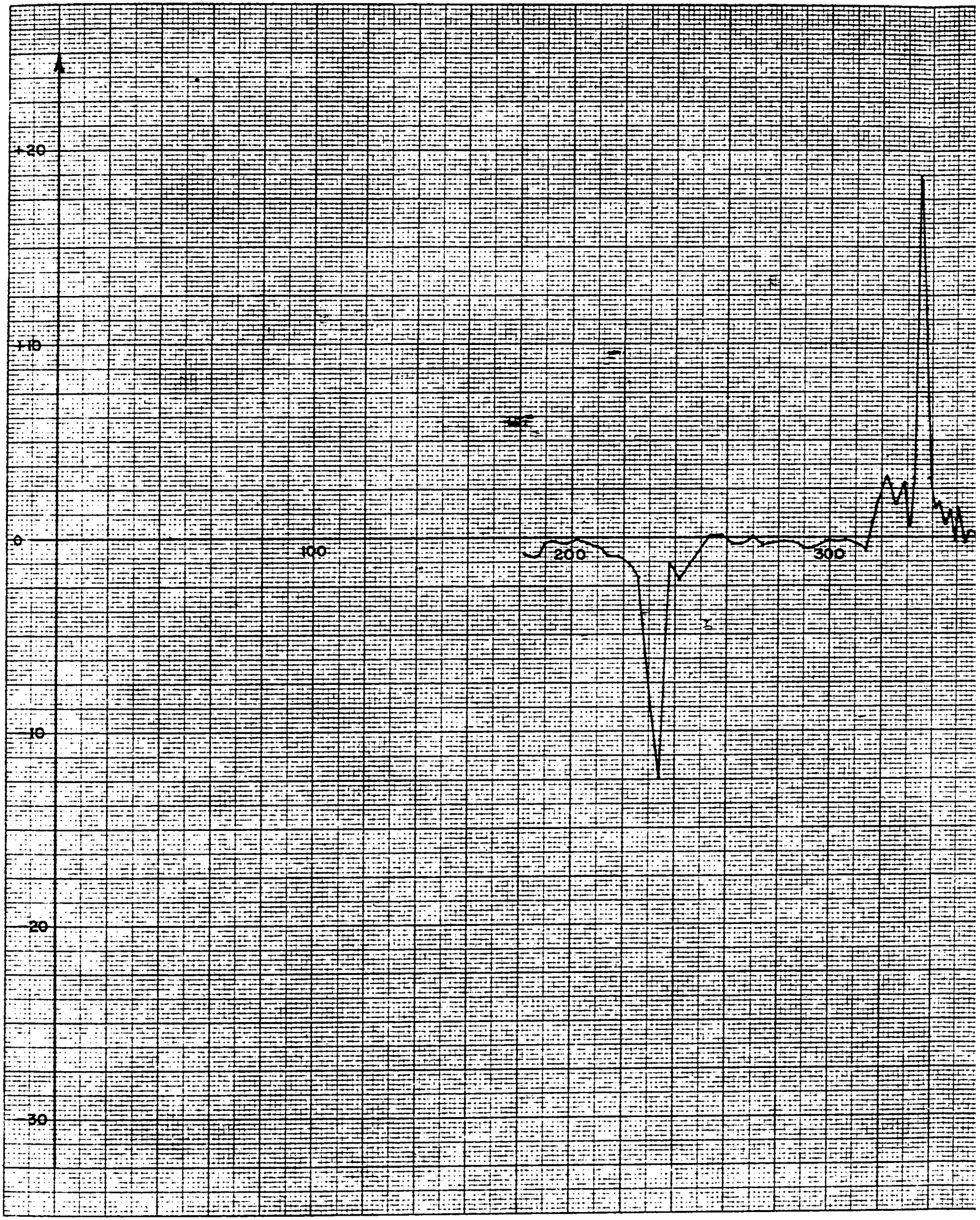
+20
10
0
100
200
300
10
20
30

FIGURE 17

$\Delta\theta(t)$

Δt

VERTICAL SCALE - 1CM = 2.5°/ MILLISECOND

HORIZ SCALE - 1CM = 20 MILLISECONDS

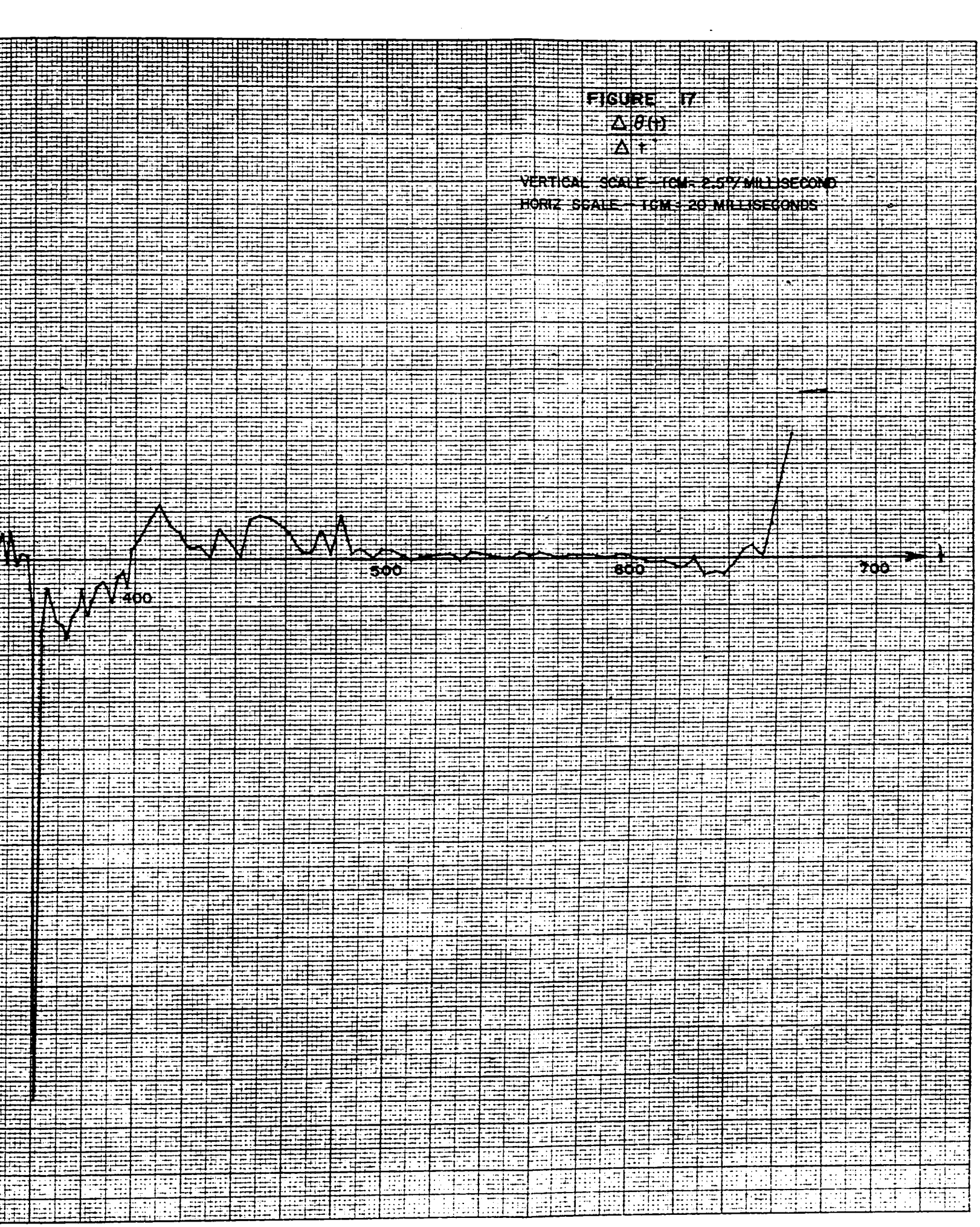

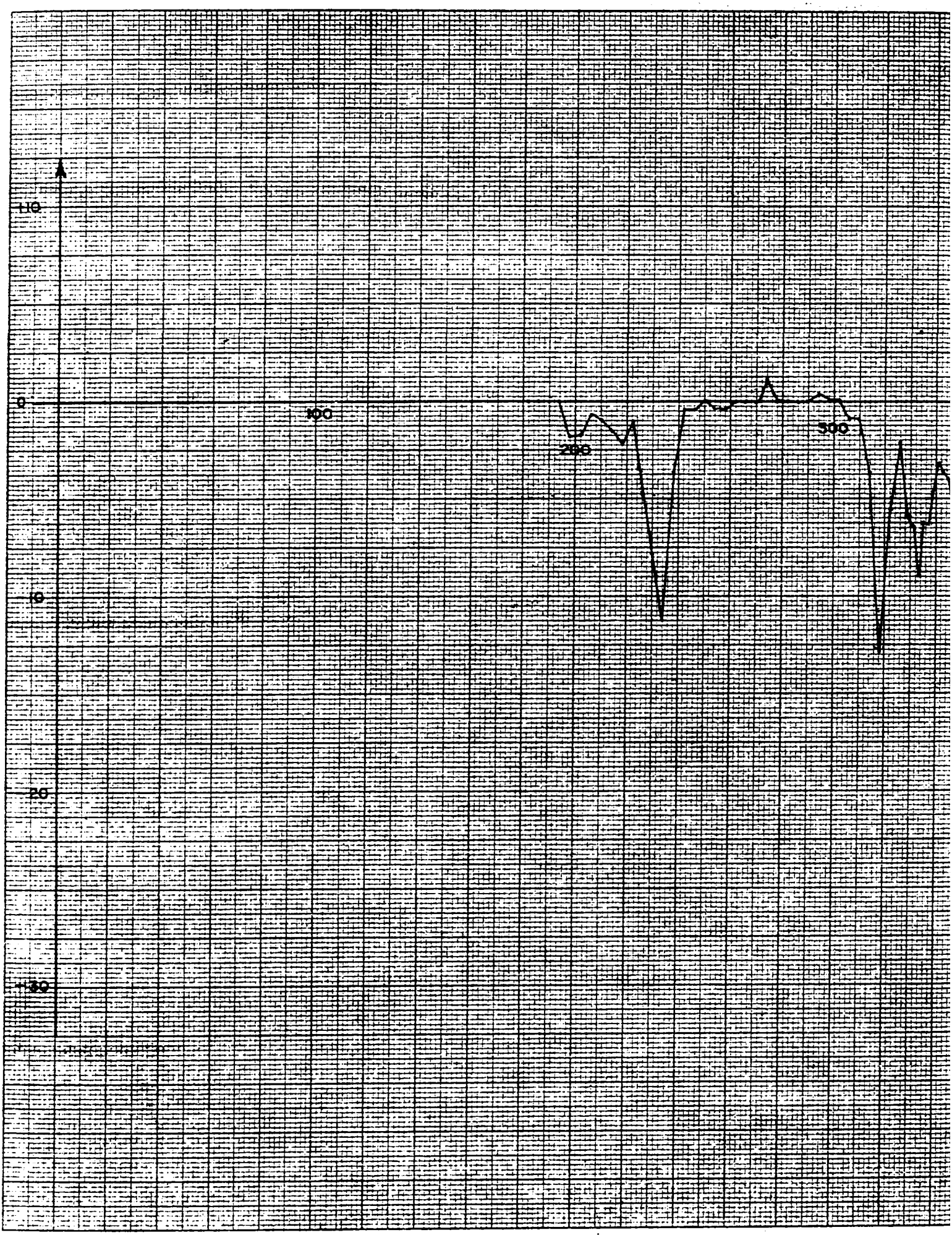
110
0
100
200
300
10
20
30

FIGURE 18

$\frac{\Delta\Phi(+)}{\Delta t}$

VERTICAL SCALE – 1 CM = 25% MILLISECOND
HORIZ SCALE – 1 CM = 20 MILLISECONDS

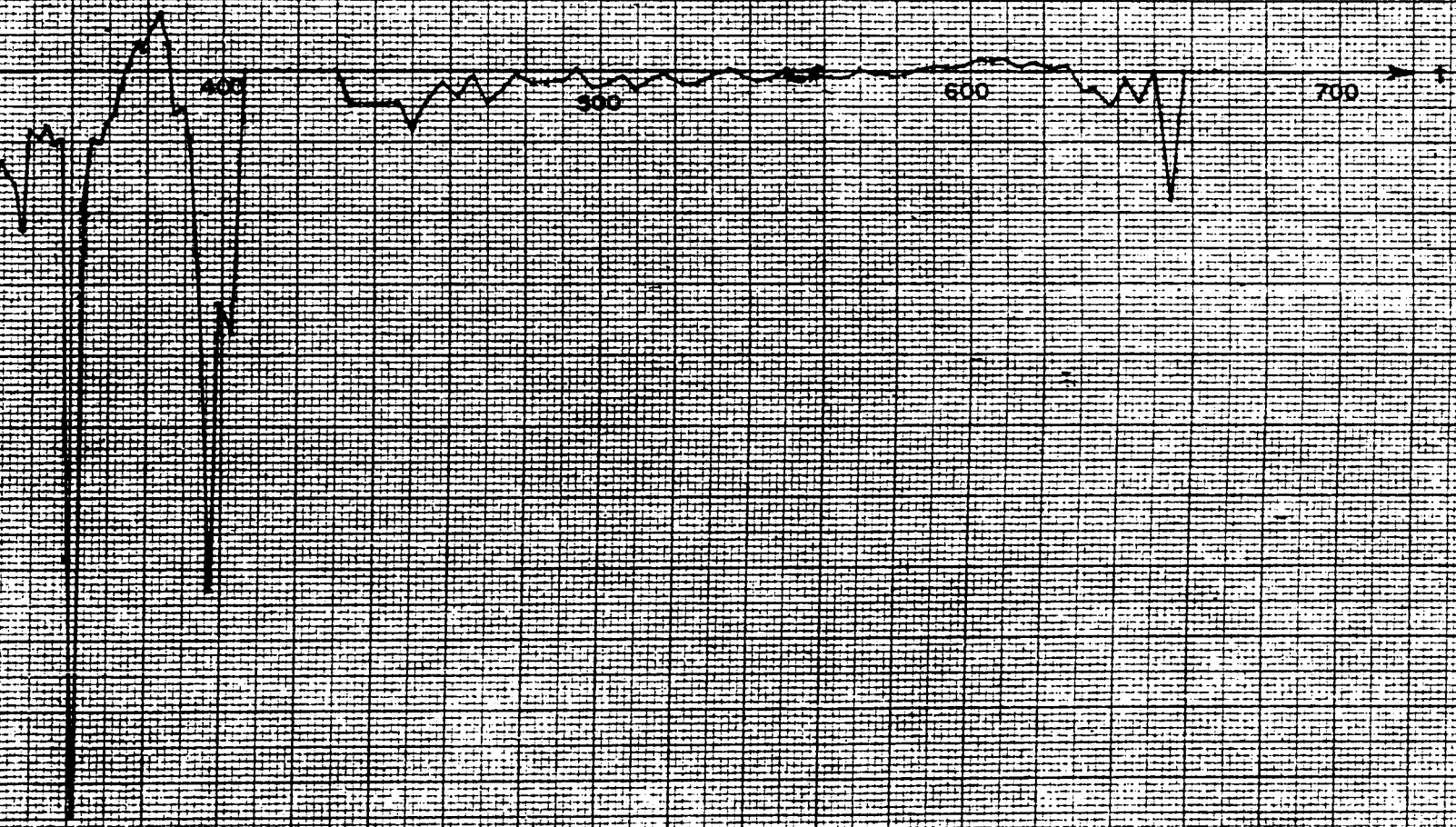

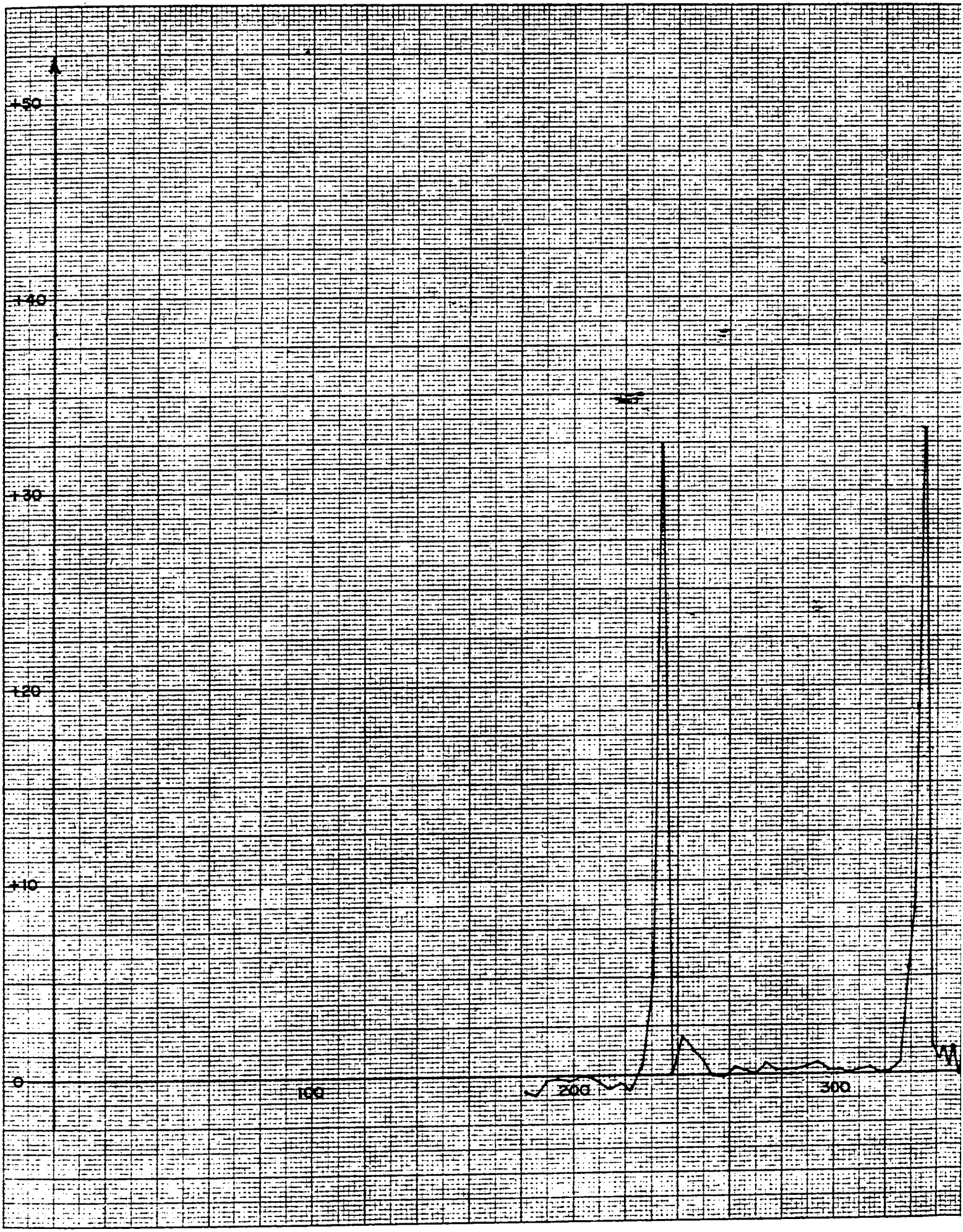
+50
+40
+30
+20
+10
0
100
200
300

FIGURE 19

$\Delta\alpha(t)$

Δt

VERTICAL SCALE – 1 CM = 2.5 MILLISECOND

HORIZ SCALE – 1 CM = 20 MILLISECONDS

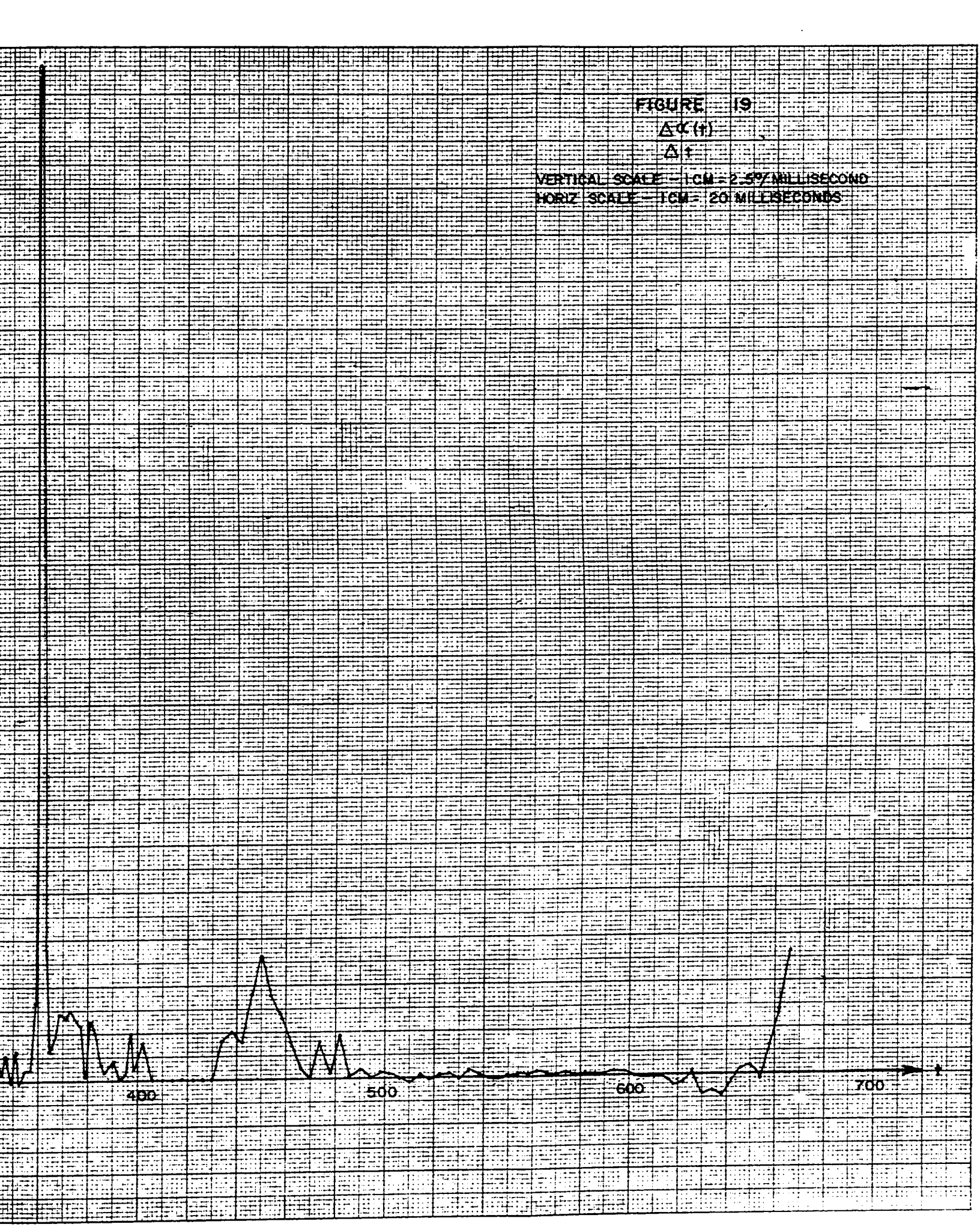

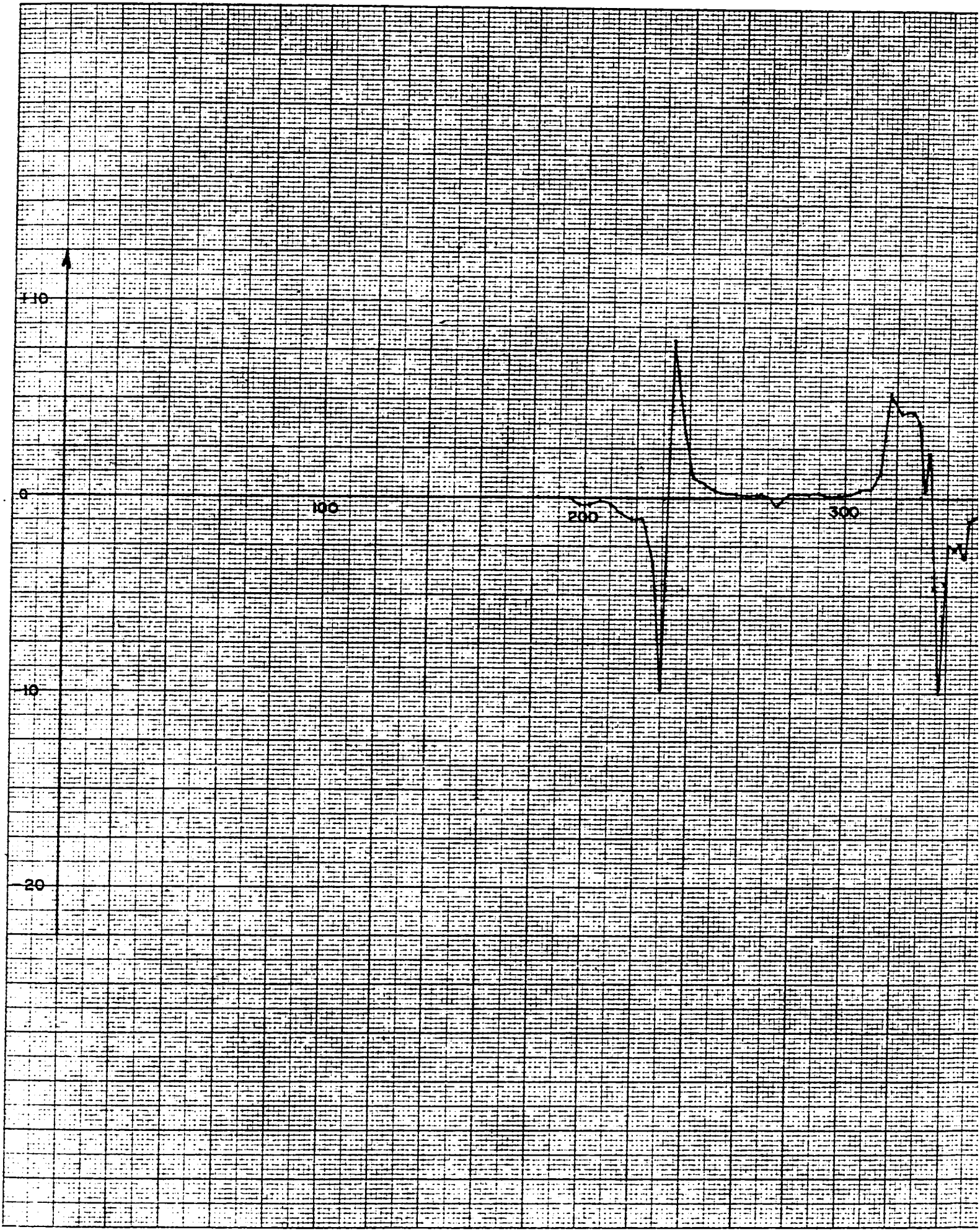
110
0
10
20
100
200
300

FIGURE 20

$\frac{\Delta \beta(t)}{\Delta t}$

VERTICAL SCALE – 1 CM = 2.5% MILLISECOND

HORIZ SCALE – 1 CM = 20 MILLISECONDS

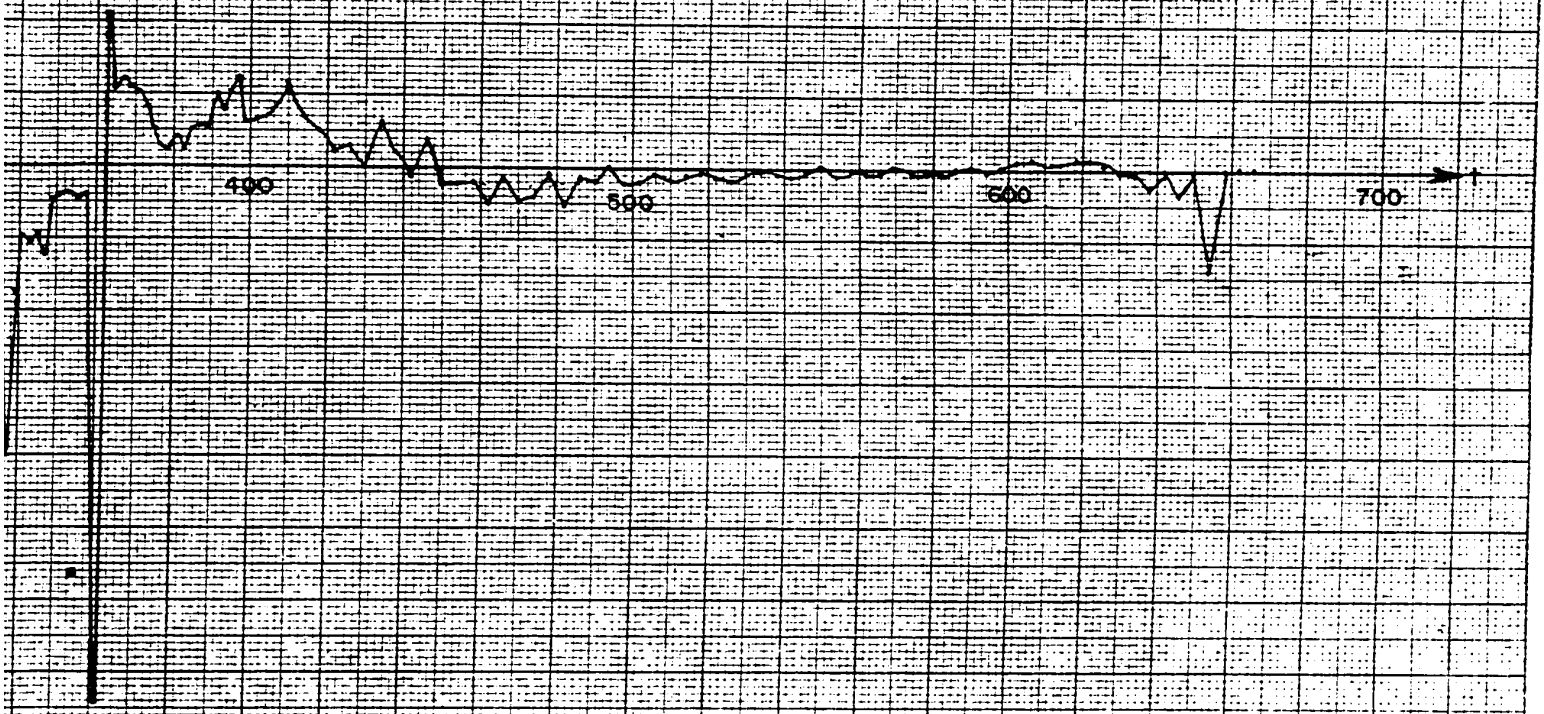

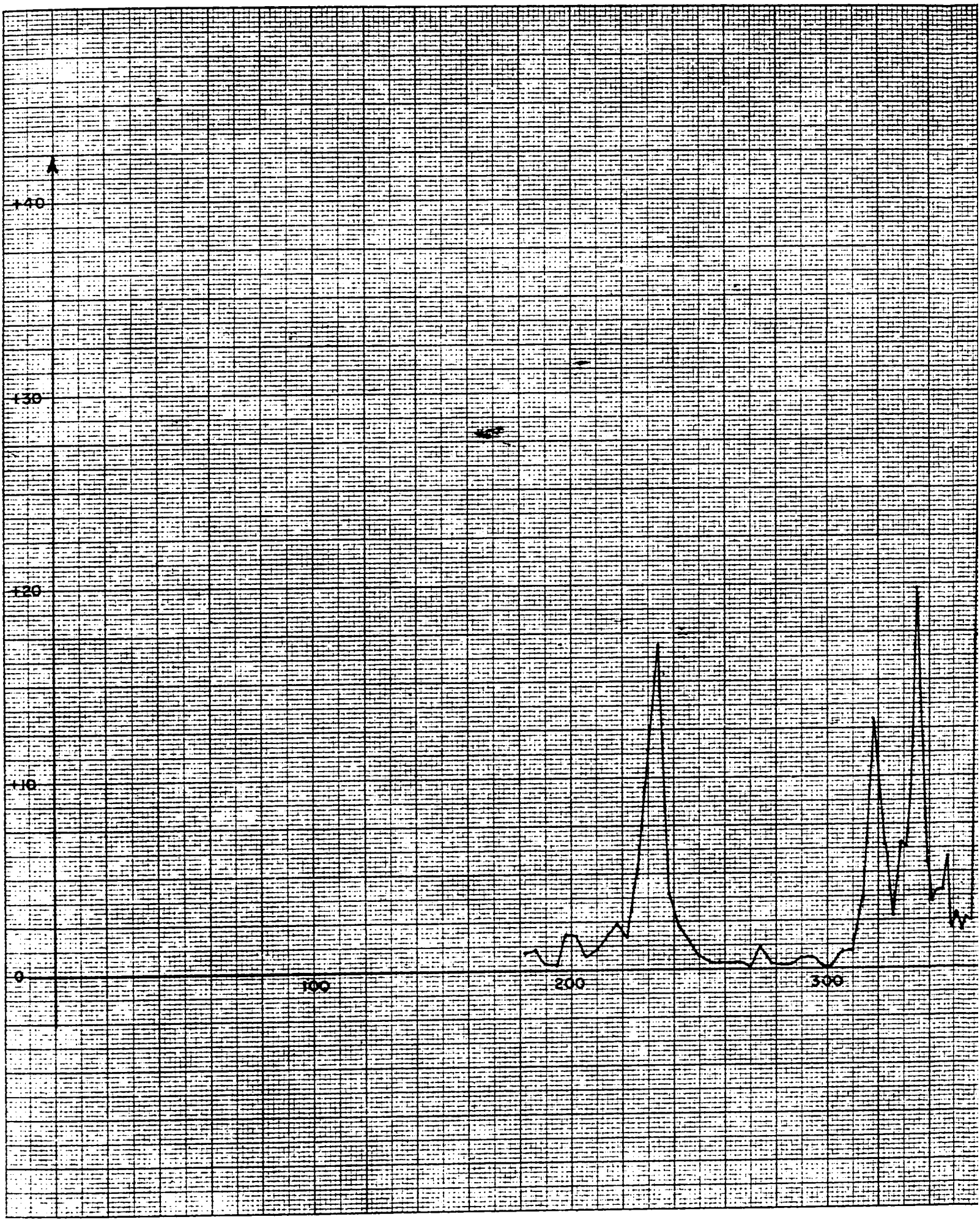
+40
+30
+20
+10
0
100
200
300

FIGURE 21

$$|w| = \left| \sqrt{\left(\frac{\Delta\theta(t)}{\Delta t}\right)^2 + \left(\frac{\Delta\phi(t)}{\Delta t}\right)^2} \right|$$

VERTICAL SCALE — 1 CM = 2.5°/MILLISECOND

HORIZ SCALE = 1 CM = 20 MILLISECONDS

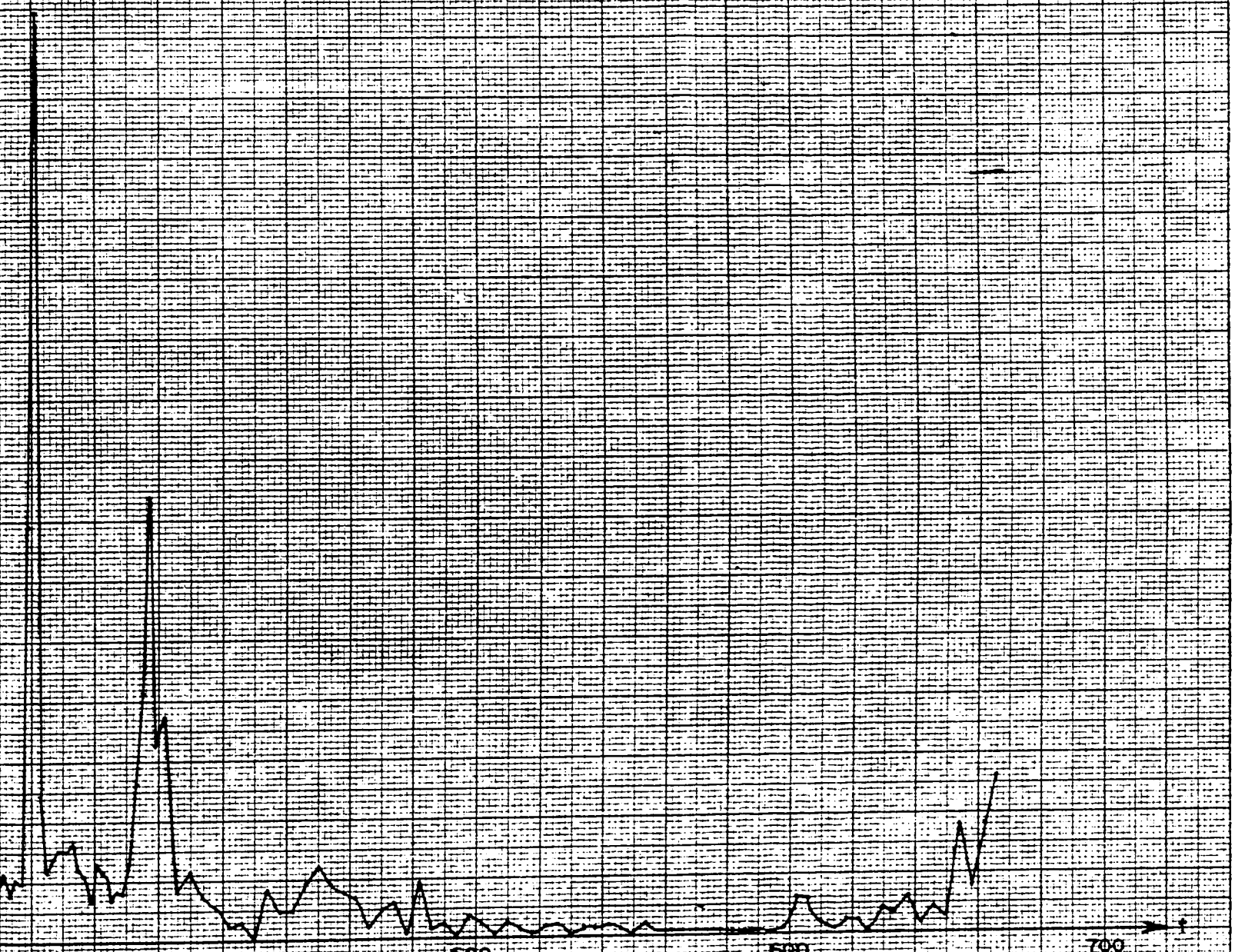

CHAPTER 8

FOURIER ANALYSIS OF THE ELECTROCARDIOGRAPHIC SIGNAL

Summary

Few investigators have given quantitative data regarding the harmonic analysis of the ECG signal. The following chapter discusses the few references available dealing with the Fourier analysis of the ECG waveform and presents the results of an analysis of $x(t)$ performed on an IBM 650 digital computer. A short note on power spectrum, autocorrelation and crosscorrelation is given. Included in the list of references is a number of qualitative reports dealing with high fidelity electrocardiography.

Fourier Analysis

The main purpose of a Fourier analysis of the ECG signal is to establish the bandwidth, which to date is still an open issue, required of electrocardiographic recording equipment. The analysis also serves to indicate that the Fourier series is inefficient for representing the ECG signal as compared to a set of orthogonalized exponential functions with complex exponents (Chapter 9).

Caldwell et al published (1932-33) the first quantitative data re Fourier analysis of an ECG signal (8~~1~~93, 6~~8~~83). The harmonic analysis was performed using a Coradi analyzer (8~~2~~94). The results of the analysis for a few frequencies were reported as given in Table 8.1.

TABLE 8.1

Harmonic	Relative Amplitude
1 (Fundamental)	1.00
2	2.36
20	3.24
30	0.75
35	1.27
40	2.27
45	1.33
50	0.94
100	2 (approximate)

The fundamental frequency was about 1.25 cps as determined from the number of heart beats per minute so that the 40th harmonic would correspond to 50 cps. Caldwell et al state that an approximate analysis (not using the Coradi analyzer) indicated that the amplitude of the 100th harmonic (125 cps was about twice that of the fundamental. This investigation was carried out to define the frequency response required of ECG recording equipment and indicate the importance of good high frequency response.

In comparing the response of a string galvanometer to the response of the research amplifier and oscillograph used to obtain the record for

harmonic analysis, the bandwidths were 50 cps and 250 cps respectively; bandwidth being defined arbitrarily by a 15% decrease in response. The results of this study were in conflict with previous investigations largely due to the fact that the records used for previous investigations were obtained with string galvanometers incapable of responding to the higher frequencies adequately. The high rates of change of potential in the ECG waveform, namely the rise and fall times of the QRS complex, give an approximate indication of the frequency response required (Chapter 4). The results given in Table 8.1 are plotted in figure 8.1 for the purpose of comparison with results to be discussed below. In briefly discussing the importance of the higher frequency components in following the QRS complex, Sayers (17) claims that variations of up to 10% in magnitude can be observed in human subjects from day to day in the higher frequency components, that is, above 200 cps, of the ECG signal. Sayers, however, does not give data to support his statement.

Scher and Young (95)(1960) performed a frequency analysis on the ECG signals recorded from some 25 subjects. The results of their analysis is reporduced in figure 8.2 for ready reference. In investigations prior to 1960 (96, 83), notching, slurring and other rapid movements of the oscilloscope beam were mentioned with the implication that useful diagnostic information could be obtained from recording the higher frequencies. However, there have also been suggestions (97) that the amount of high frequency information is limited. Scher and Young attempted to resolve this question by making a qualitative frequency analysis of the ECG signal. Prior to the work of Scher and Young, only Caldwell et al (1932-33) had reported quantitative frequency analysis results. The equipment used to record the ECG signal had a frequency response well in excess of the recorder itself which was capable of a paper speed sufficient to resolve 0.5 millisecond deflections, that is frequencies up to 1000 cps.

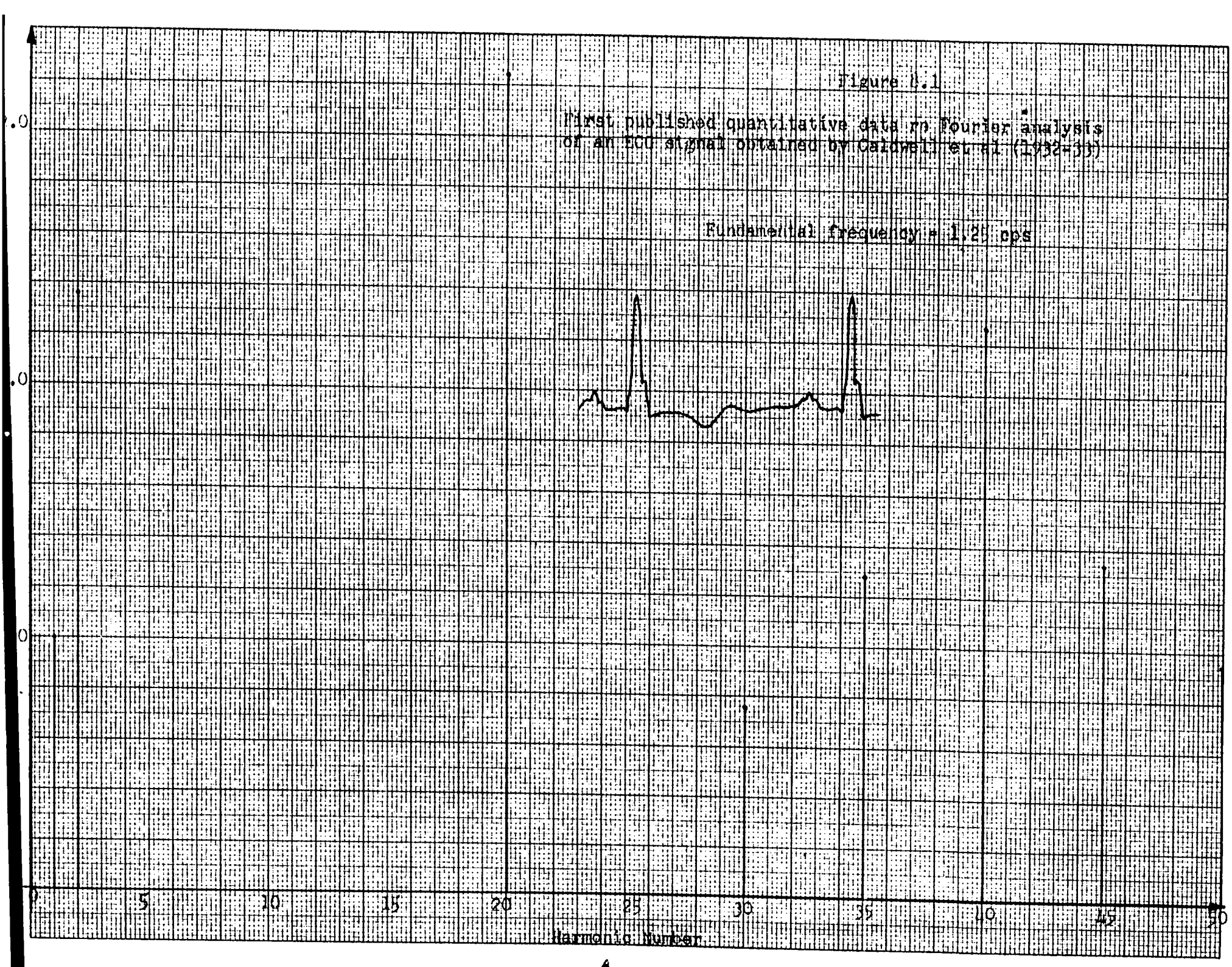
Figure 8.1
First published quantitative data on Fourier analysis of an ECG signal obtained by Caldwell et al (1932-33)
Fundamental frequency = 1.25 cps
.0
.0
0
0
5
10
15
20
25
30
35
40
45
50
Harmonic Number

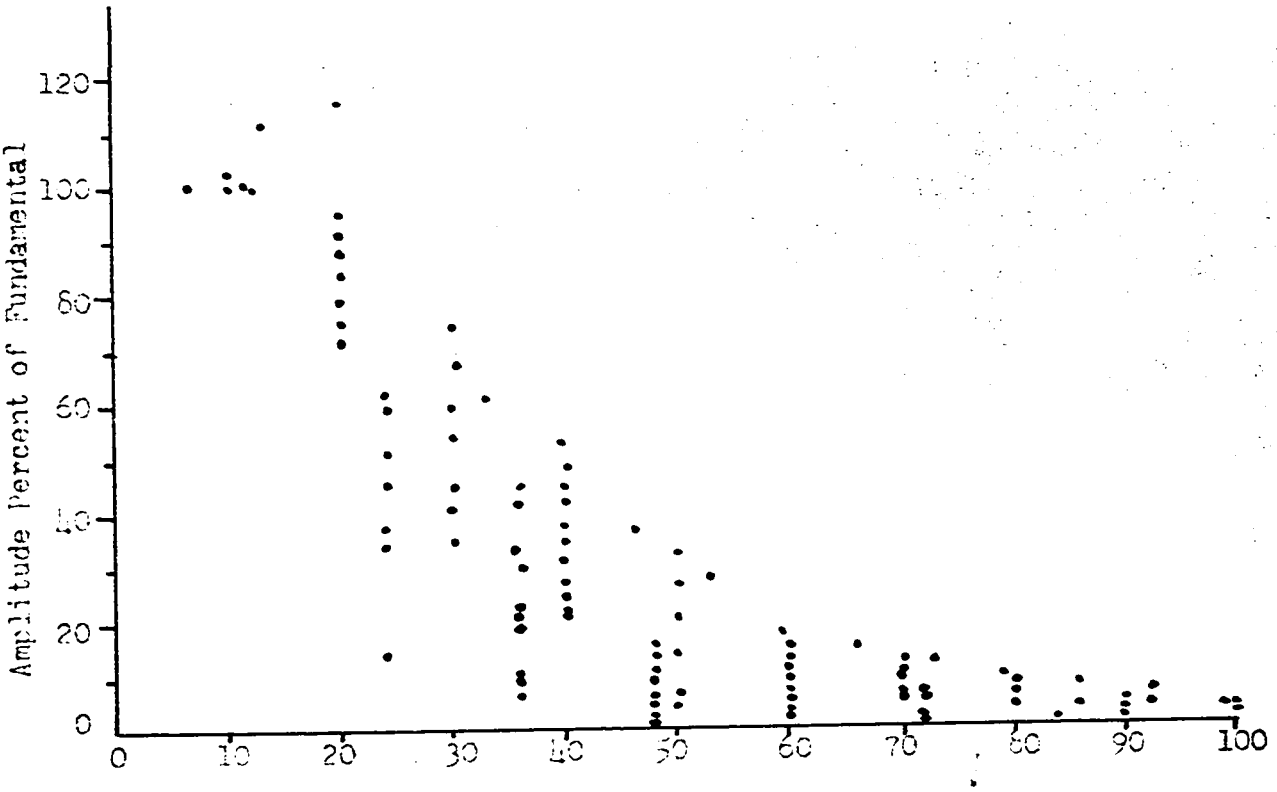

Figure 8.2

Frequency analysis of ECG signals (recorded from 25 subjects) carried out by Scher and Young (1960)

After appropriate enlarging of the photographic records, the outline of the waveforms were carefully cut out and mounted on a photoelectric waveform generator (8~~6~~98) feeding a General Radio waveform analyzer and associated recording equipment. From their analysis Scher and Young conclude that frequencies of 100 cps or higher are less than 10% of the amplitude of the fundamental and that frequencies above 100 cps contribute less than 2% to the total area of the ECG signal. Their results are consistent with Gilford (8~~5~~97) but are in disagreement with Langner (8~~4~~96) and Caldwell et al (8~~1~~93, 6~~6~~83).

A Fourier analysis of $x(t)$[1], figure 7.1, performed on an IBM 650 digital computer[2] at the University of Ottawa is shown in figures 8.3 and 8.4. The results of the analysis follows the general pattern of the results obtained by Scher and Young in that the envelope of the amplitude spectrum are of approximately the same form, keeping in mind that figure 8.3 is for only one signal and figure 8.2 is plotted for a number of signals. Figure 8.3 shows the Fourier analysis performed on $x(t)$ for one complete heart cycle with a period of 640 milliseconds or fundamental frequency of 1.56 cps as measured from P wave onset to P wave onset. The 40th harmonic corresponds to approximately 62 cps and has an amplitude of approximately 6% of the fundamental.

Figure 8.4 shows the Fourier analysis performed on an interval (arbitrarily chosen) containing the QRS pulse and the start of the T wave. The period of the interval was 162 milliseconds corresponding to a fundamental frequency of 6.21 cps. The 20th harmonic corresponds to approxi-

---

[1] $x(t)$, $y(t)$ and $z(t)$ were recorded using Electronics for Medicine Physiological Recording equipment. The preamplifiers of this equipment have a frequency response of 0.1 to 600 cps. The bandwidth of the preamplifiers can be reduced by switching in high and low pass filters.

[2] The analysis required 2 hours of computer time. To prove out the computer program a trial run was performed using a simple example

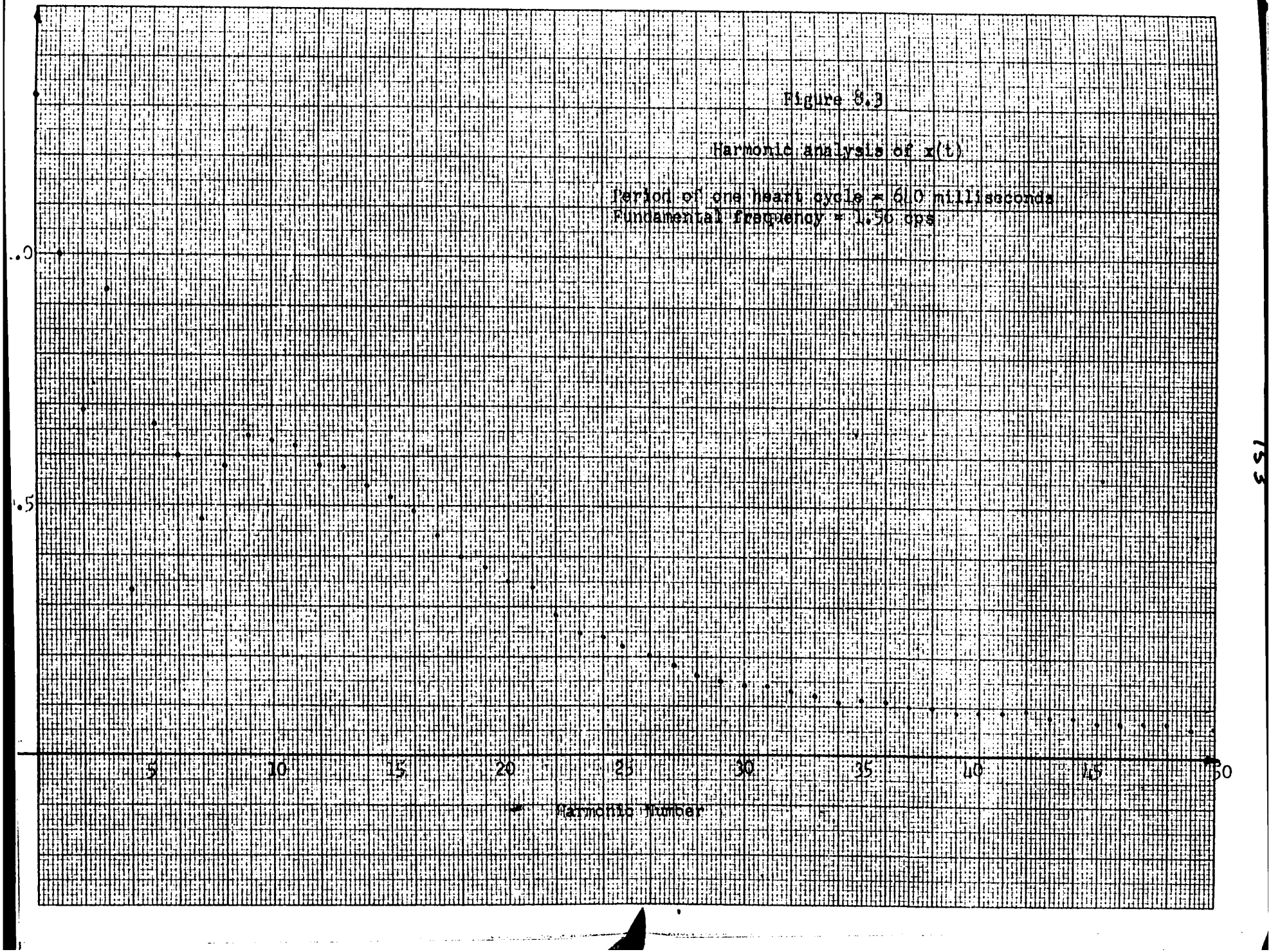
Figure 8.3
Harmonic analysis of x(t)
Period of one heart cycle = 640 milliseconds
Fundamental frequency = 1.56 cps
1.0
.5
5
10
15
20
25
30
35
40
45
50
Harmonic Number

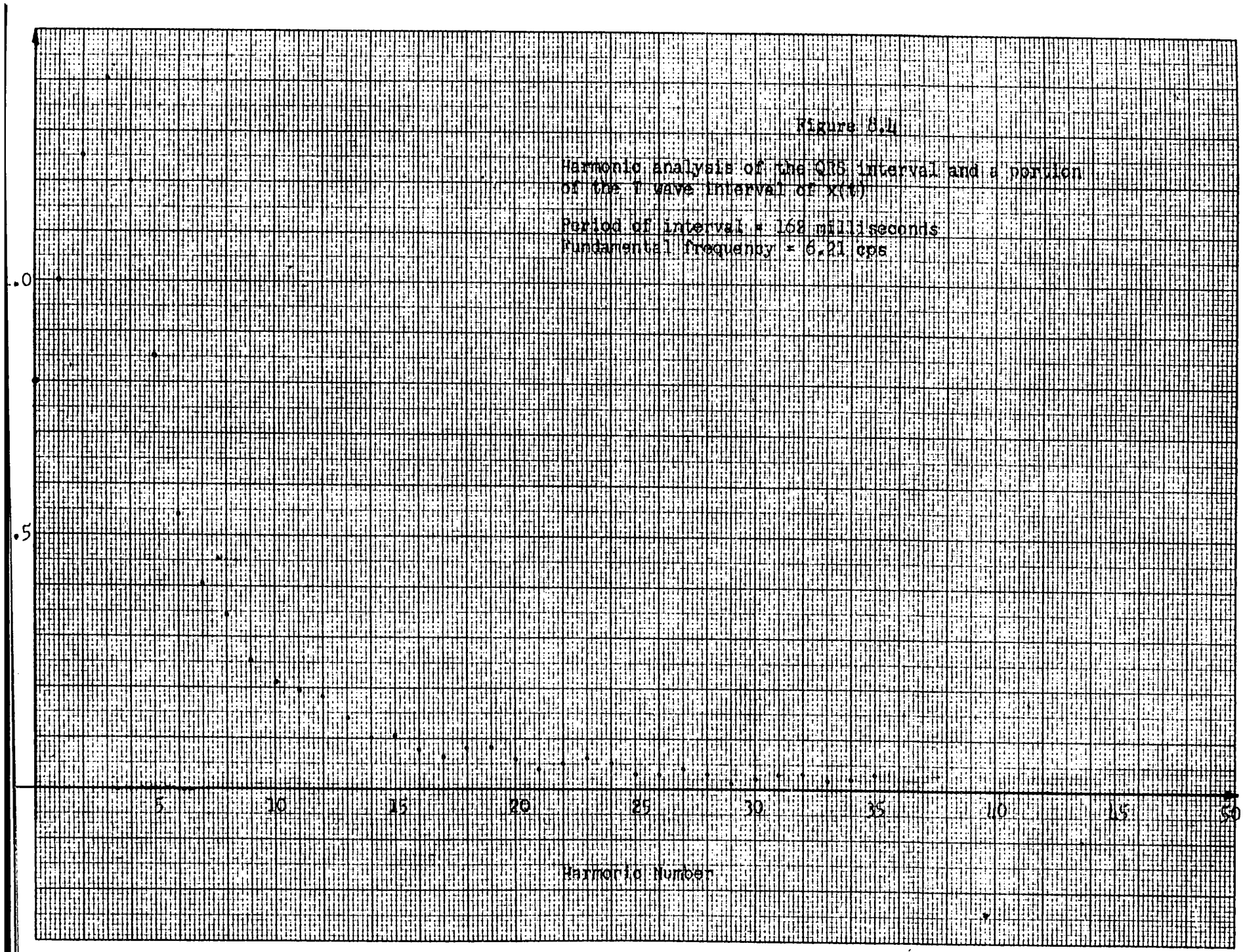

Figure 8.4

Harmonic analysis of the QRS interval and a portion of the T wave interval of x(t)

Period of interval = 168 milliseconds
Fundamental frequency = 6.21 cps

mately 125 cps and has an amplitude of 6% relative to the fundamental.

The dc component of ECG signals results from the asymmetry of the waveforms about the baseline (zero) which corresponds to the isoelectric point (origin) on a VCG display. Since the Fourier series consists of symmetrical functions, that is, sine and cos functions, an analysis requires a dc term to represent the asymmetry of the ECG signal. The importance of properly identifying the baseline of an ECG signal and the necessity of considering the dc component in circuit and system design has already been mentioned elsewhere in this thesis.

Related to the harmonic analysis of the ECG signal are the qualitative observations reported in the literature under the topic of high fidelity electrocardiography (8.96, 8.97, 8.100 to 8.104). Kerwin (8.100)(1953) reported on a qualitative study dealing with the effect of system bandwidth on the ECG signal waveform. The effect of bandwidth was illustrated by passing an ECG signal through a system, the bandwidth of which could be set at 50, 100, 200 and 6400 cps, and comparing the resulting display of a rectangular pulse rise time and an ECG signal waveform visually. Kerwin suggested the use of higher paper speeds in recording equipment as being necessary to bring out the high frequency components of the ECG. This is warranted for research work, but the significance of higher frequencies in pathologic processes remains to be evaluated. Kerwin did not give quantitative results in the terms of harmonic analysis.

The work of Langner and Geselowitz reported in (8.104)(1960) is of interest in that illustrations of the result of passing an ECG signal through a high pass filter are given indicating the residual signal remaining with increasing cut off frequency (3 db down). They suggested the use of an RMS meter to measure the energy content of the residual

signal but resorted to CRO displays in their work for reasons of simplicity.

Finally, it is worthwhile to discuss briefly a limited number of reports available in the literature dealing with the power spectrum, autocorrelation and crosscorrelation of the ECG signal[3]. Franke et al (8 ~~13~~ 105) (1962) studied the high frequency components in the electrocardiogram by means of a power spectrum analysis obtained by analog computation. The ECG signal was filtered by a variable band-pass filter (Krohn Hite, ultra low frequency band-pass 333-A) the output of which, after suitable amplification, was fed to an electronic squaring circuit. The output voltage of the squaring circuit is proportional to the signal power in frequency band determined by the band-pass filter. Finally, the output of the squaring circuit was fed to an integration circuit the output of which is proportional to the power spectral density of the input signal. The frequency bands used were: 0 - 60, 30 - 60, 40 - 80, 60 - 120, 90 - 180, 130 - 260, 180 - 360, 250 - 500, and 350 - 700 cps. From their study, Franke et al demonstrated that practically all of the energy in the higher frequency bands is concentrated in the QRS complex. Furthermore, they point out that the small relative amplitude of the high frequency part of the ECG signal spectrum is not sufficient reason to conclude that the higher frequencies do not contribute significant diagnostic information and that the only relevant quantity is the signal-to-noise ratio. By the power spectral method, Franke et al claim that components as high as 3000 cps, well above the noise level, were found in some subjects.

---

[3]The literature also contains a number of interesting reports on the power spectrum, autocorrelation and crosscorrelation of electroencephalograms (EEG), phonocardiograms (PCG), and other physiological signals.

Angelakos and Shepherd (8 ~~14~~ 106)(1957) give a good discussion on the meaning of autocorrelation and its use in finding hidden periodicities in otherwise meaningless waveforms such as the ECG during ventricular fibrillation. To obtain the autocorrelation function, they used a computer developed at the Massachusetts Institute of Technology (8 ~~15~~ 107)(1955). Koyama et al (8 ~~16~~ 108)(1962) used an analog correlator (Model CCA-22, Sony, Corp., Tokyo, Japan) to obtain the autocorrelation and crosscorrelation of the ECG during ventricular fibrillation induced in dogs in order to re-evaluate the findings of Angelakos and Shepherd regarding the periodicities of fibrillation. Finally, the bibliography lists further papers (8 ~~17~~ 109 ~~to~~ to 8 ~~20~~ 112) on the topics of the power spectrum and correlation function of the ECG signal.

CHAPTER 9

REVIEW OF THE APPLICATIONS OF SIGNAL ANALYSIS TO THE REPRESENTATION OF ELECTROCARDIOGRAPHIC SIGNALS

Summary

The following chapter is a review of the application of signal analysis theory by Huggins and Young to the representation of ECG signals and subsequent classification of the signals using the representation. The representation uses a set of orthogonalized exponential functions which form the basis of a multidimensional signal space. The intrinsic component theory is also discussed. The material presented will be mainly descriptive and will refer to various mathematical techniques and concepts. The purpose of this chapter is to present an understanding of the work carried out by Huggins and Young through the association of various ideas and concepts and without resorting to rigorous mathematical details. Although the theoretical mathematical foundations used by Huggins and Young are well established, and the feasibility of their technique has been demonstrated, the diagnostic usefulness of the technique has yet to be demonstrated by further experimental studies. Mention is also made of the factor analysis technique used by Scher et al.

The signal analysis concept as used in communication engineering and other fields can be considered to be composed of two problems; the classification problem and the representation problem. Both the classification problem and the representation problem as related to the application of signal analysis to ECG waveforms have been investigated by Huggins and Young (~~2.5~~ 25, ~~7.1~~ 86, ~~9.1~~ 113, ~~9.2~~ 114, ~~9.3~~ 115). As previously mentioned in Chapter 1, once a signal is described in some definite manner, the classification problem can readily be handled by established statistical methods with the aid of a digital computer.

Perhaps the problem of signal representation can best be discussed briefly with respect to the field of communication engineering (~~9.4~~ 116). As the communication art grows more sophisticated and involved, the communications engineer is faced with the problem of dealing with complicated signals. The communications engineer seeks a set of analytical tools whereby he may render the behavious of complicated signals easy to manipulate in mathematical computations and simple to understand. Similar problems arise in the fields of seismology, electroencephalography, aeronautical structural engineering, etc. Though the problem of representing a general signal S has not yet been solved, there are techniques available for representing certain restricted classes of signals in the set of all possible signals S such that the representation in some sense facilitates computation, analysis or "seeing what goes on" in the generation and processing of signal waveforms. Though difficulties may be present, certain theoretical or practical advantages make these techniques noteworthy.

There are many aspects or attributes of a signal that may be of interest. For example, in a speech signal one might be interested in the semantic content, identifying the words that make it up, waveform, intelligibility to the listener. These aspects are intuitively related, but a good representation of one attribute, say waveform, may not be related in a one to one manner with another attribute, say identification. It is necessary to set certain restrictions, the first restriction being that one is interested in characterizing the aspect of "waveform" which is usually given as a function of time. Secondly, the characterization, as already mentioned, must be useful in the sense of ease of computation and understanding "what goes on". The problem of the communications engineer is thus quite analagous to the problem encountered in ECG diagnosis by the cardiologist.

As suggested elsewhere in this report and in the literature, electrocardiographic diagnosis of heart ailments depends on the subjective interpretation of an experienced specialist, a cardiologist. Huggins and Young, using their background gained from signal analysis and representation problems in communications engineering (95)[117], have attempted to find an efficient representation of the ECG waveform. To enable statistical analysis of signals, such as the ECG waveform, by means of digital computers, the first problem is to describe each ECG by a collection of discrete numbers, that is, an efficient representation must be found. To find an efficient representation means to approximate the signal with the smallest number of basis signals and maintain a specified accuracy of approximation. In other words, the ECG signal is decomposed into a linear

combination of a prescribed set of component signals called a basis. By measuring the amount of each component signal, the pertinent information in the ECG can be represented by a collection of numbers.

The problem of finding an efficient representation thus becomes the problem of finding or choosing an appropriate set of basis signals. Pipberger et al (~~5.2~~ 67; Chapter 5) decomposed the ECG signal by means of the sampled data approach which uses pulses as the basis components. The ECG signal, as well as other physiological signals, have been decomposed by means of the spectral analysis method (Chapter 8; ~~9.6~~, ~~9.7~~, ~~9.8~~ 119 120 121) which uses the sine-cosine functions of a Fourier series as basis components. Both the sinusoidal and the sampled data representations of the ECG signal are easily accomplished with present day instrumentation and so are practical from this standpoint. However, to obtain a sufficiently accurate representation of the ECG signal, a large number of frequency components or sampling points are required and the problem of statistical analysis becomes impractical. For this reason, the conventional technique for automatic interpretation of the ECG uses the sampled data process only to convert the analog ECG signal into a digitized format. The digital computer is then used as a memory device and is instructed to measure, according to pattern recognition programs discussed in Chapter 5, the clinically useful parameters established over the years by the experience of cardiologists.

Huggins and Young chose to decompose the ECG signal using a set of orthogonalized exponential functions of time. They have demonstrated the feasibility of first representing (decomposing) the QRS and T portions of the ECG signal with acceptable fidelity with only 12 such components and

then using this relatively compact representation for classifying ECG waveforms. Using the 12 exponential components, the average error of approximation is 5% (for the QRS and T waves only, the P wave was not considered). In comparison, using 12 sinusoidal components in a Fourier series representation results in an average error energy of 28% to 48%. To limit the error to 5% requires a dc component and 28 sine and cosine components.

In discussing the problem of finding an efficient representation of an arbitrary signal by means of a set of basic components, the concept of a signal vector in a multi-dimensional signal space proves useful. This concept treats the set of all possible signals S in a very generalized way. That is, a collection (ensemble) of signals are considered to be vectors in an n-dimensional signal (Hilbert) space. For each signal (function of time), there is a corresponding signal vector the length and direction of which corresponds to the energy and waveform respectively of the signal. In our context, "signal" refers to the ECG waveform. To reconstruct a signal from a signal vector means to project the signal vector into a certain subspace which is equivalent physically to measurements performed by a particular type of instrumentation. In effect, the signal vector is projected onto the appropriate coordinates of the n-dimensional signal space and the resulting projections, when combined linearly (summed) yield the signal.

As has been suggested earlier in this chapter, the problem of representing a general signal S has not yet been solved, but it is possible to represent certain restricted classes of signals. The class of signals

of interest here is that composed of all possible ECG waveforms. Before proceeding further, it should be emphasized that the signal vector should not be confused with the heart dipole vector. The signal vector is a fixed vector which represents the entire ECG signal by a single point in the n-dimensional (Hilbert or abstract) space. The heart dipole vector, on the other hand, is a time varying vector at a fixed location in physical space. The signal vector represents the time structure of the signal, the length corresponding to energy and the direction to waveshape. In contrast, the dipole vector consists of three spatial components $x(t)$, $y(t)$ and $z(t)$, each of which can be represented by a signal vector in signal space. The three signals together represent the time and space structure of the dipole.

The concept of signal space is perhaps best illustrated by a simple example. Consider the simple triangular and square signals shown in figure 9.1 and defined by

$$f(t) = t \qquad 0 \leq t \leq \pi \tag{9.1}$$

$$g(t) = \pi \qquad 0 \leq t \leq \pi$$

The Fourier series expansion over the interval $0 \leq t \leq \pi$ yields.

$$f(t) = 2 \sin t - \frac{2 \sin 2t}{2} + \frac{2 \sin 3t}{3} \cdots\cdots \tag{9.2}$$

$$g(t) = 4 \sin t + \frac{4 \sin 3t}{3} + \cdots\cdots\cdots\cdots$$

which may be rewritten as

$$|f\rangle = |fa\rangle + |\varepsilon_f\rangle \tag{9.3}$$

$$|g\rangle = |ga\rangle + |\varepsilon_g\rangle$$

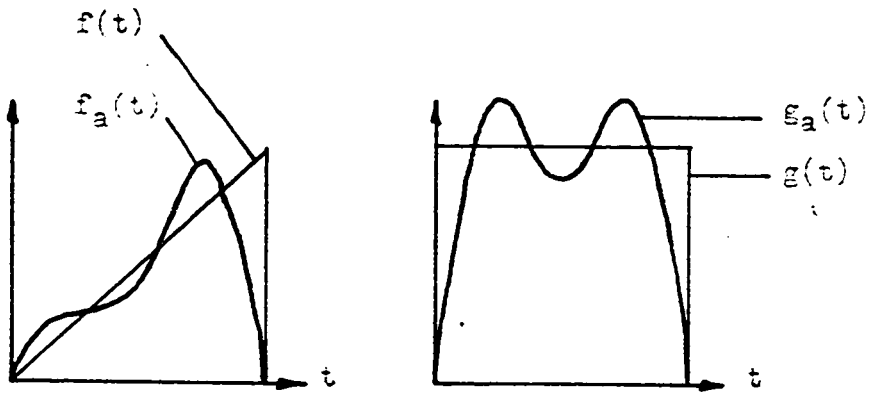

$f(t) = t, 0 \leq t \leq \pi \qquad g(t) = \pi, 0 \leq t \leq \pi$

$$f_a(t) = 2 \sin t - \sin 2t + \frac{2}{3} \sin 3t$$

$$g_a(t) = 4 \sin t + \frac{4}{3} \sin 3t$$

Figure 9.1

Representation of triangular wave and square wave by Fourier series.

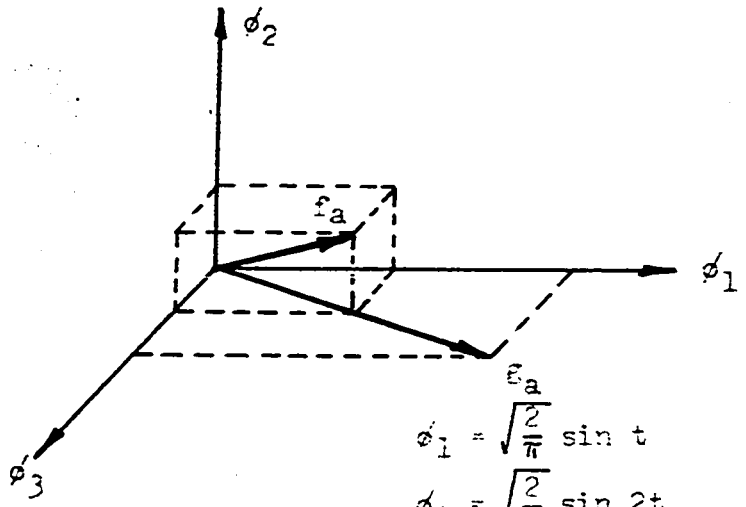

$$\phi_1 = \sqrt{\frac{2}{\pi}} \sin t$$

$$\phi_2 = \sqrt{\frac{2}{\pi}} \sin 2t$$

$$\phi_3 = \sqrt{\frac{2}{\pi}} \sin 3t$$

Figure 9.2

Signal space spanned by three sine functions.

where

$$|f_a\rangle = \sqrt{2\pi}\left(\sqrt{\frac{2}{\pi}}\sin t\right) + \sqrt{\frac{2\pi}{2}}\left(-\sqrt{\frac{2}{\pi}}\sin 2t\right) + \sqrt{\frac{2\pi}{3}}\left(\sqrt{\frac{2}{\pi}}\sin 3t\right)$$

$$|g_a\rangle = 2\sqrt{2\pi}\left(\sqrt{\frac{2}{\pi}}\sin t\right) + \frac{2\sqrt{2\pi}}{3}\left(\sqrt{\frac{2}{\pi}}\sin 3t\right) \qquad (9.4)$$

The notation $|\ \rangle$ (due to Dirac, see 9.118a) indicates signal vector. $|\varepsilon_f\rangle$ and $|\varepsilon_g\rangle$ in equations 9.3 are the error vectors resulting from approximating the true signals by a finite number of terms in the Fourier series expansion.

If we now define

$$|\phi_1\rangle = \sqrt{\frac{2}{\pi}}\sin t$$

$$|\phi_2\rangle = -\sqrt{\frac{2}{\pi}}\sin 2t \qquad (9.5)$$

$$|\phi_3\rangle = \sqrt{\frac{2}{\pi}}\sin 3t$$

as the basis or component functions then equations 9.4 may be written as

$$|f_a\rangle = \sqrt{2\pi}\,|\phi_1\rangle + \sqrt{\frac{2\pi}{2}}\,|\phi_2\rangle + \sqrt{\frac{2\pi}{3}}\,|\phi_3\rangle$$

$$|g_a\rangle = 2\sqrt{2\pi}\,|\phi_1\rangle + \sqrt{\frac{2\pi}{3}}\,|\phi_3\rangle \qquad (9.6)$$

Keeping in mind that the basis functions defined in 9.5 are the first three terms of the Fourier series, one can simply write the amplitude coefficients in the form of a vector,

$$|f_a\rangle = \left(\sqrt{2\pi}, \sqrt{\frac{2\pi}{2}}, \sqrt{\frac{2\pi}{3}}\right)$$

$$|g_a\rangle = \left(2\sqrt{2\pi}, 0, \frac{2}{3}\sqrt{2\pi}\right) \qquad (9.7)$$

Figure 9.2 shows the signal subspace spanned by the three Fourier components $|\phi_1\rangle$, $|\phi_2\rangle$ and $|\phi_3\rangle$. The components and the error $|\varepsilon\rangle$ are mutually orthogonal. The approximation of the triangular and square waves, $|f_a\rangle$, $|g_a\rangle$, may be interpreted as the projections of signals $|f\rangle$ and $|g\rangle$ onto the chosen three dimensional subspace where the amount of each component of the projections is given by 9.7. Figure 9.1 indicates the approximation of the triangular and square waves by the first three components of the Fourier series. The approximation could be improved to any desired degree by using additional, say n, components of the Fourier series expansion. In signal space, this amounts to considering an n-dimensional subspace which corresponds to the use of n basis functions. The problem of efficient signal representation is to select the smallest possible set of basis functions which can represent the members of a class of signals with acceptable accuracy. That is, the problem is to find a simple set of component functions onto which the projection of the signals of interest will have maximum average energy which is equivalent to minimizing the average error of representing the signals in the least-square sense.

As suggested above, ECG signals have been decomposed using various types of basis functions. Huggins and Young chose to represent the ECG waveform with a set of orthognolized exponentials. That is, each ECG signal is decomposed into the same set of exponential time functions

$$\sum_{i} a_i \exp(-a_k t \pm j\beta_k t) \qquad (9.8)$$

which form the basis or coordinates of a multi-dimensional signal space. Orthogonolized exponentials were chosen partly because they resemble the typical pattern of ECG waveforms and partly because certain relatively

simple analog instrumentation techniques are available for such a basis. If a satisfactory representation of the ECG signal can be obtained using exponentials, a simple electrical filter network (orthonormal filter) (9.5, 9.9, 9.10) may be synthesized to form an equivalent signal generator which will generate the approximating ECG signal.

As indicated in equation 9.8, orthognolized exponentials in general have complex exponents. If in particular, the exponents are real and equal then the set of orthognolized exponentials are called Laguerre functions, figure 9.3a. In initial studies, Huggins and Young used Laguerre functions to represent the ECG signal because they are the simplest orthognolized set and because of simplicity of instrumentation. Using 20 components, a reasonable approximation to the ECG signal was achieved. The Laguerre functions are in effect a special set of exponentials in that the exponents are not complex. Since a Fourier series representation of a signal can be written in exponential form, the Fourier series is also a special set of orthognolized exponential functions which is made up of exponentials with purely imaginary exponents. Neither of the choices, that is, the use of Laguerre functions or simusoidal functions, is made with any particular regard to the characteristics of the signal to be represented and so these sets of basic functions are not necessarily the most efficient possible. In subsequent studies Huggins and Young developed an iterative procedure, using a digital computer, to determine a set of basic exponential functions with complex exponents that are "matched" to a given class of signals, in particular, the class of ECG signals. The details of the procedure are given in (25) and (9.1). The basis determined consisted of 12 exponentials with complex exponents (figure 9.3b) spanning a twelve-dimensional signal space. This represents a considerable improvement as compared to

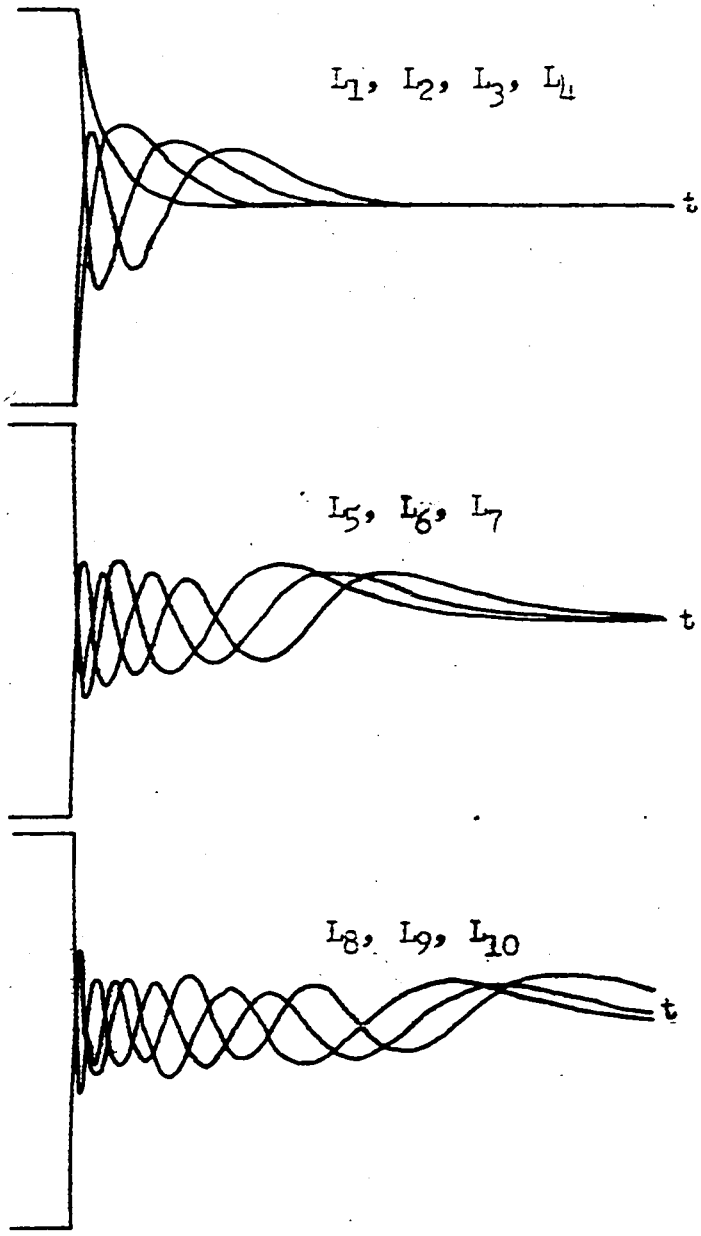

Figure 9.3a

Laguerre functions

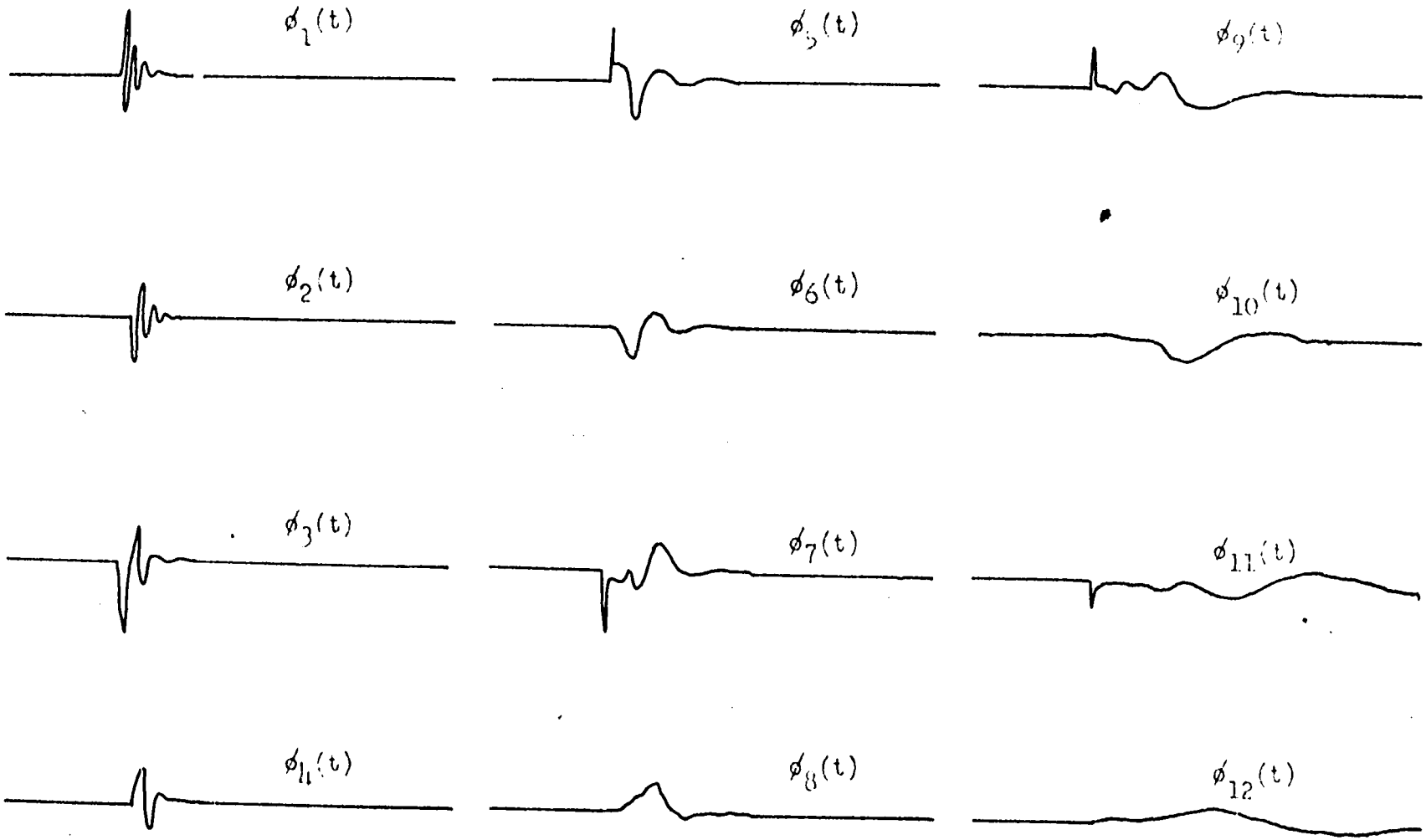

Figure 9.3b

Orthogonal exponential functions with complex exponents

representations using Fourier series or Laguerre functions and suggests that complex exponents seem best for representing ECG signals.

The problem of finding the most efficient set of complex exponents, that is the set of complex exponents best matched to the class of signals of interest has no straightforward solution. The iterative procedure used to find a set of basic exponentials developed by Huggins and Young is partly emperical and the basis determined is by no means unique. The iterative procedure and the basis determined, however, have proven to be very practical for ECG representation. Huggins and Young also suggest that other procedures may someday be developed to find the set of matched exponents.

Recall now that once the ECG signal is decomposed into the chosen set of 12 exponential time functions, the ECG signal is represented as a single point in a twelve-dimensional signal space. Supposedly, the points in the signal space representing the same heart malfunction will cluster together in some way in signal space. To verify this hypothesis, it has been demonstrated on a limited scale that ECG signals recorded from 51 subjects with a variety of known pathological conditions myocardial infarction, hypertrophy and conduction defects can be classified with the aid of a digital computer operating on the orthonormal exponential representation of the ECG signal. The mathematical details of the classification procedure are given in reference (25, pp. 85-97).

Finally, Huggins and Young have developed a new theory for electrocardiography, the intrinsic component theory (25, ~~9.2~~ 114). According to

the dipole theory, the heart vector can be defined as the resultant dipole vector of all current sources and sinks in the heart, the relative spatial orientation of the sources and sinks varying with time. In contrast to the dipole theory and its extension to multipole theory, the intrinsic component theory enables one to regard the heart as electrically consisting of several sets of spatially stationary current sources and sinks, the intensities of which all vary with time in proportion to a single common time factor. That is, each component represents an equivalent assemblage of sources and sinks which change their magnitudes during the heart cycle but do not change their relative spatial orientation (as is true physiologically).

The voltage V(p,t) measured on the body surface at a point P can be demonstrated to be separable into time and space functions. That is, the dipole and multipoles can be decomposed according to their spatial relationship such that each component is a function of time. Parameters such as the location of the point P, heart location and body shape affect the space function portion of the voltage V(p,t). Huggins and Young suggest that it is not necessary to decompose ECG signals into time variable dipole or multipole components according to their spatial structure. Instead, one should consider decomposing the ECG signal into components in terms of different temporal characteristics, that is, waveform. Since time is one-dimensional and physical space is three dimensional, Huggins and Young suggest it is easier to formulate a theory based on temporal characteristics rather than spatial structure of the body and leads and have developed their suggestion into the above mentioned intrinsic component theory.

This new approach is a variation of the eigenvalue process (9, 124) which is well known to mathematics and physicists and which is termed factor analysis by statisticians. Physically, an eigenvalue process is equivalent to a rotation of a corrdinate system where the eigenvectors describe the new coordinate system in terms of the original coordinate system.

The ECG actually measured on the body surface can be decomposed into intrinsic components with the aid of a digital computer such that the components are orthogonal (uncorrelated) with one another in the time domain. If n simultaneous measurements or leads, say $x_1, x_2, \ldots\ldots x_n$ are obtained for a subject, the n measurements are usually not entirely independent. By using the eigenvalue process as detailed in references (25) and (9, 114) m intrinsic components defined by

$$u_k(t) = \sum_{i=1}^{n} e_{ik}\, x_i(t) \qquad (9.9)$$

can be evaluated where $m \leq n$. Assuming that a sufficient number of simultaneous measurements n have been made such that an ECG measured at any point on the body surface is expressible by a linear combination of the measurements, then equation 9.9 indicates that the n ECG's measured can be thought of as being generated by the same set of m intrinsic components. That is, each ECG is a linear combination of the m intrinsic components. In terms of intrinsic components, the voltage measured at any point p may be written as

$$V(p,t) = \sum_{k=1}^{m} e_k(p)\; u_k(t) \qquad (9.10)$$

The differences in the waveforms of the n ECG's measured are due to the

locations of the point p at which each measurement was made so the coefficient $c_k(p)$ is a function of space and relates the k^{th} intrinsic component, which is a function of time only, and the field point p. Equation 9.10 indicates that the intrinsic components enable us to separate the time and space functions of the voltage $V(p,t)$.

It is interesting to note that Scher et al (29) in their factor analysis of the QRS complex have essentially calculated the intrinsic components for a number of normal subjects but did not attach a physical meaning to the components (factors) in terms of spatially stationary current sources and sinks as Huggins and Young have done. That is, Huggins and Young have shown that each ECG signal may be considered to be a linear combination of m intrinsic component, $u_k(t)$, one can imagine there exists a spatially stationary set of current sources and sinks that vary in amplitude with time according to the time function $u_k(t)$. The word "intrinsic" is used because the temporal characteristics of the intrinsic components exist intrinsically in the measured ECG signals and depend on the waveform of the signals only regardless of where the measurement is taken.

Huggins and Young suggest that their theory may provide a better representation of the physical process than the multipole theory because the cardiac tissue is an assemblage of spatially fixed dipoles discharging in an ordered temporal sequence and creating a field on the body surface which may or may not, especially in the case of heart disease, resemble that of a dipole. The intrinsic component theory is thus no more unreal that the multipole theory and is more practical since it lends itself to digital computer computation whereas the multipole theory is somewhat

impractical (see Chapter 1, footnote 4).

For a single ECG dipole, the application of the intrinsic component theory provides a mathematical foundation for VCG rotation (see Chapter 2 and 5 re coordinate rotation) and the components are easily visualized physically. The effect of coordinate rotation, as mentioned elsewhere in this report, is to reduce apparent differences in ECG's and VCG's resulting from different heart orientations. Assuming we have a time-varying dipole as the "ECG source" and an orthogonal lead system insensitive to heart position, the three signals x(t), y(t) and z(t), figure 9.4a, are sufficient, to describe the heart activity under dipole theory and should enable calculation of corresponding signals relative to any other set of mutually perpendicular axes. Application of the eigenvalue procedure to the conventional x(t), y(t), z(t) components effects a transformation which results in the new intrinsic components u(t), v(t) and w(t), figure 9.4b, and which can be interpretted as a coordinate rotation. The u(t), v(t) and w(t) components describe the time information of the ECG's and are given by

$$\begin{aligned} u(t) &= e_{xu}\, x(t) + e_{yu}\, y(t) + e_{zu}\, z(t) \\ v(t) &= e_{xv}\, x(t) + e_{yv}\, y(t) + e_{zu}\, z(t) \\ w(t) &= e_{xw}\, x(t) + e_{yw}\, y(t) + e_{zu}\, z(t) \end{aligned} \qquad (9.11)$$

where e_{xu}, e_{yu}, etc. are the direction cosines which indicate the spatial orientation of the new coordinate system axes u, v and w with respect to the old coordinate system axes x, y and z. The instrinsic components

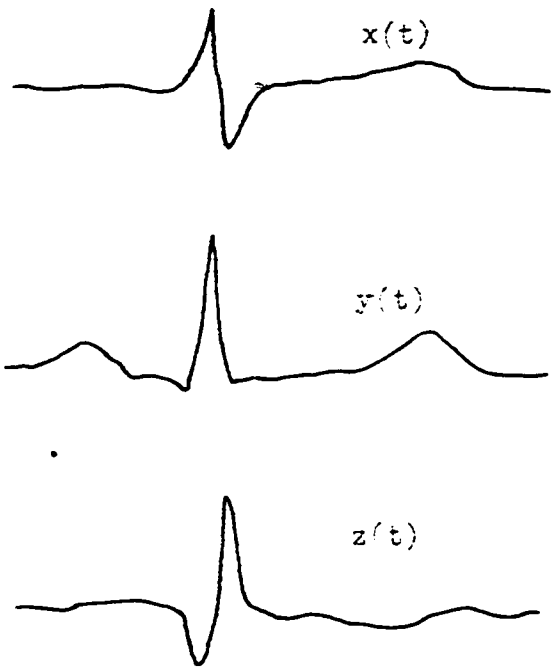

Figure 9.4a

Dipole components, x(t), y(t), and z(t).

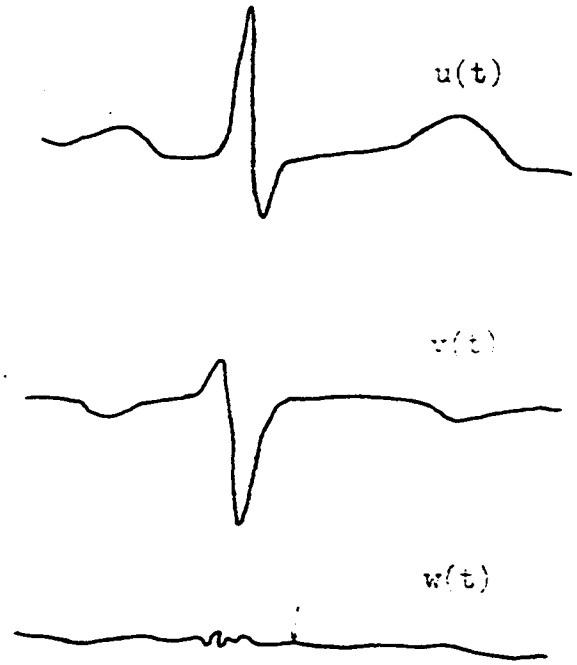

Figure 9.4b

Intrinsic components of a dipole u(t), v(t), and w(t).

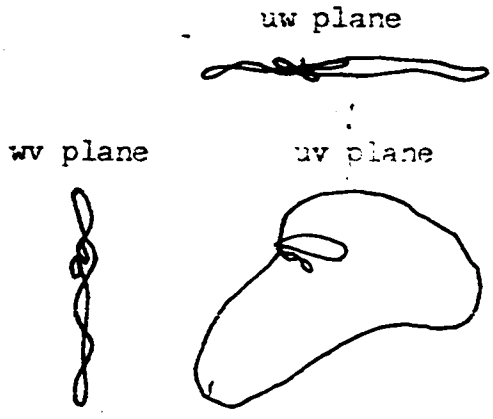

Figure 9.4c

Essential loop of the vectorcardiogram

are unique, that is they do not depend upon the particular set of orthogonal axes from which the calculation is made. In other words, the results would be the same if the original ECG signals were recorded on another orthogonal set of axes, say x', y', z'.

The vectorcardiograms corresponding to u(t), v(t) and w(t) are shown in figure 9.4c. The essential loop of the vectorcardiogram lies in the uv plane and the w axis is the direction of the "polar-vector" mentioned in Chapter 5. If desired, the essential loops of the P, QRS, and T intervals could be evaluated separately.

In concluding it should be emphasized that the technique used by Huggins and Young to represent the ECG signal is an elegant way to represent arbitrary waveforms in general and is not restricted to electrcardiographic or other physiological waveforms. At present, the ECG signal seems to lend itself more readily to mathematical manipulations than other physiological waveforms and so electrocardiography provides a good starting point for developing the application of signal analysis techniques to physiological waveforms.

CONCLUSION

The foregoing presentation dealing with the topic of ECG analysis and diagnosis using computers has been based on information gathered from numerous and varied sources. The investigation primarily reviews known and tried techniques and attempts to organize the problems into a logical context such that the problems are placed into proper perspective for the purpose of planning and acessing the worth of extending various lines of investigation in ECG and VCG research work. The author hopes that the reader has found something of interest in the material presented and apologizes if the presentation is perhaps disjointed in some instances.

For clinical evaluation, the curves calculated in Chapter 7 using the digital computer should be obtained for a number of subjects, some of which have specific types of heart malfunction. Certainly, with the pilot study reported in this thesis, such a project, if properly organized, could be carried out with a minimum of tedium in spite of the fact that an analog-digital converter and a digital plotting board may not form part of a readily available digital computer facility. Such a project would, among other things, help evaluate the worth of developing an electronic analog system to display angular velocity, linear velocity and the like. An analog facility[1] is already available at Ottawa General Hospital for displaying linear velocity. The use of the digital computer to obtain linear velocity curves can provide a useful complement to the study of linear velocity curves obtained on the analog facility

---

[1] Developed recently for Dr. F. Berkman by Mr. O.Z. Roy of the Medical Electronics group, Radio & Electrical Engineering Division of the National Research Council of Canada.

by providing a method for helping to establish the bandwidth specification of a practical analog differentiator (Recall from Chapter 4 that the ideal analog differentiator can only be approximated in practice). A comparison of the linear velocity curves given in Chapter 7 with the analog linear velocity records obtained at the Ottawa General Hospital using differentiators of different bandwidths indicates, that the higher the bandwidth of the analog differentiators, the better the agreement between the two sets of records. The analog records, however, are considerably more noisy.

It is worthwhile to repeat that the variety of displays discussed contain redundant information and an evaluation of the diagnostic usefulness of the individual displays is required. The diagnostic usefulness of the individual displays could well be a function of the abnormalities of the heart.

Finally, the application of signal analysis concepts reviewed in Chapter 9, provides a promising new approach to analyzing ECG signals.

APPENDIX

Summary

The following section presents a review of some elementary vector analysis and the equations for cartesian to spherical coordinate transformation. This material is reproduced here for ready reference in conjunction with reading Chapters 4 and 7.

Space Curves

Let $\underline{r}(t)$ be a vector depending on a single scalar variable t. (For the purpose of this report, t is the time variable). If $\underline{r}(t)$ is a "position vector" (heart vector)[1] joining the origin o of a three dimensional coordinate system and any point (x_1, x_2, x_3)[2] then

$$\underline{r}(t) = x_1(t)\underline{i} + x_2(t)\underline{j} + x_3(t)\underline{k}$$

and specification of the vector function $\underline{r}(t)$ defines x_1, x_2, x_3 as functions of the scalar variable t where $\underline{i}$, $\underline{j}$, $\underline{k}$ are unit vectors in the direction of ox_1, ox_2, ox_3 respectively.

---

[1] To correlate mathematical and ECG terminology, the appropriate mathematical terms are followed by descriptive information in parentheses to relate them to ECG terminology.

[2] Although the material presented here is given for three dimensional "physical" or "geometric" space, (x_1, x_2, x_3) is used in place of (x, y, z) to suggest that a vector function need not be restricted to three dimensional "physical" space but can also be considered in the more general context of an n-dimensional abstract space.

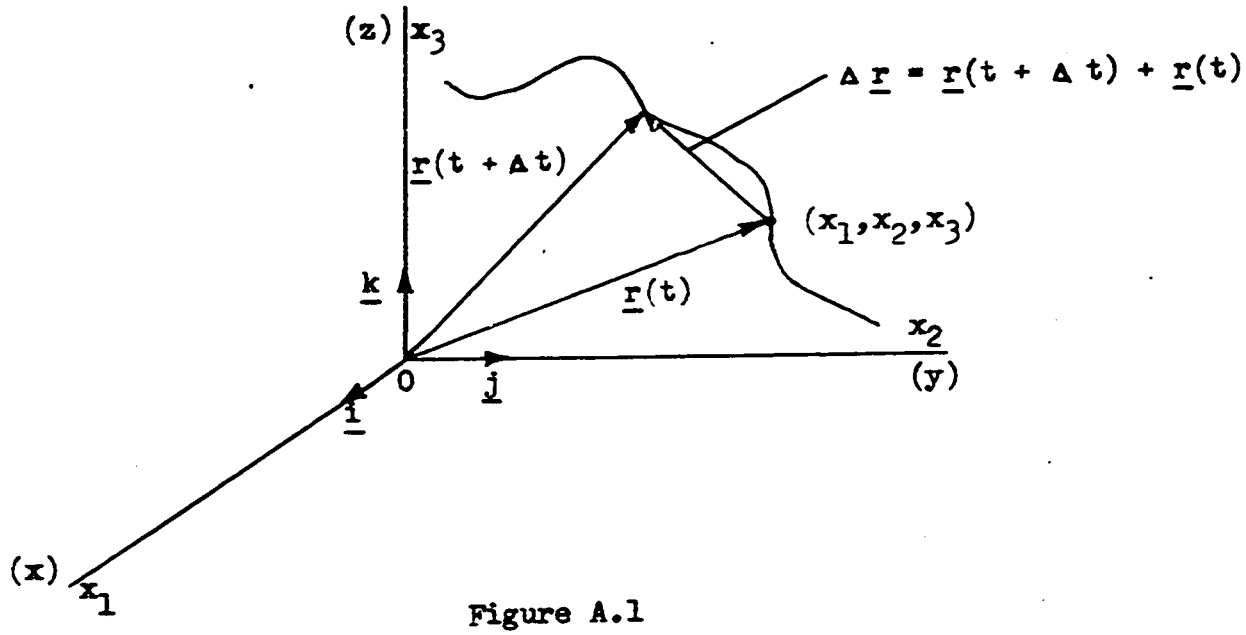

Figure A.1

As t changes, the terminal point of $\underline{r}$ describes a space curve (heart vector loop) having the parametric equations:

$$x_1 = x_1(t), \quad x_2 = x_2(t), \quad x_3 = x_3(t)$$

(This set of parametric ~~equa~~ equations correspond to the three orthogonal components of the heart vector x(t), y(t), z(t).)

Differentiation

Now, $\dfrac{\Delta \underline{r}}{\Delta t} = \dfrac{\underline{r}\,(t + \Delta t) - \underline{r}(t)}{\Delta t}$ is a vector in the direction of $\Delta \underline{r}$ where Δt denotes an increment in t[3]. The ordinary derivative of the vector $\underline{r}(t)$ with respect to the scalar t is given by

$$\frac{d\underline{r}}{dt} = \lim_{\Delta t \to 0} \frac{\Delta \underline{r}}{\Delta t} = \lim_{\Delta t \to 0} \frac{\underline{r}(t + \Delta t) - \underline{r}(t)}{\Delta t}$$

---

[3]Note that $\Delta \underline{r} = \underline{r}(t + \Delta t) \leftarrow \underline{r}(t)$ is a vector addition and not an algebraic addition and so must be resolved into algebraic operations in designing an analog system. e.g. the magnitude of $\underline{r}(t)$ is given by

If the limit exists, $\frac{d\underline{r}}{dt}$ will be a vector in the direction of the tangent to the space curve at(x_1, x_2, x_3) and is given by

$$\frac{d\underline{r}}{dt} = \frac{dx_1}{dt}\,\underline{i} + \frac{dx_2}{dt}\,\underline{j} + \frac{dx_3}{dt}\,\underline{k}$$

If t is the time variable $\frac{d\underline{r}}{dt}$ represents the linear velocity $\underline{v}(t)$ with which the terminal point of $\underline{r}(t)$ describes the curve.

Thus, $$\frac{d\underline{r}}{dt} = \underline{v}(t) = v_1(t)\,\underline{i} + v_2(t)\,\underline{j} + v_3(t)\,\underline{k}$$ [4]

where $\frac{dx_i}{dt} = v_i(t)$ $\qquad i = 1, 2, 3$

Since $\frac{d\underline{r}}{dt}$ is itself a vector depending on t, we can consider its derivatives with respect to t. If this derivative exists, it is denoted by $\frac{d^2\underline{r}}{dt^2}$. In a like manner, higher order derivatives are described. If t is the time variable, then $\frac{d^2\underline{r}(t)}{dt^2} = \frac{d\underline{v}(t)}{dt}$ represents the linear acceleration $\underline{a}(t)$ of the terminal point of $\underline{r}$ along the curve.

Thus, $$\frac{d^2\underline{r}}{dt^2} = \underline{a}(t) = \frac{d\underline{v}}{dt} = \frac{dv_1}{dt}\,\underline{i} + \frac{dv_2}{dt}\,\underline{j} + \frac{dv_3}{dt}\,\underline{k}$$

or $$\underline{a}(t) = a_1(t)\underline{i} + a_2(t)\underline{j} + a_3(t)\underline{k}$$

where $\frac{dv_i}{dt} = a_i(t)$ $\qquad i = 1, 2, 3$

---

[4] In the various scalar time displays of ECG signals, one must be careful to differentiate between $\left|\frac{d\underline{r}}{dt}\right| = |\underline{v}(t)|$ which is the magnitude of the linear velocity and $\frac{d\,|\underline{r}(t)|}{dt}$ which is the slope of the magnitude $|\underline{r}(t)|$ curve of the vector $\underline{r}(t)$.

To summarize, the derivatives of the components of $\underline{r}(t)$, namely $x_1(t)$, $x_2(t)$, $x_3(t)$ give $v_1(t)$, $v_2(t)$, $v_3(t)$ and $a_1(t)$, $a_2(t)$, $a_3(t)$ which are the components of $\underline{v}(t)$ and $\underline{a}(t)$ respectively. (If t is the time variable, and denoting $x_1(t)$, $x_2(t)$, $x_3(t)$ by $x(t)$, $y(t)$, $z(t)$ as the components of the heart vector, then the derivatives of $x(t)$, $y(t)$, $z(t)$ yield $v_x(t)$, $v_y(t)$, $v_z(t)$ and $a_x(t)$, $a_y(t)$ $a_z(t)$ which are the components of $\underline{v}(t)$ and $\underline{a}(t)$ respectively). It is appropriate to mention at this point, that unlike the derivatives of functions in cartesian coordinates, the derivatives of functions in spherical coordinates require careful interpretation. The material below will illustrate this comment.

Spherical Coordinates

Normally, spherical coordinates in terms of r, θ (latitude or elevation), and ϕ (longitude or azimuth) are given as in figure A.2. In some cases, spherical polar coordinates are used and θ_p (polar angle or colatitude) is used in place of θ.

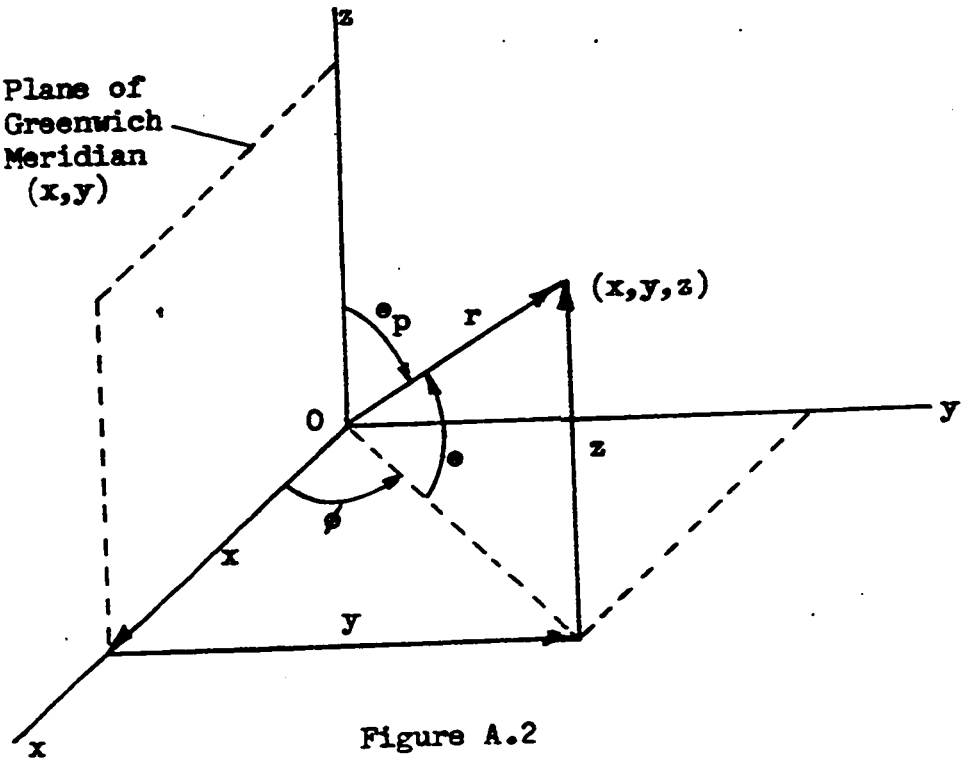

Figure A.2

$$|r| = \sqrt{x^2 + y^2 + z^2}$$

$$\theta = \arcsin \frac{z}{r} \qquad 0^\circ < \theta < \pm 90^\circ$$

$$\phi = \arctan \frac{y}{x}$$

For polar spherical coordinates

$$\theta_p = \arcsin \frac{\sqrt{x^2 + y^2}}{r} \qquad 0^\circ < \theta_p < 180^\circ$$

In terms of the x, y, z coordinates, the first derivatives of r, θ, ϕ are given by:[5]

$$\dot{r} = \frac{dr}{dt} = \frac{x\dot{x} + y\dot{y} + z\dot{z}}{\sqrt{x^2 + y^2 + z^2}}$$

$$\dot{\theta} = \frac{d\theta}{dt} = \frac{(x\dot{x} + y\dot{y})\frac{z}{\rho} - \dot{z}\rho}{\sqrt{x^2 + y^2 + z^2}} \qquad \text{where } \rho^2 = x^2 + y^2$$

$$\dot{\phi} = \frac{d\phi}{dt} = \frac{x\dot{y} - y\dot{x}}{x^2 + y^2}$$

For the purposes of Chapter 7, aligning the x, y, z axes indicates in figure A.2 with the body as per figure 1 of Chapter 3, the convention used for r, θ, ϕ is indicated in figure A.3. The equations used to obtain r, θ, ϕ from x, y, x are:

$$r = \sqrt{x^2 + y^2 + z^2}$$

$$\theta = \arcsin \frac{\pm y}{r} \qquad 0^\circ \leq \theta \leq \pm 90^\circ$$

$$\phi = \arcsin \frac{\pm z}{\sqrt{z^2 + x^2}} \qquad 0^\circ \leq \phi \leq \pm 180^\circ$$

---

[5] Corben and Stehle, Classical Mechanics, J. Wiley & Sons, 1950, p. 20.

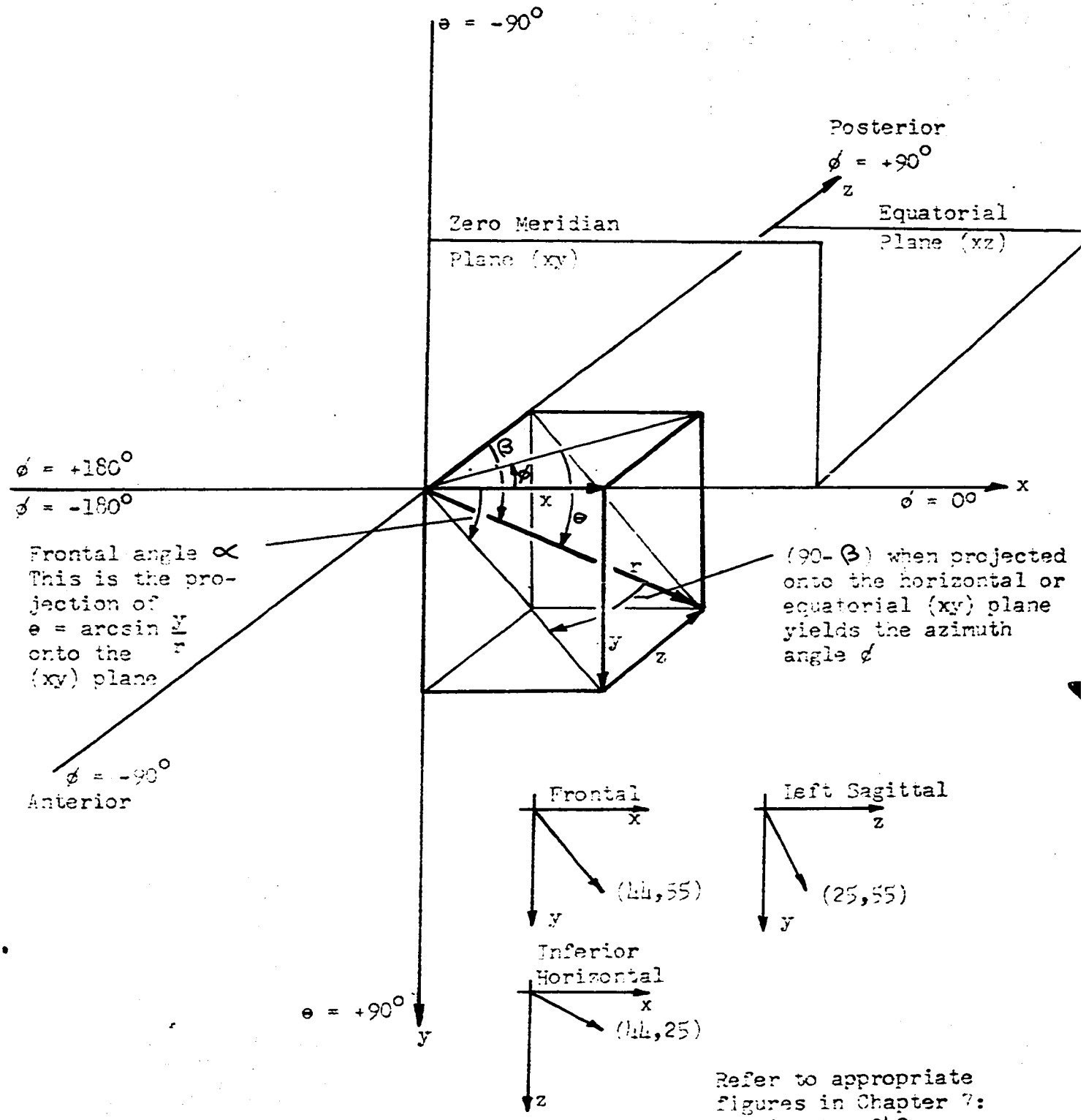

Refer to appropriate figures in Chapter 7:
At time t = 340
(x,y,z) → (+44,+55,+25)
which corresponds to
(r,θ,φ) → (74.4,47°,29°)

Figure A.3

COMPARISON OF SPHERICAL COORDINATE CONVENTIONS

Convention / Angle	Convention used in Chapter 7, Figures 8 and 9.	Abildskov's Convention, Chapter 7, Figures 10 and 11.
Equatorial plane	Transverse (horizontal) xy plane	Frontal xy plane
Azimuth or Longitude measured in equatorial plane.	$\phi(t)$ $0^\circ \leq \phi \leq \pm 180$ 0° corresponds to +ve x axis $+90^\circ$ corresponds to +ve z axis 0° to $+180^\circ$ is in posterior hemisphere (z is +ve)* 0° to -180° is in anterior hemisphere (z is -ve)*	$\alpha(t)$ $0^\circ \leq \alpha \leq \pm 180^\circ$. 0° corresponds to +ve x axis $+90^\circ$ corresponds to +ve y axis 0° to $+180^\circ$ is in inferior hemisphere (y is +ve) 0° to -180° is in superior hemisphere (y is -ve)
Elevation or Latitude measured with respect to equatorial plane	$\theta(t)$ $0^\circ \leq \theta \leq \pm 90^\circ$ 0° to $+90^\circ$ is in inferior hemisphere (y is +ve) 0° to -90° is in superior hemisphere (y is -ve)	$\beta(t)$ $0^\circ \leq \beta \leq \pm 90^\circ$ 0° to $+90^\circ$ is in posterior hemisphere (z is +ve) 0° to -90° is in anterior hemisphere (z is -ve)
Polar Axis	+y	+z
Colatitude or Polar Angle measured with respect to polar axis	$\theta_p(t)$ $0^\circ \leq \theta_p \leq +180^\circ$	$\beta_p(t)$ $0^\circ \leq \beta_p \leq +180^\circ$

* Corresponds to Helm's notation figure 3.3b which uses inferior view rather than superior view for the transverse (horizontal) plane VCG loop.

Angular Velocity

Most commonly, the term angular velocity is applied to rotational motion. It can, however, be extended to any motion of a point with respect to any axis. (Note that in speaking of the angular velocity of a point with respect to an axis of rotation, one implies that the point is located by a position vector with respect to some reference and one really is considering the rate of change of angular orientation of the position vector.)

Consider, first, a two dimensional position vector $\underline{P}$ specified in polar coordinates were O is the origin and point P is the terminus of the position vector at(r, θ).[6] Take a unit vector $\underline{i}$ along OP, a unit vector $\underline{j}$ perpendicular to OP in the direction of θ increasing, and a unit vector $\underline{k}$ forming a positive orthogonal triad with $\underline{i}$ and $\underline{j}$. The triad $\underline{i}$, $\underline{j}$, $\underline{k}$ form a rigid frame of reference. As P moves to P', this

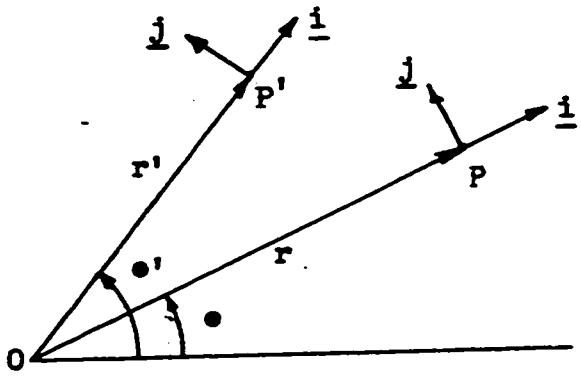

Figure A.4

triad is in motion about the $\underline{k}$-axis with angular speed $\dot{\theta}$, and hence has an angular velocity $\underline{w} = \underline{k}\,\dot{\theta}$ where $\dot{\theta}$ denotes $\frac{d\theta}{dt}$, that is, the rate of change of angle θ with respect to time t. In other words, angular velocity

---

[6] The following material was extracted from:
E.A. Milne, Vectorial Mechanics, Methuen & Co. Ltd., 1948, pp. 173 - 174.

is a vector quantity represented by a vector along the axis of rotation (and pointed in the direction required by the right hand rule.) [illegible]

Consider now the three dimension position vector $\underline{P}$ specified in spherical polar coordinates (r, θ, ϕ) as defined by figure A.5. Let $\underline{i}$ be a unit vector in the direction OP, $\underline{j}$ a unit vector perpendicular to OP in the plane zOP and with sense in the direction of θ increasing.

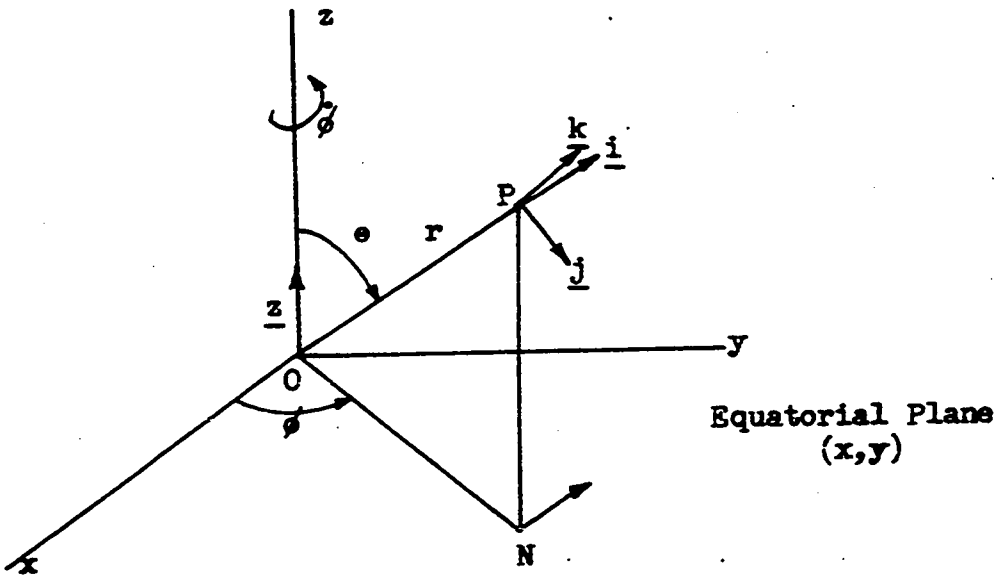

Figure A.5

Let $\underline{k} = \underline{i} \wedge \underline{j}$ i.e.) $\underline{i}$, $\underline{j}$, $\underline{k}$ form a positive orthogonal triad. The plane zOP has angular speed $\dot{\phi}$ about Oz, and so the plane defined by $\underline{i}$ and $\underline{j}$ has the angular velocity $\dot{\phi}\underline{z}$ where $\underline{z}$ is a unit vector along Oz. Relative to the point moving with this angular velocity, the triad $\underline{i}$, $\underline{j}$, $\underline{k}$ has the angular speed $\dot{\theta}$ about an axis through P parallel to $\underline{k}$. Hence, by the theorem of relative angular velocities,[7] the angular velocity of the triad $\underline{i}$, $\underline{j}$, $\underline{k}$ relative to the reference frame Oxyz is given by $\underline{w} = \dot{\phi}\underline{z} + \dot{\theta}\underline{k}$. This is a vector addition. For example, if a top is spinning about an axis which is simultaneously being tipped toward the table, the resultant

---

[7] E.A. Milne, op. cit., p. 166.

angular velocity is the vector sum of the angular velocities of spin and tipping. When $\underline{w}$ is not constant in time, the direction of $\underline{w}$ is called the instantaneous axis and motion of P is perpendicular to the instantaneous direction of $\underline{w}$. The angular speed is given by $|\underline{w}| = \left|\sqrt{\dot{\phi}^2 + \dot{\theta}^2}\right|$. In other words, $\underline{w} = \dot{\phi}\underline{z} + \dot{\theta}\underline{k}$ gives the "true" or "maximum projection" of angular velocity as a function of time with respect to the instantaneous axis which is changing orientation continuously.

To illustrate the comment made above which stated that "unlike the derivatives of functions in cartesian coordinates, the derivatives of functions in spherical coordinates require careful interpretation", the equations which give the component velocities and accelerations of the point P specified by the position vector $\underline{P}$ are respectively[8]

$$\underline{v}(t) = \frac{d\underline{P}}{dt} = \dot{r}\,\underline{i} + r\,\dot{\theta}\,\underline{j} + r\,\dot{\phi}\sin\theta\,\underline{k}$$

$$\underline{a}(t) = \frac{d^2\underline{P}}{dt^2} = \underline{i}(\ddot{r} - r\dot{\theta}^2 - r\dot{\phi}^2\sin^2\theta) + \underline{j}\left(\frac{1}{r}\frac{d}{dt}(r^2\dot{\theta}) - r\dot{\phi}^2\sin\theta\cos\theta\right)$$

$$+ \underline{k}\,\frac{1}{r\sin\theta}\,\frac{d}{dt}\,(r^2\sin^2\theta\,\dot{\phi})$$

The components are in the direction of r increasing($\underline{i}$), θ increasing($\underline{j}$) and ϕ increasing($\underline{k}$). Compared to their counterparts in cartesian coordinates, these two equations are considerably more involved and so it is more practical to work in cartesian coordinates when obtaining linear velocity v(t) and acceleration a(t). In a similar way that the first derivative of linear velocity yields linear acceleration, one can also obtain angular acceleration or the rate of change of angular velocity by evaluating the first derivative of angular velocity.

---

[8] E.A. Milne, op. cit., pp. 174 - 175.

REFERENCES

1. Massie, E. and Walsh, T.J., Clinical Vectorcardiography and Electrocardiography, Year Book Publisher Inc., Chicago, 1960.

2. Schmitt, O.H., Okajima, M. and Blaug, M., "Skin Preparation and Electrocardiographic Lead Impedance", Digest of the 1961 International Conference on Medical Electronics, New York, July 21, 1961, p. 266.

3. Lamb, L.E., Fundamentals of Electrocardiography and Vectorcardiography, C.C. Thomas, Publisher, Springfield, Illinois, 1957.

4. Franke, E.K., Braunstein, J.R. and Zellner, D.C., "Study of High Frequency Components in Electrocardiogram by Power Spectrum Analysis", Circulation Research, Vol. 10, June 1962, pp. 870 - 879.

5. Knickerbocker, G.G. and Kouwenhoven, W.B., "Electrical Techniques and the Heart in Health and Disease", Electrical Engineering, October 1961, pp. 761 - 766.

6. Engle, R.L., Jr., Davis, B.J., "The Meaning of Medical Diagnosis", Digest of the 1961 International Conference on Medical Electronics, New York, July 21, 1961, p. 9.

7. Frank, E., "The Elements of Electrocardiographic Theory", A.I.E.E. Trans. on Communications and Electronics, May, 1953, pp. 125 - 134.

8. Okada, R.H., "A Critical Review of Vector Electrocardiography", I.E.E.E. Transactions on Bio-Medical Electronics, Vol. BME - 10, July 1963, pp. 95 - 98.

9. Geselowitz, D.B., "Multipole Representation for an Equivalent Cardiac Generator", Proc. IRE, Vol. 48, No. 1, January 1960, pp. 75 - 79.

10. Frank, E., "An Accurate Clinically Practical System for Spatial Vectorcardiography", Circulation, 13: 737, 1956.

11. Stallman, F.W., Pipberger, H.V., "Automatic Recognition of Electrocardiographic Waves by Digital Computer," Circulation Research, Vol. 9, November 1961, pp. 1138 - 1143.

12. Pipberger, H.V., "Use of Computers in the Interpretation of Electrocardiograms", Circulation Research, Vol. 11, September 1962, pp. 555 - 562.

13. Pipberger, H.V. and Stallman, F.W., "Use of Computers in ECG Interpretation", American Heart Journal, Vol. 64, No. 2, August 1962, pp. 285 - 286.

14. Caseres, C.A., "How Can the Waveforms of a Clinical Electrocardiogram be Measured Automatically by a Computer?" I.R.E. Trans. on Bio-Med. Elect., Vol. BME - 9, January 1962, pp. 21 - 22.

15. Schmitt, O.H., "The Present Status of Vectorcardiography," Archives of Internal Medicine, Vol. 96, May 1955, pp. 574 - 593.

16. Forsyth, G.E., J. von der Groeben and Toole, J.G. "Vectorcardiographic Diagnosis with the Aid of ALGOL", Communications of the A.C.M., pp. 118 - 122.

17. Sayers, B. McA., "A Spatial Magnitude Electrocardiograph", American Heart Journal, 49: 336, 1955.

18. McFee, R., "A Trigonometric Computer with Electrocardiographic Applications", Review of Scientific Instruments, Vol. 21, No. 5, May 1950, pp. 420 - 426.

19. Dower, G.E., Moore, A.D., Park, W.K.R., Poole, E.G. and Yuan, J., "A New Computer for Three-Dimensional Electrocardiography". 1958 I.R.E. Canadian Convention Record, p. 459.

20. Park, W.R.K., "A Polarcardiograph Computer". M.A.Sc. Thesis, University of British Columbia, 1954.

21. Poole, E.G., "A Spherical Polarcardiograph Computer", M.A.Sc. Thesis, University of British Columbia, 1954.

22. McFee, R., Parungao, A and Mueller, W., "An Electronic Coordinate Transformer for Electrocardiography", I.R.E. Trans. on Bio-Med. Elect., Vol. BME-8, No. 1, January 1961, pp. 52 - 54.

23. Koechlin, R., "Project of a Coordinated Instrumentation between Several Centres of Electrocardiography", Digest of the 1961 International Conference on Medical Electronics, p. 213.

24. Hagen, W.K. and Horowitz, M., "Estimating the Amount of Information in an ECG Signal by use of Information Theory". Paper presented at the 15th Annual Conference in Engineering in Medicine and Biology, November 4 - 7, 1962, Chicago, Illinois.

25. Young, T.Y., "Representation and Analysis of Signals Part X, Signal Theory and Electrocardiography", Ph.D. Thesis, The Johns Hopkins University, May 1962.

26. Brinberg, L. Quantitative Vectorelectrocardiography. Waverly Press Inc., Baltimore, Maryland, 1960.

27. Carberry, W.J., Steinberg, C.A., Tolles, W.E. and Freiman, A.H., "Automatic Methods for the Analysis of Physiological Data", Topics in Electronics, Vol. II, 1961, published by Airborne Instruments Laboratory, Long Island, New York.

28. Steinberg, C.A., Abrahams, S. and Caseres, C.A., "Pattern Recognition in the Clinical Electrocardiogram", I.R.E. Trans. on Bio-Med. Elect., Vol. BME - 9, January 1962, pp. 23 - 30.

29. Scher, A.M., Young, A.C. and Meredith, W.M., "Factor Analysis of the Electrocardiogram", Circulation Research, Vol. 8, May, 1960, pp. 519 - 526.

30. Northern News, Northern Electric Co., Montreal, Canada, Vol. XXXVI, No. 20, November 18, 1963.

31. Greenwood, Holdam, MacRae Electronic Instruments, MIT Radiation Laboratory Series, Vol. 21, McGraw Hill Book Co., Toronto, 1948.

32. Crufts Laboratory Staff Electronic Circuits and Tubes, McGraw Hill Books Co., Toronto, 1947, pp. 854 - 855.

33. McG. Ross, H., Shuffrey, A. "An Electronic Square Law Circuit", Journal of Scientific Instruments, 25: 200, 1948.

34. Chance, B.H., MacNichol, E.F., Sayre, D., Williams, F. Waveforms, MIT Radiation Laboratory Series, Vol. 19, McGraw Hill Book Co., Toronto, 1949, p. 683.

35. De Cote, R., Horwath, W.J. "An Electronic Computer for Electrocardiography", IRE Transactions on Bio-Medical Electronics, Vol. PGME-8, 1955.

36. Milnor, W.R., Talbot, S.A., Newman, E.V. "A Study of the Relationship between Unipole Leads and Spatial Vectorcardiograms using the Panoramic Vector Cardiograph", Circulation, Vol. 7, October, 1953, pp. 545 - 558.

37. Pipberger, H.V., Carter, T.N. "Analysis of the Normal and Abnormal Vectorcardiogram in its Own Reference Frame", Circulation, Vol. 26, May 1962, pp. 827 - 840.

38. Abildskov, J.A., Ingerson, W.E., Hisey, B.L. "A Linear Time Scale for Vectorcardiographic Data", Circulation, Vol. 14, October, 1956, p. 556.

39. Sayer, B.M., Silberberg, F.G., Durie, D.F. "The Electrocardiographic Spatial Magnitude Curve in Man", American Heart Journal, 49: 323, 1955.

40. McFee, R. and Johnston, F.D.
"Electrocardiographic Leads"
Part I Introduction, Circulation, 8: 554, 1953.
Part II Analysis, Circulation, 9: 255, 1954.
Part III Synthesis, Circulation, 9: 868, 1954.

41. Hellerstein, H.K., Hamlin, R.
"QRS Component of the Spatial Vectorcardiogram and of the Spatial Magnitude and Velocity Electrocardiogram of the Normal Dog",
The American Journal of Cardiology, December, 1960, pp. 1049-1061.

42. Frank, E.
"An Accurate Clinically Practical System for Spatial Vectorcardiography",
Circulation, Vol. 13, May 1956, pp. 737 - 749.

43. Frank, E.
"A Direct Experimental Study of Three Systems of Vectorcardiography",
Circulation, Vol. 10, July 1954, pp. 101 - 113.

44. Helm, R.A.
"Vectorcardiographic Notation",
Circulation, Vol. 13, 1956, p. 581.

45. Committee on Electrocardiography, American Heart Association:
"Recommendations for Standardization of Electrocardiographic and Vectorcardiographic Leads",
Circulation, Vol. 10, 1954, p. 564.

46. Brink, R.W.
A First Year of College Mathematics (with Spherical Trigonometry),
D. Appleton - Century Co., New York, 1937.

47. Valley and Wallman
Vacuum Tube Amplifiers
MIT Radiation Laboratory Series, Vol. 18, p. 80.

48. Korn and Korn
Electronic Analog Computers
McGraw Hill Book Co., 2nd Edition

49. U.S. Patent 2,634,909

50. Karplus
Analog Simulation
McGraw Hill Book Co., 1958.

51. Jackson, A.S.
Analog Computation
McGraw Hill Book Co., 1960.

52. Smith, G.W. and Wood, R.C.
Principles of Analog Computation
McGraw Hill Book Co., 1959.

53. Langner, P.H., Geselowitz, D.B.
"First Derivative of the Electrocardiogram"
Circulation Research, Vol. 10, February 1962, pp. 220 - 226.

54. Ford, R.L.
"Differentiating Circuits"
Electronic Engineering, December 1953, pp. 519 - 521.

55. Geiss, G.R., Glomb, J.D.G.
"Development of an Adaptive Control System"
Polytechnic Institute of Brooklyn
Research Report No. PIBMRI - 827 - 60, Sept. 19, 1960,
pp. 28 - 33.

56. Nikiforuk, P.N.
"A Technique for Non-linear Function Generation"
Electronic Engineering, March 1955, pp. 118 - 119.

57. Kovach, L.D., Comley, W.
"A New, Solid State, Nonlinear Analog Component"
IRE Transactions on Electronic Computers, December 1960,
pp. 496 - 503.

58. Murphy, C.G.
Basic Automatic Control Theory
Van Nostrand, 1957.

59. Celinski, O., Rimawi, I.H.
"Classification of Analog Multipliers",
Instruments and Control Systems", Vol. 37, No. 6,
June 1964, pp. 149 - 156.

60. Electronic Multiplier Instruction Manual,
Donner Scientific Co., Concord, California.

61. Keister, G.L.
"A Compact Multiplier Puts the Hall Effect to Work",
Control Engineering, November, 1955, pp. 94 - 99.

62. Glinski, G.S., Landolt, J.P.
"Theory and Practice of Hall Effect Multipliers",
1961 IRE International Convention Record, Part 2.

63. Landolt, J.P.
"The Hall Effect Multiplier - A Contribution to Analog
Multiplier Technology",
M.Sc. Thesis, University of Ottawa, October 1961.

64. Tommerdahl, J.B.
"A Preamplifier for an Electrocardiograph Monitoring System",
IRE Trans. on Bio-Med. Elect., January 1961, pp. 55 - 58.

65. Roy, O.Z.
"An Electronic Heart Beat Simulator and a Cardiac Tachometer",
IRE Trans. on Med. Elect., PGME-11, July 1958, pp. 48 - 52.

66. Taback, L., Marden, E., Mason, H.L., Pipberger, H.V.
"Digital Recording of Electrocardiographic Data for Analysis by a Digital Computer",
IRE Trans. on Med. Elect., Vol. ME-6, No. 3, September 1959, pp. 167 - 171.

67. Pipberger, H.V., Freis, E.D., Taback, L., Mason, H.L.
"Preparation of Electrocardiographic Data for Analysis by Digital Electronic Computer",
Circulation, Vol. 21, March 1960, pp. 413 - 418.

68. Suckling, E.E.
Bioelectricity,
McGraw Hill Book Co., 1961.

69. Berson, A.S., Stallman, F.W., Pipberger, H.V.
"Digital Computer Analysis of Electrocardiographic Data",
Digest of the 1961 International Conference on Medical Electronics, New York, July 1961, p. 232.

70. Steinberg, C.A., Carberry, W.J., McBride, J.M., Caceres, C.A.
"Pattern Recognition in the Electrocardiogram",
Digest of the 1961 International Conference on Medical Electronics, New York, July 1961, p. 233.

71. Caseres, C.A., Steinberg, C.A., Abraham, S., Carberry, W.J., McBride, J.M., Tolles, W.E., Rikki, A.E.
"Computer Extraction of Electrocardiographic Parameters",
Circulation, Vol. 25, February 1962, pp. 356 - 362.

72. Rikki, A.E., Tolles, W.E., Steinberg, C.A., Carberry, W.J., Freiman, A.H., Abraham, S., Caceres, C.A.
"Computer Analysis of Electrocardiographic Measurements",
Circulation, Vol. 24, September 1961, pp. 643 - 649.

73. Steinberg, C.A.
"Computers Will Aid in the Diagnosis of Heat Disease",
Topics in Electronics, Vol. 1, March 1960,
Published by Airborne Instruments Laboratory,
Deer Park, Long Island, New York.

74. Steinberg, C.A., Tolles, W.E., Freiman, A.H., Abraham, S, Caceres, C.A.
"Techniques for the Use of the Digital Computer as an Aid in the Diagnosis of Heart Disease",
Paper presented at Eastern Joint Computer Conference, December 14, 1961, Sheraton Park Hotel, Washington 16, D.C.
(see Topics in Electronics, Vol. 1, March 1960, Airborne Instruments Laboratory, Deer Park, Long Island, New York.)

75. Pipberger, H.V., Arms, R.J., Stallman, F.W.
"Automatic Screening of Normal and Abnormal Electrocardiograms by Means of a Digital Electronic Computer",
Proc. Soc. Exp. Biol. and Med., 106: 130, 1961.

76. Pipberger, H.V., Stallman, F.W., Berson, A.S.
"Automatic Analysis of the P-QRS-T Couples of the Electrocardiogram by Digital Computer",
Annals of Internal Medicine, Vol. 57, No. 5, November, 1962, pp. 776 - 787.

77. Forsythe, G.E., von der Groeben, J., Toole, J.G.
"Vectorcardiographic Diagnosis with the Aid of ALGOL",
Communications of the ACM, pp. 118 - 122.

78. von der Groeben, J.
"The Spatial Frequency Distribution of the QRS Loop as Studied on 154 Normal Individuals",
American Heart Journal, Vol. 59, June 1960, pp. 875 - 891.

79. von der Groeben, J.
"Spatial Representation of Cardiac Vectors with the Aid of Tabulated Functions",
American Heart Journal, Vol. 52, 1956, p. 562.

80. von der Groeben, J.
"A Comprehensive Mapping of Spatial Vectorcardiographic Data",
American Heart Journal, Vol. 56, 1958, p. 510.

81. Okajima, M., Stark, L. Whipple, G., Yasui, S.
"Computer Pattern Recognition Techniques: Some Results with Real Electrocardiographic Data",
I.E.E.E. Trans. on Bio-Medical Electronics, July 1963, pp. 106 - 114.

82. Stark, L. et al.
"Digital-Computer Diagnosis of the Electrocardiogram by Using Pattern-Recognition Techniques".
Quarterly Progress Report No. 65, April 15, 1962 pp. 231 - 238.
Massachusetts Institute of Technology, Cambridge, Mass.

83. Ried and Caldwell
"Research in Electrocardiography", Annals of Internal Medicine, Vol. 7, 1933 - 34, p. 369.

84. Weiss, H.
"Estimating Experimental Errors", Machine Design, June 7, 1962, pp. 154 - 157.

85. Clark, W.A.
"Computer - Generated Displays of Bioelectric Data Processing",
Digest of the 1961 International Conference on Medical Electronics, New York, July 1961, p. 97.

86. Young, T.Y., Huggins, W.H.
"On the Representation of Electrocardiograms,"
I.E.E.E. Trans. on Bio-Med. Elect., July 1963, pp. 86 - 95.

87. Abildskov, J.A., Hisey, B.L., Ingerson, W.E.
"The Magnitude and Orientation of Ventricular Excitation Vectors in the Normal Heart and Following Myocardial Infarction", American Heart Journal, Vol. 55, No. 1, January 1958, pp. 104 - 113.

88. Stratbucker, R.A., Hyde, C.M., Wixon, S.A.
"The Magnetocardiogram - A New Approach to Fields Surrounding the Heart",
I.E.E.E. Trans. on Bio-Medical Electronics, Vol. BME-10, No. 4, October 1963, pp. 145 - 149.

89. Hildebrand, F.B.
Introduction to Numerical Analysis, McGraw Hill, New York, 1956.

90. Milne
Numerical Calculus, Princeton University Press, 1949.

91. Kopal
Numerical Analysis, J. Wiley and Sons, 1955.

92. O'Donohue, J.P.
"A Note on Using Cascaded Simple Averages for Obtaining Acceleration Information",
Proc. I.R.E., January 1962, p. 187.

93. Caldwell, Oler and Peters.
"An Improved Form of Electrocardiograph",
Review of Scientific Instruments, 111, pp. 277 - 286, 1932.

94. James, Nichols and Phillips.
Theory of Servo-Mechanisms
MIT Radiation Laboratory Series, Vol. 25, p. 283.

95. Scher, A.M., Young A.C.
"Frequency Analysis of the Electrocardiogram",
Circulation Research, Vol. 8, March 1960, pp. 344 - 346.

96. Langner, P.H.
"The Value of High Fidelity ECG Using the CRO and an Expanded Time Scale",
Circulation, Vol. 5, 1952, p. 249.

97. Gilford, S.R.
"High Fidelity Electrocardiography",
Proc. of Second Joint AIEE - IRE Conference on Electronics in Nucleonics and Medicine, New York, October 31, 1949.

98. Sunstein, D.E.
"Photoelectric Waveform Generator",
Electronics, 22: 100, 1949.

99. Whittaker and Robinson.
Calculus of Observations, Blackie and Sons, Ltd., London, 1949.

100. Kerwin, A.J.
"The Effect of Frequency Response of Electrocardiographs on the Form of Electrocardiograms and Vectorcardiograms",
Circulation, Vol. 8, July 1953, p. 98..

101. Langner, P.H.
"Further Studies in High Fidelity ECG Myocardial Infarction",
Circulation, Vol. 8, July 1953, p. 905.

102. Langner, P.H.
"High Fidelity ECG - Further Studies Including the Comparative Performance of Four Different ECG's",
American Heart Journal, Vol. 45, May 1953, p. 683.

103. Panel Discussion on "Future Research in Electrocardiography" held at the Conference on Modern Concepts of Electrocardiography and Methods of ECG Data Processing. September 11, 1959. Veterans' Administration Hospital, Mt. Alto, 2650 Wisconsin Ave., N.W., Washington 7, D.C.

104. Langner, P.H., Geselowitz, D.B.
"Characteristics of the Frequency Spectrum in the Normal Electrocardiogram and in Subjects Following Myocardial Infarction",
Circulation Research, Vol. 8, May 1960, pp. 577 - 584.

105. Franke, E.K., Braunstein, J.R., Zellner, D. C.
"Study of High Frequency Components in Electrocardiogram by Power Spectrum Analysis",
Circulation Research, Vol. 10, June 1962, pp. 870 - 879.

106. Angelakos, E.T., Shepherd, G.M.
"Autocorrelation of Electrocardiographic Activity During Vectricular Fibrillation",
Circulation Research, 5: 657, 1957.

107. Barlow, J.S., Brown, R.M.
"An Analog Correlator System for Brain Potentials",
MIT, Res. Lab. Electr., Techn. Report No. 300, 1955.

108. Koyama, S., Harumi, K., Suzuki, K., Watanabe, H., Takahashi, N.
"Autocorrelation and Crosscorrelation of Electrocardiographic Record During Ventricular Fibrillation",
Japanese Heart Journal, Vol. 3, No. 3, May 1962, pp. 269 - 274.

109. Franke, E.K., Braunstein, J.R., Power, J.R.
"Power Spectrum ~~"Autocorrelation~~ Analysis of the High Frequency Electrocardiogram",
Paper read at the Biophysical Society meeting, Boston, Feb. 5, 1958.

110. Franke, E.K., Braunstein, J.R.
"Autocorrelation Analysis of the High Frequency Electrocardiogram",
Paper presented at the 11th Annual Conference on Electrical Techniques in Medicine and Biology,
Minneapolis, November 19 - 21, 1958.

111. Favret, A.G.
"Autocorrelation Techniques Applied to the Fetal Electrocardiogram",
Digest of the 1961 International Conference on Medical Electronics,
New York City, July 16 - 21, 1961, p. 5.

112. Raoult, P.
"Correlation Function and Fourier Analysis",
Digest of the 1961 International Conference on Medical Electronics,
New York City, July 16 - 21, 1961, p. 273.

113. Young, T.Y., Huggins, W.H.
"Representation and Analysis of Signals, Part VIII,
"Representation of Electrocardiogram by Orthogonalized Exponentials"
Report No. AFCRL-187, The Johns Hopkins University, March 1961.

114. Young, T.Y., Huggins, W.H.
"The Intrinsic Component Theory of Electrocardiography"
IRE Trans. on Bio-Med. Elect., October 1962, pp. 214 - 221.

115. Young, T.Y., McDonough, R.N., Huggins, W.H., Lai, D.C.
"Matched Exponents for Representation of Electrocardiograms"
Digest of 1961 International Conference on Medical Electronics,
p. 237.

116. Baghdady (editor)
Lectures on Communication System Theory,
McGraw Hill Book Co., 1961, Chapter 10.

117. Huggins, W.H.
"Representation and Analysis of Signals; Part I, The Use of
Orthogonalized Exponentials"
Report No. AFCRC-TR-57-357.
The John Hopkins University, September 1957.

118. Lai, D.C.
"Representation and Analysis of Signals; Part VI, Signal Space
Concepts and Dirac's Notation",
Report No. AFCRC-TN-60-167
The John Hopkins University, January 1960.

119. Lowenberg, E.C.
"Signal Theory Applied to the Analysis of Electroencephalograms"
IRE Trans. on Medical Electronics, Vol. ME-7, January 1960,
pp. 7 - 12.

120. Gerbarg, D.S., Holocomb, F.W., Hoffer, J.F., Bading, C.E.,
Schultz, G.L., Sears, R.E.
"Analysis of Phonocardiogram by a Digital Computer",
Circulation Research, Vol. II, September 1962, pp. 569 - 576.

121. Gerbarg, D.S., Taranta, A., Spagnuolo, M., Hoffer, J.J.
"Computer Analysis of Phonocardiograms",
Progress in Cardiovascular Diseases, Vol. 5, No. 4,
January 1963, pp. 393 - 405.

122. Kautz, W.H.
"Transient Synthesis in the Time Domain"
IRE Trans. on Circuit Theory, Vol. CT-1, No. 3, September 1954, pp. 29 - 39.

123. Lee, Y.W.
Statistical Theory of Communication
J. Wiley and Sons Inc., 1960.

124. Goldstein, H.
Classical Mechanics
Addison-Wesley Publishing Co., Cambridge, Mass. 1957.

V I T A

Name: Nickolas Andrew Bobey

Born: Winnipeg, Canada June 9, 1937.

Educated:

Primary: Lord Selkirk School 1943 - 1952 Winnipeg, Canada

Secondary: Lord Selkirk High School 1952 - 1954 Winnipeg, Canada

University: University of Manitoba 1954 - 1959 Winnipeg, Canada

Degree: B.Sc. (E.E.) Communications option May 1959.